

Alternative splicing of MALT1 controls signaling and activation of CD4⁺ T cells

Dissertation

zur Erlangung des Doktorgrades der Naturwissenschaften
an der Ludwig-Maximilians-Universität München
Fakultät für Biologie

angefertigt am

Helmholtz Zentrum München

Deutsches Forschungszentrum für Gesundheit und Umwelt
Institut für Molekulare Toxikologie und Pharmakologie
Abteilung Zelluläre Signalintegration

vorgelegt von

Isabel Meininger

München, den 11.08.2016

1. Gutachter: Prof. Dr. Daniel Krappmann

2. Gutachter: Prof. Dr. Michael Boshart

Tag der Abgabe: 11.08.2016

Tag der mündlichen Prüfung: 27.03.2017

Table of contents

Table of contents.....	III
List of figures.....	VII
List of tables.....	IX
1 Summary.....	1
1 Zusammenfassung.....	3
2 Introduction.....	5
2.1 T cells in adaptive immune responses.....	5
2.1.1 The adaptive immune system.....	5
2.1.2 T cell activation and differentiation.....	6
2.2 TCR-induced signaling pathways.....	9
2.2.1 T cell receptor and co-receptors.....	9
2.2.2 Proximal T cell receptor signaling events.....	9
2.2.3 NFAT, ERK and AP-1 activation.....	12
2.3 CARMA1, BCL10 and MALT1 facilitate canonical NF- κ B and JNK signaling.....	13
2.3.1 The transcription factor NF- κ B.....	13
2.3.2 CBM complex components.....	15
2.3.3 CBM assembly triggers NF- κ B and JNK signaling.....	17
2.3.4 MALT1 in T cell activation.....	21
2.4 Alternative splicing.....	24
2.4.1 General concept of alternative splicing.....	24
2.4.2 Alternative splicing in T cell activation.....	26
2.5 Aims of the study.....	28
3 Results.....	29
3.1 Functional analysis of MALT1 isoforms.....	29
3.1.1 Evolutionary conservation of MALT1 isoforms.....	29
3.1.2 Design of MALT1 mutants to analyze individual TRAF6 binding sites.....	30
3.1.3 T6BM1 encoded by MALT1 exon7 contributes to the activation of T cell signaling pathways.....	32
3.1.4 MALT1 exon7 supports TRAF6 and NEMO recruitment to reinforce MALT1 scaffolding function.....	34
3.1.5 MALT1 isoforms do not differ in their protease function.....	36
3.2 Role of MALT1 isoforms in T cell activation and differentiation.....	38

3.2.1	T cell receptor signaling induces MALT1A expression in primary CD4 ⁺ T cells	38
3.2.2	MALT1A expression is enhanced in activated T cell subsets	40
3.2.3	Alternative MALT1 splicing is induced in human CD4 ⁺ T cells	41
3.2.4	Design and evaluation of morpholino oligomer to prevent MALT1A expression	42
3.2.5	MALT1A upregulation supports NF-κB and JNK signaling	45
3.2.6	TCR-induced MALT1A expression supports T cell activation	48
3.2.7	Alternative MALT1 splicing does not influence T cell fate decisions	49
3.3	Regulation of alternative MALT1 splicing by the splicing factor hnRNP U	52
3.3.1	A siRNA screen identifies hnRNP U as a critical splicing regulator of alternative MALT1 splicing	52
3.3.2	mRNA stability of <i>MALT1</i> isoforms is not affected by hnRNP U	54
3.3.3	hnRNP U binds to <i>MALT1</i> pre-mRNA in proximity to exon7	55
3.3.4	hnRNP U-mediated exon7 skipping depends on exon7 adjacent intronic sequences	56
3.3.5	TCR-induced exon7 inclusion in CD4 ⁺ T cells is modulated by hnRNP U	59
3.3.6	hnRNP U counteracts T cell activation	61
4	Discussion	63
4.1	TCR ligation induces alternative MALT1 splicing	65
4.2	hnRNP U negatively regulates exon7 inclusion	67
4.3	Exon7 inclusion augments MALT1 scaffolding function	70
4.4	Alternative MALT1 splicing is dispensable for MALT1 protease activity	73
4.5	The MALT1 isoform ratio is critical for T cell activation	75
4.6	TCR-mediated control of alternative MALT1 splicing	78
4.7	Conclusion and perspectives	82
5	Materials	85
5.1	Instruments and equipment	85
5.2	Chemicals	87
5.2.1	General chemicals	87
5.2.2	Cell culture	89
5.2.3	Stimulants, inhibitors and cytokines	90
5.3	Enzymes and Kits	90
5.4	Mice strains	91
5.5	Eukaryotic cell lines	92
5.6	Bacteria	92

5.7	Vectors and oligonucleotides.....	92
5.7.1	Vectors	92
5.7.2	shRNAs	94
5.7.3	siRNAs and morpholino.....	95
5.7.4	EMSA oligonucleotides	96
5.7.5	Primer for qPCR and semi-qPCR.....	96
5.8	Antibodies.....	98
5.8.1	Antibodies for cell purification, stimulation and differentiation.....	98
5.8.2	FACS antibodies	98
5.8.3	Primary antibodies for Western Blot.....	99
5.8.4	Secondary antibodies for Western Blot.....	100
5.8.5	RNA-binding protein immunoprecipitation (RIP) antibodies.....	100
5.9	Buffers and solutions	100
6	Methods	102
6.1	Cell culture	102
6.1.1	Storage of cell lines	102
6.1.2	Cultivation of adherent cells	102
6.1.3	Cultivation of suspension cells.....	102
6.1.4	Isolation and cultivation of primary murine CD4 ⁺ T cells.....	102
6.1.5	Isolation and cultivation of primary human CD4 ⁺ T cells	103
6.1.6	Immunization and isolation of different murine T cell subsets.....	104
6.2	Cell transfection and transduction	104
6.2.1	Transfection of Jurkat T cells by electroporation.....	104
6.2.2	Transfection of Jurkat T cells with siRNA and morpholino	105
6.2.3	Lentiviral transduction of Jurkat T cells	105
6.2.4	Adenoviral transduction of primary, murine CD4 ⁺ T cells.....	106
6.3	Cell stimulation and differentiation.....	107
6.3.1	Stimulation of Jurkat T cells and primary human CD4 ⁺ T cells	107
6.3.2	Stimulation of primary murine CD4 ⁺ T cells	107
6.3.3	<i>In vitro</i> differentiation of murine CD4 ⁺ T cells.....	109
6.4	Flow cytometry and cell sorting	109
6.4.1	Staining of surface molecules	110
6.4.2	Intracellular cytokine staining.....	110
6.4.3	Sorting of primary murine CD4 ⁺ T cells.....	111
6.5	Molecular biology methods	111

6.5.1	Polymerase chain reaction (PCR)	111
6.5.2	DNA restriction digestion, agarose gel electrophoresis and DNA extraction.....	112
6.5.3	DNA ligation and transformation of <i>Escherichia coli</i>	112
6.5.4	Cultivation of <i>E. coli</i> and plasmid preparation	113
6.5.5	DNA sequencing	113
6.5.6	RNA isolation.....	113
6.5.7	Reverse transcription into cDNA	114
6.5.8	Quantitative real-time PCR (qPCR) and semi-quantitative PCR (semi-qPCR) 114	
6.6	Biochemical and immunological methods	115
6.6.1	Preparation of whole cell lysates.....	115
6.6.2	Co-immunoprecipitation and Strep-Tactin pulldown	116
6.6.3	RNA-binding protein immunoprecipitation.....	116
6.6.4	SDS polyacrylamide gel electrophoresis (SDS-PAGE).....	117
6.6.5	Western Blot (WB).....	118
6.6.6	MALT1 activity detection using MALT1 activity based probes	118
6.6.7	Electrophoretic mobility shift assay (EMSA)	119
6.7	Statistical analysis.....	120
7	Abbreviations.....	121
8	References	131
9	Appendix	150
9.1	Publications	150
9.2	Acknowledgments	151

List of figures

Figure 2.1: CD4 ⁺ T helper cell differentiation.	7
Figure 2.2: Proximal T cell receptor signaling.....	11
Figure 2.3: Molecular structure of CARMA1, BCL10, and MALT1.....	16
Figure 2.4: NF-κB and JNK activation by the CBM complex.....	19
Figure 2.5: MALT1 protease promotes optimal T cell activation.....	23
Figure 2.6: Regulatory sequences and factors in alternative splicing.....	25
Figure 3.1: Domain structure and evolutionary conservation of MALT1 isoforms.	30
Figure 3.2: Generation of Jurkat T cell lines stably expressing MALT1 TRAF6 binding mutants.....	31
Figure 3.3: MALT1 is required for NF-κB and JNK signaling.	32
Figure 3.4: T6BM1 encoded by MALT1A exon7 supports NF-κB and MAPK activation.....	33
Figure 3.5: T6BM1 within MALT1 exon7 is functional and enhances MALT1 scaffolding function.....	35
Figure 3.6: Inclusion of exon7 does not alter MALT1 protease activity.	37
Figure 3.7: Primary CD4 ⁺ T cells lack Malt1A and predominantly express Malt1B.	38
Figure 3.8: TCR stimulation induces exon7 inclusion and thus MALT1A expression in CD4 ⁺ T cells.	40
Figure 3.9: Activated T cell subsets display enhanced MALT1A expression levels.....	41
Figure 3.10: TCR stimulation upregulates MALT1A expression in human CD4 ⁺ T cells.....	42
Figure 3.11: Design of morpholino to prevent MALT1A induction.....	43
Figure 3.12: Morpholino prevents TCR-induced MALT1A induction in CD4 ⁺ T cells.....	44
Figure 3.13: Morpholino does not affect T cell signaling in the absence of MALT1A.....	45
Figure 3.14: TCR-induced MALT1A induction augments T cell signaling.....	46
Figure 3.15: Inhibition of MALT1A induction does not alter MALT1 protease function.	47
Figure 3.16: MALT1A induction is required for optimal CD69 and CD25 upregulation and IL-2 production.	49

Figure 3.17: Optimization of TH1 and TH17 cell differentiation conditions.....	50
Figure 3.18: Alternative MALT1 splicing does not influence T cell effector differentiation.	51
Figure 3.19: The splicing regulator hnRNP U negatively regulates exon7 inclusion and thus MALT1A expression in Jurkat T cells.....	53
Figure 3.20: mRNA stability of MALT1 isoforms is not affected by hnRNP U.....	55
Figure 3.21: hnRNP U binds to <i>MALT1</i> pre-mRNA near exon7.	56
Figure 3.22: <i>Cis</i> -regulatory sequences around exon7 control alternative MALT1 splicing....	57
Figure 3.23: hnRNP U-mediated exon7 skipping is regulated by two regulatory sequences located 100-200 bp upstream and downstream of exon7.	58
Figure 3.24: hnRNP U acts as a negative regulator of MALT1A induction in CD4 ⁺ T cells..	60
Figure 3.25: Knockdown of hnRNP U diminishes activation of CD4 ⁺ T cells.	62
Figure 4.1: Putative model for modulation of T cell activation by alternative MALT1 splicing.....	64
Figure 4.2: Looping out model for hnRNP U-mediated exon7 skipping.....	70
Figure 4.3: Model for the regulation of exon7 inclusion by multiple splicing factors.	81
Figure 6.1: Schematic of stimulation of OT-II CD4 ⁺ T cells with T cell-depleted, OVA-loaded APCs.	108

List of tables

Table 1: List of general vectors.....	92
Table 2: List of additional vectors.....	94
Table 3: Sequences of shRNAs for adenoviral knockdown of hnRNP U.....	95
Table 4: Sequences of individual siRNAs.....	95
Table 5: Sequences of morpholinos.	95
Table 6: EMSA oligonucleotide sequences.	96
Table 7: Murine primer sequences.	97
Table 8: Human primer sequences.	98
Table 9: PCR standard protocol.	111
Table 10: PCR standard program.	112
Table 11: qPCR standard protocol.	114
Table 12: qPCR standard program.	114
Table 13: Semi-qPCR standard protocol.....	115
Table 14: Semi-qPCR standard program.	115
Table 15: Labling of DNA probes.....	119
Table 16: EMSA standard protocol.....	120

1 Summary

T cells are central players of adaptive immune responses. Engagement of the T cell receptor (TCR) by specific antigens together with a CD28 co-stimulus promotes T cell activation, proliferation, and differentiation into T cell effector subsets with distinct functions. TCR/CD28 co-ligation induces activation of the canonical NF- κ B signaling cascade, which requires the assembly of CARMA1, BCL10, and MALT1 into a high-molecular weight complex called the CBM complex. The paracaspase MALT1 acts both as a molecular scaffold and as a protease to mediate T cell activation and effector functions. As part of the CBM complex, MALT1 scaffold recruits the E3 ligase TRAF6 to channel upstream TCR signaling to the canonical IKK/NF- κ B pathway and JNK signaling. TCR ligation also induces MALT1 protease activity, which modulates T cell responses by cleaving several signaling mediators and post-transcriptional regulators. In the present study, two alternative splice variants of MALT1, MALT1A and MALT1B, were identified. The aim was to analyze the impact of both MALT1 isoforms on T cell activation and functions, and to investigate the regulation of alternative MALT1 splicing.

Database research revealed the existence of two isoforms of MALT1, MALT1A and MALT1B, which are highly conserved in mammals. Both isoforms harbor two C-terminal TRAF6 binding motifs (T6BM2/3), but differ in inclusion (MALT1A) or exclusion (MALT1B) of a 33 bp exon7, comprising an additional TRAF6 binding motif (T6BM1). Mutating individual TRAF6 binding sites demonstrated that T6BM1 within exon7 recruits TRAF6 and contributes to the activation of NF- κ B and JNK signaling, revealing that the presence of exon7 enhances MALT1 scaffolding function. In contrast, exon7 inclusion is dispensable for MALT1 paracaspase activity. Furthermore, MALT1 isoform expression levels and functions have been analyzed in primary, murine CD4⁺ T cells. Whereas naive CD4⁺ T cells expressed almost exclusively the shorter splice variant MALT1B, TCR stimulation triggered exon7 inclusion and thus MALT1A expression, which was also observed in T cells with an activated phenotype such as effector T cells and T follicular helper (T_{FH}) cells. TCR-driven MALT1A induction augmented NF- κ B and JNK signaling and expression of T cell activation markers CD69, CD25, and IL-2, revealing that MALT1A upregulation is required for optimal T cell activation. In contrast, T cell differentiation processes are not affected by alternative MALT1 splicing, since both isoforms promoted T_H1 and T_H17 differentiation to the same extent. Screening of critical splicing factors controlling alternative MALT1 splicing

identified hnRNP U as a negative regulator of exon7 inclusion. Downregulation of hnRNP U promoted enhanced TCR-induced MALT1A expression and CD4⁺ T cell activation. hnRNP U associates with *MALT1* pre-mRNA and two sequences of approximately 100 bp 5' and 3' of exon7 were identified as putative hnRNP U binding regions that facilitate exon7 exclusion. The data demonstrate that hnRNP U controls alternative splicing of MALT1 and that TCR-induced splicing of MALT1 enhances relative MALT1A expression, which augments MALT1 scaffolding function to enhance downstream signaling and to promote optimal T cell activation. The findings reveal that the functions of the central T cell signaling mediator MALT1 are controlled by alternative splicing, and that this regulation shapes the outcomes of T cell responses.

1 Zusammenfassung

T Zellen übernehmen eine zentrale Rolle bei der adaptiven Immunantwort. Die Stimulation des T Zell Rezeptors (TCR) durch ein spezifisches Antigen zusammen mit einem CD28 Kostimulus führt zur Aktivierung, Proliferation und schließlich zur Differenzierung von naiven T Zellen in distinkte Effektor T Zellen. Auf molekularer Ebene bewirkt die TCR/CD28 Kostimulation unter anderem eine Aktivierung des kanonischen NF- κ B Signalweges, wofür die Assemblierung des CARMA1/BCL10/MALT1 (CBM) Komplexes von entscheidender Bedeutung ist. Eine zentrale Komponente des CBM Komplexes stellt die Paracaspase MALT1 dar, welche sowohl als Gerüstprotein als auch als Protease fungiert. Die Gerüstfunktion ermöglicht MALT1 die E3 Ligase TRAF6 zu rekrutieren und schließlich TCR-Signale zum kanonischen IKK/NF- κ B und JNK Signalweg zu übermitteln. Auch die Proteasefunktion von MALT1 wird nach TCR Stimulation aktiviert, welche verschiedene Signalmoleküle und posttranskriptionelle Regulatoren spaltet und dadurch T Zellantworten moduliert. In der vorliegenden Arbeit wurden zwei alternative Spleißvarianten von MALT1, MALT1A und MALT1B, identifiziert. Ziel dieser Arbeit war es den Einfluss beider MALT1 Isoformen auf die Aktivierung und Funktion von T Zellen zu analysieren sowie die Regulation des alternativen Spleißprozesses zu untersuchen.

Datenbank-Recherchen offenbarten, dass mit MALT1A und MALT1B zwei MALT1 Isoformen existieren, die in Säugetieren stark konserviert sind. Beide Isoformen besitzen zwei TRAF6 Bindungsmotive im C-Terminus (T6BM2/3), aber unterscheiden sich in der Inklusion (MALT1A) oder Exklusion (MALT1B) eines 33 bp langen Exon7, welches eine zusätzliche TRAF6 Bindungsregion T6BM1 kodiert. Durch Mutation der individuellen TRAF6 Bindungssequenz in Exon7 konnte gezeigt werden, dass T6BM1 in der Lage ist TRAF6 zu binden und zur Aktivierung des NF- κ B und JNK Signalweges beizutragen. Dies lässt darauf schließen, dass die Gerüstfunktion von MALT1 durch die Anwesenheit von Exon7 verstärkt wird. Im Gegensatz dazu bleibt die Proteaseaktivität bei der Einfügung von Exon7 unbeeinflusst. Weiterhin wurde die Expression und die Funktion beider Isoformen in primären, murinen CD4⁺ T Zellen untersucht. Dabei zeigte sich, dass naive CD4⁺ T Zellen fast ausschließlich die kürzere Isoform MALT1B exprimieren, während TCR Stimulation die Inklusion von Exon7 und somit die Expression von MALT1A bewirkte. Dieses Phänomen wurde auch in aktivierten T Zellen wie zum Beispiel in Effektor T Zellen und T_{FH} Zellen beobachtet. Die TCR-vermittelte Induktion von MALT1A verstärkte die Aktivierung von

NF- κ B und JNK sowie die Hochregulation der Aktivierungsmarker CD69, CD25 und IL-2, was darauf schließen lässt, dass eine erhöhte MALT1A Expression zu einer optimalen T Zellaktivierung beiträgt. Da beide Isoformen die Differenzierung in T_H1 und in T_H17 Zellen gleich stark begünstigten, wird deutlich, dass alternatives MALT1 Spleißen für die T Zelldifferenzierung irrelevant ist. Bei der Suche nach möglichen Spleißfaktoren, welche alternatives Spleißen von MALT1 regulieren, konnte hnRNP U als Negativregulator der Exon7 Inklusion identifiziert werden. Eine Herunterregulation von hnRNP U führte zu einer erhöhten MALT1A Expression nach TCR Stimulation und einer verstärkten T Zellaktivierung. hnRNP U bindet an die prä-mRNA von *MALT1* und zwei Sequenzen mit einer Länge von 100 bp in der Nähe von Exon7 wurden als mögliche hnRNP U Bindungsregionen identifiziert. Unsere Daten zeigen, dass hnRNP U alternatives Spleißen von MALT1 reguliert und TCR-induziertes Spleißen von MALT1 zu einer vermehrten Produktion von MALT1A führt, was die Gerüstfunktion von MALT1 verstärkt und somit eine optimale T Zellaktivierung ermöglicht. Es wird deutlich, dass alternatives Spleißen die Funktion eines zentralen Signalschalters im T Zellsignalweg reguliert, welcher die finale T Zellantwort moduliert.

2 Introduction

2.1 T cells in adaptive immune responses

The mammalian immune system protects hosts effectively from foreign antigens, such as microbes, viruses, and toxins, and recognizes and eliminates cancer cells (Chaplin, 2010; Warrington et al., 2011). Two main defense strategies can be delineated: innate immunity and adaptive immunity. Whereas innate immunity provides an immediate, but unspecific (antigen-independent) defense against infections (Gonzalez et al., 2011), adaptive immune responses are highly antigen-specific, but appear later as they require expansion of specific adaptive immune cells (Chaplin, 2010; Murphy et al., 2008). Key features of the adaptive immune system are its ability to distinguish between self and non-self, and to produce immunological memory (Abbas et al., 2014). Innate and adaptive immunity cooperate to combat an infection with high efficiency, and deregulation of both contributes to the development of diseases such as autoimmunity, immunodeficiency, and cancer (Warrington et al., 2011).

2.1.1 The adaptive immune system

The major players of the adaptive immune system are T and B lymphocytes. B lymphocytes arise from bone marrow stem cells and fully mature in secondary lymphoid organs (Murphy et al., 2008). Mature B cells are activated by soluble and cell-bound antigens and differentiate into antibody secreting plasma cells or long lived memory B cells (Abbas et al., 2014; Warrington et al., 2011). Secretion of antibodies can promote neutralization of pathogens or toxins, induction of phagocytosis, or activation of the complement system to protect the host from infection (Abbas et al., 2014; Parkin and Cohen, 2001). Thus, B cells play a crucial role in antibody-mediated immunity, also known as humoral immunity (Warrington et al., 2011). The humoral strategy mainly eliminates extracellular microbes, failing to detect intracellular pathogens. Defense against intracellular pathogens is facilitated by cell-mediated immunity, which relies on circulating T lymphocytes that originate from hematopoietic stem cells in the bone marrow and mature in the thymus to promote destruction of pathogen-infected phagocytes or other infected host cells (Abbas et al., 2014; Germain, 2002; McNeela and Mills, 2001).

In order to recognize distinct antigens, T and B lymphocytes express T cell receptors (TCRs) and B cell receptors (BCRs), respectively (Boehm, 2012). Due to the large array of foreign antigens, a high diversity of antigen-receptors differing in their antigen specificity is generated by somatic recombination of gene segments (Abbas et al., 2014). In contrast to B cells, T lymphocytes only detect foreign antigens that are presented by major histocompatibility complex (MHC) molecules, which are expressed on the surface of antigen presenting cells (APCs), such as dendritic cells, macrophages, B cells, or epithelial cells (Pitcher and van Oers, 2003; Warrington et al., 2011). MHC molecules can be classified as class I or class II molecules based on whether they present peptides derived from intracellular (class I) or extracellular (class II) proteins (Vyas et al., 2008). MHC class I and class II present both self-peptides as well as foreign peptide fragments. Two major subpopulations of T lymphocytes are known, which recognize different types of antigen-MHC complexes: CD4⁺ or T helper (T_H) cells and CD8⁺ or cytotoxic T lymphocytes. Whereas CD8⁺ T cells recognize peptides bound to MHC class I molecules expressed on all nucleated cells, CD4⁺ T cells are restricted to MHC class II-bound antigens located on professional APCs such as dendritic cells, macrophages, and B cells (Vyas et al., 2008; Warrington et al., 2011). Thereby, CD4⁺ and CD8⁺ T cells can distinguish between self-antigens and foreign antigens. CD8⁺ T cells are involved in the destruction of nucleated cells infected with intracellular pathogens like viruses or cytoplasmic bacteria. In contrast, CD4⁺ T cells do not possess any cytotoxic activity, but are able to activate other immune cells including B cells, macrophages, and other leukocytes, to mediate an immune response (Chaplin, 2010). Upon encountering their cognate antigens, CD4⁺ and CD8⁺ T lymphocytes become activated, proliferate and differentiate into effector or memory T cells, which are able to provide immediate or long-term protection, respectively (Abbas et al., 2014; Chang et al., 2014).

2.1.2 T cell activation and differentiation

Mature CD4⁺ and CD8⁺ T cells are released from the thymus into the blood stream and are considered to be naive before they encounter a specific antigen (Abbas et al., 2014; Zhu et al., 2010). They migrate to secondary lymphoid organs such as the spleen and lymph nodes, where they encounter and recognize their cognate antigen. Naive T cells are characterized by high levels of the surface markers CD62L (CD62 ligand or L-selectin) and CCR7 (CC chemokine receptor 7), which facilitate T cell entrance into lymph nodes through high-endothelial venules (HEVs) by detecting adhesion molecules and chemokines (Berard and

Tough, 2002). Upon recognition of a foreign antigen, T cells enlarge and proliferate. They downregulate CD62L and secrete cytokines, like interleukin (IL)-2, that further supports their proliferation and survival (Bachmann and Oxenius, 2007). Activated T cells upregulate the activation markers CD69, CD25 and CD44 on their surface. While the C-type lectin CD69 supports retention of activated T lymphocytes in secondary lymphoid organs (Shiow et al., 2006), upregulation of the IL-2 receptor subunit CD25 further amplifies IL-2-mediated expansion (Malek, 2008). Surface expression of the hyaluronic acid receptor CD44 occurs later and is considered to be critical for the migration of effector T cells to sites of infection (Baaten et al., 2010).

Depending on the cytokine milieu, the antigen dose and the type of APC, CD4⁺ and CD8⁺ T cells differentiate into specific effector cells (Ley, 2014; Luckheeram et al., 2012; Zhu et al., 2010). Regarding CD4⁺ T cell differentiation, several distinct effector subtypes can be distinguished (Figure 2.1).

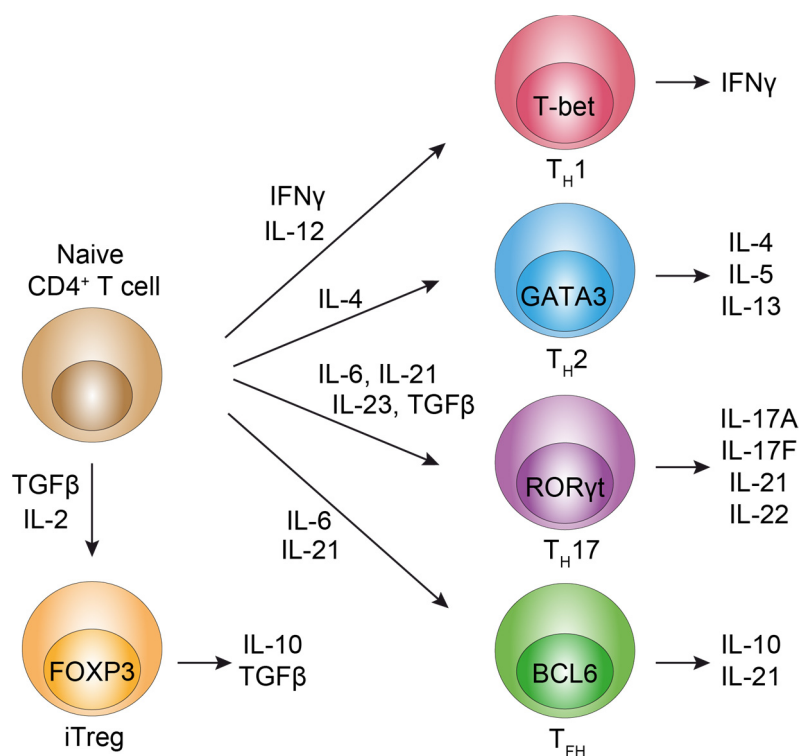


Figure 2.1: CD4⁺ T helper cell differentiation. Depending on the cytokine milieu and other factors, CD4⁺ T cells can differentiate into T_H1, T_H2, T_H17, T_{FH} and iTreg cells. Each subtype secretes a distinct set of cytokines and thus adopts a specific function within the immune system. BCL6 (B cell chronic lymphocytic leukemia/lymphoma 6), FOXP3 (forkhead box p3), GATA3 (GATA binding protein 3), IFN (interferon), IL (interleukin), iTreg (induced regulatory T cell), RORγt (RAR-related orphan receptor gamma t), T-bet (T-box transcription factor), T_{FH} (follicular T helper), TGFβ (transforming growth factor beta), T_H (T helper).

In response to cytokines such as IFN γ (interferon γ) and IL-12, CD4⁺ T cells differentiate into TH1 cells characterized by the expression of the transcription factor T-bet (T-box transcription factor) (Szabo et al., 2000). TH1 cells further secrete IFN γ , which represents a positive feedback loop to reinforce TH1 differentiation and induces the activation of phagocytes to eliminate intracellular pathogens (Luckheeram et al., 2012). To combat extracellular parasites, T cells of the TH2 subtype are generated in response to IL-4 (Swain et al., 1990). TH2 cells express GATA3 (GATA binding protein 3) and produce IL-4, IL-5 and IL-13, which are critical for IgE (immunoglobulin E) production of B cells, eosinophil activation, and mucus secretion (Deo et al., 2010; Ley, 2014). Therefore, TH2 cells play a key role in allergic diseases (Luckheeram et al., 2012). In addition to TH1 and TH2 cells, a third lineage of effector T helper cells has been identified called TH17 cells (Korn et al., 2009; Luckheeram et al., 2012). TH17 cell differentiation relies on the cytokines IL-6, IL-21, IL-23, and TGF β (transforming growth factor beta), as well as the transcription factor ROR γ t (RAR-related orphan receptor gamma t) (Figure 2.1) (Ivanov et al., 2006; Korn et al., 2009). By producing IL-17A, IL-17F, IL-21 and IL-22, TH17 cells induce the release of antimicrobial peptides and the recruitment of neutrophils and thus contribute to the clearance of bacterial and fungal infections (Waite and Skokos, 2012). An additional CD4⁺ T cell subtype are follicular T helper (TFH) cells characterized by the expression of PD-1 (programmed cell death protein-1), ICOS (inducible T cell co-stimulator), and CXCR5 (CXC chemokine receptor type 5) as well as the transcription factor BCL6 (B cell chronic lymphocytic leukemia/lymphoma 6) (Ma et al., 2012). TFH cells develop in response to cytokines like IL-21 and IL-6. In turn, they are able to secrete IL-21 and IL-10 and thus provide help for B cells to differentiate into antibody-producing plasma cells or long-lived memory B cells (Luckheeram et al., 2012; Ma et al., 2012). In order to prevent disproportionate immune responses, CD4⁺ T cells can also differentiate into suppressor T cells, known as induced regulatory T cells (iTregs), which are distinct from thymus derived natural Tregs (nTregs) (Chaplin, 2010). iTreg differentiation requires TGF β and IL-2. Those cells are characterized by the expression of the transcription factor FOXP3 (forkhead box p3) and the secretion of anti-inflammatory cytokines IL-10 and TGF β , which suppress immune activation (Luckheeram et al., 2012). Therefore, Tregs play a major role in the maintenance of immune homeostasis and peripheral self-tolerance (Sakaguchi et al., 2009).

2.2 TCR-induced signaling pathways

2.2.1 T cell receptor and co-receptors

T cell-mediated immune responses require the detection of a foreign antigen by the TCR. The TCR consists of a highly variable α/β heterodimer that recognizes peptide antigens presented by MHC proteins (Murphy et al., 2008). It associates with the CD3 complex, consisting of CD3 γ , CD3 δ and CD3 ϵ protein chains, and a homodimer of ζ chains to form the TCR complex (Figure 2.2). Both, the CD3 complex and the ζ dimer harbor one or more immunoreceptor tyrosine-based activation motifs (ITAMs), which are crucial for coupling TCR ligation to the activation of intracellular signaling pathways (Love and Hayes, 2010; Malissen, 2008). Engagement of a TCR by an antigen-MHC complex initiates phosphorylation of ITAMs creating a binding platform for molecules involved in proximal TCR signaling (Sharpe and Abbas, 2006). Recognition of antigen-MHC complexes is supported by the co-receptors CD4 or CD8, which bind to MHC class II or MHC class I molecules, respectively (Gascoigne, 2008; Vyas et al., 2008). CD4 and CD8 co-receptors also contribute to ITAM phosphorylation by associating with the tyrosine kinase LCK (lymphocyte-specific protein tyrosine kinase) (Schulze-Luehrmann and Ghosh, 2006). However, productive T cell activation requires a second signal, since TCR stimulation alone leads to apoptosis or a state of unresponsiveness, called anergy (Schmitz and Krappmann, 2006). Therefore, T cells express co-stimulatory molecules such as CD28 co-receptors, which specifically recognize the proteins B7.1 (CD80) or B7.2 (CD86) expressed on the surface of APCs (Abbas et al., 2014; Chen and Flies, 2013). Co-receptor-mediated signaling augments weak TCR-induced signals to promote efficient T cell activation and a productive immune response (Schmitz and Krappmann, 2006). Collectively, the additional co-stimulatory signal provides a mechanism to prevent autoreactive and aberrant T cell responses (Chen and Flies, 2013).

2.2.2 Proximal T cell receptor signaling events

Upon stimulation of the TCR together with a co-stimulus, the T cell undergoes extensive cytoskeletal remodeling resulting in the formation of the immunological synapse (IS), which forms at the cell-cell interface between APC and T cell (Alarcon et al., 2011; Smith-Garvin et al., 2009). Proximal signaling molecules and receptors are enriched within the IS and

associate with the TCR. The synapse consists of supramolecular activation clusters (SMACs), which can be divided into the central SMAC (cSMAC), the surrounding peripheral SMAC (pSMAC), and the distal SMAC (dSMAC) (Kumari et al., 2014; Yu et al., 2013). pSMAC and dSMAC mainly contain integrin adhesion molecules, glycoproteins, and protein tyrosine phosphatases and thereby promote synapse formation and stabilization. The cSMAC, however, clusters TCRs together with CD28 co-receptors and other signaling molecules such as PKC θ (protein kinase C θ) enabling sustained TCR signaling (Alarcon et al., 2011; Smith-Garvin et al., 2009). Upon prolonged T cell activation, co-inhibitory molecules are recruited to the IS leading to termination of TCR signaling (Chen and Flies, 2013). Thus, the immunological synapse provides a platform for the recruitment and enrichment of receptors and accessory proteins that induce both signal amplification and termination (Guy and Vignali, 2009; Yu et al., 2013).

The initiation of proximal T cell signaling requires the recruitment of Src family kinases to the TCR (Paul and Schaefer, 2013; Schulze-Luehrmann and Ghosh, 2006). Upon antigen binding, FYN and the CD4/CD8-associated kinase LCK are recruited to the TCR complex and phosphorylate conserved ITAM motifs within the CD3 subunits (Figure 2.2) (Schulze-Luehrmann and Ghosh, 2006; Smith-Garvin et al., 2009). Phosphorylation of ITAMs allows the recruitment and activation of ZAP70 (zeta-chain-associated protein kinase 70 kDa), which is central for the activation of downstream signaling mediators (Paul and Schaefer, 2013; Smith-Garvin et al., 2009). ZAP70 phosphorylates several substrates such as the transmembrane adapter LAT (linker for activation of T cells) and the cytosolic protein SLP76 (Src homology 2 (SH2)-domain containing leukocyte protein of 76 kDa) (Paul and Schaefer, 2013). In turn, both proteins serve as docking sites for the recruitment of effector molecules such as PLC γ 1 (phospholipase C γ 1), the p85 subunit of PI3K (phosphoinositide 3 kinase), the adapters GRB2 (growth factor receptor-bound protein 2) and GADS (GRB2-related adapter downstream of Shc) as well as the GEFs (guanine nucleotide exchange factors) VAV1 and SOS (son of sevenless) (Figure 2.2) (Schulze-Luehrmann and Ghosh, 2006; Smith-Garvin et al., 2009).

The activation of PLC γ 1 results in the hydrolysis of PIP $_2$ (phosphatidyl inositol 4,5-bisphosphate), generating the second messengers inositol 1,4,5-trisphosphate (IP $_3$) and diacylglycerol (DAG) (Paul and Schaefer, 2013). Whereas IP $_3$ triggers activation of the transcription factor NFAT (nuclear factor of activated T cells), membrane-associated DAG together with the GEF SOS promotes activation of the Ras (rat sarcoma)-ERK1/2

(extracellular signal-regulated kinase 1/2) pathway resulting in activation of the transcription factor AP-1 (activator protein-1) (Brownlie and Zamoyska, 2013; Smith-Garvin et al., 2009). Moreover, production of DAG is critical for PKC θ -dependent activation of CARMA1 (caspase-recruitment domain (CARD)-containing MAGUK 1), which in turn recruits BCL10 (B cell chronic lymphocytic leukemia/lymphoma 10) and its constitutive binding partner MALT1 (mucosa associated lymphoid tissue lymphoma translocation protein 1) (Schulze-Luehrmann and Ghosh, 2006; Thome et al., 2010). CARMA1, BCL10 and MALT1 assemble to form the high-molecular weight CBM complex that links TCR ligation to the canonical NF- κ B (nuclear factor kappa B) pathway (see section 2.3). Overall, TCR stimulation triggers the activation of three major transcription factors: NFAT, AP-1 and NF- κ B (Figure 2.2) (Padhan and Varma, 2010).

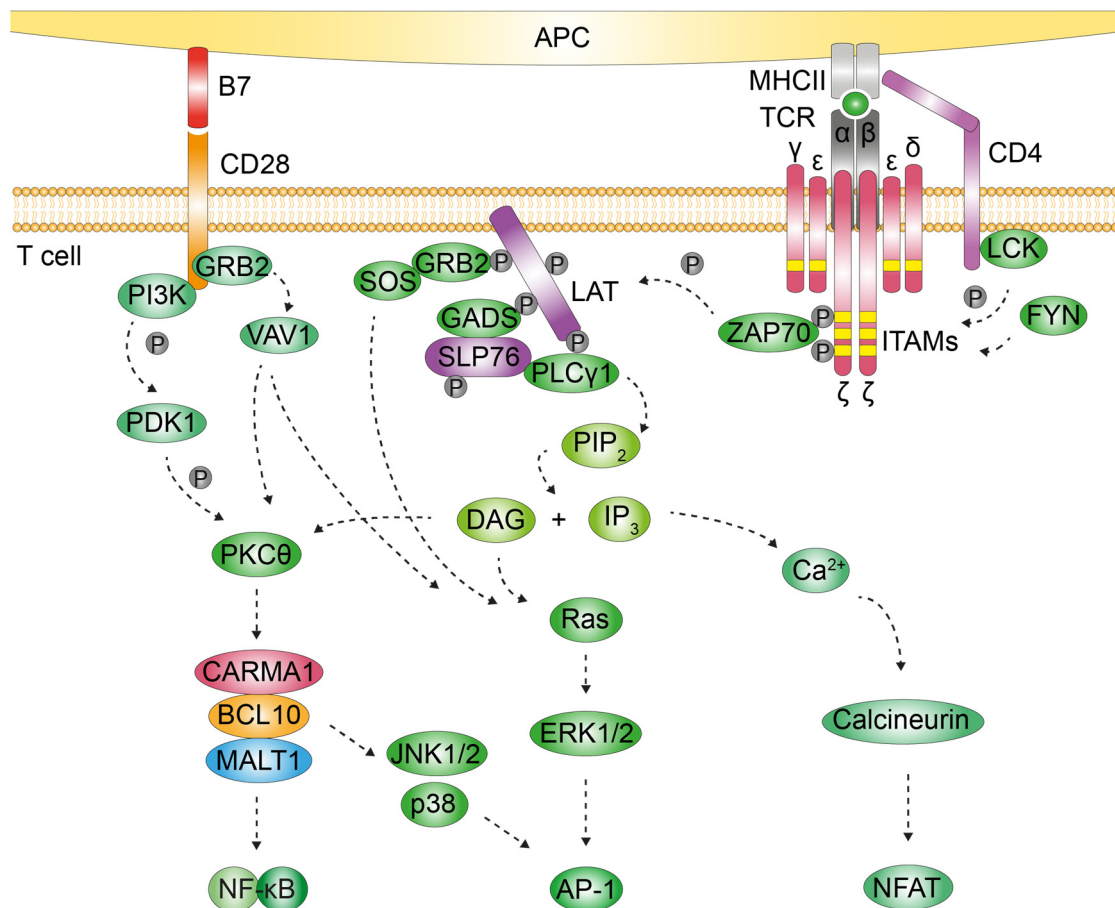


Figure 2.2: Proximal T cell receptor signaling. Antigen presentation by the MHC class II complex triggers activation of CD4⁺ T cells. Upon TCR ligation, the Src family kinases FYN and LCK phosphorylate ITAM motifs (marked in yellow) within the CD3 subunits resulting in the activation of receptor proximal kinases. In turn, the adapter proteins LAT and SLP76 are phosphorylated and recruit several signaling mediators to stimulate activation of the transcription factors NFAT, AP-1 and NF- κ B. Stimulation of the CD28 co-receptor further supports TCR-induced signaling. Abbreviations are explained in the main text.

To induce efficient T cell activation, stimulatory signals from the CD28 co-receptor are necessary. It has been suggested, that CD28 co-engagement supports T cell signaling by triggering activation of two pathways (Figure 2.2) (Schmitz and Krappmann, 2006; Schulze-Luehrmann and Ghosh, 2006). On the one hand, the CD28 co-receptor associates with the p85 regulatory subunit of PI3K. Upon ligand binding, PI3K is activated and converts PIP₂ into PIP₃ (phosphatidyl inositol 3,4,5-trisphosphate) serving as a docking site for several pleckstrin homology (PH) domain-containing proteins, including phosphoinositide-dependent kinase 1 (PDK1), its target protein kinase B (PKB or AKT), and the GEF VAV1 (Schulze-Luehrmann and Ghosh, 2006; Smith-Garvin et al., 2009). Binding of PDK1 to PIP₃ activates PDK1 and induces its binding to PKC θ and CARMA1 at the immunological synapse, thereby prompting PKC θ activation, CBM complex assembly and NF- κ B signaling (see section 2.3) (Park et al., 2009). The second pathway that is induced upon CD28 co-receptor ligation relies on GRB2 and VAV1 (Schulze-Luehrmann and Ghosh, 2006; Thaker et al., 2015). Via GRB2, VAV1 is recruited to the CD28 co-receptor and activated inducing signaling in many directions: VAV1 drives actin cytoskeleton reorganization, supports activation of NF- κ B via PKC θ , and is also involved in NFAT, AP-1 and JNK (c-Jun N-terminal kinases) signaling (Schmitz and Krappmann, 2006; Schulze-Luehrmann and Ghosh, 2006; Thaker et al., 2015). Collectively, CD28 co-receptor signaling augments TCR signals (Park et al., 2009; Schulze-Luehrmann and Ghosh, 2006).

2.2.3 NFAT, ERK and AP-1 activation

Activation of NFAT is regulated by calcium (Ca²⁺) release into the cytosol in response to IP₃ binding to receptors on the endoplasmatic reticulum (Macian, 2005). Increased cytosolic Ca²⁺ levels promote activation of the Ca²⁺-dependent phosphatase calcineurin, which in turn dephosphorylates cytosolic NFAT proteins, enabling their nuclear translocation (Figure 2.2) (Padhan and Varma, 2010). NFAT activation exclusively requires TCR ligation without CD28 co-stimulation. Upon TCR ligation without a co-stimulus, active NFAT proteins promote the expression of anergy-inducing genes. However, in the case of TCR/CD28 co-stimulation, NFAT can interact with other transcription factors such as AP-1 to induce transcription of target genes that play a major role in T cell proliferation and differentiation (Heissmeyer et al., 2004; Macian, 2005).

T cell activation also triggers activation of the MAPK (mitogen activated protein kinase) ERK1/2, which is facilitated by Ras (Figure 2.2) (Kortum et al., 2013; Smith-Garvin et al., 2009). Two GEFs, DAG-dependent RasGRP (Ras guanyl nucleotide-releasing protein) and SOS are required to convert Ras-GDP into Ras-GTP resulting in Ras activation (Kortum et al., 2013; Stone, 2011). In turn, Ras activates the serine-threonine kinase RAF-1, which triggers a protein kinase cascade leading to activation of the MAPKs ERK1/2 (Smith-Garvin et al., 2009). Specifically, the MAPK activation cascade relies on the activation of MAPK kinase kinases (MAP3Ks) such as RAF-1 that stimulates MAPK kinases (MAP2Ks or MKKs), which in turn activate MAPKs. Finally, MAPKs drive activation of the transcription factor AP-1 (Chuang et al., 2000; Smith-Garvin et al., 2009). AP-1 represents a large family of dimeric protein complexes mainly composed of members of the Fos or Jun family (Padhan and Varma, 2010; Shaulian and Karin, 2002). Activation of ERK1/2 causes induction of *c-Fos* mRNA and elevates c-Fos protein levels (Padhan and Varma, 2010). c-Fos binds to pre-existing Jun proteins (mainly c-Jun) in the nucleus to form the transcription factor AP-1. AP-1 regulates a broad range of cellular processes as cell proliferation, death, survival and differentiation (Padhan and Varma, 2010; Shaulian and Karin, 2002; Zhang and Liu, 2002).

2.3 CARMA1, BCL10 and MALT1 facilitate canonical NF- κ B and JNK signaling

Activation of the TCR by antigenic ligands stimulates activation of PKC θ , which initiates formation of a high-molecular weight complex consisting of CARMA1, BCL10, and MALT1 (CBM complex). The CBM signalosome channels upstream TCR/CD28 signaling to canonical NF- κ B signaling and JNK activation (Blonska and Lin, 2009; Wegener and Krappmann, 2007). Mice with a specific deletion in CARMA1, BCL10 or MALT1 fail to activate NF- κ B and to induce a productive immune response, indicating the necessity of these signaling mediators in lymphocyte activation (Thome et al., 2010).

2.3.1 The transcription factor NF- κ B

The transcription factor NF- κ B plays a key role in the immune system, as its activation promotes immune and inflammatory responses, drives cell survival and proliferation, and thus contributes to the development and the maintenance of the immune system (Hayden and Ghosh, 2012; Oeckinghaus and Ghosh, 2009). Due to its broad physiological role, it is not

surprising that deregulation of NF- κ B signaling contributes to the development of severe diseases such as immunodeficiency, autoimmunity, and cancer (Oeckinghaus and Ghosh, 2009).

In mammals, the NF- κ B transcription factor family consists of five members: c-Rel, p65 (RelA), RelB, p50 (NF- κ B1), and p52 (NF- κ B2), which are able to form homo- or heterodimers with distinct transcriptional activity (Gerondakis et al., 2014; Oeckinghaus and Ghosh, 2009). All members contain an N-terminal Rel-homology domain (RHD), which harbors sequence elements enabling dimerization, binding to inhibitory I κ B (inhibitor of NF- κ B) proteins, as well as nuclear translocation and the recognition of DNA elements (Gerondakis et al., 2014; Schulze-Luehrmann and Ghosh, 2006). However, only the Rel proteins p65 (RelA), c-Rel and RelB possess a conserved transactivation domain (TAD) in the C-terminus, allowing them to initiate transcription. In resting cells, NF- κ B is maintained in an inactive state in the cytosol by the binding of cytosolic inhibitory I κ B proteins such as I κ B α , I κ B β , and I κ B ϵ (Gerondakis et al., 2014; Gilmore, 2006; Hayden and Ghosh, 2012). These inhibitory proteins contain multiple ankyrin repeats mediating interaction with the RHD domain of NF- κ B proteins and thereby masking the nuclear localization sequence (NLS) and DNA binding regions (Gerondakis et al., 2014; Oeckinghaus and Ghosh, 2009). NF- κ B activation requires stimulus-induced I κ B degradation allowing NF- κ B nuclear translocation and concomitant target gene expression (Oeckinghaus and Ghosh, 2009). Active NF- κ B promotes re-synthesis of I κ B proteins such as I κ B α representing a negative regulatory feedback mechanism to limit the NF- κ B response (Oeckinghaus and Ghosh, 2009). As I κ B α harbors a nuclear export sequence (NES), newly synthesized I κ B α removes NF- κ B dimers from DNA, masks their NLS and supports their export into the cytosol (Karin, 1999).

In general, the NF- κ B pathway can be divided into the classical or canonical pathway, and the alternative or non-canonical NF- κ B signaling pathway (Hayden and Ghosh, 2012). Canonical signaling depends on p50, p65 (RelA), and c-Rel, whereas the non-canonical pathway promotes nuclear translocation of p52-RelB dimers (Gerondakis et al., 2014). Stimulation of the TCR by antigenic ligands primarily drives canonical NF- κ B signaling, which relies on activation of the I κ B kinase (IKK) complex consisting of the catalytic subunits IKK α (IKK1) and IKK β (IKK2) and the regulatory component NEMO (NF- κ B essential modulator)/IKK γ (Hinz and Scheidereit, 2014).

2.3.2 CBM complex components

TCR-induced IKK activation specifically requires formation of the CBM complex consisting of the molecular scaffold protein CARMA1, the adaptor BCL10, and its constitutive binding partner MALT1 that contains proteolytic activity (Thome et al., 2010).

CARMA1 (also known as CARD11 or Bimp3) was initially identified in a bioinformatic approach as a 130 kDa CARD containing scaffold protein (Bertin et al., 2001; Gaide et al., 2001; McAllister-Lucas et al., 2001). It is one of three members of the CARMA family, including CARMA1, CARMA2 and CARMA3, which share high sequence and structure homology, but differ in their tissue expression pattern. In contrast to CARMA2 and CARMA3, CARMA1 is the only CARMA protein expressed in hematopoietic tissues (Blonska and Lin, 2011). CARMA1 contains several protein-protein interaction domains (Figure 2.3). It encodes an N-terminal CARD domain, which serves as a protein-protein interaction site (Hara and Saito, 2009; Kao et al., 2015). Via heterotypic CARD-CARD interactions, CARMA1 recruits the adapter protein BCL10 upon TCR stimulation (Gaide et al., 2002; Li et al., 2012). The CARD domain is followed by the coiled-coil (CC) domain and the linker region (Thome et al., 2010). The CC domain is critical for signal activation by facilitating CARMA1 oligomerization, but it also stabilizes a closed, inactive conformation of CARMA1 (see below), which is underscored by the finding that various mutations in the CC region promote constitutive NF- κ B signaling (Lamason et al., 2010; Lenz et al., 2008; Tanner et al., 2007). The linker region contains multiple phosphorylation sites, which are necessary for CBM complex formation upon TCR stimulation (Matsumoto et al., 2005; Sommer et al., 2005). In resting cells, the linker acts as a repressor by interacting with CARMA1 CARD-CC keeping CARMA1 in a closed, inactive conformation (McCully and Pomerantz, 2008). Furthermore, CARMA1 contains a C-terminal MAGUK domain, consisting of a PDZ (PSD-95/DLG/ZO1 homology), a SH3 (Src homology 3), and a GUK (guanylate kinase) domain (Funke et al., 2005). The MAGUK mediates membrane association, which is crucial for the recruitment of CARMA1 to the immunological synapse (Hara et al., 2004; Wang et al., 2004). On top of this, intra- or intermolecular interactions of the SH3 and GUK domains facilitate CARMA1 multimerization, required for CBM complex assembly (Hara et al., 2015).

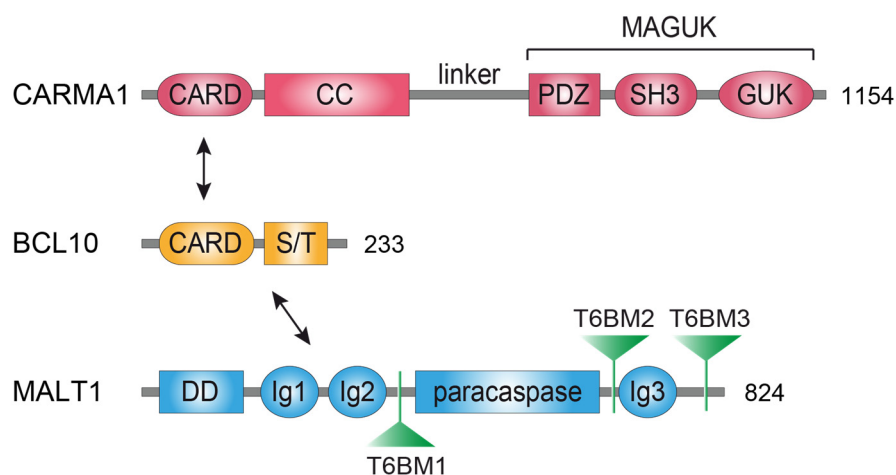


Figure 2.3: Molecular structure of CARMA1, BCL10, and MALT1. The scaffold protein CARMA1 contains an N-terminal CARD domain that mediates recruitment of the adapter protein BCL10 via heterotypic CARD-CARD interactions. In turn, BCL10 is constitutively associated with the N-terminus of the paracaspase MALT1. CARD (caspase-recruitment domain), CC (coiled-coil), PDZ (PSD-95/DLG/ZO1 homology), SH3 (Src homology 3), GUK (guanylate kinase), S/T (Ser/Thr)-rich domain, DD (death domain), Ig (immunoglobulin)-like domains, T6BM1/2/3 (TRAF6 binding motifs 1/2/3).

The adapter protein BCL10 (27 kDa) was originally identified as a recurrent t(1;14)(p22;q32) translocation in MALT lymphoma leading to its overexpression (Willis et al., 1999). It consists of an N-terminal CARD domain, which binds to CARMA1 CARD upon stimulation (Figure 2.3) (Thome et al., 2010). In its monomeric form, BCL10-CARD contains a highly dynamic structure, which tends to form stable filaments especially in the presence of CARMA1 (Bertin et al., 2001; Guet and Vito, 2000). While BCL10 binds to CARMA1 only upon stimulation, it is constitutively associated with MALT1 and this interaction is mediated by the BCL10 CARD and adjacent residues (Langel et al., 2008; Wegener et al., 2006). Moreover, BCL10 harbors an unstructured Ser/Thr-rich region in the C-terminus, which stabilizes BCL10-MALT1 interaction and can be modulated by phosphorylation (Wegener et al., 2006). Collectively, BCL10 serves as a critical bridging factor within the CBM complex.

MALT1 was first identified from the recurrent translocation t(11;18)(q21;q21) in MALT lymphoma that creates the oncogenic fusion protein cIAP2 (cellular inhibitor of apoptosis 2)-MALT1 (also API2-MALT1), consisting of the N-terminal domain of cIAP2 and the C-terminal paracaspase-Ig3 domain of MALT1 (Rosebeck et al., 2016). MALT1 is a 92 kDa protein harboring an N-terminal death domain (DD), three immunoglobulin-like domains (Ig-like domains), and a paracaspase (caspase-like) domain (Figure 2.3). In addition, MALT1 contains three binding motifs for the E3 ligase TRAF6 (tumor-necrosis factor associated receptor-associated factor 6) (T6BM1/2/3) (Noels et al., 2007; Sun et al., 2004). The

interaction between MALT1 and BCL10 relies on the N-terminal DD and the Ig1 and Ig2 domains within MALT1 (Langel et al., 2008; Lucas et al., 2001).

MALT1 is a protease, whose activity is induced upon CBM complex assembly (Coornaert et al., 2008; Rebeaud et al., 2008). In mammals, MALT1 protease shares high sequence homology to caspases (Hulpiau et al., 2015; Uren et al., 2000). MALT1 is a cysteine protease harboring two conserved residues, Cys464 and His415, within the caspase-like domain mediating its catalytic activity (Wiesmann et al., 2012; Yu et al., 2011). However, while caspases exhibit their enzymatic activity by cleaving their substrates after Asp residues, MALT1 is an Arg-specific protease revealing that MALT1 is more closely related to Arg/Lys-specific metacaspases found in plants, fungi and parasites (Hachmann et al., 2012; Uren et al., 2000; Vercammen et al., 2007). The exact mechanism how MALT1 is activated within the CBM complex upon antigen-receptor stimulation is incompletely understood. However, resolution of the paracaspase structure has provided new insights into the functional mechanism of MALT1 activation and, based on this, a two-step activation model has been suggested (Wiesmann et al., 2012; Yu et al., 2011). In its unliganded form, MALT1 protease is in a dimeric but inactive state. The C-terminal Ig3 domain exerts an auto-inhibitory function by folding back to the caspase-like domain, preventing formation of the catalytic machinery and thus the processing of substrates (Wiesmann et al., 2012). Upon substrate binding, the paracaspase-Ig3 domain undergoes conformational changes resulting in the release of Ig3-mediated auto-inhibition of the caspase-like domain (Staal and Beyaert, 2012; Wiesmann et al., 2012; Yu et al., 2011). In contrast to many caspases, MALT1 activation does not require an auto-proteolytic cleavage reaction and is only active in its full-length form (Eitelhuber et al., 2015; Hachmann et al., 2015). Interestingly, monoubiquitination of Lys644 within the Ig3 domain has been reported to induce MALT1 activity upon T cell stimulation, which further underscores the relevance of the Ig3 domain for MALT1 activation (Pelzer et al., 2013).

2.3.3 CBM assembly triggers NF- κ B and JNK signaling

Upon T cell co-stimulation, CARMA1, BCL10 and MALT1 assemble into a high-order filamentous signaling complex (Oeckinghaus et al., 2007; Qiao et al., 2013). Initial CBM complex assembly requires structural rearrangements within CARMA1. In resting cells, CARMA1 adopts a closed, inactive conformation mediated by intra-molecular interactions

between the linker and the CARD-CC domains (Jattani et al., 2016; McCully and Pomerantz, 2008). Following T cell stimulation, CARMA1 is recruited to the immunological synapse and is phosphorylated on Ser552 and Ser645 by PKC θ causing a shift from its closed (auto-inhibitory) to its open (active) conformation (Matsumoto et al., 2005; Sommer et al., 2005). In its open conformation, CARMA1 recruits pre-assembled BCL10-MALT1, which induces the formation of BCL10 filaments and the activation of MALT1 protease (Qiao et al., 2013). The critical role of Ser645 phosphorylation for CBM assembly is underscored by the identification of the phosphatase, PP2A (protein phosphatase 2A) that counteracts CARMA1 phosphorylation, CBM complex formation and NF- κ B activation (Eitelhuber et al., 2011). PKC θ -mediated phosphorylation of CARMA1 is essential for initial CBM assembly, but it is not sufficient to trigger robust downstream signaling. A number of other phosphorylation events on CARMA1 by numerous protein kinases are required for downstream signaling. For example, CARMA1 is also phosphorylated by HPK1 (hematopoietic progenitor kinase1), AKT, and CamKII (calmodulin-dependent protein kinase II) promoting enhanced CARMA1-induced signaling (Brenner et al., 2009; Cheng et al., 2014; Ishiguro et al., 2006).

As well as providing an activating function, phosphorylation of CARMA1 can also promote CBM disassembly and signaling termination (Bidere et al., 2009; Moreno-Garcia et al., 2009). In addition, phosphorylation and ubiquitination of BCL10 dampens CBM activity (Ishiguro et al., 2007; Lobry et al., 2007; Scharschmidt et al., 2004; Wegener et al., 2006; Zeng et al., 2007). For example, IKK β phosphorylates a stretch of Ser residues (134/136/138/141/145) in the C-terminus of BCL10 and thereby disturbs its interaction with MALT1, and impairs NF- κ B signaling and ensuing T cell activation (Wegener et al., 2006). Thus, TCR ligation does not only promote CBM assembly, but also initiates several negative feedback mechanisms to prevent aberrant T cell signaling.

Assembly of the CBM complex serves as a critical step for activation of the IKK complex (Figure 2.4) (Thome et al., 2010). Recruitment of the IKK complex to the CBM signalosome is facilitated by the attachment of K63-linked polyubiquitin chains to BCL10 and MALT1, which are specifically recognized by the polyubiquitin binding motif of NEMO (Oeckinghaus et al., 2007; Wu and Ashwell, 2008). In line with this, removal of MALT1 ubiquitin chains by the deubiquitinase A20 (also known as tumor necrosis factor α -induced protein 3 (TNFAIP3)) counteracts T cell activation (Duwel et al., 2009). Initiation of K63-linked ubiquitination events mainly relies on the scaffolding function of MALT1, as it recruits the E3 ligase TRAF6 through its TRAF6 binding motifs (Oeckinghaus et al., 2007). Subsequently, TRAF6

oligomerizes and becomes activated, which results in the conjugation of K63-linked polyubiquitin chains to MALT1 and NEMO (Oeckinghaus et al., 2007; Shambharkar et al., 2007). In addition, formation of Met1-linked ubiquitin chains on BCL10 by the linear ubiquitin chain assembly complex (LUBAC) may contribute to IKK recruitment and thus canonical NF- κ B signaling (Satpathy et al., 2015). The LUBAC consists of HOIL1 (heme-oxidized IRP2 ubiquitin ligase 1), the catalytic subunit HOIP (HOIL1-interacting protein; also known as RNF31), and SHARPIN (SHANK-associated RH domain interacting protein) (Tokunaga and Iwai, 2012). The association of LUBAC with the CBM complex contributes to canonical NF- κ B signaling (Dubois et al., 2014; Tokunaga and Iwai, 2012).

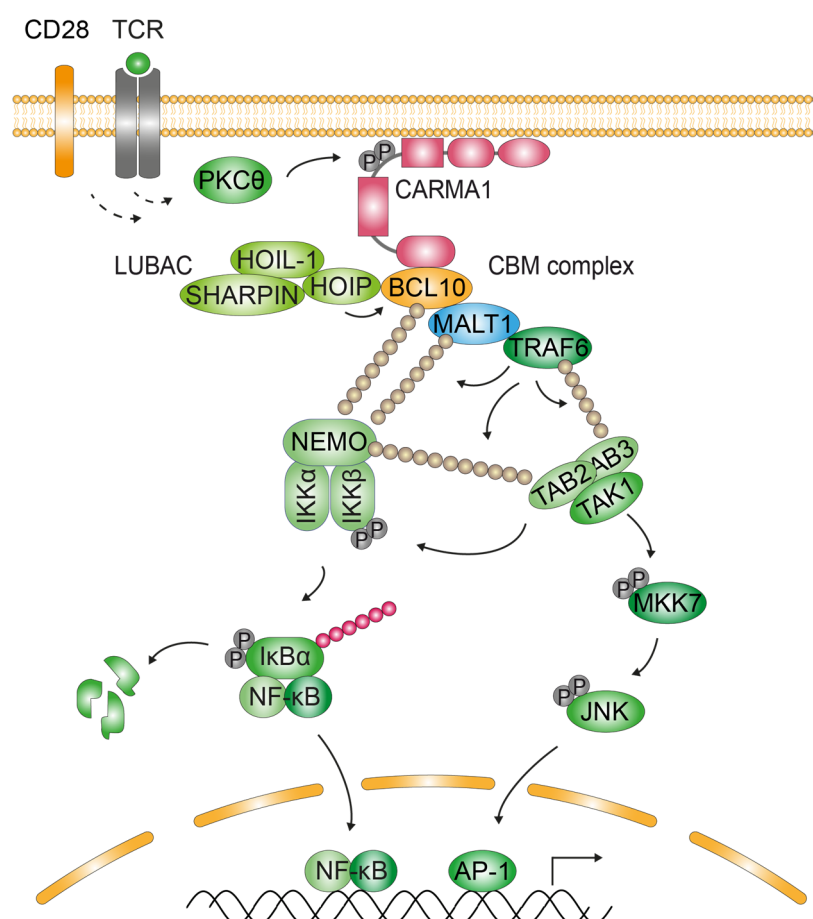


Figure 2.4: NF- κ B and JNK activation by the CBM complex. TCR ligation activates PKC θ , which in turn phosphorylates CARMA1 triggering CBM complex assembly. MALT1 recruits the E3 ligase TRAF6, inducing ubiquitination of MALT1 and NEMO. The linear ubiquitin chain assembly complex (LUBAC) supports NF- κ B signaling by associating with the CBM complex and potentially by conjugating linear ubiquitin chains to BCL10. Finally, overall polyubiquitination recruits the IKK and the TAB2/3-TAK1 complex resulting in IKK β phosphorylation. Active IKK β phosphorylates I κ B α and triggers its ubiquitin-dependent proteasomal degradation, which enables translocation of canonical NF- κ B members into the nucleus to promote target gene expression. TAK1 also activates MKK7 to phosphorylate JNK, which contributes to c-Jun accumulation and thus AP-1 activation. Abbreviations are explained in the main text.

IKK complex activation depends on phosphorylation of two Ser residues (Ser177/181) within IKK β (Hinz and Scheidereit, 2014). IKK β phosphorylation is induced by TAK1 (transforming growth factor β activated kinase-1), which is recruited to ubiquitinated BCL10, MALT1 and NEMO via the ubiquitin-binding domains of its adapters TAB2 and TAB3 (TAK1 binding protein 2/3) (Figure 2.4) (Oeckinghaus et al., 2007; Sun et al., 2004). In turn, the activated IKK complex phosphorylates inhibitory I κ B proteins such as I κ B α on Ser32 and Ser36 (Israel, 2010; Oeckinghaus and Ghosh, 2009). Phosphorylated I κ B α is recognized by β -transducin repeat containing protein (β -TrCP), which serves as a subunit of the SCF (Skp1-Cullin-Roc1/Rbx/Hrt1-F-box) E3 ligase complex. SCF $^{\beta$ -TrCP induces K48-linked ubiquitination of phosphorylated I κ B α leading to its proteasomal degradation and a concomitant release of NF- κ B dimers, most commonly p50:p65 heterodimers, which then translocate into the nucleus to promote target gene expression (Hayden and Ghosh, 2012). Canonical NF- κ B signaling controls inflammatory responses, proliferation and survival and therefore its activity must be transient and properly controlled, for example by the NF- κ B-dependent induction of the negative regulator I κ B α (Shih et al., 2011).

Upon TCR/CD28 stimulation, CBM complex formation also promotes activation of the JNK pathway (Figure 2.4). The JNK family is a subfamily of MAPKs and consists of three proteins (JNK1, JNK2 and JNK3), which are all expressed in two different isoforms (46 kDa and 54 kDa) and activate a number of transcription factors, including AP-1 (Johnson and Lapadat, 2002). Whereas JNK3 expression is restricted to the brain, heart, and testis, JNK1 and JNK2 are ubiquitously expressed and play important roles in T cell activation (Blonska and Lin, 2009). JNKs phosphorylate c-Jun and drive phosphorylation of the AP-1 family member ATF2 (activating transcription factor 2), resulting in c-Jun induction and thus increased AP-1 levels (Padhan and Varma, 2010; Shaulian and Karin, 2002). Activation of JNK depends on phosphorylation by the upstream kinases MKK4/MKK7 (Liu and Lin, 2005; Zarubin and Han, 2005). CARMA1-deficient T cells exhibit defects in JNK signaling and it has been suggested that the CBM complex facilitates the recruitment of kinases mediating JNK phosphorylation and activation (Hara et al., 2003; Jun et al., 2003). Indeed, it has been reported that the IKK activating kinase TAK1 serves as an upstream kinase of JNK. TCR stimulation triggers the recruitment of TAK1 to CARMA1-activated BCL10 oligomers, which are also associated with the MAP2K MKK7 and JNK2 facilitating JNK2 activation and concomitant c-Jun accumulation (Blonska and Lin, 2009; Blonska et al., 2007). In line with this, MALT1 is also required for optimal JNK signaling in T cells (Gewies et al., 2014;

Jaworski et al., 2014). Thus, CARMA1, BCL10 and MALT1 not only activate IKK/NF- κ B signaling, but also mediate crosstalk to the JNK pathway. In addition to JNK activation, CBM complex formation also supports activation of the MAPK p38 (see Figure 2.2), but the underlying mechanisms are not well defined.

2.3.4 MALT1 in T cell activation

MALT1 plays a crucial role in lymphocyte activation. This is evidenced by the fact, that T lymphocytes from MALT1-deficient mice display impaired TCR-induced NF- κ B signaling and concomitant activation, proliferation, and cytokine responses (Ruefli-Brasse et al., 2003; Ruland et al., 2003). This is recapitulated in humans, where patients with a genetic MALT1 defect show abrogated NF- κ B activation and T cell proliferation (Jabara et al., 2013; McKinnon et al., 2014; Punwani et al., 2015). MALT1 also adopts a key role in T cell fate decisions (Brustle et al., 2015; Brustle et al., 2012).

In an attempt to further dissect the functions of MALT1, in particular its scaffolding and paracaspase activities in lymphocytes, mice expressing paracaspase mutant MALT1 (*Malt1^{PM}* mice) have been generated (Bornancin et al., 2015; Gewies et al., 2014; Jaworski et al., 2014; Yu et al., 2015). MALT1 protease inactivation resulted in reduced T cell proliferation and IL-2 secretion, revealing that MALT1 protease supports optimal T cell activation. Moreover, MALT1 knockout mice show severe defects in T_H17 cell differentiation, demonstrating the importance of MALT1 in T cell fate decisions (Brustle et al., 2012). Analysis of MALT1 paracaspase mutant mice revealed that the proteolytic activity of MALT1 is required for the generation of T_H17 cells (Bornancin et al., 2015). Consequently, both MALT1-deficient and MALT1 paracaspase mutant mice were protected from T_H17-driven experimentally induced autoimmune encephalomyelitis (EAE) suggesting that MALT1 paracaspase might serve as a promising target for the treatment of autoimmune diseases (Bornancin et al., 2015; Brustle et al., 2012; Gewies et al., 2014; Jaworski et al., 2014). In addition to the generation of effector T cells such as T_H17 cells, the development of Treg cells also relies on MALT1 and in particular on its paracaspase activity (Bornancin et al., 2015; Brustle et al., 2015; Gewies et al., 2014; Jaworski et al., 2014). MALT1 protease dead mice developed severe autoimmune diseases as the residual lymphocyte activation by MALT1 scaffolding function can no longer be counterbalanced due to a lack of Treg cells. It thus becomes clear that MALT1 plays a dual

role, functioning not only to promote immune activation, but also to regulate immune homeostasis.

With the discovery of MALT1 protease, several MALT1 substrates have been identified (Figure 2.5). MALT1 cleaves its substrates after Arg and the consensus cleavage motif LXP/SR↓G has been suggested (Klein et al., 2015). By cleaving a subset of regulators involved in NF- κ B and JNK signaling, it was initially believed that MALT1 paracaspase promotes optimal T cell activation by modulating TCR-induced signaling pathways. For example, the deubiquitinase A20 negatively regulates NF- κ B activation by removing K63-linked polyubiquitin chains from MALT1 and is cleaved by MALT1 upon TCR ligation (Coornaert et al., 2008; Duwel et al., 2009). Moreover, MALT1-directed cleavage of the non-canonical NF- κ B family member RelB appears to strengthen canonical NF- κ B activation as inactivated RelB can no longer interfere with RelA or c-Rel DNA binding (Hailfinger et al., 2011). MALT1 not only inactivates negative regulators of NF- κ B signaling, but also cleaves positive regulatory factors, such as the LUBAC subunit HOIL-1, upon T cell stimulation (Douanne et al., 2016; Elton et al., 2015; Klein et al., 2015). In addition, MALT1-mediated inactivation of the deubiquitinase CYLD (cylindromatosis) results in enhanced JNK signaling in Jurkat T cells (Staal et al., 2011). However, data from MALT1 paracaspase mutant mice demonstrate that MALT1 protease activity has only limited effects on TCR-driven IKK/NF- κ B activation and is not required for JNK signaling (Gewies et al., 2014; Jaworski et al., 2014). Of note, MALT1 also cleaves itself (auto-cleavage) as well as its constitutive binding partner BCL10 (Baens et al., 2014; Rebeaud et al., 2008). Although it has been demonstrated that BCL10 cleavage supports T cell adhesion to fibronectin, the relevance of both MALT1 auto-cleavage and BCL10 inactivation for lymphocyte activation remains unclear.

The identification of the ribonuclease Regnase-1 (also known as Zcc3h12a and MCPIP1) and the RNA-binding proteins Roquin-1 and Roquin-2 as MALT1 substrates has revealed new insights into the biological function of MALT1 paracaspase (Figure 2.5) (Jeltsch et al., 2014; Uehata et al., 2013). Regnase-1, Roquin-1, and Roquin-2 destabilize numerous pro-inflammatory transcripts to prevent aberrant T cell activation (Leppek et al., 2013; Matsushita et al., 2009; Uehata et al., 2013). Consequently, MALT1-directed cleavage of Regnase-1 and Roquins resulted in stabilization of pro-inflammatory transcripts including *Il2*, *Ikbns*, and *IkB ζ* , which are crucial for the generation of T_H17 cells (Jeltsch et al., 2014; Uehata et al., 2013). Thus, in contrast to MALT1 scaffolding function, MALT1 paracaspase mainly has a

modulatory role: it contributes to optimal T cell activation and differentiation by regulating post-transcriptional gene expression.

Since constitutive MALT1 activity is associated with autoimmune diseases and lymphoma, many efforts have been undertaken to develop specific MALT1 inhibitors. Small molecule inhibitors, such as the phenothiazine-derivatives Mepazine and Thioridazine represent promising candidates for pharmacologic inhibition of MALT1 protease as they reportedly attenuate EAE induction and have shown promising effects in preclinical lymphoma models (Mc Guire et al., 2014; Nagel et al., 2012).

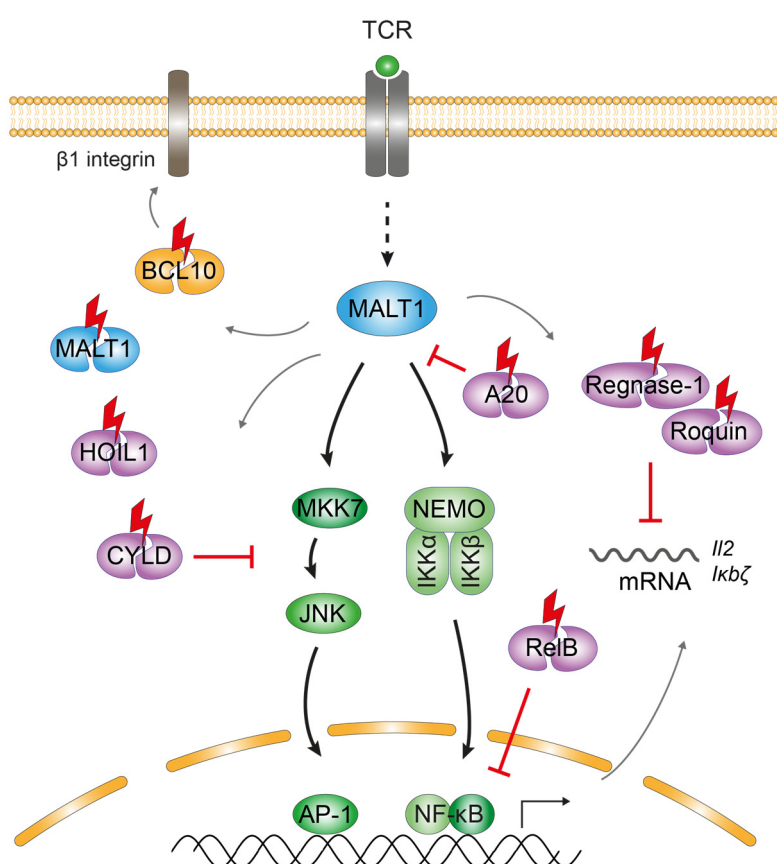


Figure 2.5: MALT1 protease promotes optimal T cell activation. Upon TCR stimulation, MALT1 paracaspase is activated, which cleaves several substrates such as BCL10, MALT1 itself, HOIL1, CYLD, A20, RelB and the RNA regulators Regnase-1 and Roquin. MALT1 paracaspase activity thereby regulates NF-κB and JNK signaling, cell adhesion, as well as mRNA stability. Abbreviations are explained in the main text.

2.4 Alternative splicing

Alternative splicing serves as a crucial mechanism to regulate gene expression as it generates multiple distinct mRNAs from a given gene and thus enriches the coding capacity of the genome (Martinez and Lynch, 2013; Tazi et al., 2009). About 95 % of human multi-exon genes are affected by alternative splicing (Pan et al., 2008; Wang et al., 2008). Several studies have identified changes in alternative splicing during T cell activation that modulate T cell antigen responses (Ip et al., 2007; Martinez et al., 2012; Sandberg et al., 2008; Wu et al., 2008).

2.4.1 General concept of alternative splicing

Pre-mRNA splicing is essential for the expression of genes in eukaryotes. The basic splicing process, performed by a macromolecular ribonucleoprotein complex, the so-called spliceosome, involves the removal of non-coding introns and the concomitant fusion of exons (Black, 2003; Chen and Manley, 2009; Matlin et al., 2005; Wahl et al., 2009). The spliceosome consists of five small nuclear ribonucleoprotein particles (snRNPs), U1, U2, U4, U5, and U6 as well as auxiliary factors like U2AF (U2 auxiliary factor), and recognizes pre-mRNA sequences positioned at the exon-intron boundaries: the 5' splice site (5' SS), the 3' splice site (3' SS), branch point sequences (BPS), and the polypyrimidine tract (PPT) (Figure 2.6) (Wahl et al., 2009). The 5' end of an intron harbors the 5' SS and is defined by the consensus sequence CAG↓GURAGU (where R is A or G), whereas the 3' end is characterized by BPS, PPT and the 3' SS AG↓G (Busch and Hertel, 2012; De Conti et al., 2013). Spliceosome binding to the splice sites is facilitated by base-pair interactions between the snRNA of the snRNPs and the RNA sequences of the splice sites (Martinez and Lynch, 2013; Wahl et al., 2009). Upon recognition of the splicing signals, the spliceosome catalyzes the splicing reaction resulting in exon ligation (De Conti et al., 2013).

Alternative splicing refers to different combinations of exon joining, resulting in the generation of multiple mRNA variants that encode proteins with distinct and sometimes even opposing functions (Busch and Hertel, 2012; Kornblihtt et al., 2013; Lynch, 2004). The most common type of alternative splicing involves alternative inclusion or exclusion of an internal “cassette” exon (Martinez and Lynch, 2013). A further form represents alternative splice site usage (alternative 5' SS or 3' SS), which occurs when two or more splice sites are located near the end of one exon (Keren et al., 2010). More rare subtypes of alternative splicing

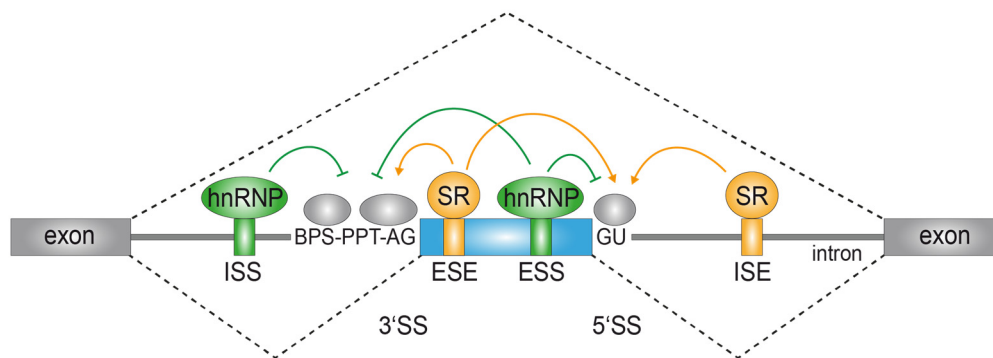


Figure 2.6: Regulatory sequences and factors in alternative splicing. Exons are defined by conserved sequences located at the exon-intron boundaries: the 5' splice site (SS), the 3' SS, branch point sequences (BPS) and the polypyrimidine tract (PPT), which are recognized by components of the spliceosome (depicted in grey). Binding of *trans*-acting factors (SR and hnRNP proteins) to *cis*-regulatory sequences (ESE, ESS, ISE, ISS) within the pre-mRNA either enhances or inhibits splice site recognition and usage. ESE (exonic splicing enhancer), ESS (exonic splicing silencer), ISE (intrinsic splicing enhancer), ISS (intrinsic splicing silencer).

include mutually exclusive exons, intron retention, alternative promoter usage, and alternative polyadenylation (Keren et al., 2010; Martinez and Lynch, 2013; Pohl et al., 2013).

Exon definition, meaning which 5' SS and 3' SS are selected by the spliceosome, depends on the strength of competing splice sites (Douglas and Wood, 2011; Wahl et al., 2009). Splice site strength is defined by how well a sequence matches the consensus sequence. Whereas strong splice sites generally lead to constitutive splicing, weak splice sites are thought to be less efficiently recognized (Kornblihtt et al., 2013; Lim and Burge, 2001; Roca et al., 2005). However, most mammalian splice sites are rather weak and thus cannot account for correct exon recognition. Therefore additional sequence elements are required to enable proper splice site selection (Wahl et al., 2009). Those *cis*-regulatory elements include sequences within exons, such as exonic splicing enhancers (ESEs) and exonic splicing silencers (ESSs), as well as intronic sequences like intronic splicing enhancers (ISEs) and intronic splicing silencers (ISSs) (Figure 2.6) (Martinez and Lynch, 2013). These elements are bound by *trans*-acting factors such as Ser/Arg-rich (SR) proteins and heterogeneous nuclear ribonucleoproteins (hnRNPs), which either positively or negatively regulate exon inclusion (Busch and Hertel, 2012; Kornblihtt et al., 2013). SR proteins usually bind to enhancer elements like ESEs via their RNA recognition motifs (RRMs). Due to their Arg/Ser (RS) domain, SR proteins are able to interact with other splicing factors and to facilitate the recruitment of the splicing machinery to the splice sites, such as U1 snRNP to 5' SS and U2 snRNP to the 3' SS. Thus, SR proteins mainly enhance exon recognition and thus promote exon inclusion (Busch and

Hertel, 2012; Douglas and Wood, 2011). hnRNP proteins also contain a RNA binding domain, in most cases the RRM domain, to recognize certain pre-mRNA sequences. To interact with other protein regulators, most hnRNPs harbor Arg/Gly/Gly repeats (RGG boxes) and glycine-, acidic- or proline-rich domains (Busch and Hertel, 2012). hnRNPs preferentially associate with silencer sequences and thus act as splicing repressors (Chen and Manley, 2009; Wahl et al., 2009). They exert their repressive function for example by preventing recruitment of snRNPs to the splice site (Zhu et al., 2001), by blocking snRNP interactions (Izquierdo et al., 2005; Sharma et al., 2005), or by looping out entire exons (Nasim et al., 2002). However, SR proteins can also function as splicing suppressors and hnRNP proteins can enhance splicing events (Martinez and Lynch, 2013). Of note, most transcripts are bound by multiple SR, hnRNP, and other regulatory proteins, and the selection of an exon for splicing is determined by the balance between the competing factors (Martinez and Lynch, 2013).

Alternative splicing can be modulated in many ways. Epigenetic factors, like chromatin structure and histone modifications, play a key function in regulating alternative splicing (Luco et al., 2011). More recently, it was also revealed that splicing can occur co-transcriptionally (Kornblihtt et al., 2013). Thereby, the pace of RNA polymerase II influences exon inclusion or exclusion (Shukla and Oberdoerffer, 2012). In addition, secondary structures like stem-loop structures in the transcript influence splice site selection (Douglas and Wood, 2011; Jin et al., 2011). Finally, alternative splicing depends on the expression and the activity of *trans*-acting factors, which can be modulated by external stimuli. Signaling pathways can alter subcellular localization, binding preferences to interaction partners, stability, and thus cellular expression levels of splicing factors (Douglas and Wood, 2011; Heyd and Lynch, 2011). In T cells, TCR signaling impacts on the function of numerous splicing factors and thus alters the pattern of alternative splicing.

2.4.2 Alternative splicing in T cell activation

Alternative splicing plays a crucial role for T cell-mediated immune responses, as many genes with known immunological functions undergo alternative splicing during T cell activation (Ip et al., 2007; Martinez et al., 2012). Alternative splicing regulates genes encoding cell surface receptors, cytokines, transcription regulators, RNA-processing molecules, and signaling molecules (Martinez and Lynch, 2013). Although numerous examples have been identified to

date, it remains largely unknown which specific factors regulate the alternative splicing events and how these factors are controlled by signaling.

One well-investigated example of alternative splicing upon T cell activation is splicing of the transmembrane phosphatase CD45 (Hermiston et al., 2003). CD45 is involved in antigen-receptor-mediated signaling and harbors three alternatively spliced exons (4, 5 and 6). The variable exons encode for segment elements that are heavily O-glycosylated in the CD45 surface protein (Zikherman and Weiss, 2008). In resting cells, distinct CD45 isoforms with variable amounts of O-glycosylated segments are expressed. However, T cell activation drives skipping of all three exons and thus promotes an increase in the expression of the shortest isoform, which lacks the O-glycosylated domains (Hermiston et al., 2003; Zikherman and Weiss, 2008). Skipping of the segments allows CD45 homodimerization, which results in a reduction in CD45 phosphatase activity and a concomitant decrease in TCR-induced signaling (Martinez and Lynch, 2013). In resting cells, exclusion of the variable exons 4, 5 and 6 can be facilitated by binding of the splicing factor hnRNP L to an activation responsive motif (ARS), which is part of silencer sequences located in exon 4 and 6 (Rothrock et al., 2003; Rothrock et al., 2005; Tong et al., 2005). However, the massive increase in exon skipping upon T cell stimulation relies on the recruitment of hnRNP LL (Oberdoerffer et al., 2008; Topp et al., 2008; Wu et al., 2008). Moreover, PTB-associated splicing factor (PSF) also contributes to TCR-induced *CD45* exon repression (Heyd and Lynch, 2010). Collectively, multiple splicing factors cooperate to fine tune CD45 function and thus T cell signaling strength.

In addition to CD45, a number of other immune regulators are also alternatively spliced upon T cell activation. For example, TCR-induced splicing of the JNK kinase MKK7 serves a positive feedback loop to increase JNK activity and concomitant T cell activation (Martinez et al., 2015). In addition, the common- γ chain (γ c or CD132), which serves as the critical signaling unit for cytokine receptors like the IL-2 receptor, undergoes alternative splicing in response to T cell activation, which results in the generation of a soluble γ c splice isoform that counteracts cytokine signaling, but enhances T_H17 responses (Hong et al., 2014). In summary, TCR-induced alternative splicing modulates T cell activation and also impacts on T cell fate decisions to facilitate optimal immune responses.

2.5 Aims of the study

Alternative splicing is a critical mechanism to control T cell functions in immune responses. Global analysis has revealed widespread alterations in the splicing pattern of genes with known functions in immune responses. Although alternative splicing of several immune regulators has been reported, little is known about alternative splicing of signaling mediators and its impact on T cell signaling, activation, and differentiation.

MALT1 paracaspase is a central regulator in adaptive immune responses and thus plays a key role in T cell activation. It acts as a scaffolding protein to activate canonical NF- κ B signaling, but also contains proteolytic activity, which modulates T cell responses (Thome et al., 2010). Database analysis identified two alternative isoforms of MALT1, MALT1A and MALT1B, which only differ in inclusion or exclusion of exon7 that encodes for 11 amino acids (aa). However, neither the expression nor the functions of both MALT1 isoforms have been investigated so far. Moreover, nothing is known about the regulatory mechanisms controlling alternative exon7 splicing.

The main aim of this study was to investigate the role of MALT1A and MALT1B in T cell responses and how the process of alternative MALT1 splicing is regulated. Initially, the expression levels of the two MALT1 isoform in T lymphocytes were determined. Furthermore, it was dissected whether exon7 inclusion modulates MALT1 scaffolding function and MALT1 paracaspase activity and thereby affects the activation of T cell signaling pathways. It was of high interest to elucidate the role of alternative MALT1 splicing in T cell activation and whether both isoforms differentially control T cell fate decisions. A further aim was to identify putative MALT1 splicing factors in a screening approach and to verify potential candidates in cellular assays. The study aimed to gain more insight into the mechanism of how splicing factors control alternative exon7 inclusion, and whether those regulators might modulate MALT1 isoform-mediated T cell responses.

3 Results

3.1 Functional analysis of MALT1 isoforms

As part of the CBM complex, MALT1 bridges upstream TCR signaling to canonical IKK/NF- κ B signaling (Thome et al., 2010). MALT1 acts as a scaffolding protein and recruits the E3 ligase TRAF6, which conjugates K63-linked ubiquitin chains to the C-terminus of MALT1 (Oeckinghaus et al., 2007). These ubiquitin chains serve as a docking site for the recruitment of NEMO and thus for the activation of the IKK complex (Oeckinghaus et al., 2007). Besides its scaffolding function, MALT1 also contains proteolytic activity that is induced upon TCR stimulation and modulates T cell activation and effector functions (Jaworski and Thome, 2015).

3.1.1 Evolutionary conservation of MALT1 isoforms

Two alternative splice variants of MALT1 have been identified by analyzing mammalian transcriptome databases: MALT1A (824 aa) and MALT1B (813 aa) (Griesbach, 2012). Both isoforms harbor a death domain (DD) and two Ig-domains (Ig1 and Ig2) in the N-terminus as well as a paracaspase domain, a third Ig domain (Ig3), and two C-terminal TRAF6 binding motifs (T6BM2/3) (Figure 3.1). However, MALT1A and MALT1B differ in a short region of 11 amino acids (aa 309-319), which is encoded by a 33 bp long exon7 located between the Ig2 and the paracaspase domain in human MALT1.

Whereas exon7 inclusion leads to the expression of MALT1A (824 aa), its exclusion promotes expression of MALT1B (813 aa). Interestingly, exon7 encodes a third TRAF6 binding motif (T6BM1), which was previously identified in the API2-MALT1 fusion oncoprotein comprising the N-terminus of API2 fused to the C-terminus of MALT1, and can induce constitutive NF- κ B signaling in MALT lymphomas (Noels et al., 2007; Rosebeck et al., 2016). The exon7 amino acid sequence, the exon/intron boundaries, the T6BM1, and the expression of the two MALT1 isoforms are highly conserved among humans, chimpanzees, mice, and rats. This evolutionary and structural conservation in mammals implies a functional relevance of maintaining the expression of both MALT1A and MALT1B.



Figure 3.1: Domain structure and evolutionary conservation of MALT1 isoforms. MALT1A (824 aa) and MALT1B (813 aa) harbor two C-terminal TRAF6 binding motifs 2 and 3 (T6BM2/3), but only MALT1A contains an additional T6BM1 encoded by exon7. The exon7 sequence is highly conserved in mammals (shown below). T6BMs are highlighted in blue or orange and other protein domains are illustrated by grey boxes. DD (death domain), Ig (immunoglobulin)-like domains.

3.1.2 Design of MALT1 mutants to analyze individual TRAF6 binding sites

MALT1 harbors two functional C-terminal TRAF6 binding sites (T6BM2 and 3) (Sun et al., 2004). A previous study from our group revealed that upon TCR stimulation, the E3 ligase TRAF6 binds to the C-terminal T6BMs and conjugates K63-linked ubiquitin chains to MALT1 (Oeckinghaus et al., 2007). The additional, highly conserved TRAF6 binding motif (T6BM1) within MALT1A was shown to be functional upon overexpression of MALT1 together with BCL10 in HEK293 cells, but its role in T cell signaling remains unknown (Noels et al., 2007). Therefore, the aim was to investigate the contribution of the individual T6BMs, in particular T6BM1, for the activation of downstream T cell signaling pathways.

First, several MALT1A and MALT1B constructs, mutated in one or more TRAF6 binding sites, were generated (Figure 3.2a). Specifically, the critical glutamates (E) within the T6BMs were mutated to alanine (A) (Sun et al., 2004). All constructs were fused to a C-terminal Flag-Strep-Strep-tag (StrepTagII) for efficient precipitation, and cloned into a lentiviral transfer vector as lentiviruses integrate into the target cell genome and allow stable MALT1 expression (see section 6.2.3). To eliminate interference of endogenous MALT1, we used MALT1-deficient Jurkat T cells (*MALT1*^{-/-}), that had been generated by CRISPR/Cas9 in our laboratory (established by T. Gehring, AG Krappmann). After lentiviral transduction, infection efficiency of MALT1-deficient T cells was assessed by co-expression of the cell surface marker human (h) Δ CD2 and was > 90 % in each case (Figure 3.2b). Although h Δ CD2

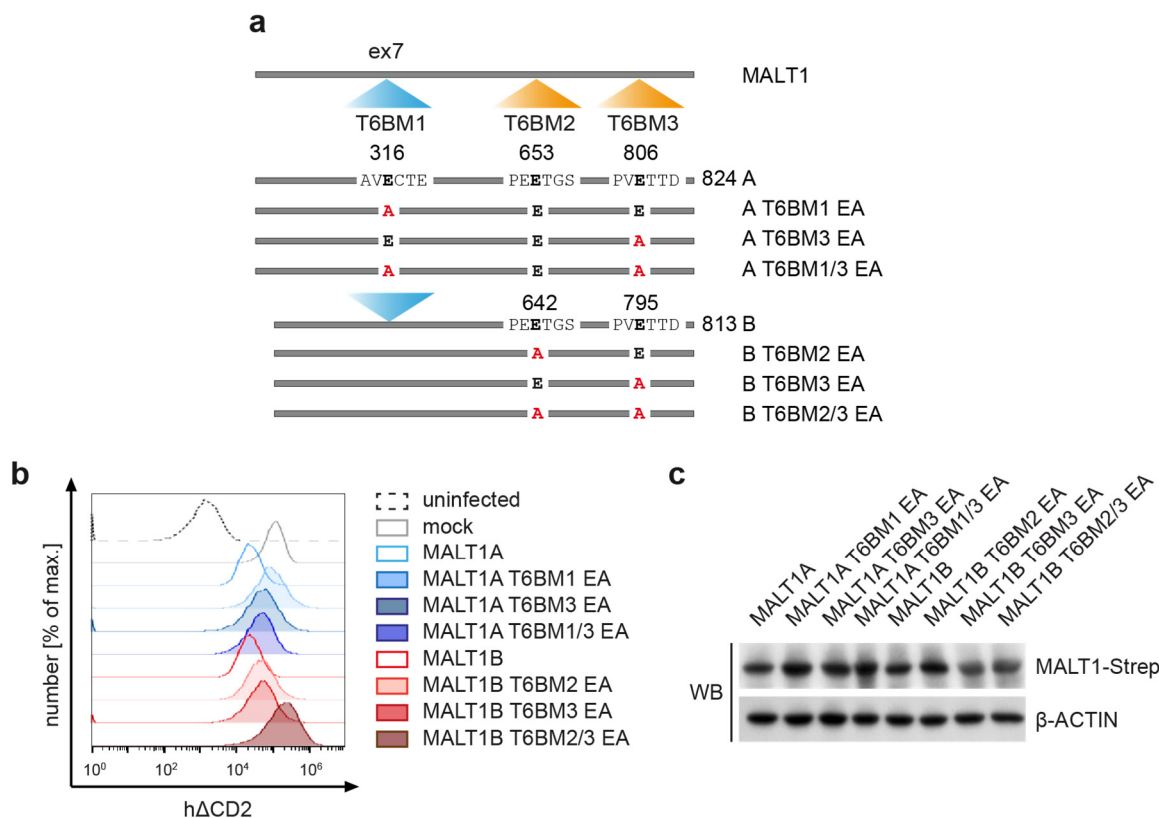


Figure 3.2: Generation of Jurkat T cell lines stably expressing MALT1 TRAF6 binding mutants. (a) Design and generation of MALT1 TRAF6 binding mutants. Different TRAF6 binding mutants were generated, containing glutamate (E) to alanine (A) point mutations within the T6BMs of MALT1A and MALT1B. (b,c) Stable expression of different MALT1 constructs in MALT1-deficient Jurkat T cells. MALT1-deficient Jurkat T cells generated by CRISPR/Cas9 were transduced with StrepTagII (mock) or MALT1-StrepTagII variants. (b) Infection efficiency was assessed by co-expression of the cell surface marker human (h) Δ CD2 using flow cytometry. Uninfected MALT1-deficient cells were used as a negative control. (c) Protein expression of MALT1-StrepTagII constructs was analyzed by Western Blot using a MALT1-specific antibody. β -ACTIN served as loading control. (MALT1-deficient Jurkat T cells were generated by T. Gehring, AG Krappmann).

surface expression varied slightly between different constructs, Western Blot (WB) analysis revealed similar protein expression levels (Figure 3.2c).

Initially, the potential of Jurkat wildtype (WT) and mock infected MALT1-deficient T cells to activate NF- κ B and MAPK signaling was compared. Thereby, cells were stimulated with P/I (Phorbol 12-myristate 13-acetate (PMA)/Ionomycin), which bypasses TCR signaling as PMA directly stimulates PKC θ and Ionomycin triggers the influx of Ca²⁺. Consequently, I κ B α is phosphorylated and concomitantly degraded by the proteasome, promoting NF- κ B activation. As expected, MALT1-deficient T cells reconstituted with the vector alone (mock) were unable to activate NF- κ B signaling (Figure 3.3). This was due to the lack of I κ B α phosphorylation and subsequent degradation, preventing release and nuclear translocation of NF- κ B. In addition, JNK and p38 phosphorylation were reduced in MALT1-deficient T cells,

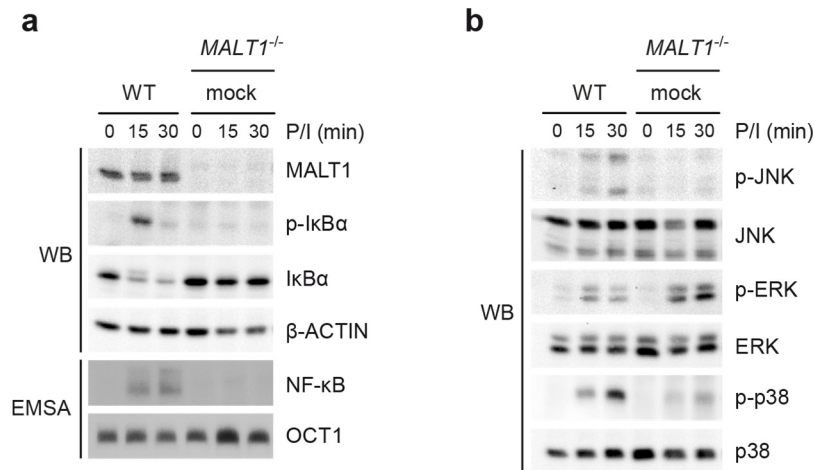


Figure 3.3: MALT1 is required for NF-κB and JNK signaling. (a,b) Jurkat WT cells and mock reconstituted MALT1-deficient Jurkat T cells (*MALT1*^{-/-}) were stimulated with P/I for the indicated time points. (a) MALT1 expression, IκBα phosphorylation and degradation were analyzed by Western Blot using the indicated antibodies. NF-κB DNA binding was analyzed by EMSA. β-ACTIN and OCT1 served as loading controls for Western Blot and EMSA, respectively. (b) MAPK signaling was investigated using the indicated phospho-specific and total protein antibodies.

whereas ERK signaling was not affected (Figure 3.3). These results are in line with observations from *Malt1* knockout mice (Ruland et al., 2003) and demonstrate that MALT1 is required for TCR-induced NF-κB and JNK signaling, but is dispensable for ERK signaling.

3.1.3 T6BM1 encoded by MALT1 exon7 contributes to the activation of T cell signaling pathways

To assess the necessity of the TRAF6 binding site within exon7 for downstream signaling, the signaling potential of MALT1A or B to that of their respective mutants was compared (Figure 3.4). Upon reconstitution of MALT1-deficient Jurkat T cells with MALT1A WT, NF-κB and MAPK activation were markedly induced (Figure 3.4a,b). According to NF-κB signaling, NF-κB DNA binding was strongest after 30 min P/I stimulation, which correlated with robust IκBα degradation (Figure 3.4a). After 60 min, NF-κB activity decreased slightly due to the re-synthesis of IκBα, which again inhibits nuclear translocation of NF-κB. Mutation of either T6BM1 in exon7 (T6BM1 EA) or T6BM3 in the C-terminus (T6BM3 EA) had no effect on IκBα phosphorylation, degradation, and NF-κB DNA binding compared to MALT1A WT (Figure 3.4a). Only the combined mutation of T6BM1 and T6BM3 (T6BM1/3 EA) abolished NF-κB signaling. Activation of JNK and p38 followed the same pattern: whereas single mutation of T6BM1 and T6BM3 did not alter JNK and p38 phosphorylation, the combined mutation of both sites impaired activation of JNK and p38 (Figure 3.4b). ERK signaling was

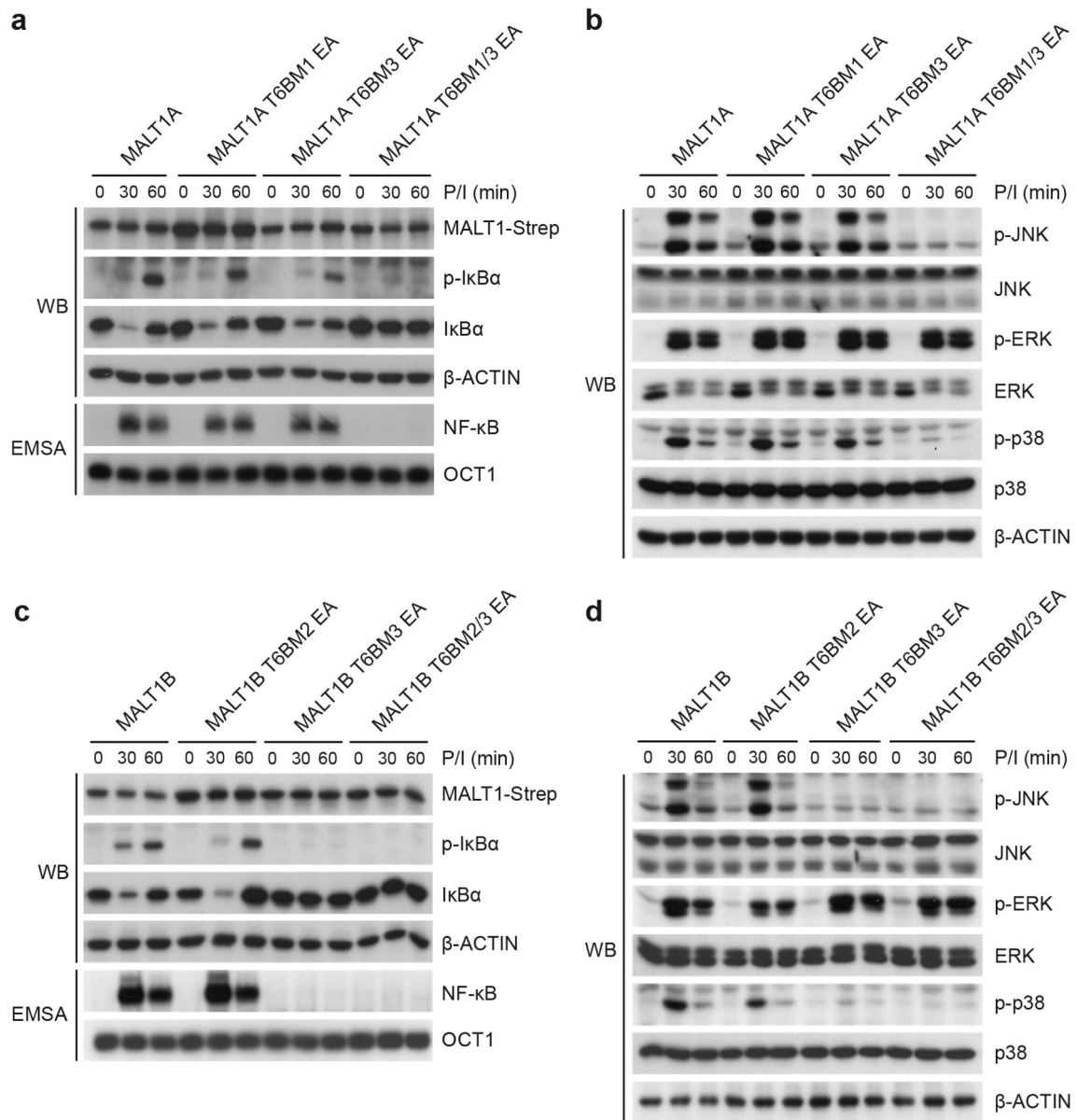


Figure 3.4: T6BM1 encoded by MALT1A exon7 supports NF- κ B and MAPK activation. (a-d) MALT1-deficient Jurkat T cells were reconstituted with Strep-tagged MALT1A, MALT1B, or TRAF6 binding mutants. Reconstituted cells were stimulated with P/I for the indicated time points. (a,c) MALT1 expression, I κ B α phosphorylation and degradation were analyzed by Western Blot using the indicated antibodies. NF- κ B DNA binding was assessed by EMSA. β -ACTIN and OCT1 were used as loading controls for Western Blot and EMSA, respectively. (b,d) MAPK signaling was investigated by Western Blot using phospho-specific and total protein antibodies as indicated. β -ACTIN served as loading control.

not altered by mutation of the TRAF6 binding sites within MALT1A. In addition, the effect of MALT1B TRAF6 binding site mutations on NF- κ B and MAPK signaling was determined (Figure 3.4c,d).

Again, MALT1B WT promoted robust activation of NF- κ B and MAPK. Mutation of T6BM2, located next to the Ig3 domain of MALT1B, did not alter NF- κ B and MAPK signaling,

whereas disruption of the most C-terminal TRAF6 binding site (T6BM3) completely impaired NF- κ B and JNK activation and decreased p38 phosphorylation (Figure 3.4c,d). Of note, mutation of TRAF6 binding sites 2 or 3 did not change ERK activity. The data reveal that T6BM3 in MALT1B and T6BM1/T6BM3 in MALT1A contribute to the activation of downstream signaling pathways, whereas T6BM2 located within the Ig3 domain is dispensable for signaling. Similar results were observed upon reconstitution of primary, murine CD4⁺ T cells with different MALT1 constructs (Griesbach, 2012).

3.1.4 MALT1 exon7 supports TRAF6 and NEMO recruitment to reinforce MALT1 scaffolding function

As demonstrated in the previous section (section 3.1.3), mutation of individual T6BMs within MALT1 affects the activation of downstream T cell signaling pathways. To analyze whether the observed effects are due to alterations in TRAF6 recruitment and CBM complex formation, we performed a Strep-Tactin pulldown (StrepT-PD) of C-terminal Strep-tagged MALT1 constructs after 30 min P/I stimulation and assessed CARMA1, BCL10, and TRAF6 binding in the pulldown fractions (Figure 3.5a). Constitutive association of MALT1 with BCL10 was not affected by mutations of T6BMs or by deletion of exon7 in MALT1B, and stimulation-induced recruitment of CARMA1 was similar among the MALT1 constructs. However, exon7 deletion in MALT1B, as well as the single mutation of T6BM1 or T6BM3 in MALT1A, clearly reduced the association between TRAF6 and MALT1. Consistent with the data from the signaling experiments (see Figure 3.4), mutation of T6BM3 in MALT1B or the combined mutations of T6BM1/T6BM3 in MALT1A completely impaired recruitment of TRAF6 (Figure 3.5a). This clearly demonstrates that in MALT1A, both the exon7-encoded T6BM1 and the most C-terminally located T6BM3 are functional, but redundant for TRAF6 binding.

The E3 ligase TRAF6 mediates MALT1 ubiquitination, which is required for recruitment and activation of the IKK complex (Oeckinghaus et al., 2007). To check whether changes in TRAF6 recruitment affect MALT1 modifications and IKK complex recruitment, pulldown fractions were stained with a MALT1-specific antibody (B12) that also detects MALT1 ubiquitin modifications. Polyubiquitination of MALT1 results in a high molecular weight smear, which appears above the main band of MALT1 (indicated by *). As expected, exon7-lacking MALT1B displayed reduced ubiquitination (indicated by *) compared to MALT1A

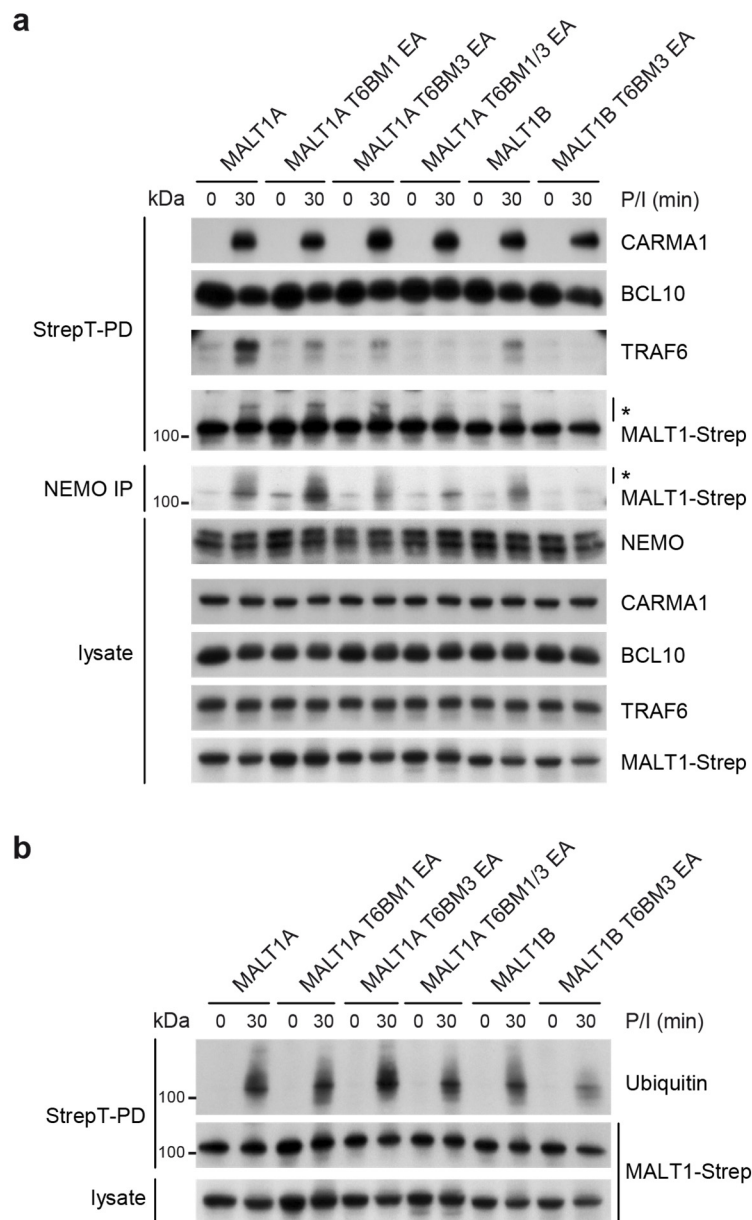


Figure 3.5: T6BM1 within MALT1 exon7 is functional and enhances MALT1 scaffolding function. (a) TRAF6 binds to T6BM1 encoded by MALT1 exon7 and contributes to NEMO recruitment. CBM complex formation and TRAF6 recruitment of MALT1 reconstituted cells were investigated by StrepT-PD after 30 min P/I stimulation. NEMO recruitment to MALT1 was monitored after NEMO IP. Precipitates and cell lysates were analyzed by Western Blot using the indicated antibodies. Modification of MALT1 by ubiquitination is marked by an asterisk (*). (b) MALT1 exon7 contributes to MALT1 ubiquitination. Reconstituted cells were stimulated with P/I for 30 min prior MALT1 protein precipitation by StrepT-PD. Pulldown and lysate samples were analyzed by Western Blot with the depicted antibodies. MALT1 ubiquitination was monitored by staining the precipitates with an ubiquitin-specific antibody.

(Figure 3.5a). In addition, the MALT1 ubiquitin smear was severely reduced in the absence of any functional TRAF6 binding site leading to a decreased association with the IKK subunit NEMO, which was monitored upon immunoprecipitation (IP) of NEMO (Figure 3.5a). In summary, both T6BM1 and T6BM3 within MALT1 are required for optimal TRAF6-

mediated MALT1 ubiquitination and subsequent IKK complex association, and therefore lead to an elevated scaffolding activity of MALT1A compared to MALT1B.

To date, TRAF6 is the only identified E3 ligase facilitating MALT1 ubiquitination in T cells (Oeckinghaus et al., 2007). To address, whether mutation of the TRAF6 binding sites impairs overall MALT1 ubiquitination, precipitated MALT1 was stained with an ubiquitin-specific antibody (Figure 3.5b). MALT1 ubiquitination was slightly reduced upon single mutation of T6BM1 in MALT1A and exon7 deletion in MALT1B, but was not further decreased by the combined mutation of T6BM1/3 in MALT1A, or the single mutation of T6BM3 in MALT1B. This suggests that additional E3 ligases than TRAF6 can promote MALT1 ubiquitination. However, although MALT1A T6BM1/3 EA and MALT1B T6BM3 EA maintain some residual ubiquitin chains, this is insufficient to activate downstream signaling. Collectively, the mutagenesis analysis reveals that both T6BM1 and T6BM3 boost TRAF6 recruitment, which supports activation of downstream T cell signaling pathways.

3.1.5 MALT1 isoforms do not differ in their protease function

MALT1 does not solely function as a scaffolding protein, but also possesses a proteolytic activity that is induced upon TCR stimulation (Coornaert et al., 2008; Rebeaud et al., 2008). Activated MALT1 protease cleaves several substrates involved in signaling and post-transcriptional gene regulation to facilitate robust T cell responses, including BCL10, A20, HOIL1, CYLD, RelB, Regnase-1 and Roquin (Coornaert et al., 2008; Elton et al., 2015; Hailfinger et al., 2011; Jeltsch et al., 2014; Klein et al., 2015; Rebeaud et al., 2008; Staal et al., 2011; Uehata et al., 2013). To assess whether exon7 inclusion affects MALT1 protease function, proteolytic MALT1 activity was measured using a MALT1 activity based probe (ABP) (Figure 3.6a) (Eitelhuber et al., 2015). ABPs have the ability to distinguish between active and inactive enzymes. The MALT1 ABP contains the BCL10-derived cleavage sequence LRSR as recognition motif and harbors a reactive electrophile AOMK (acyloxymethyl ketone), which covalently binds to MALT1. ABP-labeling with the fluorophore BODIPY (boron-dipyrrromethene) enables detection of active MALT1-ABP complexes in a fluorescence scan (Eitelhuber et al., 2015). To analyze MALT1 activity, StrepT-PDs of mock, MALT1A and MALT1B expressing cells were performed and the precipitates were labeled with fluorescently-labeled ABP (Figure 3.6b). Upon P/I stimulation

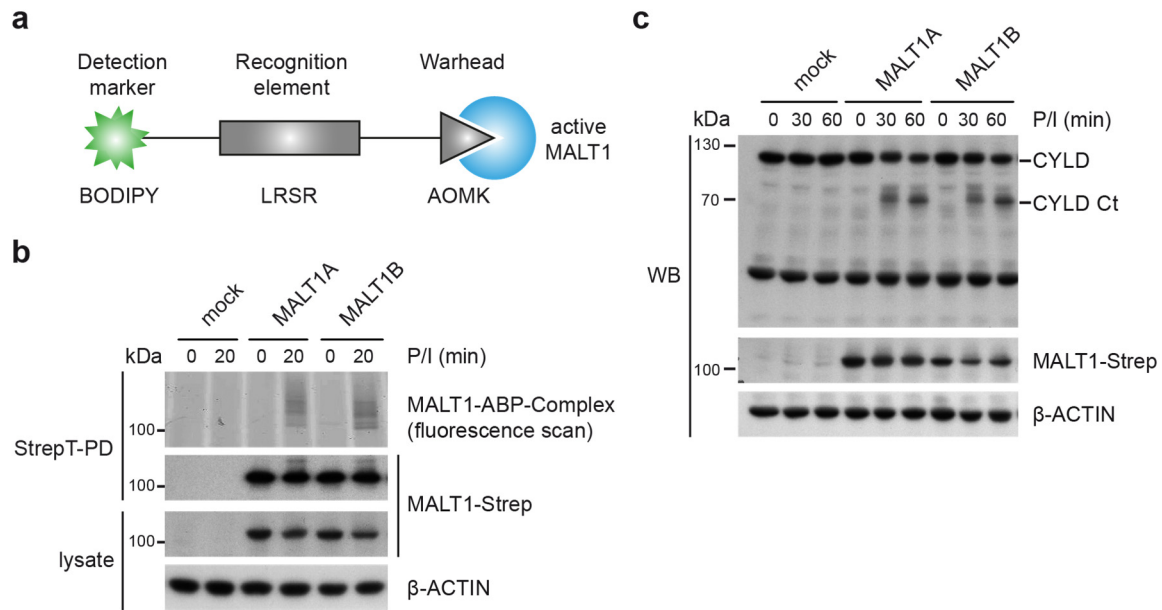


Figure 3.6: Inclusion of exon7 does not alter MALT1 protease activity. (a) An activity-based probe (ABP) containing the BCL10-derived cleavage sequence LRSR was used to specifically measure proteolytic MALT1 activity. Binding to MALT1 is facilitated by AOMK and active MALT1-ABP complexes are detectable by the fluorophore BODIPY. (b) MALT1 isoforms display similar proteolytic MALT1 activity. Mock, MALT1A or MALT1B expressing Jurkat T cells were stimulated for 20 min with P/I prior to StrepT-PD. Precipitates were incubated with BODIPY-labeled ABP before loading onto a 9 % SDS gel and active MALT1-ABP complexes were visualized by a fluorescence scan. Pull-down samples and cell lysates were analyzed by Western Blot, where β -ACTIN served as loading control. (c) CYLD cleavage is comparable in MALT1A and MALT1B expressing cells. Reconstituted Jurkat T cells were stimulated with P/I for the indicated time points. Lysates were analyzed for CYLD cleavage by Western Blot using the indicated antibodies. The applied CYLD antibody detects full-length and the C-terminal CYLD cleavage fragment appearing at ~ 70 kDa (CYLD Ct).

MALT1 activity was induced, but did not differ between MALT1A and MALT1B expressing cells (Figure 3.6). In accordance with previous experiments, active MALT1 was heavily polyubiquitinated after stimulation indicated by the high molecular weight smear above 100 kDa. To confirm the observed results, MALT1 activity was further monitored by analyzing MALT1 substrate cleavage. Upon TCR stimulation, MALT1 cleaves the deubiquitinase CYLD (~ 110 kDa) generating an N-terminal (40 kDa) and a C-terminal (CYLD Ct, 70 kDa) fragment, whereby the latter can be detected using a CYLD-specific antibody raised against the C-terminus (Staal et al., 2011). CYLD cleavage was induced upon P/I stimulation of transduced Jurkat T cells and was similar in both MALT1A and MALT1B expressing cells (Figure 3.6c). As expected, mock transduced cells were unable to cleave CYLD due to the lack of endogenous MALT1. Collectively, the data reveal that alternative splicing of MALT1 does not affect MALT1 protease activity and subsequent substrate cleavage.

3.2 Role of MALT1 isoforms in T cell activation and differentiation

3.2.1 T cell receptor signaling induces MALT1A expression in primary CD4⁺ T cells

Inclusion of exon7 in MALT1 contributes to the activation of downstream signaling pathways in transduced Jurkat T cells. As exon7 is highly conserved in mammals, it was investigated whether alternative MALT1 splicing is also relevant for signaling and activation in primary mouse T cells. We first designed primer pairs that selectively amplify *Malt1A* (ex5-ex7/8) or *Malt1B* (ex5-ex6/8) (Figure 3.7a). To analyze mRNA expression levels in murine T cells, CD4⁺ T cells were freshly isolated from spleen and lymph nodes of BALB/c mice and MALT1 isoform expression was measured by quantitative PCR (qPCR or real-time (RT) PCR), whereby hydroxymethylbilane synthase (*Hmbs*) served as internal control.

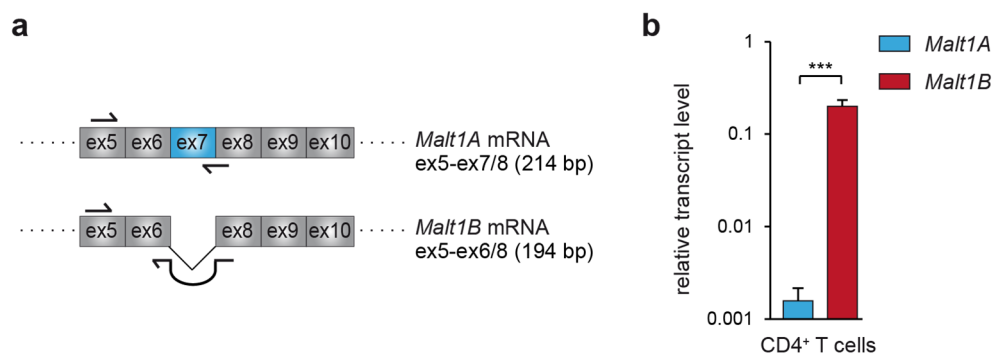


Figure 3.7: Primary CD4⁺ T cells lack *Malt1A* and predominantly express *Malt1B*. (a) Schematic of *Malt1* primers used for specific amplification of murine *Malt1A* (ex5-ex7/8; 214 bp) and murine *Malt1B* (ex5-ex6/8; 194 bp). (b) *Malt1A* and *Malt1B* mRNA levels in CD4⁺ T cells from BALB/c mice were analyzed by qPCR using isoform-specific ex5-ex7/8 or ex5-ex6/8 primers. Transcript levels were normalized to *Hmbs* mRNA levels. Depicted is the mean \pm SD (n=3) (b). ***p < 0.001; unpaired *t*-test.

Quantitative PCR revealed a more than ~ 100 fold higher expression of the shorter isoform *Malt1B* compared to *Malt1A* (Figure 3.7b). As MALT1A was hardly detectable, one can conclude that primary, unstimulated CD4⁺ T cells contain reduced levels of the longer splice variant MALT1A and mainly express MALT1B.

T cell activation correlates with drastic changes in alternative splicing patterns (Martinez et al., 2012). Therefore, *Malt1A* and *Malt1B* mRNA expression levels were further elucidated after 3 h anti-CD3 and/or anti-CD28 stimulation (Figure 3.8a). Whereas CD3 antibodies engage the TCR, CD28 antibodies stimulate the CD28 co-receptor. Stimulation of CD4⁺ T cells with anti-CD3 alone or anti-CD3/ CD28 in combination induced *Malt1A* expression

by a factor 10-12, whereas incubation with anti-CD28 alone failed to upregulate *Malt1A* expression. In contrast, *Malt1B* levels were only slightly altered by anti-CD3 or anti-CD3/CD28 treatment (factor 2-4). TCR-induced induction of *Malt1A* was further confirmed by semi-quantitative PCR (semi-qPCR), in which the samples are compared within the exponential amplification phase of the PCR reaction (Figure 3.8b). Thereby, *Malt1A* levels markedly increased after 3 h or 6 h anti-CD3 stimulation, but decreased again after 18 h (Figure 3.8b left panel). Compared to anti-CD3/CD28 or anti-CD28 alone, 6 h of anti-CD3 treatment induced *Malt1A* most efficiently (Figure 3.8b right panel). Again, *Malt1B* was only moderately enhanced, which was also observed for overall *Malt1* expression (Griesbach, 2012). Thus, T cell activation mediates exon7 inclusion and anti-CD3 stimulation alone was sufficient to induce alternative splicing of MALT1.

As CD3 antibodies only stimulate the TCR-associated CD3 complex, and do not directly engage the antigen-binding pocket, it was determined whether alternative MALT1 splicing is also induced upon stimulation of the TCR antigen-binding site with a real antigenic peptide. Therefore, OT-II T cells were utilized, which bear a transgenic TCR that specifically recognizes a chicken ovalbumin peptide (OVA, aa 323-339) presented by MHC class II proteins expressed on the surface of APCs.

First, irradiated, T cell-depleted APCs (TCR β ⁻) from *wt* mice were incubated with OT-II T cells (TCR β ⁺) in a ratio 1:1 (Figure 3.8c upper panel). To activate OT-II T cells, APCs were pulsed with OVA peptide and incubated with OT-II T cells for different time points. To check OVA-mediated OT-II activation, we gated on OT-II cells (TCR β ⁺) and examined surface expression of the activation marker CD69, whose expression was enhanced with increasing time points (Figure 3.8c lower panel). Since splicing occurs earlier than CD69 upregulation, alternative MALT1 splicing was analyzed after 6 h OVA stimulation (Figure 3.8d). Consistent with the effects observed following anti-CD3 stimulation, OVA-mediated OT-II stimulation promoted *Malt1A* induction, but only mildly altered *Malt1B* levels (Figure 3.8d). The effects were not as pronounced as in the anti-CD3 treated T cells, but the upregulation of *Malt1A* was statistically significant. Thus, TCR stimulation with a MHC/peptide complex also induces alternative splicing of MALT1 leading to exon7 inclusion. Although MALT1B is the dominant isoform, TCR stimulation increases the MALT1A versus MALT1B expression ratio in CD4⁺ T cells.

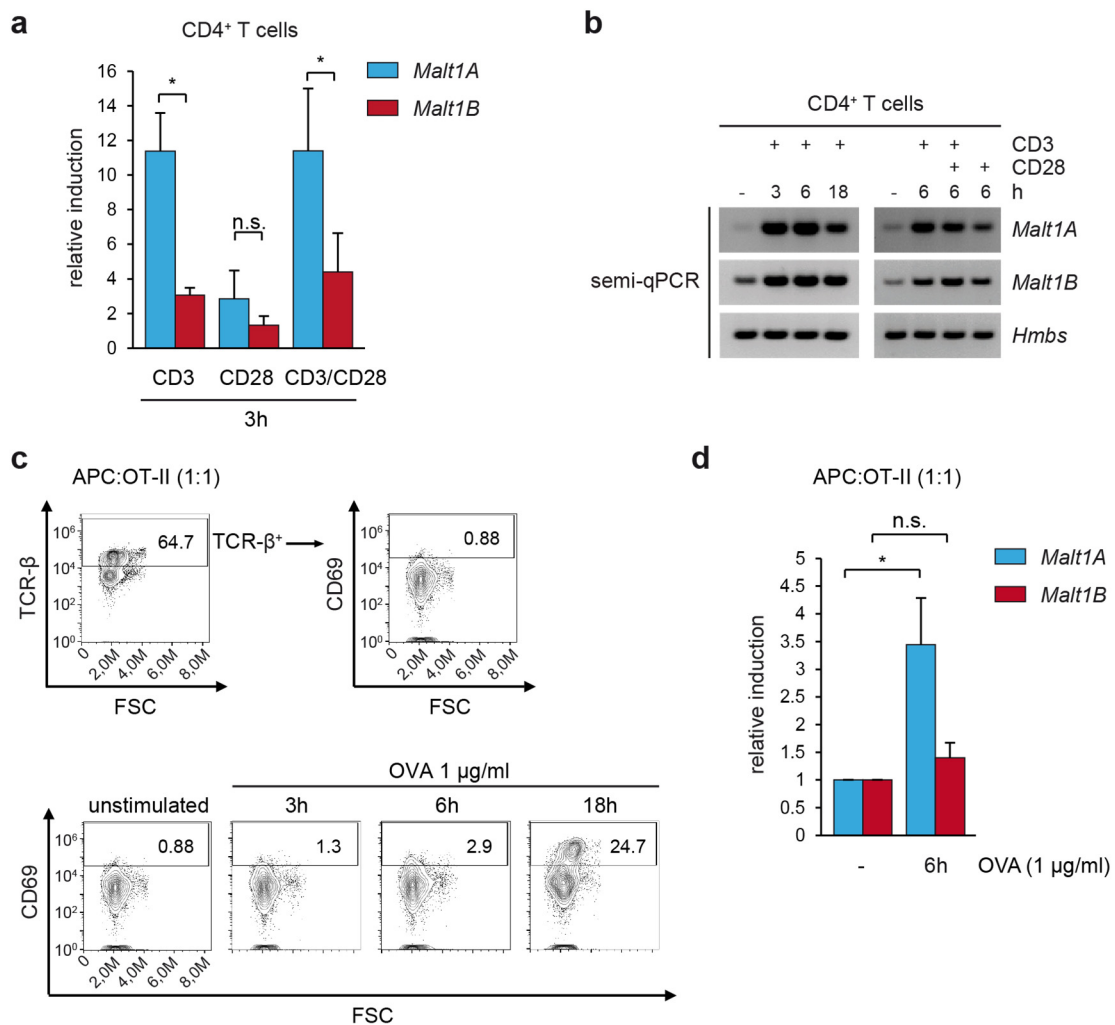


Figure 3.8: TCR stimulation induces exon7 inclusion and thus MALT1A expression in CD4⁺ T cells. (a,b) CD4⁺ T cells from BALB/c mice were stimulated with anti-CD3, anti-CD28, or both antibodies for the indicated time points. (a) *Malt1A* and *Malt1B* expression was measured by qPCR using isoform-specific primers and normalized to *Hmbs* levels. Relative induction was calculated relative to unstimulated control. (b) For semi-qPCR analysis, amplification of *Malt1A* and *Malt1B* was stopped after 35 cycles and 28 cycles, respectively. *Hmbs* served as internal control. (c,d) T cell-depleted APCs (TCRβ⁻) from *wt* mice were incubated with OT-II T cells (TCRβ⁺) in a ratio 1:1. For OT-II T cell activation, APCs were pulsed with 1 μg/ml OVA peptide and incubated with OT-II T cells for the indicated time points. (c) OT-II T cell activation was monitored by gating CD69 surface expression in TCRβ⁺ cells using flow cytometry. (d) *Malt1A* and *Malt1B* expression levels were analyzed in OT-II CD4⁺ T cells cultured for 6 h with *wt* APCs unloaded or loaded with 1 μg/ml OVA. Transcript levels were normalized to *Hmbs*. Relative induction was determined comparative to unloaded APCs cultured 1:1 with OT-II T cells. Data show the mean ± SD (n=3) (a,d). *p < 0.05; n.s. not significant; unpaired *t*-test.

3.2.2 MALT1A expression is enhanced in activated T cell subsets

TCR ligation promotes T cell activation and differentiation into distinct effector subsets such as TH1, TH2, TH17 and the more recently identified TFH cells (Chang et al., 2014). All subtypes differ in their cytokine expression pattern to fulfill distinct functions during an immune response (Luckheeram et al., 2012). As alternative MALT1 splicing is induced upon

T cell stimulation (see Figure 3.8), it was determined whether elevated MALT1A levels are also seen in activated T cell effector subsets. To promote the generation of effector T cells, BALB/c mice were immunized and splenic CD4⁺ T cells were isolated after 7 days. Out of the pool of CD4⁺ T cells (~ 71 %), naive T cells (CD62L⁺CD44⁻, ~ 62 %), effector T cells (CD62L⁻CD44⁺, ~ 24 %) and specifically T_{FH} cells (CXCR5⁺PD-1⁺, ~ 12 %) were purified (Figure 3.9a) (performed by J. Kranich, Institute for Immunology, LMU München).

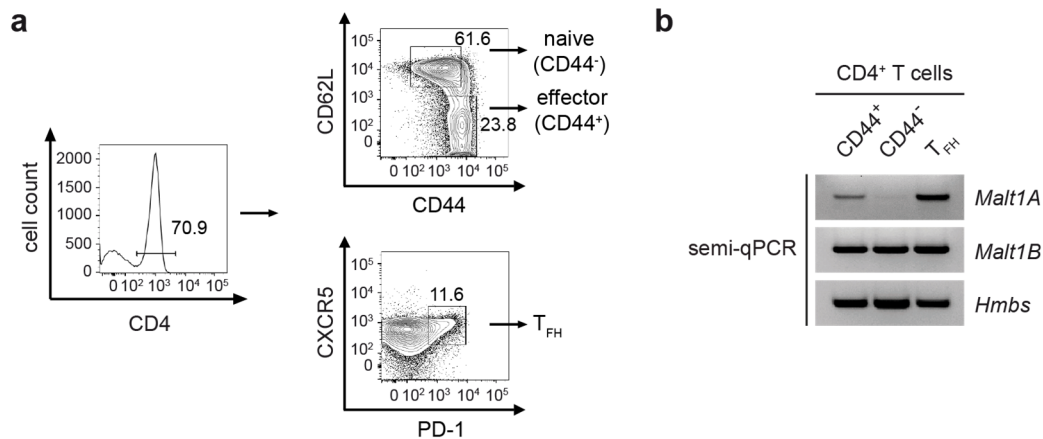


Figure 3.9: Activated T cell subsets display enhanced MALT1A expression levels. (a) Splenic CD4⁺ T cells were isolated from immunized BALB/c mice and were further sorted for naive CD62L⁺CD44⁻ T cells, activated CD62L⁻CD44⁺ effector T cells and CXCR5⁺PD-1⁺ T follicular helper (T_{FH}) cells as indicated. (Immunization and sorting was performed by J. Kranich, Institute for Immunology, LMU München). (b) After RNA isolation, *Malt1A* and *Malt1B* mRNA expression was investigated by semi-qPCR using isoform-specific primer pairs. Again, *Hmbs* served as internal control. Depicted is one of four independent experiments.

RNA was isolated from different T cell subsets and mRNA expression levels of *Malt1A* and *Malt1B* were analyzed by semi-qPCR using isoform-specific primers (see Figure 3.7a). For semi-qPCR, we first varied the number of PCR cycles to determine the exponential phase of the PCR reactions. Afterwards, the samples were reamplified, stopped in the exponential phase and loaded on an agarose gel to compare isoform expression levels. Whereas *Malt1B* transcript levels were similar between naive and effector T cells, *Malt1A* expression was upregulated in effector cells and T_{FH} cells, but not in the naive T cell subset (Figure 3.9b). Thus, alternative MALT1 splicing also drives MALT1A induction *in vivo* in activated T cells, which might be required to facilitate optimal immune responses.

3.2.3 Alternative MALT1 splicing is induced in human CD4⁺ T cells

MALT1A was induced in murine CD4⁺ T cells upon T cell activation. To elucidate if alternative MALT1 splicing also occurs in human T cells, we purified CD4⁺ T cells from

peripheral blood mononuclear cells (PBMCs) from four healthy donors and assessed MALT1 isoform levels in resting cells and upon anti-CD3/CD28 stimulation. After RNA isolation, mRNA expression levels were analyzed using human *MALT1A* (ex6/7-ex10) and *B* (ex5-ex6/8) specific primers (Figure 3.10a). Unstimulated human CD4⁺ T cells expressed more *MALT1B* than *MALT1A* (factor 4-5) (Figure 3.10b left panel), and anti-CD3/CD28 stimulation induced *MALT1A* expression (5 fold), but not as strong as in murine CD4⁺ T cells (Figure 3.10b right panel). Moreover, *MALT1B* levels were also upregulated by a factor 2-3 upon stimulation, which only slightly increases the *MALT1A*/*MALT1B* ratio. Although the effects are less pronounced than in murine CD4⁺ T cells, one can conclude that MALT1 also undergoes alternative splicing in human, peripheral T cells.

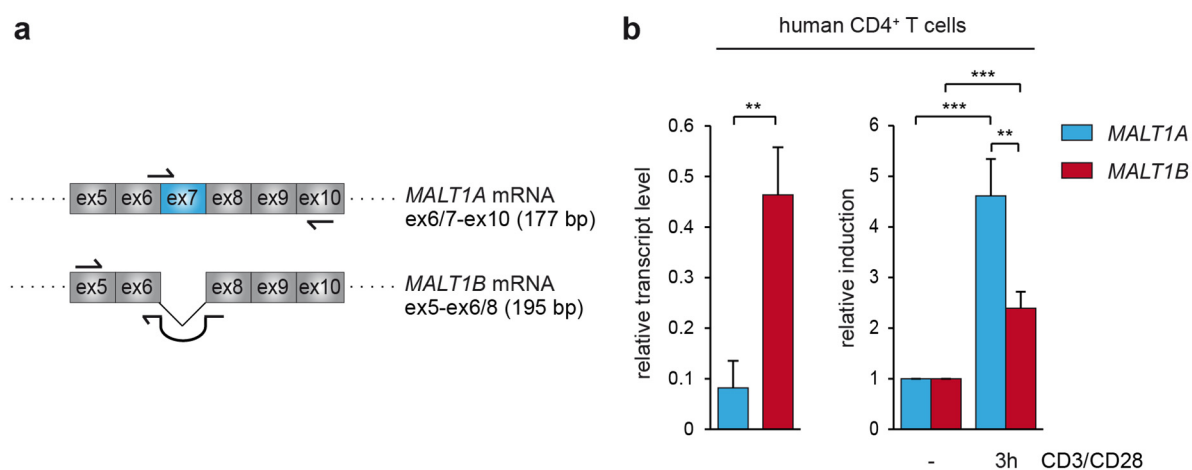


Figure 3.10: TCR stimulation upregulates MALT1A expression in human CD4⁺ T cells. (a) Schematic depiction of primers specific for human *MALT1A* (ex6/7-ex10; 177 bp) and human *MALT1B* (ex5-ex6/8; 195 bp). (b) Primary human CD4⁺ T cells were isolated from peripheral blood mononuclear cells (PBMCs) from four donors. Purified cells were stimulated with anti-CD3/CD28 for 3 h and MALT1 isoform expression was measured by qPCR using human *MALT1A*- or *MALT1B*-specific primers. *MALT1* transcript levels were normalized to RNA polymerase II (*RP2*) mRNA levels and relative induction was calculated compared to unstimulated cells. Depicted is the mean \pm SD (n=4) (b). **p < 0.01; ***p < 0.001; unpaired *t*-test.

3.2.4 Design and evaluation of morpholino oligomer to prevent MALT1A expression

As MALT1 exon7 supported signaling in Jurkat T cells, it was investigated whether exon7 inclusion also supports signaling and activation in primary, murine T cells. Therefore, a vivo-morpholino oligomer (MO) was designed, which targets the exon7-intron7 boundary of the *Malt1* pre-mRNA and thereby should prevent splice site selection resulting in exon7 skipping (Figure 3.11a). First, it was tested how efficiently the designed MO blocked exon7 inclusion in mouse embryonic fibroblasts (MEFs), which express both MALT1 isoforms and thus do

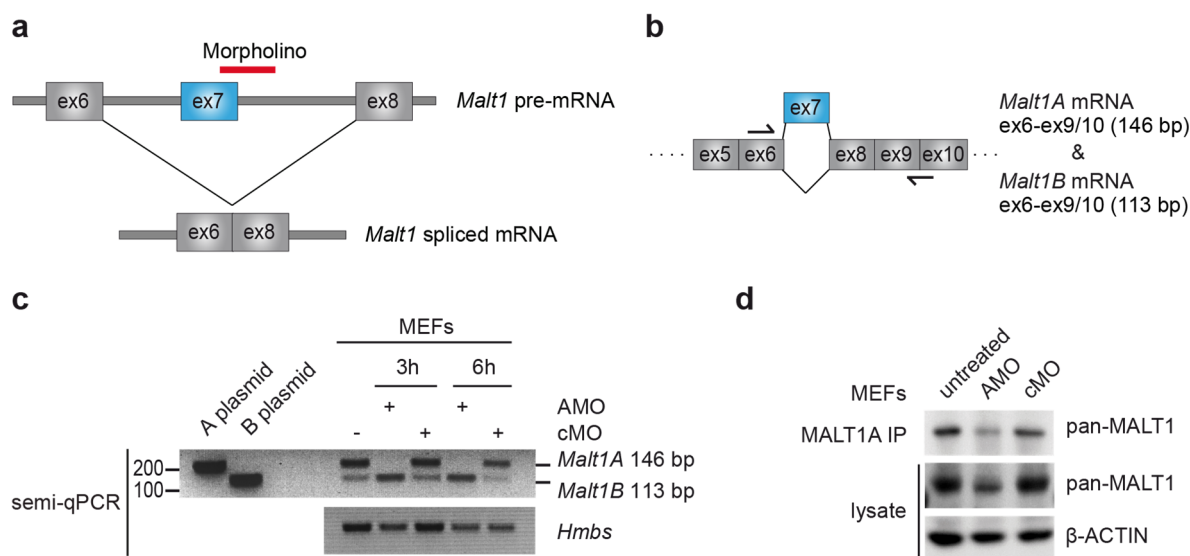


Figure 3.11: Design of morpholino to prevent MALT1A induction. (a) Model for vivo-morpholino (MO)-induced prevention of MALT1A expression. MO was designed against the exon7-intron7 boundary (5' splice site) in *Malt1* pre-mRNA to prevent spliceosomal recognition and exon7 inclusion. (b) Design of primer pairs for the simultaneous amplification of *Malt1A* and *Malt1B* (ex6-ex9/10; 146 bp *Malt1A*; 113 bp *Malt1B*). (c,d) Morpholino treatment impairs MALT1A expression in mouse embryonic fibroblasts (MEFs). MEFs were treated with morpholino against MALT1A (AMO), control MO (cMO) or remained untreated. (c) *Malt1A* and *Malt1B* mRNA expression was analyzed by semi-qPCR and isoform size was assessed by loading *MALT1A* and *MALT1B* plasmid DNA. *Hmbs* transcript levels served as internal control. (d) MALT1A was precipitated by using a MALT1A-specific antibody raised against MALT1 exon7. Precipitates and cell lysates were stained with a total MALT1 antibody. β -ACTIN served as loading control.

not require stimulation-induced MALT1A induction. After incubation with MALT1A morpholino (AMO) or control morpholino (cMO) for 3 h or 6 h, MEFs were analyzed for their MALT1 isoform expression levels by semi-qPCR using a primer pair (ex6-ex9/10) that amplifies *Malt1A* and *B* simultaneously (Figure 3.11b,c).

AMO treatment completely abolished *Malt1A* mRNA expression and shifted alternative splicing towards enhanced *Malt1B* levels (Figure 3.11c). In contrast, cMO incubation did not alter the *Malt1* isoform ratio (Figure 3.11c). AMO treatment also reduced MALT1A protein expression (Figure 3.11d). This was monitored by MALT1A IP using an antibody raised against MALT1 exon7, whose specificity has been confirmed in previous experiments upon ectopic MALT1A expression in HEK293 cells (Griesbach, 2012). Thus, the designed MO selectively reduced MALT1A expression in MEFs.

The efficiency of MO incubation was further tested in murine CD4⁺ T cells, which require TCR ligation to initiate alternative MALT1 splicing. Therefore, isolated CD4⁺ T cells were incubated with AMO or cMO prior to anti-CD3 or anti-CD3/CD28 stimulation and *Malt1* isoform expression was analyzed by semi-qPCR and qPCR (Figure 3.12a-c).

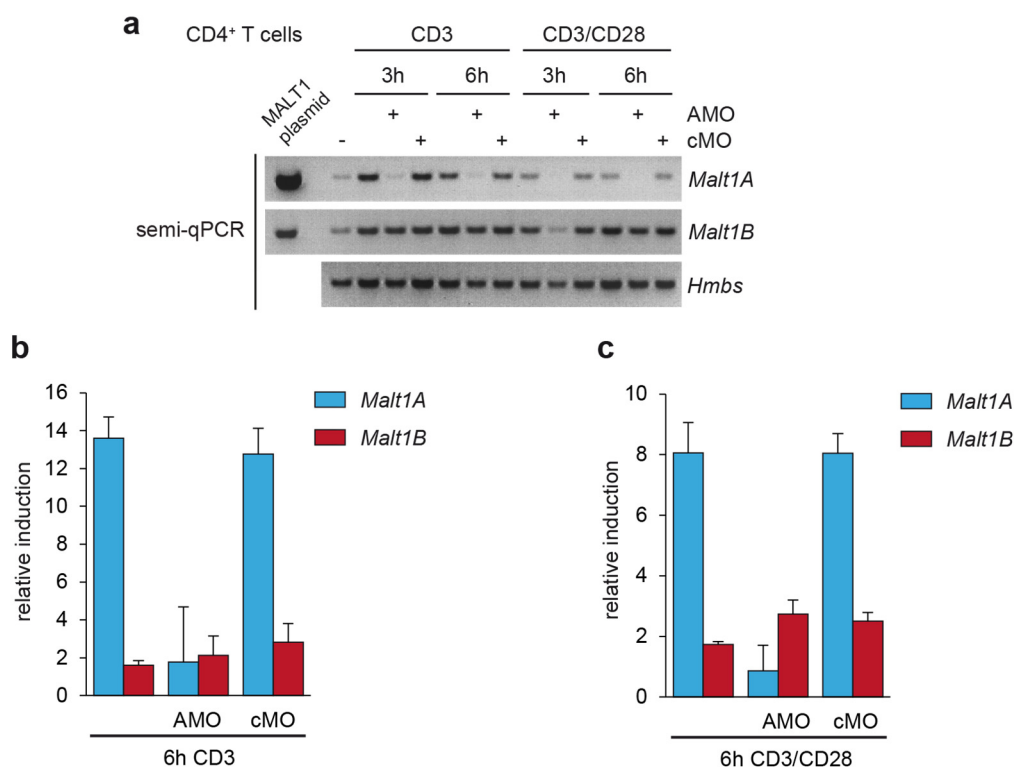


Figure 3.12: Morpholino prevents TCR-induced MALT1A induction in CD4⁺ T cells. (a-c) CD4⁺ T cells from BALB/c mice were treated with AMO, cMO or left untreated for 3 h before anti-CD3 or anti-CD3/CD28 stimulation for the indicated time points. (a) *Malt1A* and *Malt1B* mRNA expression was investigated by semi-qPCR using isoform-specific primer pairs. *MAL T1* plasmid DNA was loaded to check isoform size. *Hmbs* served as internal control. (b,c) *Malt1* isoform levels were analyzed by qPCR using the same primers as in (a). Transcript levels were normalized to *Hmbs* and relative induction was determined in comparison to unstimulated samples. Depicted is the mean \pm SD (n=3) (b,c).

Selective amplification with *Malt1A*- or *B*-specific primer pairs revealed that AMO treatment completely abolished anti-CD3- or anti-CD3/CD28-mediated *Malt1A* induction, whereas *Malt1B* expression was not affected (Figure 3.12). Again, anti-CD3 stimulation alone induced a more efficient *Malt1A* upregulation (Figure 3.12a,b) than anti-CD3/CD28 treatment (Figure 3.12a,c). In summary, the designed MO against MALT1A serves as a useful tool to selectively prevent MALT1A upregulation in CD4⁺ T cells.

Although unstimulated, primary CD4⁺ T cells lack MALT1A expression, it was examined, whether MO treatment of resting cells may have unwanted side effects and already influences T cell signaling pathways. Therefore, freshly isolated murine CD4⁺ T cells were left untreated or incubated with AMO or cMO before they were stimulated with anti-CD3/CD28 or P/I. As exon7 inclusion in Jurkat T cells mainly influences JNK and NF- κ B signaling, we focused on the analysis of those signaling pathways. Neither NF- κ B signaling nor JNK activation was

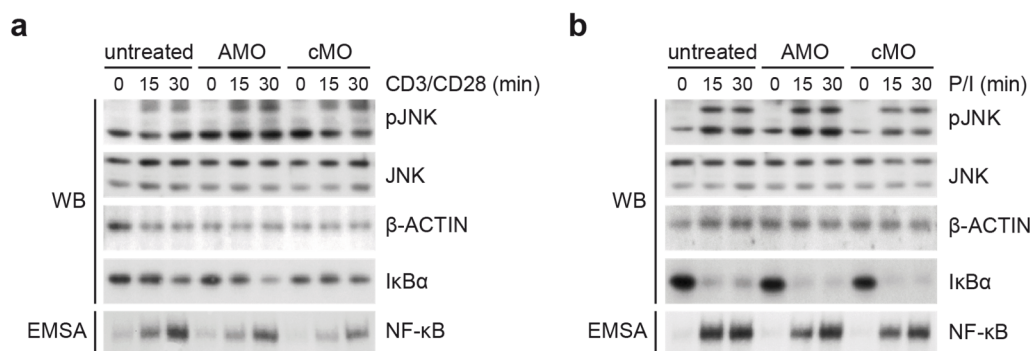


Figure 3.13: Morpholino does not affect T cell signaling in the absence of MALT1A. (a,b) After MO treatment, CD4⁺ T cells were directly stimulated with anti-CD3/CD28 (a) or P/I (b) for the indicated time points. JNK phosphorylation and IκBα degradation were analyzed by Western Blot using the indicated antibodies. NF-κB activation was monitored by EMSA.

altered in AMO treated cells, revealing that AMO does not interfere with T cell signaling in the absence of MALT1A (Figure 3.13a,b). Thus, AMO can be further used for the analysis of downstream signaling pathways upon MALT1A upregulation.

3.2.5 MALT1A upregulation supports NF-κB and JNK signaling

TCR ligation triggers exon7 inclusion and thus MALT1A induction. Since exon7 harbors a functional TRAF6 binding motif and can contribute to the activation of NF-κB and JNK signaling in Jurkat T cells, the aim was to investigate whether upregulation of MALT1A in murine CD4⁺ T cells augments T cell signaling. Therefore, freshly isolated CD4⁺ T cells were pre-treated with anti-CD3 to induce MALT1A expression, and activation of downstream signaling was monitored after re-stimulation with P/I to bypass upstream TCR stimulation that might be altered upon CD3 pre-treatment.

Without pre-treatment, IκBα is phosphorylated within 10 min and completely degraded after 20 min P/I stimulation resulting in nuclear translocation of NF-κB (Figure 3.14a). NF-κB signaling was strongly enhanced upon anti-CD3 pre-treatment. With respect to MAPK signaling, anti-CD3 pre-treated cells showed pronounced JNK activation, whereas ERK and p38 signaling were not affected (Figure 3.14b). To determine whether enhanced NF-κB and JNK activation is due to MALT1A upregulation, the designed AMO was utilized. Primary T cells were incubated with AMO or cMO prior to anti-CD3 pre-treatment and re-stimulated with P/I. Again, CD3 pre-treatment promoted stronger NF-κB activation and slightly enhanced JNK phosphorylation in untreated or cMO treated cells (Figure 3.14c,d). In T cells,

which lack MALT1A expression due to AMO incubation, NF- κ B DNA binding was dramatically reduced compared to cMO treated cells (~ 4 fold at 30 min) and was comparable to CD4⁺ T cells without anti-CD3 pre-treatment (Figure 3.14c). I κ B α levels are low after AMO incubation, which could be due to decreased re-synthesis of I κ B α in the presence of AMO. Regarding MAPK activation, JNK phosphorylation was slightly reduced after AMO treatment, but ERK and p38 activation were not affected (Figure 3.14d). Collectively, TCR-mediated MALT1A induction enhances MALT1 scaffolding function to promote optimal NF- κ B and JNK activation.

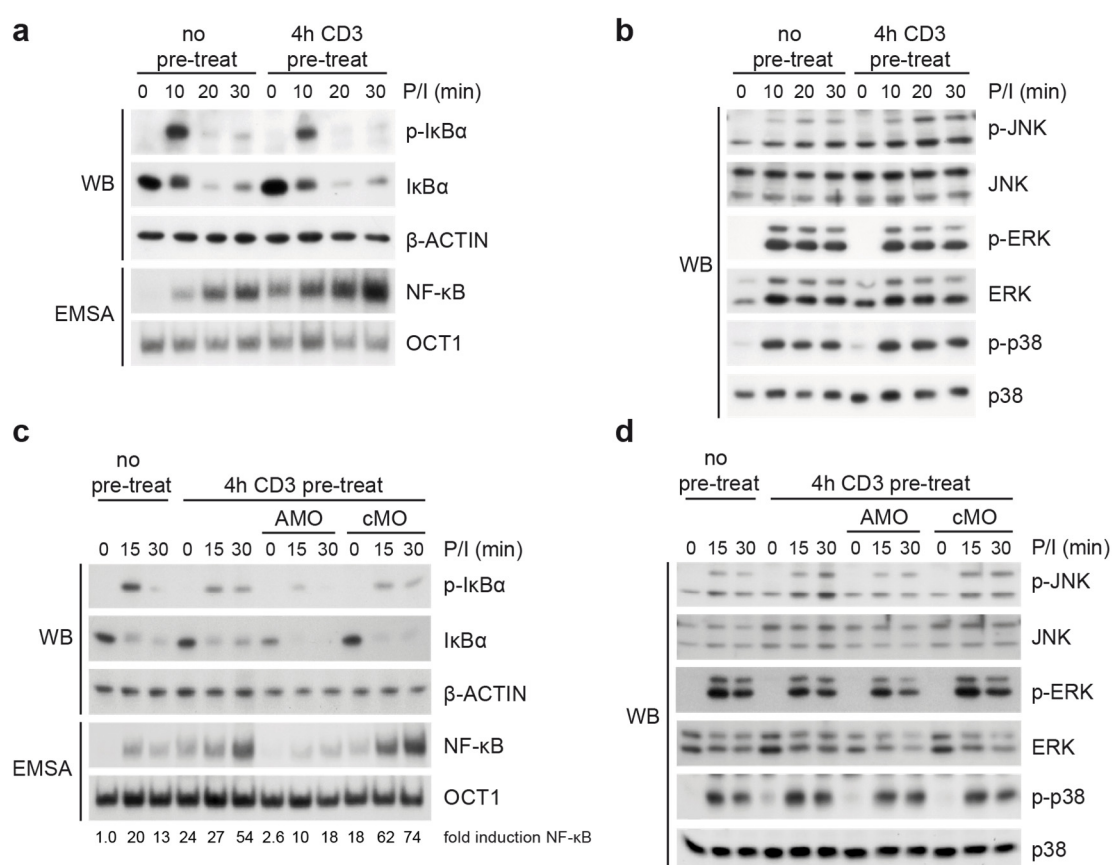


Figure 3.14: TCR-induced MALT1A induction augments T cell signaling. (a,b) Anti-CD3 pre-treatment of CD4⁺ T cells enhances NF- κ B and JNK signaling. CD4⁺ T cells from BALB/c mice were either pre-treated with anti-CD3 for 4 h or left untreated. Afterwards, the cells were stimulated with P/I for the indicated times. (a) To analyze NF- κ B signaling, I κ B α phosphorylation and degradation were analyzed by Western Blot using the indicated antibodies. NF- κ B activation was assessed by EMSA. β -ACTIN and OCT1 were used as loading controls. (b) MAPK signaling was investigated by monitoring JNK, ERK and p38 phosphorylation in Western Blot analysis with the illustrated antibodies. (c,d) Anti-CD3-mediated MALT1A induction accounts for optimal NF- κ B and JNK activation. Untreated, AMO or cMO treated CD4⁺ T cells were pre-treated with anti-CD3 for 4 h prior to secondary P/I stimulation. (c) NF- κ B signaling was analyzed as in (a). NF- κ B fold induction was calculated by quantification of NF- κ B signal relative to OCT1 control. Active NF- κ B levels in untreated, unstimulated cells were set to 1. (d) Analysis of MAPK signaling was performed as in (b).

It has been reported that JNK activation depends on CYLD cleavage by MALT1 paracaspase in Jurkat T cells (Staal et al., 2011). As JNK activation was slightly enhanced upon MALT1A induction in primary CD4⁺ T cells (see Figure 3.14), it was investigated whether proteolytic MALT1 activity and concomitant CYLD cleavage is augmented upon MALT1A upregulation.

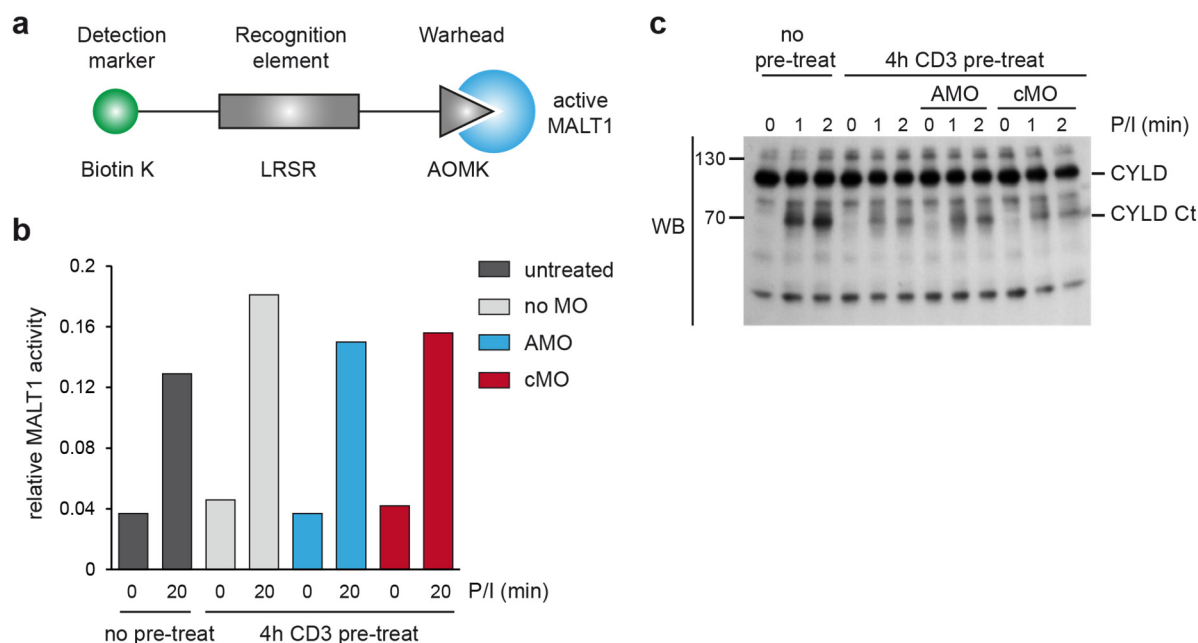


Figure 3.15: Inhibition of MALT1A induction does not alter MALT1 protease function. (a) Schematic of an ABP probe used for detecting active MALT1. The structure of the ABP is similar to the probe described in Figure 3.6a, but contains a Biotin detection marker. (b) MALT1 proteolytic activity is independent of MALT1A induction. CD4⁺ T cells were treated with AMO, cMO or kept untreated prior to anti-CD3 pre-treatment. Afterwards, cells were re-stimulated with P/I for 20 min before incubation with the biotinylated MALT1 ABP probe. Active MALT1 ABP complexes were immobilized on a streptavidin-coated plate and were detected by an enzyme-linked activity-sorbent assay (ELASA). MALT1 activity was calculated relative to background levels. Depicted is one experiment (n=1). (c) CYLD cleavage is not affected by MALT1A induction. CD4⁺ T cells were treated with MO or kept untreated prior to anti-CD3 pre-treatment and subsequent P/I re-stimulation for the indicated time points. CYLD cleavage was analyzed by Western Blot using a CYLD antibody detecting full-length and the C-terminal CYLD cleavage fragment appearing at ~ 70 kDa.

For monitoring MALT1 paracaspase activity, a Biotin-coupled MALT1 ABP was used (Figure 3.15a) (Eitelhuber et al., 2015). CD4⁺ T cells were incubated with AMO or cMO and pre-treated with anti-CD3 followed by P/I re-stimulation and incubation with the Biotin-ABP. MALT1 ABP complexes can be immobilized on streptavidin-coated plates and active MALT1 is detectable using a MALT1-specific antibody.

As expected, T cell stimulation induced activation of MALT1 paracaspase (Figure 3.15b). However, MALT1 activity did not differ between AMO and cMO treated cells, revealing that inhibition of MALT1A induction does not affect MALT1 protease function. Regarding MALT1 substrate cleavage, CYLD cleavage was reduced upon anti-CD3 pre-treatment, but was not altered by AMO incubation upon P/I re-stimulation (Figure 3.15c). Finally, MALT1 protease activity is not influenced by MALT1A induction and therefore does not account for enhanced JNK activation.

3.2.6 TCR-induced MALT1A expression supports T cell activation

MALT1A induction leads to enhanced NF- κ B and JNK signaling (see Figure 3.14). As activation of both pathways is required for optimal T cell activation, it was addressed whether an increase in MALT1A expression results in a more robust T cell activation. T cell activation correlates with upregulation of the surface markers CD69 and CD25, which prolong lymphocyte retention in secondary lymphoid organs and support T cell expansion, and can be monitored by flow cytometry (Malek, 2008; Shiow et al., 2006).

Stimulation of murine CD4⁺ T cells with anti-CD3/CD28 promoted a strong induction of CD69 and CD25 surface expression, but was reduced in the absence of MALT1A (Figure 3.16a). This was further confirmed by quantification of CD69 and CD25 mean fluorescence intensity (MFI) (Figure 3.16b). Moreover, activated T cells produce IL-2, whose expression is induced by several transcription factors including NF- κ B (Schulze-Luehrmann and Ghosh, 2006). IL-2 is an important cytokine for mediating T cell survival, proliferation, and differentiation (Bachmann and Oxenius, 2007). When cells were stained for intracellular IL-2, the amount of IL-2 positive cells in AMO treated CD4⁺ T cells was reduced (Figure 3.16c,d), which correlates with decreased *Il2* transcript levels (Figure 3.16e). The results reveal that TCR-induced MALT1A upregulation is required to promote optimal CD69, CD25 and IL-2 expression and thus to facilitate more robust T cell activation.

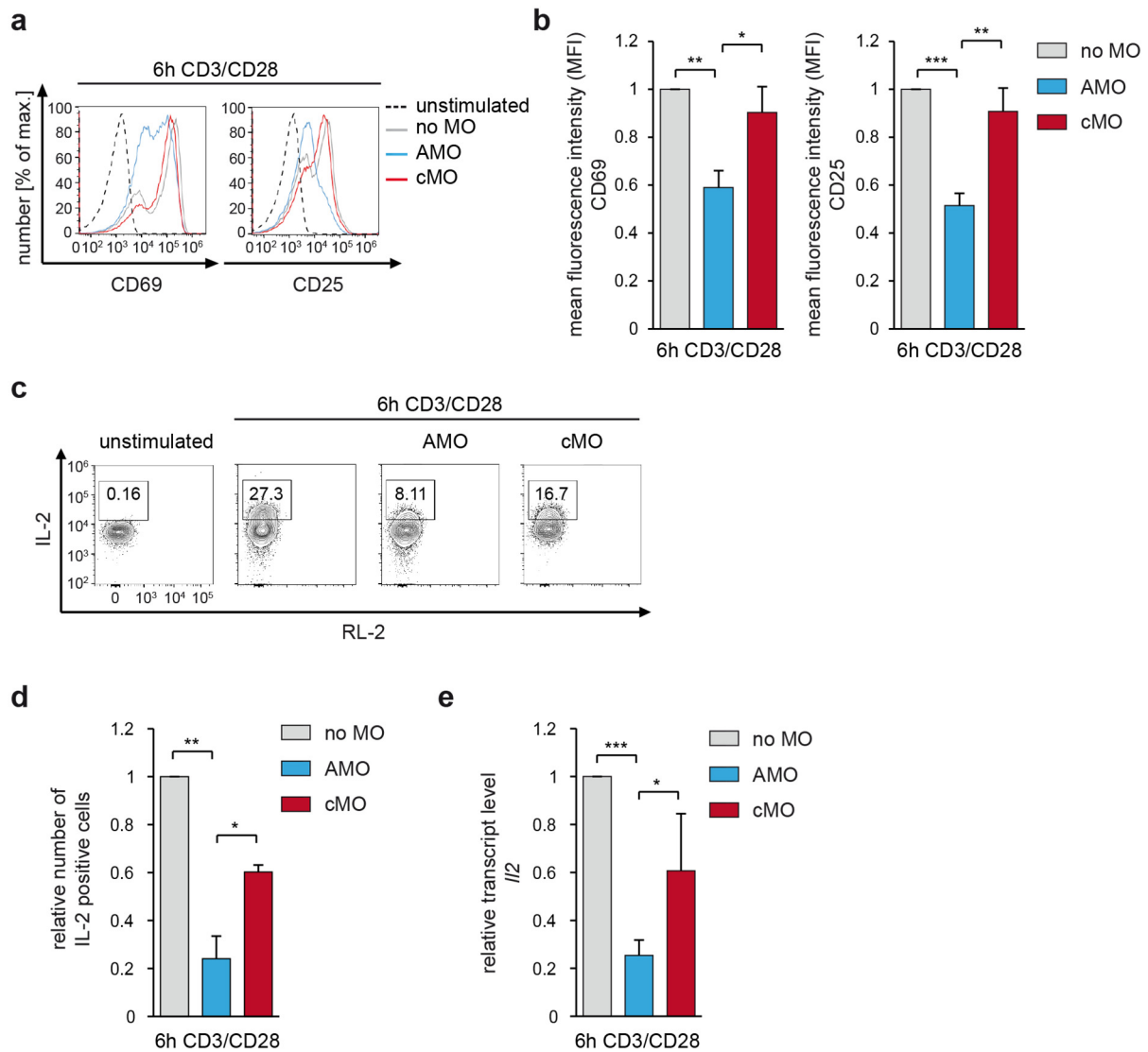


Figure 3.16: MALT1A induction is required for optimal CD69 and CD25 upregulation and IL-2 production. (a-e) CD4⁺ T cells from BALB/c mice were left untreated or were treated with AMO or cMO before 6 h anti-CD3/CD28 stimulation. (a) Cell surface expression of CD69 and CD25 was monitored by flow cytometry. (b) Calculation of mean fluorescence intensity (MFI) of CD69 and CD25. (c) Viable CD4⁺ T cells were fixed and stained for intracellular IL-2 and staining was analyzed by flow cytometry. Fluorescence of IL-2 was plotted against the empty channel red laser 2 (RL-2). (d) The number of IL-2 positive cells as gated in (c) was quantified comparative to stimulated control cells (no MO). (e) *Il2* mRNA expression levels in CD4⁺ T cell (no MO, AMO or cMO treated) were analyzed by qPCR using *Il2*-specific primers. *Hmbs* levels served as internal control. Depicted is the mean \pm SD (n=3) (b,d,e). *p < 0.05; **p < 0.01; ***p < 0.001; unpaired *t*-test.

3.2.7 Alternative MALT1 splicing does not influence T cell fate decisions

Upon activation, CD4⁺ T cells differentiate into distinct effector subsets (Luckheeram et al., 2012). Data from MALT1 paracaspase mutant mice revealed that MALT1 protease is required for the generation of TH17 cells, which play a crucial role in the defense against bacterial and fungal infections and are associated with several autoimmune diseases (Bornancin et al., 2015; Waite and Skokos, 2012). To elucidate the relevance of alternative MALT1 splicing for

T cell differentiation, T_H1 and T_H17 differentiation conditions were first optimized in *wt* and *Malt1*^{-/-} T cells. Thereby, limiting stimulation conditions were used to gain an optimal readout for monitoring MALT1 isoform-specific effects in subsequent experiments. In particular, naive $CD4^+$ T cells from *wt* and *Malt1*^{-/-} mice were stimulated with irradiated APCs and increasing concentrations of anti-CD3 (0.1-3 $\mu\text{g/ml}$), and were subsequently analyzed for their potential to differentiate into IL-17A-producing T_H17 cells and IFN γ -secreting T_H1 cells. As expected, MALT1-deficient $CD4^+$ T cells were unable to differentiate into T_H17 cells, but also T_H1 differentiation was reduced under the used stimulation conditions (Figure 3.17). At a concentration of 1 $\mu\text{g/ml}$ anti-CD3, differentiation into T_H1 and T_H17 cells was optimal and used for further experiments.

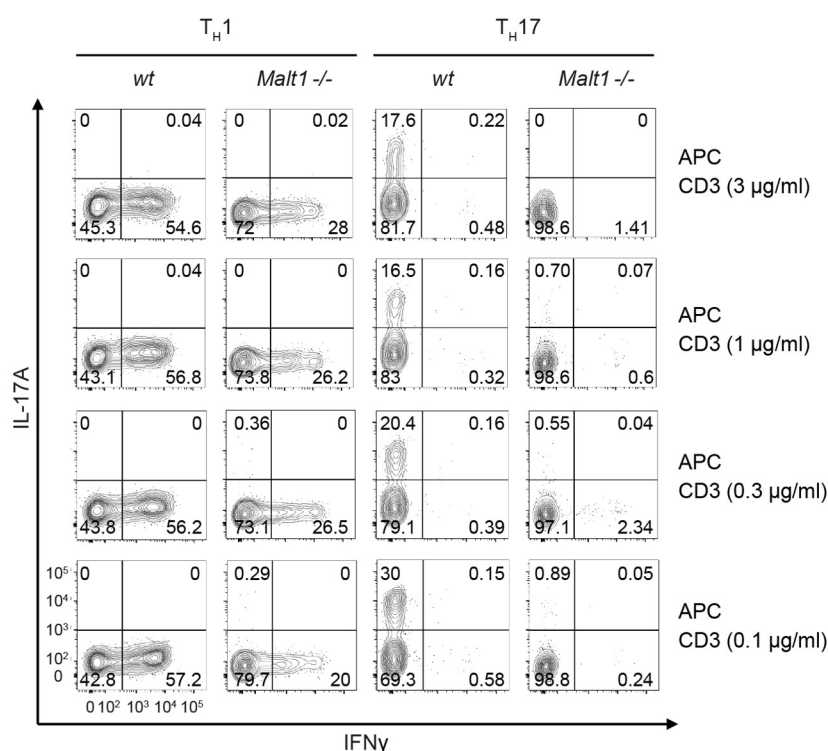


Figure 3.17: Optimization of T_H1 and T_H17 cell differentiation conditions. $CD4^+$ T cells from *wt* and *Malt1*^{-/-} mice were treated with irradiated APCs in a ratio 1:10 with increasing concentrations of anti-CD3 antibodies under T_H1 or T_H17 polarizing conditions. After re-stimulation, intracellular expression of the T_H1 marker IFN γ and the T_H17 marker IL-17A in viable $CD4^+$ T cells were determined by flow cytometry.

To analyze the impact of exon7 inclusion on T_H1 and T_H17 differentiation, an adenoviral approach was used (Warth and Heissmeyer, 2013). We infected naive $CD4^+$ T cells from *Malt1*^{-/-}R26/CAG-CAR $\Delta 1^{\text{stop-fl}}$ *Cd4-Cre* mice with adenoviruses encoding MALT1A,

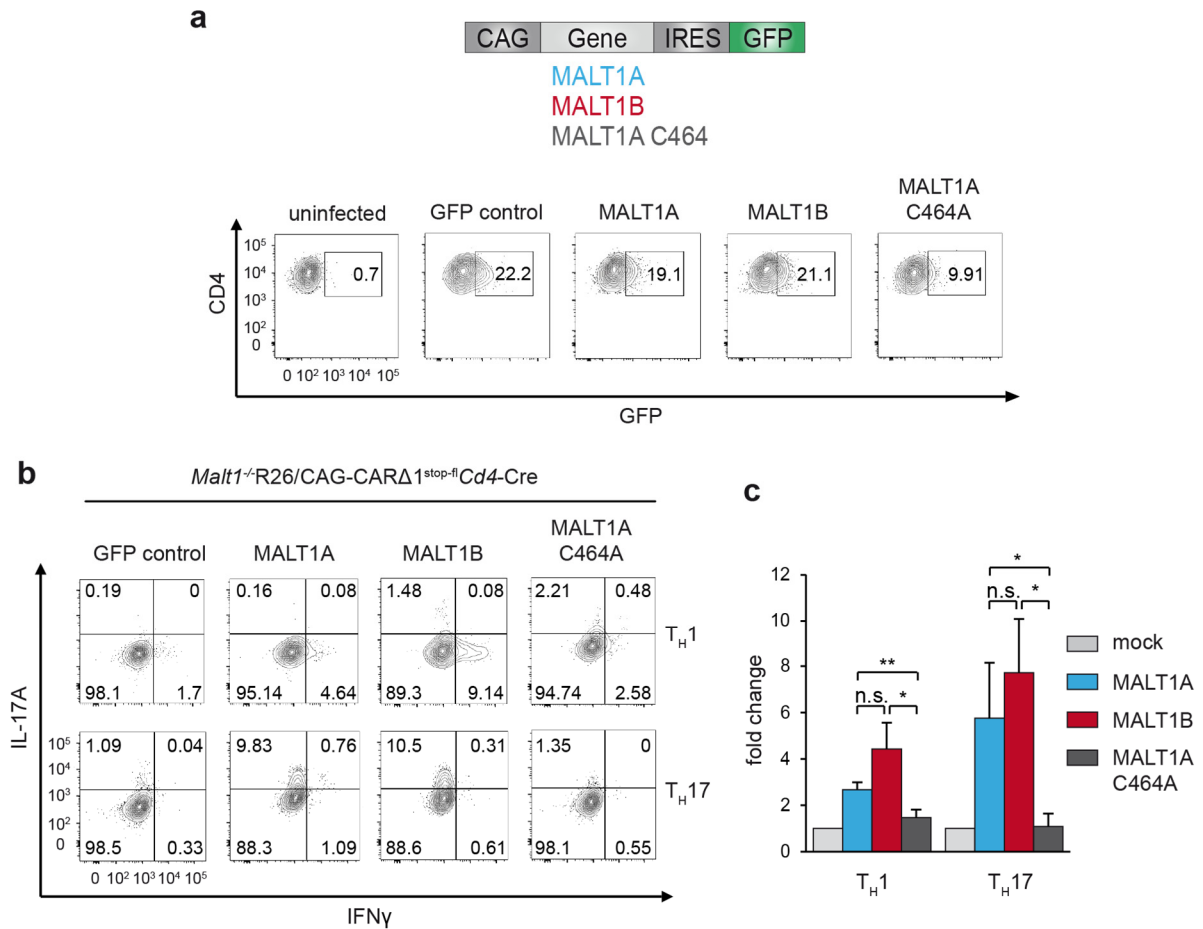


Figure 3.18: Alternative MALT1 splicing does not influence T cell effector differentiation. (a-c) CD4⁺ T cells from *Malt1^{-/-}R26/CAG-CARΔ1^{stop-fl}Cd4-Cre* mice were transduced with adenoviruses containing mock, MALT1A, MALT1B or MALT1A C464A and co-expressing IRES–GFP. (a) Scheme of adenoviral constructs used for MALT1 expression in CD4⁺ T cells. GFP expression was investigated by flow cytometry and GFP⁺ cells were used for further analysis. (b) Adenovirally reconstituted CD4⁺ T cells were cultured under T_H1 or T_H17 polarizing conditions and re-stimulated with P/I. GFP⁺ T cells were analyzed for intracellular IFN γ and IL-17A levels by flow cytometry. Numbers in quadrants represent percentage of IFN γ or IL-17A-positive cells. (c) The number of IFN γ and IL-17A positive cells was calculated relative to mock infected cells. Data show mean \pm SD (n=4) (c). *p < 0.05; **p < 0.01; n.s. not significant; unpaired *t*-test.

MALT1B or a catalytically inactive mutant MALT1A C464A (Figure 3.18a). CD4⁺ T cells from *Malt1^{-/-}R26/CAG-CARΔ1^{stop-fl}Cd4-Cre* mice are susceptible to adenoviral transduction as they express a truncated, signaling-deficient version of the human coxsackie adenovirus receptor (CARΔ1) (Heger et al., 2015).

Transduction efficiency was determined by co-expression of the infection marker green fluorescent protein (GFP). An infection efficiency of either ~ 9 % (MALT1A C464A) or ~ 20 % (GFP control, MALT1A, MALT1B) was obtained (Figure 3.18a). Using the optimized differentiation conditions, T_H1 and T_H17 cell differentiation of reconstituted cells was monitored by staining for IFN γ and IL-17A (Figure 3.18b,c). T_H17 cell differentiation

was similar in MALT1A and B expressing cells. Although the frequencies of IFN γ -producing T_{H1} cells were enhanced in MALT1B reconstituted T cells compared to MALT1A expressing cells, the difference was not significant. As expected, T cells reconstituted with the catalytically inactive mutant MALT1A C464A failed to differentiate into T_{H17} cells and only a small population became T_{H1} cells (Figure 3.18c,d), confirming the necessity of MALT1 protease activity for effector T cell differentiation. The results demonstrate that modulation of MALT1 scaffolding function by alternative splicing is crucial for T cell activation, but does not affect MALT1 protease activity and thus T cell fate decisions.

3.3 Regulation of alternative MALT1 splicing by the splicing factor hnRNP U

3.3.1 A siRNA screen identifies hnRNP U as a critical splicing regulator of alternative MALT1 splicing

The decision as to whether an alternative exon is included or excluded in the mature mRNA largely depends on protein regulators, which bind to *cis*-regulatory sequences within exons or introns and thereby modulate splice site recognition (Chen and Manley, 2009; Kornblihtt et al., 2013). To identify putative splicing regulators controlling alternative MALT1 splicing, a small interfering RNA (siRNA) screen was conducted in Jurkat T cells expressing both MALT1 isoforms. In this approach, Jurkat T cells were transfected with different smart pool siRNAs in order to knock down RNA-binding proteins that have been associated with splicing, and analyzed the *MALT1A* versus *MALT1B* expression ratio. In an initial approach, a siRNA library containing 76 siRNAs against RNA-binding factors with putative splicing activity was used and relative *MALT1* expression was determined by radioactive PCR (Figure 3.19a).

Knockdown of several factors like RBMS1 (RNA-binding motif single-stranded-interacting protein 1), hnRNP C or hnRNP H2 influenced the MALT1 isoform ratio by promoting exon7 skipping (Figure 3.19a). However, knockdown of hnRNP U (also known as scaffold attachment factor A [SAF-A]) had the strongest effect on alternative MALT1 splicing: hnRNP U downregulation caused a ~ 2 fold enhancement in exon7 inclusion and thus shifted the *MALT1* isoform ratio towards *MALT1A* expression (Figure 3.19a).

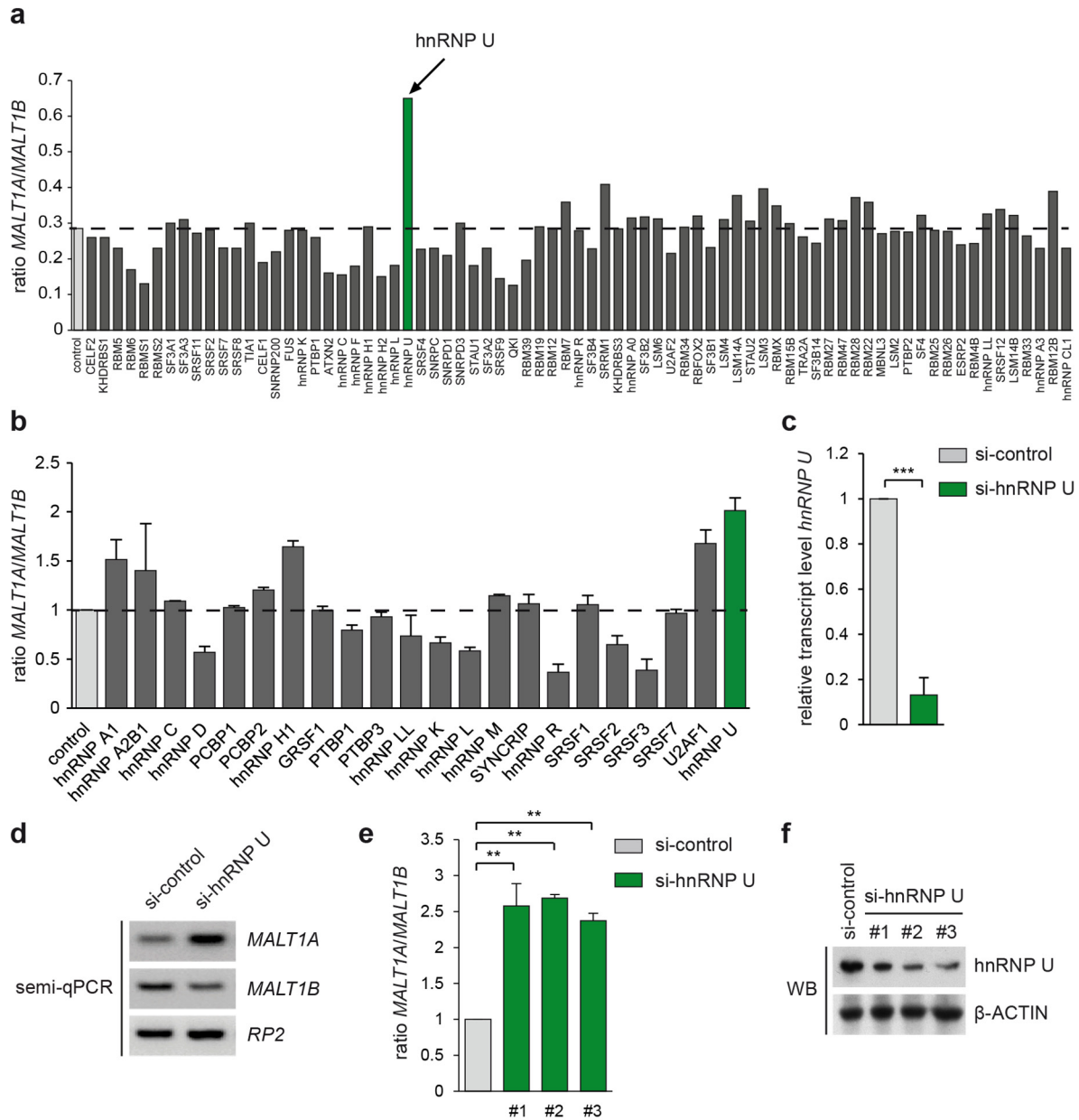


Figure 3.19: The splicing regulator hnRNP U negatively regulates exon7 inclusion and thus *MALT1A* expression in Jurkat T cells. (a-c) Identification of RNA-binding proteins involved in alternative *MALT1* splicing using two siRNA approaches. (a) Jurkat T cells were transfected with smart pool siRNAs targeting putative splicing regulators. *MALT1A/B* mRNA expression was measured by radioactive PCR. (b) Jurkat T cells were transfected as in (a) and analyzed by qPCR using *RP2* as internal control. In (b), relative *MALT1A* versus *MALT1B* expression of control cells was set to 1. (c) *hnRNP U* knockdown was confirmed by qPCR. *hnRNP U* expression was normalized to *RP2* and calculated relative to si-control (d) Jurkat T cells were transfected with a smart pool siRNA against hnRNP U and *MALT1* isoform expression was analyzed by semi-qPCR. *RP2* transcript levels served as internal control. (d) After transfection of si-control or three independent siRNAs against hnRNP U, the *MALT1A/MALT1B* ratio was analyzed by qPCR. Transcript levels were normalized to *RP2* and the *MALT1* isoform ratio of control cells was set to 1. (e) Knockdown of hnRNP U by three independent siRNAs (#1, #2, #3) was monitored by Western Blot using the indicated antibodies. Depicted is the mean \pm SD (n=3) (c,e). **p < 0.01; ***p < 0.001; unpaired *t*-test.

In parallel, we performed a second, more focused screen targeting 22 splicing factors, which have already been described to regulate alternative splicing events. A siRNA library was used to knock down the potential splicing regulators and the *MALTI* isoform ratio was evaluated using qPCR (Figure 3.19b). Knockdown of hnRNP U was confirmed by qPCR (Figure 3.19c) and an increase in *MALT1A* expression upon hnRNP U knockdown was also observed by semi-qPCR (Figure 3.19d). Comparing both screens, depletion of protein factors like hnRNP C, hnRNP K, or hnRNP R had differential effects on alternative MALT1 splicing, which can be due to different siRNA libraries and experimental conditions. However, hnRNP U popped up in both approaches with the most striking effect on MALT1 isoform expression and thus served as the most reliable candidate. The relative increase in *MALT1A* versus *MALT1B* expression was further confirmed using three independent siRNAs against hnRNP U (Figure 3.19e), whose knockdown efficiency was monitored by WB (Figure 3.19f). In summary, our results indicate that hnRNP U serves as a negative regulator of exon7 inclusion and thus *MALT1A* expression in Jurkat T cells, as hnRNP U downregulation resulted in an increased *MALT1A* versus *MALT1B* ratio.

3.3.2 mRNA stability of *MALTI* isoforms is not affected by hnRNP U

hnRNP U is involved in various biological processes including gene transcription (Kim and Nikodem, 1999; Kukalev et al., 2005; Obrdlik et al., 2008), X chromosome inactivation (Hasegawa et al., 2010), and modulation of splicing events (Huelga et al., 2012; Vu et al., 2013; Xiao et al., 2012; Ye et al., 2015). It has been also reported that hnRNP U regulates mRNA stability by binding to the 3' untranslated region (3' UTR) (Yugami et al., 2007). Although *MALT1A* and *B* are transcribed from the same gene and thus harbor an identical 3' UTR, it needs to be excluded whether the observed effect of hnRNP U on *MALT1A/B* ratio is due to alterations in mRNA stability. Therefore, control and hnRNP U-depleted Jurkat T cells were treated with Actinomycin D, which blocks transcription and thereby enables determination of mRNA decay. *MALT1A* and *MALT1B* mRNA levels were measured by qPCR and calculated relative to untreated cells.

Upon downregulation of hnRNP U, *MALT1A* mRNA was slightly more stabilized compared to si-control treated cells, but the increase was not significant (Figure 3.20a). Regarding *MALT1B*, no differences in the mRNA decay rate were observed between control and hnRNP U-depleted cells (Figure 3.20b). Although only slight effects were monitored, the data imply

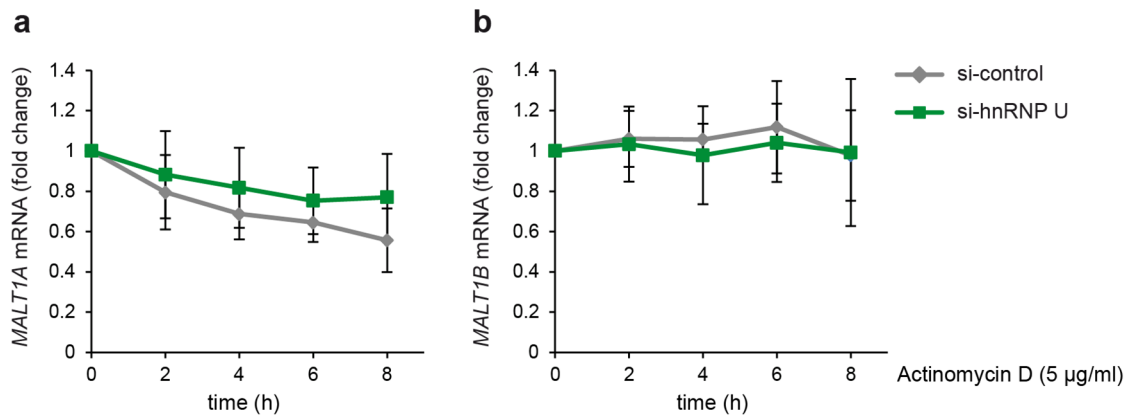


Figure 3.20: mRNA stability of MALT1 isoforms is not affected by hnRNP U. (a,b) Jurkat T cells were transfected with smart pool siRNA against hnRNP U and afterwards treated with Actinomycin D (5µg/ml) for 0 h, 2 h, 4 h, 6 h or 8 h. *MALT1A* (a) and *MALT1B* (b) mRNA expression were measured by qPCR and normalized to *RP2*, *PPIB*, *GAPDH* and *18S* rRNA levels. *MALT1* isoform expression of untreated samples was set to 1. Depicted is the mean \pm SD (n=5) (a,b).

that hnRNP U does not stabilize *MALT1B* mRNA or destabilize *MALT1A* mRNA. Therefore, one can conclude that hnRNP U rather modulates MALT1 isoform ratio by alternative splicing.

3.3.3 hnRNP U binds to *MALT1* pre-mRNA in proximity to exon7

hnRNP proteins can exert splicing enhancing or silencing activities by binding to regulatory sequences located within exons or introns (Kornblihtt et al., 2013). More recently, genome-wide analysis revealed that hnRNP proteins preferentially bind near alternatively spliced exons (Huelga et al., 2012). Therefore, the binding of hnRNP U to *MALT1* pre-mRNA near exon7 (between intron5 and intron9) and in a more distant region (exon2) was investigated. This was performed in Jurkat T cells by RNA-binding protein IP (RIP) using anti-hnRNP U or IgG control antibodies. Thereby, enrichment of distinct *MALT1* pre-mRNA regions was analyzed by qPCR (Figure 3.21a). Upon precipitation of hnRNP U, the pre-mRNA of *MALT1* around exon7 was enriched compared to IgG control and hnRNP U-depleted cells. Moreover, hnRNP U binding was highest within or in close proximity to exon7. No significant accumulation of an intron1-exon2 fragment was observed upon hnRNP U RIP, revealing that hnRNP U specifically binds to exon7 surrounding regions. Association of hnRNP U with *MALT1* pre-mRNA was also seen by semi-qPCR using primers specifically amplifying the region in6/ex7-in7 (Figure 3.21b). Collectively, hnRNP U binds to *MALT1* pre-mRNA in vicinity to the alternatively spliced exon7.

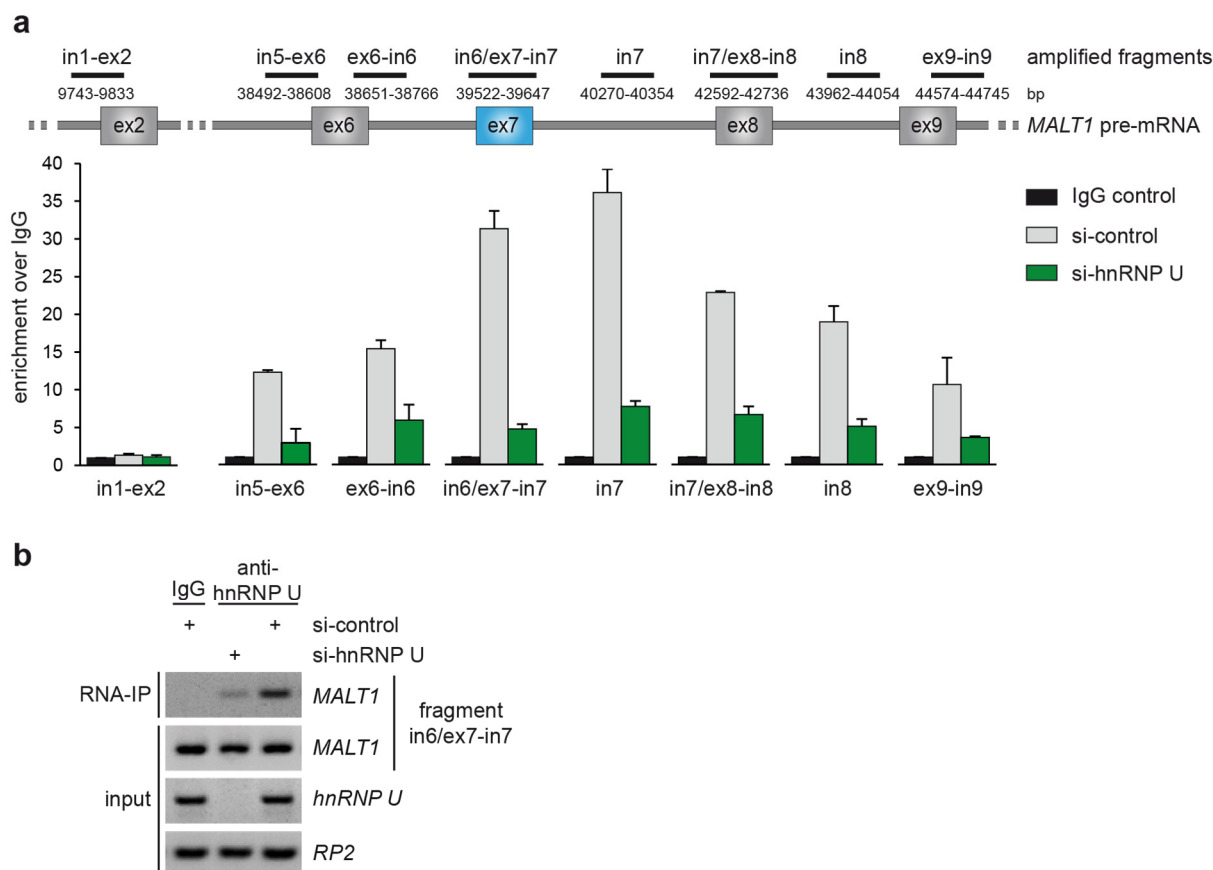


Figure 3.21: hnRNP U binds to *MALT1* pre-mRNA near exon7. (a,b) After transfection with si-control or si-hnRNP U, Jurkat T cells were lysed and incubated with IgG control or anti-hnRNP U antibodies. 10 % of total lysate were saved as input. (a) Precipitates were analyzed for *MALT1* pre-mRNA enrichment by qPCR using primers amplifying the depicted fragments. RIP RNA fractions were normalized to RNA input and calculated relative to IgG control (IgG control set as 1). Primers amplifying in1-ex2 of *MALT1* pre-mRNA served as negative control. (b) Association with *MALT1* pre-mRNA was detected by semi-qPCR using primers amplifying the in6/ex7-in7 fragment. mRNA expression of *MALT1*, *hnRNP U* and *RP2* in the input fraction were used as controls. Depicted is the mean \pm SD (n=2) (a).

3.3.4 hnRNP U-mediated exon7 skipping depends on exon7 adjacent intronic sequences

Splicing regulation can be facilitated by binding of hnRNP or SR proteins to exonic or intronic sequences within the pre-mRNA (Chen and Manley, 2009). hnRNP U attaches to *MALT1* pre-mRNA around exon7 (see Figure 3.21), but it remains unknown whether *cis*-regulatory sequences around exon7 contribute to exon inclusion or skipping.

Therefore, we made use of a minigene containing constitutive exon3 and exon7 of the transmembrane phosphatase *CD45*, which are efficiently recognized by the splicing machinery and thus permanently spliced (Figure 3.22a) (Motta-Mena et al., 2010). In order to

investigate alternative exon7 usage, *MALT1* exon7 and adjacent intronic sequences of variable length (minigenes M5 and M6) were cloned into the *CD45* minigene, between exon3 and exon7 (Figure 3.22a). Minigenes M5 and M6 were transfected into Jurkat T cells and exon7 usage was analyzed by PCR using two vector backbone primers (Figure 3.22b). Whereas transfection of the longer construct M6 resulted in equivalent exon7 inclusion/exclusion, exon7 was almost completely skipped in cells expressing the shorter minigene M5 (Figure 3.22b), revealing that regulatory sequences around exon7 control alternative exon7 splicing. Enhanced exon7 inclusion in M6 transfected cells might be due to additional enhancer elements, which are located within M6 but are absent in M5. To elucidate the impact of hnRNP U on exon7 splicing, hnRNP U was knocked down prior to minigene transfection. hnRNP U downregulation led to enhanced exon7 inclusion in both minigenes (Figure 3.22b), which further demonstrates its negative regulatory function regarding exon7 splicing. Thus, alternative *MALT1* splicing is regulated by enhancer and silencer elements located within or in proximity to exon7. hnRNP U most probably binds to silencer sequences and thereby counteracts exon7 inclusion.

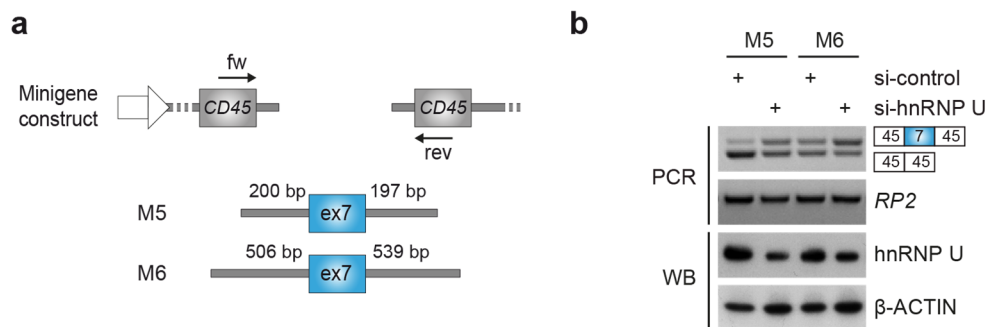


Figure 3.22: *Cis*-regulatory sequences around exon7 control alternative *MALT1* splicing. (a) Design of exon7 spanning minigenes M5 and M6. *MALT1* pre-mRNA fragments comprising exon7 were cloned into a vector harboring two constitutive *CD45* exons (exon3 and exon7). *CD45* forward (fw) and *CD45* reverse (rev) primers (indicated by arrows) were used for splicing analysis. (b) Control and hnRNP U knockdown cells were transfected with minigenes M5 or M6 and alternative exon7 inclusion was monitored by PCR utilizing *CD45*-specific primer pairs. *RP2* served as internal control. hnRNP U levels were analyzed by Western Blot, in which β-ACTIN was used as loading control.

To further localize the *cis*-regulatory sequences required for hnRNP U-mediated exon7 exclusion, four additional minigenes (M1, M2, M3 and M4) were generated by stepwise removal of intronic sequences upstream and downstream of exon7 (Figure 3.23a). Together with M5 and M6, minigenes M1, M2, M3, and M4 were transfected into Jurkat T cells and

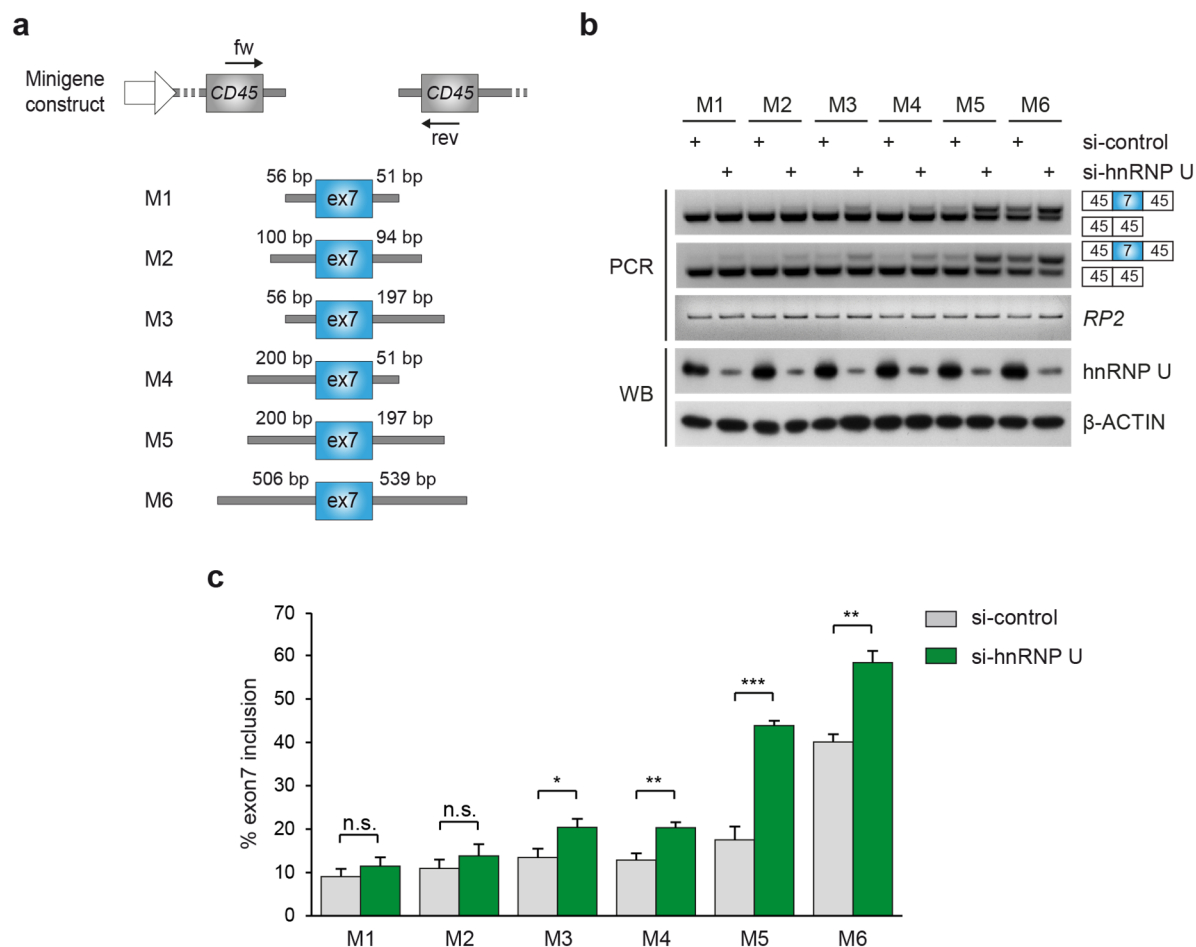


Figure 3.23: hnRNP U-mediated exon7 skipping is regulated by two regulatory sequences located 100-200 bp upstream and downstream of exon7. (a) Schematic of exon7-spanning minigenes M1-M6. *MALTI* pre-mRNA comprising minigenes harboring exon7 and flanking intronic sequences were cloned into a *CD45* exon3/exon7-containing plasmid. *CD45* forward (fw) and *CD45* reverse (rev) primers were used for splicing analysis. (b) Minigenes M1-M6 were transferred into si-control and si-hnRNP U transfected cells and afterwards analyzed for exon7 inclusion and exclusion by PCR using *CD45*-specific primers. Amplification of *RP2* was used as loading control. hnRNP U and β -ACTIN levels were analyzed by Western Blot. (c) Quantification of relative exon7 inclusion. Exon7 expression was quantified and normalized to *RP2* levels. To determine the percentage of exon7 inclusion, exon7 expression was calculated relative to total minigene expression. Data show the mean \pm SD (n=3) (c). * $p < 0.05$; ** $p < 0.01$; *** $p < 0.001$; n.s. not significant; unpaired *t*-test.

alternative exon7 usage was monitored by PCR. Again, exon7 inclusion was reduced in M5 compared to M6 expressing cells. Exon7 was almost completely excluded in shorter minigenes M1-M4 indicating the presence of exon7 surrounding silencer sequences (Figure 3.23b).

To investigate hnRNP U-related effects, exon7 splicing was monitored upon hnRNP U knockdown. While hnRNP U downregulation promoted increased exon7 inclusion in minigenes M5 and M6, exon7 was less included in M3 and M4 and was completely absent in

M1 and M2 (Figure 3.23b). Quantification of three experiments revealed that hnRNP U knockdown most strongly affected exon7 inclusion of minigene M5, which comprises 200 bp 5' and 197 bp 3' of exon7 (Figure 3.23c). As M1 and M2 are insensitive but M3 and M4 are still responsive to hnRNP U knockdown, the data suggest that hnRNP U regulated sequences are positioned between 200 bp and 100 bp 5' and 94 bp and 197 bp 3' of exon7.

3.3.5 TCR-induced exon7 inclusion in CD4⁺ T cells is modulated by hnRNP U

In previous experiments, hnRNP U was identified as a critical regulator of alternative MALT1 splicing in Jurkat T cells. To investigate whether hnRNP U also regulates TCR-mediated exon7 inclusion in primary CD4⁺ T cells, hnRNP U knockdown was performed in CD4⁺ T cells from R26/CAG-CARΔ1^{stop-fl}Cd4-Cre mice by using small hairpin RNA (shRNA) expressing adenoviruses. Thereby, two independent shRNAs against hnRNP U (hnRNP U #1 and #2) were used, and U6 empty served as control virus. Infected CD4⁺ T cells were sorted based on GFP co-expression (Figure 3.24a) and afterwards stimulated with anti-CD3/CD28 to induce exon7 inclusion. Analysis of hnRNP U transcript levels revealed that adenoviral transfer of sh-hnRNP U #1 and #2 led to efficient downregulation of hnRNP U (Figure 3.24b). To investigate the effects on MALT1 splicing, *Malt1A* and *Malt1B* mRNA levels between control and hnRNP U knockdown cells were compared. Indeed, *Malt1A* expression was increased (~ 3 fold) upon TCR stimulation in the absence of hnRNP U, whereas *Malt1B* levels were only mildly affected (Figure 3.24c).

To assess whether enhanced exon7 inclusion upon TCR ligation correlates with a decrease in hnRNP U expression, CD4⁺ T cells were stimulated with anti-CD3 and changes in *hnRNP U* transcript levels were analyzed. Surprisingly, expression of the exon7 suppressor hnRNP U was increased upon T cell stimulation, but also exon7 splicing enhancers that had been identified in both screens (like hnRNP L, hnRNP R, SRSF3) were upregulated (Figure 3.24d). In summary, one can conclude that hnRNP U acts as a regulator of TCR-induced alternative splicing of MALT1. However, the degree of exon7 inclusion might not be controlled by a single splicing factor, but rather by a complex network of splicing enhancers and silencers.

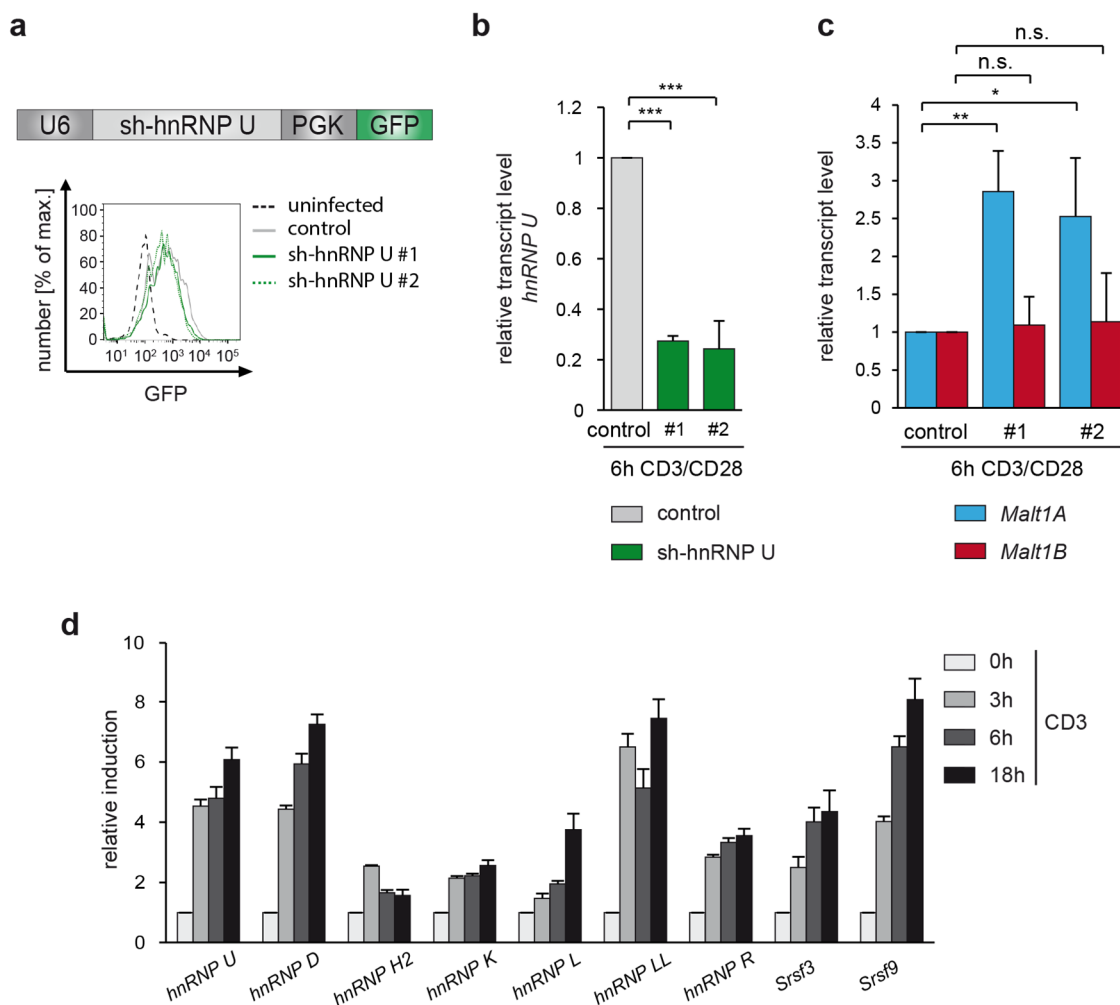


Figure 3.24: hnRNP U acts as a negative regulator of MALT1A induction in CD4⁺ T cells. (a) Scheme of adenoviral construct targeting hnRNP U knockdown. U6 promoter drives sh-hnRNP U expression, whereas PGK promoter enables GFP co-expression. Successful transduction of CD4⁺ T cells from R26/CAG-CARΔ1^{stop}-^{fl}Cd4-Cre mice with control or sh-hnRNP U adenoviruses was monitored by GFP co-expression. (b,c) After adenoviral transduction of CD4⁺ T cells with either control (U6 promoter only) or two hnRNP U adenoviruses (#1 and #2), GFP⁺ CD4⁺ T cells were sorted and stimulated with anti-CD3/CD28 stimulation for 6 h. (b) By using qPCR, *hnRNP U* knockdown was analyzed relative to *Hmbs* expression. *hnRNP U* levels in control infected cells were set to 1. (c) Analysis of *Malt1A* and *Malt1B* transcript levels of either control or sh-hnRNP U transduced cells. qPCR was performed using *Hmbs* as internal control and *Malt1* isoform expression of control infected cells was set to 1. (d) Expression levels of different *Sr* and *hnRNP* proteins in CD4⁺ T cells from Balb/c mice were investigated after anti-CD3 stimulation using qPCR. *Hmbs* levels were used for normalization and relative induction was determined relative to unstimulated cells. Depicted is the mean ± SD (n=3) (b,c,d). *p < 0.05; **p < 0.01; ***p < 0.001; n.s. not significant; unpaired *t*-test.

3.3.6 hnRNP U counteracts T cell activation

TCR stimulation induces alternative MALT1 splicing leading to MALT1A upregulation, which is required for sustained T cell activation (see section 3.2.6). As hnRNP U is critical for alternative MALT1 splicing, the question was raised whether modulation of alternative MALT1 splicing by hnRNP U also accounts for T cell activation. Therefore, we again knocked down hnRNP U by adenoviral transduction of CD4⁺ T cells from R26/CAG-CARΔ1^{stop-fl}*Cd4*-Cre mice and checked for T cell activation markers after stimulation.

Infection of CD4⁺ T cells with control or two sh-hnRNP U adenoviruses was monitored by GFP co-expression. According to sh-hnRNP U transduced cells, GFP^{low} cells represent uninfected T cells with normal hnRNP U levels, whereas GFP^{high} cells express sh-hnRNP U facilitating hnRNP U knockdown. By gating on GFP^{low} cells, no differences in CD69 or CD25 surface expression levels were observed between control and sh-hnRNP U infected cells (Figure 3.25a-c). However, GFP^{high} cells, which downregulate hnRNP U expression, display enhanced CD25 and CD69 levels in comparison to control infected cells (Figure 3.25a-c). Notably, the effects on CD69 levels were quite weak, which can be explained by the rapid upregulation of intracellular CD69 at the cell surface upon T cell activation. MFI calculation of GFP^{low} and GFP^{high} expressing cells further revealed that CD69, and especially CD25, surface expression are increased in GFP^{high} hnRNP U-depleted cells (Figure 3.25b,c). To analyze IL-2 production upon hnRNP U downregulation, we sorted for GFP⁺ CD4⁺ T cells to exclude effects from uninfected cells and measured *Ii2* transcript and IL-2 protein levels. Knockdown of hnRNP U by sh-hnRNP U #1 augmented *Ii2* mRNA levels (Figure 3.25d) and also enhanced the number of IL-2 positive cells in comparison to control infected cells (Figure 3.25e). Our findings reveal that hnRNP U negatively regulates T cell activation most likely by dampening MALT1A induction. Upon hnRNP U knockdown, MALT1A induction is enhanced resulting in a more robust CD69 and CD25 upregulation as well as IL-2 production. Taken together, the splicing factor hnRNP U counteracts exon7 inclusion and thereby modulates the cellular MALT1 isoform expression ratio, which shapes the outcome of T cell activation.

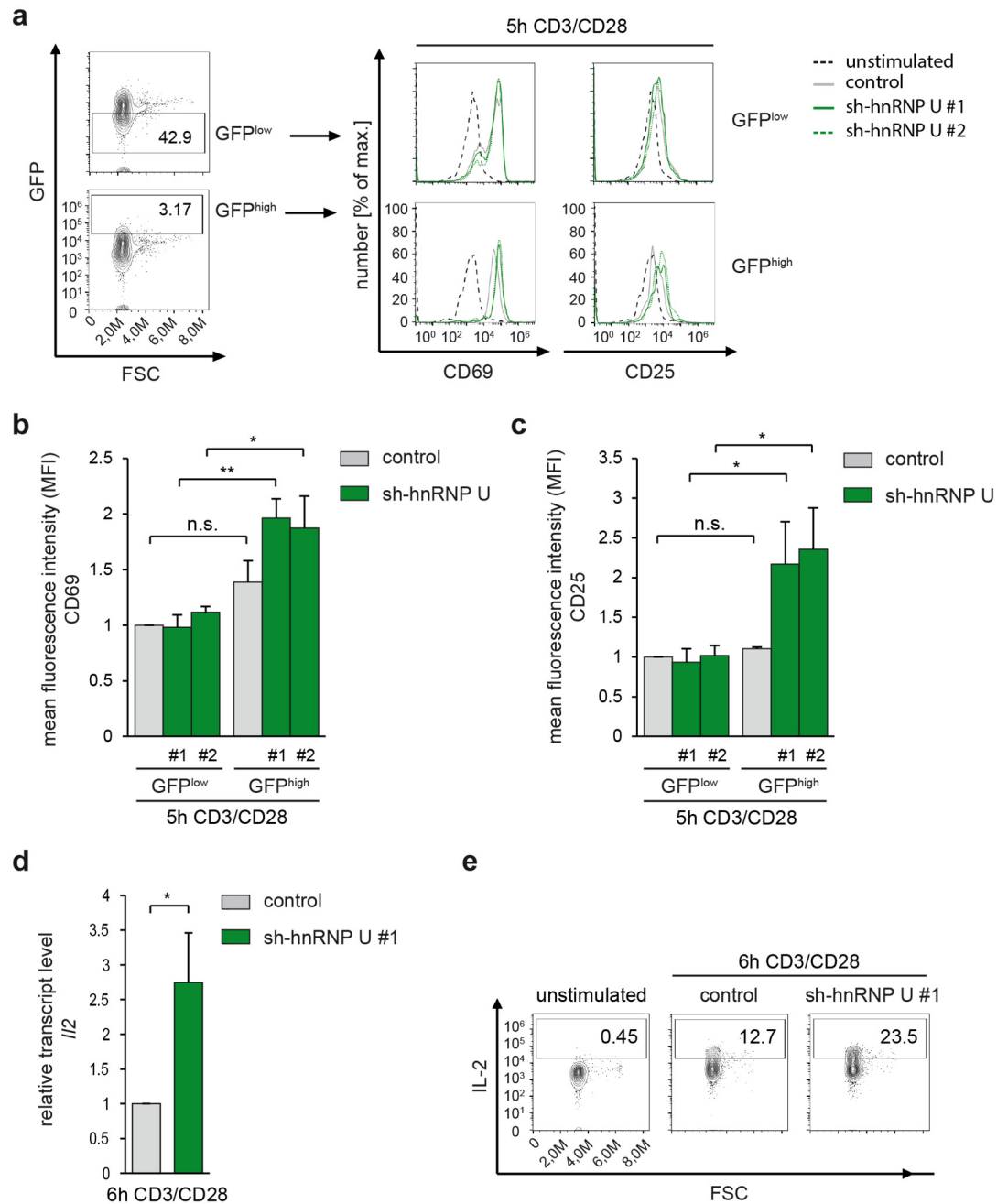


Figure 3.25: Knockdown of hnRNP U diminishes activation of CD4⁺ T cells. (a-e) CD4⁺ T cells from R26/CAG-CARΔ1^{stop-fl}Cd4-Cre mice were infected with control or sh-hnRNP U and afterwards stimulated with anti-CD3/CD28. (a) Infected cells were gated for GFP^{low} and GFP^{high} expression and analyzed for their CD69 and CD25 surface levels. (b,c) MFI values of CD69 (b) and CD25 (c) expression were compared between GFP^{low} (no hnRNP U knockdown) and GFP^{high} (hnRNP U knockdown) cells and calculated relative to control infected, GFP^{low} expressing cells. (d,e) After adenoviral transduction, GFP⁺ CD4⁺ T cells infected with control or sh-hnRNP U#1 were sorted prior to anti-CD3/CD28 stimulation. (d) Relative *Il2* mRNA levels were determined by qPCR using *Hmbs* as housekeeping gene. (e) Intracellular IL-2 levels were analyzed by flow cytometry. Depicted is the mean ± SD (n=3) (b,c,d). *p < 0.05; **p < 0.01; n.s. not significant; unpaired *t*-test

4 Discussion

Recognition of a specific antigen by the TCR activates a network of downstream signaling pathways and consequently triggers T cell activation, proliferation, and differentiation into specific effector subsets. As part of the CBM complex, MALT1 paracaspase is a key player in adaptive immune responses, and mice lacking MALT1 expression are immunodeficient (Ruefli-Brasse et al., 2003; Ruland et al., 2003). MALT1 acts as a scaffolding protein by recruiting the E3 ligase TRAF6 to promote IKK activation (Oeckinghaus et al., 2007; Sun et al., 2004), but also harbors proteolytic activity to modulate T cell responses (Coornaert et al., 2008; Rebeaud et al., 2008). Recently, high-throughput genomic studies have revealed that T cell activation is accompanied by widespread changes in alternative splicing patterns, indicating an essential role of alternative splicing for T cell functions during an immune response (Ip et al., 2007; Martinez et al., 2012). Although proteins with known immunological functions have been described to undergo alternative splicing, little is known about how alternative splicing modulates the functions of intracellular signaling mediators and how this affects T lymphocyte biology.

In the present study, it was demonstrated that expression and function of MALT1 is modulated by alternative splicing, which influences the activation of downstream signaling pathways and thereby shapes the outcome of T cell activation. Alternative splicing of MALT1 generates two splice variants, MALT1A and MALT1B, that differ in inclusion (MALT1A) or exclusion (MALT1B) of an 11 aa long exon7. TCR stimulation induces MALT1A expression, which augments MALT1 scaffolding function and fosters CD4⁺ T cell activation. The splicing factor hnRNP U negatively regulates exon7 inclusion and thereby modulates T cell activation. Based on the obtained results, one can suggest the following model (Figure 4.1). Murine, resting CD4⁺ T cells predominantly express the shorter isoform MALT1B, which lacks exon7 and only harbors the two C-terminal TRAF6 binding sites (T6BM2/3). hnRNP U impairs exon7 inclusion and thus MALT1A expression by binding to exon7 adjacent sequences within the *MALT1* pre-mRNA. Initial stimulation of primary MALT1B expressing CD4⁺ T cells results in CBM complex formation (not shown) and TRAF6 recruitment to the C-terminal T6BM3 within MALT1B leading to IKK/NF- κ B and JNK/AP-1 activation. NF- κ B and AP-1 promote target gene expression, which causes a basal induction of T cell activation markers CD69, CD25, and IL-2. Whereas MALT1A expression is still suppressed by hnRNP U upon initial stimulation, prolonged T cell activation leads to increased exon7 inclusion and thus

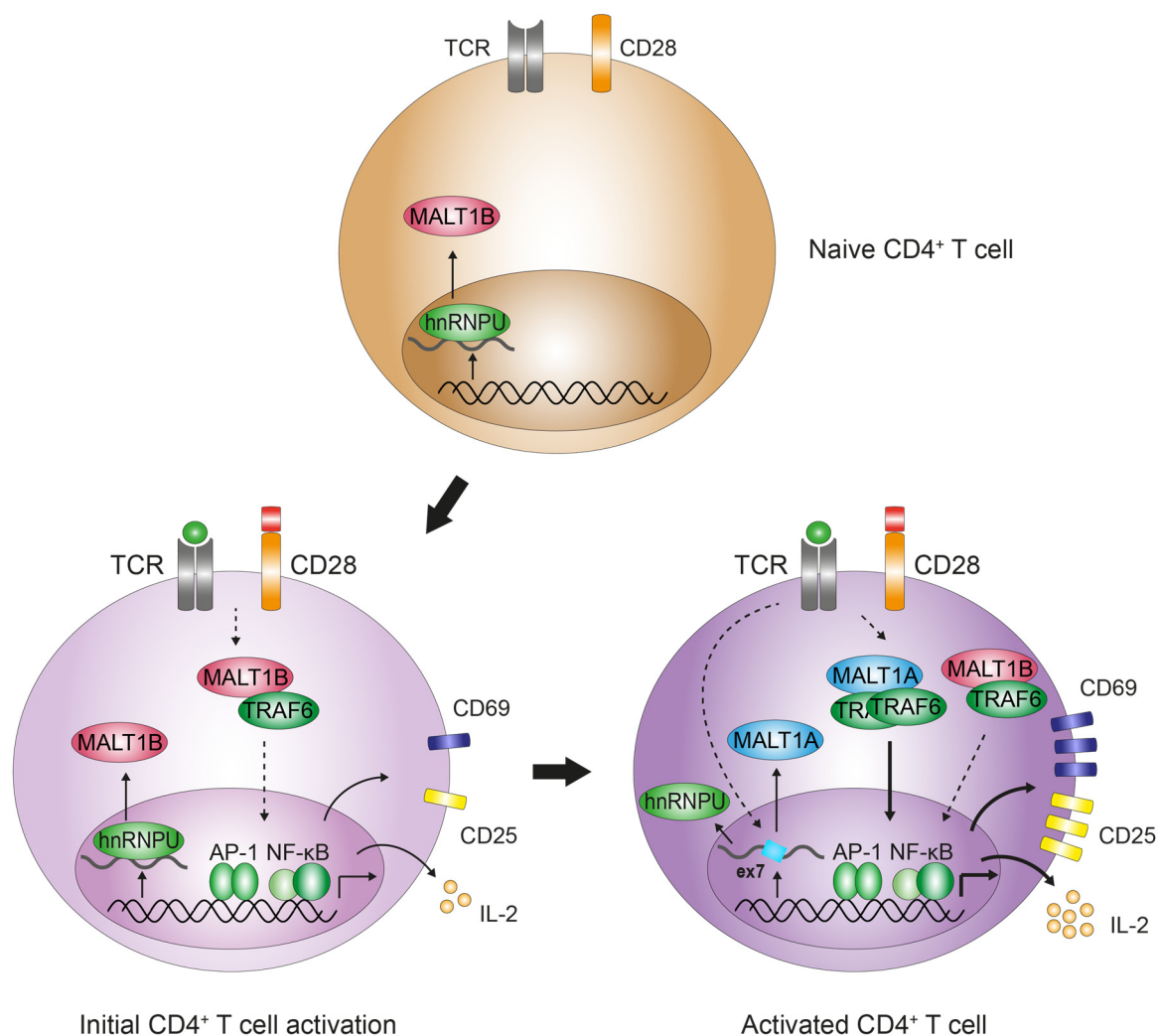


Figure 4.1: Putative model for modulation of T cell activation by alternative MALT1 splicing. In naive CD4⁺ T cells, exon7 inclusion is repressed by hnRNP U leading to the expression of the shorter splice isoform MALT1B. Upon initial T cell activation, MALT1B recruits the E3 ligase TRAF6 via its C-terminal TRAF6 binding motif promoting IKK and JNK activation (not shown), which leads to IKK/NF- κ B and JNK/AP-1 activation. As a result, T cells upregulate the activation markers CD69 and CD25 and secrete IL-2. Prolonged T cell stimulation promotes exon7 inclusion probably by releasing hnRNP U from the *MALT1* pre-mRNA leading to MALT1A induction. In contrast to MALT1B, MALT1A recruits TRAF6 via two functional TRAF6 binding sites and activates NF- κ B and JNK more strongly resulting in more robust expression of CD69, CD25, and IL-2.

MALT1A induction. Thereby, hnRNP U is probably replaced from the *MALT1* pre-mRNA. MALT1A harbors an additional functional TRAF6 binding site (T6BM1) that strongly enhances NF- κ B and slightly increases JNK signaling, forcing more robust NF- κ B and AP-1 activation, which strengthens T cell activation. Although hypoactive MALT1B is still the dominant isoform, elevated levels of the hyperactive isoform MALT1A, in combination with MALT1B, drive more robust signaling than T cells expressing solely MALT1B. Collectively,

hnRNP U controls TCR-mediated MALT1A induction, which modulates MALT1 scaffolding function to shape the outcome of T cell activation.

4.1 TCR ligation induces alternative MALT1 splicing

It is estimated that more than 90 % of mammalian multi-exon genes are alternatively spliced, with a bias towards genes that are expressed in the immune system, particularly in T cells (Lynch, 2004; Pan et al., 2008; Wang et al., 2008). High-throughput analyses revealed that many immunologically relevant kinases, phosphatases, cell surface receptors, signaling adapters and transcription factors undergo alternative splicing in response to T cell activation (Ip et al., 2007; Martinez et al., 2012). The present study demonstrates that the intracellular signaling mediator MALT1 is alternatively spliced upon TCR stimulation of murine CD4⁺ T cells. MALT1A induction was also observed in human CD4⁺ T cells isolated from peripheral blood, but to a lesser extent than in the murine system. The differences in MALT1A/MALT1B isoform levels in humans and mice might be due to the fact that the cells were isolated from different compartments (peripheral blood versus spleen and lymph nodes), where they fulfill distinct effector functions. The less efficient MALT1A upregulation in human T cells can explain why alternative exon7 usage of MALT1 was never reported in global high-throughput analyses. Those screening approaches mainly analyzed alternative splicing changes in primary human CD4⁺ T cells or Jurkat T cells, but not in murine CD4⁺ T cells (Ip et al., 2007; Martinez et al., 2012). Thereby, the stimulation-induced change in exon7 inclusion might not have reached the minimal detection threshold to be identified as a reliable alternative splicing event. It is also likely that the 33 bp long exon7 is too short to be detected in such global analyses using exon arrays. However, it was clearly demonstrated that MALT1A is significantly induced in both murine and human CD4⁺ T cells providing one of the first examples that a central regulator of TCR signaling is regulated by alternative splicing.

In the study, TCR/CD28 co-stimulation, or even TCR ligation alone, promoted MALT1A expression. Induction of MALT1A was driven by both anti-CD3/CD28 antibodies as well as OVA-peptides, but was more profound in antibody-stimulated cells, which might represent the stronger TCR stimulus. It can be assumed that MALT1A induction correlates with the strength of TCR stimulation, but further experiments using differing amounts of stimulatory antibodies or OVA-peptides need to be performed to reinforce this notion. Nevertheless, it

can be concluded that TCR-driven signaling pathways are required to activate alternative MALT1 splicing. Several immunologically relevant proteins like the co-stimulatory receptor CTLA-4 (cytotoxic T lymphocyte antigen-4) or the intracellular signaling mediator FYN have been reported to undergo alternative splicing in response to TCR stimulation, but the underlying signaling pathways mediating exon inclusion or skipping are unknown (Magistrelli et al., 1999; Rothrock et al., 2003). A more recent study demonstrates that exon2 of the JNK kinase MKK7 is excluded upon T cell stimulation and that the JNK signaling pathway itself accounts for alternative MKK7 splicing (Martinez et al., 2015). In addition, the Ras-MAPK pathway has been implicated in TCR-induced alternative splicing events, being involved in the regulation of the transmembrane phosphatase CD45, whose extracellular domain contains three variable exons that are skipped upon TCR ligation (Heyd and Lynch, 2010; Lynch and Weiss, 2000). The reported findings reveal, that not one major but rather several signaling mediators such as protein kinases are capable of triggering alternative splicing events. Since those factors often modulate the functions of regulatory splicing factors, it seems likely that TCR-induced signaling pathways alter hnRNP U activity in order to promote exon7 inclusion (see section 4.6). The signaling pathways that drive alternative MALT1 splicing could not be elucidated in the present study, but will be addressed in future experiments by selective inhibition of central signaling mediators.

Activation of alternative splicing by external stimuli mostly generates isoforms with different biological functions (Kornblihtt et al., 2013). T cell activation promotes numerous exon inclusion as well as exon exclusion events, which induce the expression of isoforms with elevated or reduced functionality (Martinez and Lynch, 2013). Alternative splicing of MALT1 is one example of how alternative splicing enriches the function of the newly generated isoform. The shorter isoform MALT1B represents the hypoactive isoform inducing moderate signaling, while the hyperactive splice variant MALT1A boosts NF- κ B and JNK activation. Although TCR ligation promoted MALT1A induction, the shorter, hypoactive variant MALT1B still remained the more abundant isoform suggesting that not the absolute protein amounts but rather the relative MALT1A vs MALT1B expression levels determine downstream effects. Elevated MALT1A levels were also observed in activated T cell subsets underscoring the relevance of an enhanced MALT1A/MALT1B ratio for T cell activation.

In addition to MALT1, also other members of the NF- κ B signaling pathway are alternatively spliced (Leeman and Gilmore, 2008). For example, stimulation of distinct cell types induces the expression of alternative splice variants of IRAK1 (interleukin 1 receptor associated

kinase 1), MyD88 (myloid differentiation factor 88) and TRAF3, which exert different effects on NF- κ B signaling than the originally expressed isoforms (Birzele et al., 2011; Janssens et al., 2002; Michel et al., 2014; Rao et al., 2005). Whereas the signal-induced isoforms of IRAK1 and MyD88 are less potent to promote NF- κ B activation, alternative TRAF3 splicing augments the NF- κ B response. Thus, activation-induced alternative splicing can both enhance and reduce cellular responses and the sum of all alternative splicing events decides to which degree a cell is activated.

By generating proteins with different functions, alternative splicing plays an important role in various cellular processes, such as cell growth, differentiation, and death (Chen and Manley, 2009). For example, relative expression of the isoforms Bcl-xS/Bcl-xL or Caspase-9a/b determines whether a cell undergoes apoptosis (Rohrbach et al., 2005; Seol and Billiar, 1999; Srinivasula et al., 1999). Moreover, alterations in the Caspase-9a/9b ratio modulate the tumorigenic capacity of non-small cell lung cancer (NSCLC) cells (Goehe et al., 2010). With respect to T cells, some alternative splicing events have been described to regulate T cell responses (Martinez and Lynch, 2013). For example, one study suggests that changes in the ratio of the Wnt-signaling associated transcription factors LEF1 (lymphoid enhancer binding factor 1) and TCF7 (transcription factor 7) might control T cell quiescence upon activation of naive CD8⁺ T cells, but the underlying mechanisms are not understood (Willinger et al., 2006). Changes in the ratio of the protein tyrosine kinase isoforms FynT and FynB have been also assumed to modulate T cell functions, since FynT upregulation promotes a more efficient IL-2 production (Davidson et al., 1992; Rothrock et al., 2003). The present study demonstrates that changes in the MALT1 isoform expression ratio impact on T cell activation and different ratios might lead to distinct T cell activation stages (see section 4.5). Single cell analyses will be required to determine precisely which MALT1 isoform expression ratio may account for inducing robust T cell responses.

4.2 hnRNP U negatively regulates exon7 inclusion

To elucidate the functional impact of alternative MALT1 splicing for T cell functions, it is critical to understand the underlying splicing mechanism. *Trans*-acting factors are key players in regulating alternative splicing as they enhance or suppress alternative exon usage (Kornbliht et al., 2013). By searching for putative candidates controlling exon7 inclusion in the *MALTI* mRNA, hnRNP U was identified as the most potent negative regulator of

alternative MALT1 splicing in two independent screening approaches in Jurkat T cells. hnRNP U is the most abundant and ubiquitously expressed hnRNP protein and has been implicated in a variety of cellular processes including mRNA stabilization (Kamma et al., 1995; Kiledjian and Dreyfuss, 1992; Yugami et al., 2007). More recent studies have revealed that hnRNP U is an important regulator of alternative splicing (Huelga et al., 2012; Vu et al., 2013; Xiao et al., 2012). Since there was no evidence that hnRNP U affects *MALTI*A or *MALTI*B mRNA stability, it is most likely that hnRNP U controls MALT1 isoform expression by counteracting exon7 inclusion. hnRNP U-mediated exon7 repression is in line with the general belief that hnRNP proteins act as splicing inhibitors (Busch and Hertel, 2012). However, within the last ten years this classical paradigm has been revised, as there are many examples of hnRNP proteins enhancing exon inclusion (Martinez et al., 2012). According to hnRNP U-regulated splicing processes, one study observed that hnRNP U promotes exon inclusion and exclusion to a similar extent, while a second study reported a preferred tendency towards exon inclusion (~70 % of alternative splicing events) (Huelga et al., 2012; Xiao et al., 2012). Nevertheless, hnRNP U clearly suppressed MALT1 exon7 splicing, which was further confirmed in an independent minigene approach. Consequently, it is not predictable whether a splicing regulator promotes exon inclusion or exclusion, because it depends on the cellular context.

hnRNP proteins can mediate splicing repression by binding to either exonic or intronic silencer elements (Kornblihtt et al., 2013). Indeed, the present study provides evidence that hnRNP U associates with the *MALTI* pre-mRNA and binding was strongly enriched in proximity to exon7 indicating the presence of silencer regions within or adjacent to exon7. Since binding studies were performed without crosslinking, it remains possible that hnRNP U does not directly target the *MALTI* pre-mRNA. hnRNP proteins act in large homopolymer complexes and it is conceivable that other complex components bridge the association between hnRNP U and its target site (Fredericks et al., 2015). Therefore, more direct binding studies such as crosslinking in combination with hnRNP U-immunoprecipitation will be performed to confirm a direct linkage between hnRNP U and *MALTI* pre-mRNA. Nevertheless, two 100 bp sequences located upstream and downstream of exon7 have been identified as putative binding regions. Of note, it is still possible that hnRNP U regulates alternative MALT1 splicing by binding to more distantly located intronic or exonic sequences within the *MALTI* pre-mRNA. To address this question, one would need to investigate the total *MALTI* pre-mRNA for putative hnRNP U binding sequences in a more global approach

using crosslinking and immunoprecipitation (CLIP). However, the interaction experiments performed in this study indicate that hnRNP U mainly associates with exon7 adjacent sequences. It has been described that hnRNP U preferentially binds to GU-rich sequences (Huelga et al., 2012; Kiledjian and Dreyfuss, 1992). The exon7 surrounding sequences were analyzed for putative silencer elements, but no striking GU-rich sequence stretches cropped up (data not shown). hnRNP U binding motifs are not well conserved, making it difficult to identify hnRNP U-responsive silencer elements. Structural studies elucidating hnRNP U binding preferences and mutational analyses of the localized 100 bp sequences could give a first hint how hnRNP U promotes exon7 skipping. Notably, hnRNP U does not solely regulate alternative splicing by sequence-specific pre-mRNA binding, but also by modulating the core splicing machinery (Xiao et al., 2012). In the latter case, hnRNP U shapes U2 snRNP maturation and thereby induces a multitude of splicing events suggesting that hnRNP U acts as a more global splicing regulator. One cannot rule out that hnRNP U contributes to exon7 skipping via interfering with the general splicing process and future studies need to unravel the exact mechanism how hnRNP U affects general splicing components. However, the preliminary identification of two putative hnRNP U binding sites upstream and downstream of exon7 suggests a “looping-out” model (Figure 4.2): hnRNP U molecules bind to two exon7 flanking silencer regions. Via protein-protein interaction, hnRNP U proteins loop out the intervening exon7 and thereby prevent splice site recognition by the spliceosome. Subsequently, exon7 is excluded resulting in the direct fusion of exon6 to exon8. Such a mechanism has already been proposed for hnRNP A1, which controls alternative splicing of its own *hnRNP A1* pre-mRNA by binding to sequences flanking alternative exon7B (Hutchison et al., 2002; Nasim et al., 2002). Although this model is rather theoretical, it provides a suitable explanation for the presence of the two exon7 flanking sequence motifs within the *MALT1* pre-mRNA.

In the screening approaches, several other splicing factors besides hnRNP U were identified that promote either exon7 inclusion (e.g. RBMS1, hnRNP L, SRSF3) or skipping (e.g. hnRNP A1, SRRM1, RBM12B). Together with the minigene approach, which revealed the presence of additional *cis*-acting RNA elements, it seems most likely that alternative *MALT1* splicing is regulated by a multitude of positive and negative regulatory *trans*-acting factors and *cis*-acting sequences rather than by hnRNP U alone. This is in line with the finding that hnRNP U can cooperate with other splicing regulators having similar or opposing effects on the alternative splicing event (Huelga et al., 2012). In addition, TCR stimulation of primary

T cells led to an upregulation of both positive and negative regulatory splicing factors, which further suggests that a complex network of splicing factors competes for MALT1 pre-mRNA binding and thereby determines the degree of exon inclusion or exclusion (see Figure 4.3 in section 4.6). To unravel the underlying splicing mechanism, the individual contribution of each splicing factor needs to be addressed in future experiments e.g. by utilizing the generated minigene system.

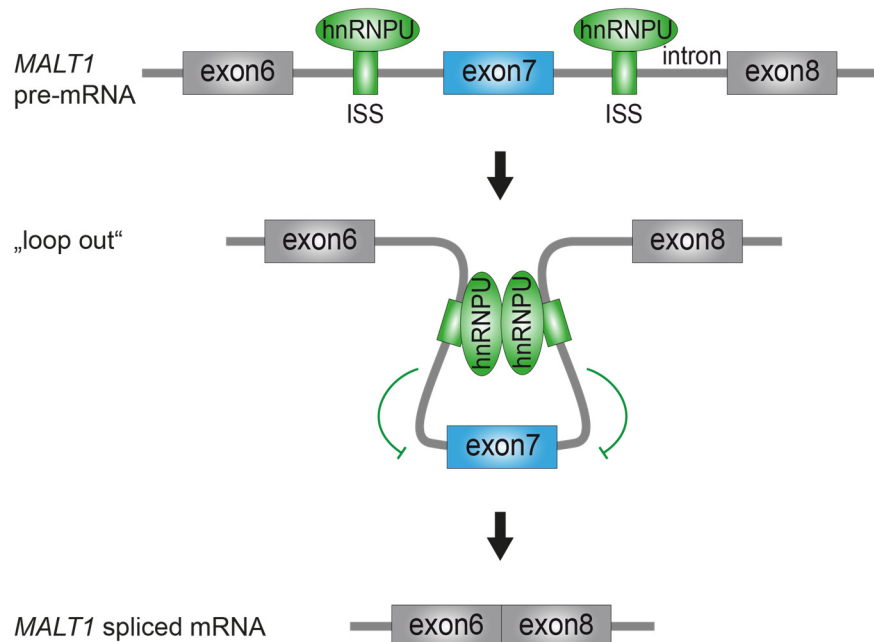


Figure 4.2: Looping out model for hnRNP U-mediated exon7 skipping. HnRNP U binds to ISSs (intronic splicing silencers; depicted in green) in the *MALT1* pre-mRNA. hnRNP U proteins interact via protein-protein interactions and “loop out” the intervening exon7. 5' and 3' splice sites of exon7 are not recognized by the spliceosome (not shown) leading to exon7 exclusion.

4.3 Exon7 inclusion augments MALT1 scaffolding function

The recruitment of TRAF6 to MALT1 has been reported to be required for the activation of the IKK/NF- κ B pathway (Oeckinghaus et al., 2007). Three TRAF6 binding sites have been mapped to MALT1, but so far only the very C-terminal TRAF6 binding motifs have been shown to contribute to TRAF6 recruitment and downstream signaling in T cells (Noels et al., 2007; Sun et al., 2004). The study provides evidence that T6BM1 encoded by exon7 recruits TRAF6 and contributes to NF- κ B activation and JNK signaling. The amount of recruited TRAF6 proteins was strongly enriched upon exon7 inclusion indicating the presence of an additional TRAF6 docking site. No complete structure of the MALT1 N-terminus is available, but one can assume that the critical glutamate (E) of T6BM1 is easily accessible. In contrast

to T6BM2 and T6BM3, the T6BM1 sequence A-V-E-C-T-E does not completely match the predicted consensus TRAF6 binding sequence P-X-E-X-X-Ar/Ac (Ar is an aromatic and Ac an acidic residue) (Ye et al., 2002). Therefore, it seems possible that T6BM1 is not a fully functional TRAF6 binding site. However, T6BM1 significantly recruits TRAF6 in our experiments. Noels et al. suggested that exon7 encodes two partial, overlapping TRAF6 binding sites, which contribute to NF- κ B activation in reporter assays (Noels et al., 2007), but our mutational analysis revealed that exon7 contains one critical glutamate and thus one TRAF6 binding motif. Moreover, the T6BM1 sequence also shows some similarities to the TRAF2 consensus binding motif P/S/T/A-X-Q/E-E suggesting that TRAF2 might also bind to T6BM1 (Ye et al., 2002). More structural information and binding studies are required to elucidate the binding properties of T6BM1.

What is the contribution of T6BM1 in conjunction with the other TRAF6 binding sites to downstream signaling? Mutational analyses in Jurkat T cells revealed that the exon7-encoded T6BM1 and the very C-terminal T6BM3 in MALT1A are relevant for signaling, whereas MALT1B only requires T6BM3. In MALT1A, one of the two T6BMs seems to be sufficient to induce full NF- κ B and JNK signaling in Jurkat T cells. In contrast, the individual TRAF6 binding motifs act more cooperatively in primary CD4⁺ T cells to mediate a full signaling response (Griesbach, 2012). One can speculate that modulation of T cell signaling strength seems to be more relevant in primary T cells than in transformed T cell lines, presumably to amplify weak TCR stimuli. Moreover, while T6BM1 and T6BM3 are functional, T6BM2 located within the Ig3 domain is dispensable for the activation of downstream signaling in Jurkat T cells. A previous study has reported that both T6BM2 and T6BM3 are relevant for signaling, but the authors only analyzed the combined mutation T6BM2/T6BM3 (Sun et al., 2004). It has been shown that the Ig3 domain plays a crucial role for MALT1 paracaspase activity, although the exact mechanism of MALT1 activation is still unknown (Wiesmann et al., 2012; Yu et al., 2011). In its inactive state the Ig3 domain adopts an auto-inhibitory conformation by folding back to the caspase-like domain, preventing MALT1 activation. Within this closed conformation the T6BM2 is most likely unable to recruit TRAF6, presumably because structural rearrangements within the Ig3 domain are required to make T6BM2 accessible for TRAF6 binding (Wiesmann et al., 2012). However, no TRAF6 binding to the T6BM2 within MALT1A or MALT1B has been detected. As CBM complex formation is not affected in cells expressing the TRAF6 binding mutants, one can exclude severe structural alterations by mutating the critical TRAF6 binding sites within MALT1. Thus,

T6BM2 seems to be a non-functional TRAF6 binding site and might be dispensable for MALT1 scaffolding function. Due to its position within the Ig3 domain, one could speculate if T6BM2 instead contributes to MALT1 paracaspase activity. It has been reported that activation of MALT1 requires monoubiquitination of K644 in the C-terminal Ig3 domain of MALT1A (Pelzer et al., 2013). Initial experiments from our group demonstrated that this process does not depend on TRAF6 (data not shown) revealing that TRAF6 binding might not be relevant for MALT1 activation. Thus, T6BM2 might fulfill other functions than recruiting TRAF6, but future structural studies are required to understand how T6BM2 might be involved in MALT1 activation.

TRAF6 is a RING-type E3 ligase that conjugates K63-linked ubiquitin chains in conjunction with the dimeric E2 enzyme Ubc13-Uev1A (Deng et al., 2000). Upon TCR ligation, TRAF6 is recruited to MALT1 leading to TRAF6 oligomerization and activation of its ligase activity (Sun et al., 2004). In turn, TRAF6 polyubiquitinates MALT1 creating a docking site for the recruitment of NEMO, which is in turn also ubiquitinated by TRAF6 (Oeckinghaus et al., 2007). In the present study, overall MALT1 ubiquitin levels and MALT1-mediated NEMO recruitment were slightly reduced in MALT1B compared to MALT1A expressing cells, suggesting that exon7 inclusion enhances TRAF6-mediated MALT1 ubiquitination and concomitant IKK complex binding. So far, it has only been reported that multiple lysine residues in the C-terminus of MALT1B are ubiquitinated by TRAF6 (Oeckinghaus et al., 2007), but it is also conceivable that TRAF6 conjugates additional ubiquitin chains to lysine residues within or adjacent to exon7 and thereby augments overall MALT1 ubiquitination. The effects on MALT1 ubiquitination were more severe upon deletion of exon7 in MALT1B than point mutation of T6BM1 in MALT1A, suggesting that the function of exon7 is not solely limited to TRAF6 recruitment. It might recruit additional E3 ligases or effector molecules, which modulate MALT1 signaling functions (see below). In addition to NEMO, MALT1 ubiquitin chains also mediate the recruitment of the TAB2/3/TAK1 complex, which promotes IKK β phosphorylation (Oeckinghaus et al., 2007; Sun et al., 2004). It was not clarified whether exon7 inclusion augments TAK1 recruitment or IKK β phosphorylation, but the fact that MALT1A ubiquitination was enhanced supports this assumption. TAK1 also serves as an upstream kinase of JNK, which stimulates the MAP2K MKK7 to promote JNK2 activation (Blonska et al., 2007). Mutations of the critical TRAF6 binding sites within MALT1 clearly abolished JNK signaling, which is in line with the observations from *Malt1* knockout mice that fail to activate JNK (Ruland et al., 2003). One can assume that T6BM1

augments MALT1 ubiquitination and thereby TAK1 recruitment, which in turn facilitates more robust activation of MKK7 and IKK β . Additional pulldown studies and IKK β kinase assays are required to unravel whether MALT1A enhances downstream signaling by augmenting activation of the TAK1/IKK β axis.

The relevance of K63-linked ubiquitin chains is underscored by the finding that T cell-specific deletion of the E2 conjugating enzyme Ubc13 impairs NF- κ B activation (Yamamoto et al., 2006). However, the relevance of TRAF6 for TCR-induced NF- κ B and JNK signaling remains questionable, since T cells from mice lacking TRAF6 expression show no abnormalities in the activation of NF- κ B and JNK upon TCR ligation (King et al., 2006). Nevertheless, this study reveals that the TRAF6 binding motifs within MALT1 are definitely required for downstream signaling. Together with the observation that single mutation of T6BM1 was less severe than exon7 deletion, one can assume that other E3 ligases might compensate for the loss of TRAF6. It has been reported that TRAF6 and TRAF2 have redundant functions, as knockdown of both proteins led to a stronger reduction of IKK activation than knockdown of one E3 ligase (Sun et al., 2004). However, no experimental evidence has been provided so far that TRAF2 associates with MALT1 or promotes MALT1 ubiquitination. Furthermore, the E3 ligase MIB2 (mindbomb E3 ubiquitin protein ligase 2) has been shown to facilitate NEMO ubiquitination in *in vitro* assays, but the relevance for CBM complex-mediated signaling remains unknown (Stempin et al., 2011). A more recent study demonstrates that the ligases cIAP1/2 support IKK activation in an oncologic scenario of BCR-driven lymphoma as they conjugate K63-linked ubiquitin chains to BCL10 (Yang et al., 2016). Whether cIAP1/2 also bind to MALT1 and mediate MALT1 ubiquitination in T cells has not been elucidated. Clearly future studies need to determine, which E3 ligases associate with MALT1 and might have redundant functions with TRAF6 to mediate MALT1 ubiquitination and subsequent IKK activation.

4.4 Alternative MALT1 splicing is dispensable for MALT1 protease activity

Besides its scaffolding function MALT1 is also a paracaspase, which is activated upon TCR stimulation and modulates T cell responses (Coornaert et al., 2008; Rebeaud et al., 2008). The enzymatic activity of MALT1 is not directly involved in IKK-mediated NF- κ B signaling, but in modulating T cell responses by cleaving substrates, which are relevant for signaling and post-transcriptional gene regulation (Bornancin et al., 2015; Gewies et al., 2014; Jaworski et

al., 2014). Inclusion of exon7 did not alter MALT1 paracaspase activity, revealing that exon7 primarily affects MALT1 scaffolding function. The production of IL-2 critically depends on MALT1 scaffolding function and is partially driven by MALT1 protease activity (Bornancin et al., 2015; Duwel et al., 2009; Jaworski et al., 2014; Oeckinghaus et al., 2007; Yu et al., 2015). Enhanced IL-2 levels were observed upon TCR-induced MALT1A upregulation in CD4⁺ T cells, which correlated with an enhanced ability to activate downstream signaling. Since there is comparable MALT1 protease activity between MALT1A and MALT1B, the more robust IL-2 production in cells with enhanced MALT1A levels is due to an increase in MALT1 scaffolding function.

MALT1 protease is essential for T cell fate decision, which was observed in *Malt1*^{-/-} and MALT1 paracaspase mutant (*Malt1*^{PM}) mice (Bornancin et al., 2015; Brustle et al., 2012; Gewies et al., 2014; Jaworski et al., 2014; Yu et al., 2015). Specifically, CD4⁺ T cells from both *Malt1*^{-/-} and *Malt1*^{PM} mice were unable to differentiate into T_H17 cells, which are known to drive pro-inflammatory responses by producing a various amount of pro-inflammatory cytokines (Bornancin et al., 2015; Brustle et al., 2012). This is in line with the results from the *in vitro* differentiation experiments, in which CD4⁺ T cells reconstituted with a catalytically inactive mutant MALT1A C464A fail to differentiate into T_H17 cells. Moreover, we also observed a decreased commitment towards the T_H1 cell lineage upon reconstitution with MALT1A C464A, whereas T_H1 cell differentiation of *Malt1*^{-/-} and *Malt1*^{PM} mice was only mildly affected (Bornancin et al., 2015; Brustle et al., 2012). Although the results might be due to the limiting differentiation and stimulation conditions, one can conclude that MALT1 protease also affects differentiation into T_H1 cells under weak stimulation conditions. In contrast, CD4⁺ T cells reconstituted with either MALT1A or MALT1B fully differentiated into T_H17 and T_H1 cells and there was no difference between MALT1A and MALT1B expressing cells. The slightly enhanced commitment of MALT1B compared to MALT1A cells might be due to different reconstitution efficiencies in the single experiments. Thus, T cell fate decisions do not depend on MALT1 scaffolding activity, but are largely controlled by MALT1 paracaspase activity. Thereby, MALT1 contributes to the generation of T_H17 effector cells by removing the post-transcriptional regulators Regnase-1 and Roquin, which dampen the upregulation of T_H17 differentiation inducing factors like IκBNS and IκBζ (Jeltsch et al., 2014; Uehata et al., 2013). Regarding other T cell subsets, the experimental setup was not optimal to monitor effects of MALT1A and MALT1B on T_H2 and Treg differentiation. Due to the fact that the generation of Treg cells also relies on MALT1

paracaspase function, it can be assumed that MALT1 isoforms would not differ in their potency to drive Treg differentiation (Bornancin et al., 2015; Gewies et al., 2014; Jaworski et al., 2014; Yu et al., 2015). However, it needs to be mentioned, that we only analyzed the differentiation potential of T cells expressing MALT1A or MALT1B only, but not different MALT1 isoform ratios. Variations in the relative MALT1 isoform expression might modulate the degree of T cell activation and thus may favor distinct cell fate decisions (see section 4.5). Single cell analyses will be a useful next step in elucidating whether relative MALT1 isoform expression modulates T cell differentiation.

MALT1 paracaspase activity has been connected to JNK signaling by cleaving the deubiquitinase CYLD (Staal et al., 2011). CYLD removes K63-linked ubiquitin chains from signaling mediators such as NEMO and TAK1 and thus serves as a negative regulator of NF- κ B and JNK signaling (Sun, 2010). Upon T cell activation, MALT1-mediated CYLD cleavage inactivates CYLD and thereby supports JNK signaling and c-Jun activation (Staal et al., 2011). The additional TRAF6 binding motif in MALT1A contributes to JNK activation and enhanced JNK phosphorylation was also observed upon MALT1A induction in primary T cells. However, MALT1 activity and CYLD cleavage were not affected by preventing MALT1A induction arguing against a role of MALT1 protease in JNK activation. This is in line with results from *Malt1^{PM}* mice that exhibit normal JNK signaling (Bornancin et al., 2015; Gewies et al., 2014; Jaworski et al., 2014), revealing that the activation of JNK relies on MALT1 scaffolding function, but not on its protease activity.

4.5 The MALT1 isoform ratio is critical for T cell activation

Although no differences in T cell differentiation have been observed, alternative MALT1 splicing clearly affected the degree of T cell activation. Elevated MALT1A levels in primary CD4⁺ T cells support the upregulation of T cell activation markers as well as IL-2 production, whereas cells with reduced MALT1A levels show moderate T cell activation. This is in line with the effects on downstream signaling, in which MALT1A upregulation promoted stronger NF- κ B and JNK signaling. IL-2 is an important T cell growth factor, and IL-2-mediated T cell proliferation is induced by its binding to its heterotrimeric cell surface receptor (Malek, 2008). It was also observed that expression of the IL-2 receptor subunit CD25 is strikingly enhanced upon MALT1A induction revealing that alternative MALT1 splicing boosts the IL-2-mediated feedback loop and concomitant T cell proliferation. These results are similar to

the observations from MALT1A and MALT1B reconstituted primary CD4⁺ T cells, in which MALT1A more potently induced IL-2 production in FACS analyses (Griesbach, 2012). As JNK signaling is dispensable for IL-2 production and concomitant T cell activation, elevated CD25 and IL-2 expression might predominantly rely on NF- κ B activation (Dong et al., 2000). Transcription of *Il2* is also driven by other transcription factors like AP-1 and NFAT (Malek, 2008), but whether AP-1 and NFAT activation are influenced upon MALT1A induction could not be elucidated during this study. In addition to IL-2, elevated CD69 levels were observed upon MALT1A induction compared to MALT1B expressing cells, but the effects were less pronounced than for CD25 and IL-2. This can be explained by the fact that a high percentage of CD69 molecules is pre-stored in intracellular vesicles and therefore rapidly upregulated upon TCR stimulation (Risso et al., 1991). Thus, the data indicate that MALT1B seems to limit T cell signaling strength and concomitant activation, while MALT1A upregulation induces stronger T cell signaling to trigger a more robust T cell response.

The relative expression of MALT1A versus MALT1B determines T cell signaling strength and the degree of T cell activation and can vary from cell to cell. It seems reasonable that different T cell activation stages might trigger distinct cell fate decisions in individual cells, as a number of reports provide evidence that not only the cytokine milieu but also the quality and the quantity of TCR signaling determine the ability to differentiate into distinct T cell subsets (Tubo et al., 2013; van Panhuys et al., 2014). One study suggests that an intermediate antigen dose promotes TH1 cell differentiation, whereas a strong TCR stimulation favors the generation of germinal center TFH cells (Baumjohann et al., 2013; Tubo et al., 2013). It was also reported that TH17 cell differentiation is favored by low-strength T cell stimulation (Purvis et al., 2010). In the present study, it was clearly demonstrated that MALT1A induction strengthens TCR signaling to NF- κ B and JNK, promoting robust T cell activation, and that MALT1A levels are sustainably enhanced in activated TFH cell subsets *in vivo*. Furthermore, TH1 and TH17 cell differentiation were slightly enhanced in MALT1B expressing cells, which only induce moderate T cell signaling. In the context of the literature, the findings suggest a model in which low MALT1A/MALT1B ratios support TH1 and TH17 cell differentiation, whereas elevated MALT1A levels favor TFH cell differentiation (Baumjohann et al., 2013; Purvis et al., 2010; Tubo et al., 2013). However, the molecular mechanisms translating distinct T cell signaling intensities into individual responses remain elusive and there are also contradictory reports proposing other antigen dosages for TH1, TH17 or TFH cell differentiation. Certainly, modulation of T cell fate decisions by TCR signaling

strength cannot be considered independently, as different cytokine milieus can guide diverse outcomes. Therefore, TCR signaling can synergize or antagonize cytokine-driven effects (Huang and August, 2015). For example, the responsiveness to IL-2 signaling largely depends on TCR-signaling strength and this dose-dependent control is critical for iTreg differentiation (Chen et al., 2003; Davidson et al., 2007; Huang and August, 2015; van Panhuys, 2016). Strong TCR signaling together with elevated IL-2 and CD25 levels upon MALT1A induction might influence the generation of iTreg cells, but further differentiation studies especially on the single cell level are required to fully understand how MALT1 isoform expression influences T cell fate decisions. Nevertheless, one can speculate that the ratio of MALT1A versus MALT1B might constitute an early bifurcation point to translate TCR signaling strength into different T cell activation stages, which differentiate into diverse effector subsets with distinct functions.

TCR-induced MALT1A induction clearly boosted activation of the NF- κ B and JNK signaling pathways, which both have been reported to influence T cell fate decisions. Activated T cell subsets express high levels of MALT1A, with the strongest upregulation being observed in T_{FH} cells. It is conceivable that elevated MALT1A levels support T_{FH} cell differentiation by inducing a strong NF- κ B response, which is in line with the findings that NF- κ B1-deficient OT-II mice were less prone to differentiate into T_{FH} cells (Serre et al., 2011). Thus, elevated NF- κ B signaling upon MALT1A induction might be one critical mechanism for driving T_{FH} cell differentiation. Moreover, NF- κ B1 is a major driver of GATA3 expression, which supports T_H2 cell differentiation (Das et al., 2001) and some components of the TCR-induced NF- κ B signaling pathway have already been associated with the generation of T_H2 cells. Ablation of PKC θ or the CBM component CARMA1 in mice inhibited T_H2 cell differentiation (Marsland et al., 2004; Medoff et al., 2006). Although no evidence was provided for a role of MALT1A or B in the generation of T_H2 cells, one can speculate whether enhanced NF- κ B signaling by elevated MALT1 isoform expression boosts T_H2 cell differentiation. Additionally, JNK signaling is involved in T cell fate decisions as MKK7-mediated JNK2 activation favors T_H1 cell differentiation (Dong et al., 2000), but the impact on the generation of other T cell effector subsets is largely unknown. Surprisingly, MALT1A expressing cells were less prone to undergo T_H1 cell differentiation compared to MALT1B cells. Again, only the effects of either MALT1A or B, but not of different MALT1 isoform ratios were analyzed. Therefore, one cannot rule out that different activation levels of NF- κ B and JNK by different MALT1 isoform ratios might favor distinct cell fate decisions.

4.6 TCR-mediated control of alternative MALT1 splicing

Alternative splicing of MALT1 is tightly regulated by hnRNP U in conjunction with other splicing regulatory proteins, which may synergize or antagonize each other, and the balance of splice factor activities determines the extent of exon7 inclusion in the mature *MALT1* mRNA. T cell stimulation leads to increased exon7 inclusion and thus MALT1A induction in primary CD4⁺ T cells, suggesting that TCR-induced signaling pathways modulate alternative MALT1 splicing mainly by altering the activity of splicing regulatory proteins. How signaling pathways shape splice factor activity is a largely unexplored field, but results from recent studies and our own experiments might give a first hint of the mechanism of TCR-induced MALT1 splicing.

Transcripts are usually associated with numerous *trans*-acting factors and subtle changes in splicing factor expression can alter the ratio of isoform expression. TCR stimulation influences the expression levels of splicing regulatory proteins, which might also be relevant for alternative MALT1 splicing (Heyd and Lynch, 2011). Indeed, TCR ligation modulated hnRNP U expression levels. Surprisingly, hnRNP U was upregulated upon stimulation, which is in conflict with the observation that MALT1A expression was simultaneously enhanced. However, at the same time putative positive regulatory splice factors, such as hnRNP R, SRSF3 and SRSF7, are induced upon TCR ligation, suggesting that alternative MALT1 splicing depends on the expression of multiple positive and negative splicing regulators. It is conceivable that increased expression of positive-regulatory splicing factors trumps the negative-regulatory impact of hnRNP U and thus promotes enhanced exon7 inclusion. One example for an alternative splicing event that is regulated by splicing factor expression levels is alternative splicing of the phosphatase CD45, which relies on the induction of hnRNP LL (Oberdoerffer et al., 2008; Topp et al., 2008; Wu et al., 2008). Upon T cell activation, hnRNP LL is upregulated and is more efficient at promoting exon repression than the basal splicing factor hnRNP L (Topp et al., 2008), but the underlying mechanism how hnRNP LL induction drives a more robust exon skipping than hnRNP L alone is still unclear. It has been suggested that both hnRNP L and hnRNP LL act independently and bind to *CD45* pre-mRNA simultaneously. Considering the increased expression of splicing regulatory proteins modulating alternative MALT1 splicing, one can assume that multiple splicing regulatory factors bind to distinct regions within the *MALT1* pre-mRNA, and that an elevated expression ratio of positive versus negative regulatory factors favors splice site selection and thus exon7

inclusion. However, it is also conceivable that splicing factors compete for *MALTI* pre-mRNA binding, in which highly expressed positive regulatory splicing factors replace negative regulatory proteins such as hnRNP U. Determining which model accounts for alternative MALT1 splicing requires the identification of responsible *cis*-regulatory elements and their *trans*-acting factors. Of note, the upregulation of relevant splicing candidates was observed on the mRNA level, but also needs to be investigated at the level of protein expression.

TCR-induced signaling pathways might not only alter splicing factor expression levels, but also their activity. Thereby, post-translational modifications especially phosphorylation events play a relevant role (Naro and Sette, 2013). Numerous signaling pathways have been implicated in several splicing processes modulating SR and hnRNP protein activity. For example, phosphorylation of the splicing factor Sam68 (Src-associated in mitosis 68 kDa) by ERK enhances Sam68-mediated variant exon5 inclusion into the *CD44* mRNA (Matter et al., 2002). Moreover, the AKT/PI3K pathway has been shown to phosphorylate hnRNP L and thereby modulate hnRNP U-regulated alternative Caspase-9a/b splicing (see below) (Vu et al., 2013). Initial inhibitor experiments in murine CD4⁺ T cells also suggest a link between TCR-induced AKT signaling and alternative MALT1 splicing (data not shown), but stimulation conditions and inhibitor concentrations need to be optimized to draw a clear conclusion. Regarding hnRNP U, it has been reported that hnRNP U is phosphorylated *in vivo* (Kiledjian and Dreyfuss, 1992) and a more recent study demonstrated that polo-like kinase 1 (PLK1) phosphorylates hnRNP U on Ser59 (Douglas et al., 2015). Whether TCR-induced AKT signaling might induce phosphorylation of hnRNP U or other splicing factors involved in alternative MALT1 splicing, needs to be further investigated. Of note, multiple other signaling pathways can be involved and might cooperate to determine the degree of exon7 inclusion.

It has been reported that signaling pathways can modulate the interaction of regulatory splice factors to their target pre-mRNAs (Heyd and Lynch, 2011; Shin and Manley, 2004; Stamm, 2008). One well-understood example of signaling-induced changes in splice factor binding properties is PTB-associated splicing factor (PSF)-mediated regulation of alternative *CD45* splicing (Heyd and Lynch, 2010). TCR ligation weakens the association of PSF and thyroid-hormone receptor-associated protein 150 (TRAP150), enabling PSF binding to *CD45* pre-mRNA mediating exon exclusion. hnRNP U preferentially binds to exon7 adjacent sequences in unstimulated Jurkat T cells. In initial RIP studies, we observed a reduced association of

hnRNP U with the *MALTI* pre-mRNA upon anti-CD3/CD28 stimulation in Jurkat T cells (data not shown), which indicates a stimulation-induced release of hnRNP U from its target site. Thereby, signaling pathways might alter hnRNP U binding affinities, as it has been shown for alternative caspase-9a/b splicing (Vu et al., 2013). In this study, hnRNP U positively regulates exon3 inclusion by binding to an RNA *cis*-regulatory element in the *caspase-9* pre-mRNA, leading to an enhanced ratio of the longer splice variant caspase-9a versus the shorter isoform caspase-9b. AKT signaling limits exon3 inclusion, as it phosphorylates the repressor protein hnRNP L, which results in enhanced binding of hnRNP L to the same RNA sequence element. Whether hnRNP L also counteracts the association of hnRNP U with *MALTI* pre-mRNA, needs to be addressed in further binding studies. The finding that several positive regulators, including hnRNP L, were identified in the two screening approaches indicates that hnRNP U could be replaced by multiple factors. How TCR-induced signaling might weaken hnRNP U binding to *MALTI* pre-mRNA is highly speculative. It is conceivable that TCR-induced signals induce structural alterations in hnRNP U and thereby affect the RNA-binding motif and its interaction to other protein regulators. Such structural changes have been reported for a number of SR proteins including SRSF1 (Ser/Arg-rich splicing factor 1) (Cho et al., 2011), but are largely unexplored for hnRNP proteins. Thus, structural studies will be important in order to understand hnRNP U binding properties.

Signaling pathways also impact on the subcellular localization of regulatory splicing factors. hnRNP proteins are concentrated in the nucleus, but can shuttle between the nucleus and the cytosol to facilitate mRNA export (Pinol-Roma, 1997). Therefore it is not surprising that signaling pathways might induce changes in the relative localization of splicing regulatory factors (Lynch, 2007). One well-documented example is hnRNP A1, which is phosphorylated and concomitantly degraded in the cytosol in response to osmotic shock preventing its association with nuclear transport factors and thus its nuclear accumulation (Guil et al., 2006; van der Houven van Oordt et al., 2000). Initially, it was reported that hnRNP U does not shuttle between nucleus and cytosol, and is restricted to the nucleus (Pinol-Roma and Dreyfuss, 1992). This observation has been revised, however, by a more recent study demonstrating that TLR signaling stimulates nuclear to cytoplasmic translocation of hnRNP U in macrophages (Zhao et al., 2012). Whether this event depends on hnRNP U phosphorylation is unclear. It is likely that TCR-induced signaling alters the nuclear-cytoplasmic distribution of hnRNP U, which favors binding of positive-regulatory factors to

MALTI pre-mRNA. Therefore, hnRNP U expression levels need to be examined in nuclear and cytosolic lysates in the course of stimulation.

The results of this study demonstrate that hnRNP U controls TCR-mediated exon7 inclusion, but additionally indicate that alternative *MALTI* splicing is regulated by a more complex network of splicing regulators. One can speculate the following model (Figure 4.3).

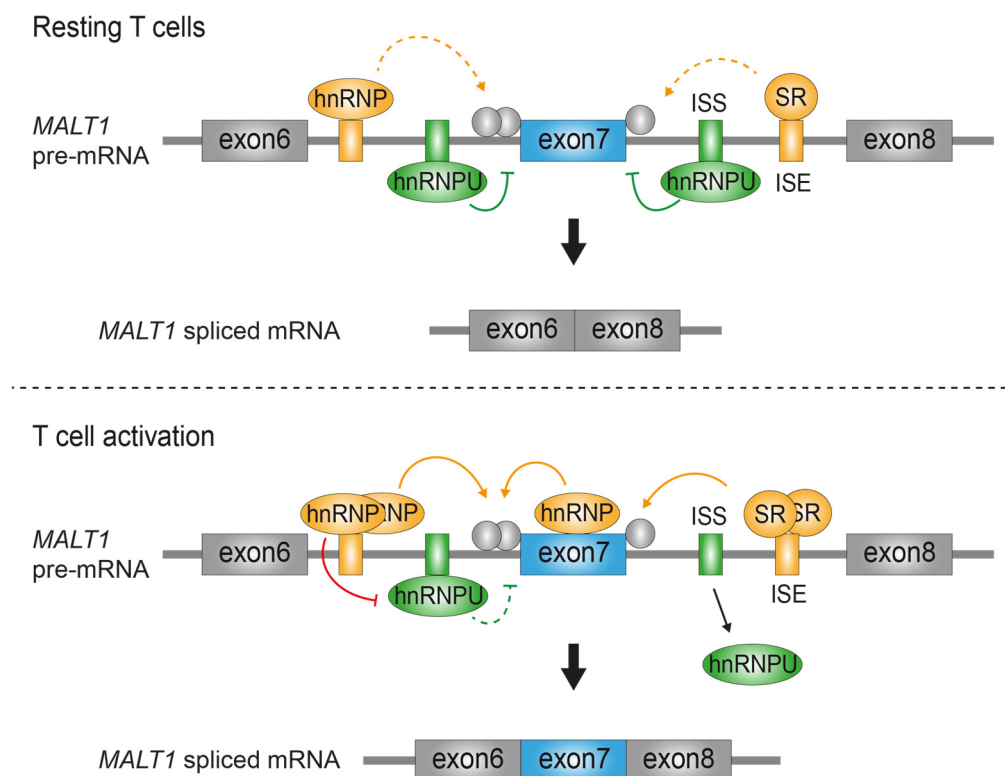


Figure 4.3: Model for the regulation of exon7 inclusion by multiple splicing factors. In resting T cells, the splicing silencer hnRNP U bind to ISSs (intronic splicing silencers; depicted in green) and positive regulatory hnRNP and SR proteins associate with enhancer elements such as ISEs (intronic splicing enhancers; depicted in yellow) within the *MALTI* pre-mRNA. hnRNP U is the dominant splicing regulator, which prevents exon7 splice site recognition by the spliceosome (depicted in grey) and thereby mediates exon7 exclusion. Upon T cell activation, both positive regulatory splicing factors and hnRNP U are induced leading to enhanced binding of positive splicing regulators, which exceed hnRNP U-mediated exon7 repression. In addition, hnRNP U might be released from the *MALTI* pre-mRNA due to a decreased affinity to its target sequences and might be exported into the cytosol. As a result, exon7 is included in the mature *MALTI* mRNA.

In resting T cells, *MALTI* pre-mRNA is bound by both hnRNP U and other positive-regulatory splicing factors. hnRNP U is the dominant splicing regulator promoting enhanced exon7 repression. Upon TCR ligation, signaling pathways are activated and increase overall splicing factor expression. Enhanced expression of positive regulatory splicing factors exceeds hnRNP U-mediated exon7 repression, leading to an enhanced degree of exon7

inclusion. Signaling pathways might also weaken hnRNP U-*MALTI* pre-mRNA binding or increase the association of positive regulatory factors with *MALTI* pre-mRNA. Moreover, the nuclear concentration of hnRNP U might be decreased due to enhanced nuclear export upon TCR ligation. It can be assumed that TCR-induced signaling regulates the functions of splicing factors implicated in alternative MALT1 splicing not by one simple mechanism, but rather by multiple steps that are required to fine tune T cell responses.

4.7 Conclusion and perspectives

Understanding the regulation of T cell responses by alternative splicing is a field of intensive research, however, the underlying mechanisms and the functional impact of those events are largely unexplored. In the present study, it was revealed that robust T cell signaling and activation requires alternative splicing of MALT1, which is controlled by a complex network of splicing factors including the negative regulator hnRNP U. It was observed that not the absolute amount, but rather the relative MALT1A versus MALT1B expression level seems to determine the degree of downstream T cell signaling and activation. Thus far, the impact of alternative MALT1 splicing has been investigated in cellular pools, but cell populations can be highly heterogeneous, meaning that MALT1 isoform levels can vary from cell to cell. Therefore, it will be a useful next step to analyze MALT1A and MALT1B expression on the single cell level by qPCR to determine whether different ratios promote distinct T cell activation stages. In this respect, it will be important to examine MALT1 isoform expression levels in activated T cell subsets and to dissect the role of different isoform ratios for T cell fate decisions.

Inclusion of exon7 in MALT1A encodes for an additional TRAF6 binding site and this was shown to enhance MALT1 scaffolding function, but not MALT1 paracaspase activity. To date, no structure of the complete MALT1 protein has been solved. Furthermore, although structures of individual MALT1 domains have been published, the structure of the entire N-terminus has not been reported. Crystallization of the N-terminus including exon7 will be necessary to understand the contribution of exon7 to MALT1A scaffolding function. MALT1A was more potent to promote JNK and NF- κ B signaling than MALT1B. It remains to be addressed whether this increase in JNK and NF- κ B activation relies on enhanced IKK activation and TAK1 binding. Therefore, additional pulldown experiments monitoring TAK1 recruitment, as well as IKK β kinase assays are required to elucidate the stronger ability of

MALT1A to stimulate downstream signaling. Moreover, mass spectrometry approaches using cells expressing MALT1A, MALT1B, and MALT1A/B TRAF6 binding mutants could reveal differences in the recruitment of downstream signaling mediators and help to identify unknown binding partners. It would be of particular interest to determine whether other E3 ligases than TRAF6 are recruited to MALT1 and mediate MALT1 ubiquitination.

Alternative MALT1 splicing critically depends on the splicing regulator hnRNP U. The putative binding sequences were narrowed to two 100 nt sequences in proximity to exon7 using a minigene approach in Jurkat T cells. hnRNP U binding can be studied using X-link IP, which directly crosslinks hnRNP U to radiolabeled RNA fragments and thus enables the visualization of hnRNP U/RNA complexes. Reducing those RNA fragments up to 20 nt in combination with distinct point mutations could be a useful strategy to pinpoint both hnRNP U binding motifs. Characterized sequences could be further studied using our established minigene system. Since multiple other splicing factors like hnRNP D, hnRNP L, hnRNP R or SRSF3 modulate alternative MALT1 splicing, it will be necessary to dissect the individual contribution of splicing regulators for exon7 inclusion. Therefore, combined knockdown of hnRNP U and other putative factors using the minigene system would reveal whether they act synergistically, antagonistically or completely independently. Moreover, determining which signaling pathways affect alternative MALT1 splicing will uncover more details about the mechanisms regulating this process. Analyzing MALT1 isoform expression and splicing factor activity following pharmacologic inhibition of critical signaling mediators such as AKT, JNK and GSK3 in primary CD4⁺ T cells would help to elucidate the connection between TCR-induced signaling pathways and alternative exon7 inclusion. In this respect, it would be relevant to address whether TCR ligation alters the phosphorylation status, binding affinities, and subcellular localization of critical splicing factors.

The present study has demonstrated that alternative MALT1 splicing has a critical role in regulating T cell functions in *ex vivo* experiments. However, MALT1 is also involved in the activation of other immune cells like B cells, mast cells and macrophages (Jaworski and Thome, 2015). Generating transgenic mouse lines expressing either MALT1A (*Malt1^{A/A}*) or MALT1B (*Malt1^{B/B}*) would be a suitable strategy to expand upon this *ex vivo* model and to elucidate the physiological relevance of alternative MALT1 splicing not only for T cell responses, but also other immune cell types. Thereby, the CRISPR/Cas9 technique can be used to generate isoform selective mouse strains. Given the results of MALT1A and MALT1B on T cell activation, one can expect that mice, which exclusively express the

hyperactive variant MALT1A, will display a more activated phenotype. It is also conceivable that MALT1A expressing mice will develop signs of autoimmune diseases and inflammation. In order to obtain a global view of the extent of the effects of alternative MALT1 splicing, it will be interesting to characterize the overall immune system of MALT1 isoform-specific mice and to monitor the activation of signaling pathways in lymphocytes and other immune cells. Moreover, MALT1 isoform selective mice might reveal whether alternative MALT1 splicing is involved in the development of immunological disorders, information that could provide promising new therapeutic avenues. Additionally, elevated MALT1A levels were not only observed upon T cell activation, but also in several B cell lymphoma cell lines (data not shown). Future studies could extend from this finding to determine the role of alternative MALT1 splicing in the development and maintenance of lymphomas.

In summary, this study has uncovered a novel mechanism by which T cell function is controlled: alternative splicing of the paracaspase MALT1. The thesis contributes to a better understanding of the functions of a central player in lymphocyte activation and represents an important starting point for future studies addressing the impact of alternative MALT1 splicing on the overall immune system and for the development of diseases.

5 Materials

5.1 Instruments and equipment

Agarose gel chambers	NeoLab, Heidelberg
Autoradiography MP films	GE Healthcare, Freiburg
Bacterial culture flasks	BD, Heidelberg
Cell-counting chamber Neubauer	NeoLab, Heidelberg
Cell culture flasks	BD, Heidelberg
Cell culture plates	BD, Heidelberg; Nunc, Rochester, USA
Cell strainer (100 μ M)	NeoLab, Heidelberg
Centrifuges:	
Centrifuge Avanti J-26 XP	Beckmann Coulter, Krefeld
Cell culture centrifuge, 5804	Eppendorf, Hamburg
Cooling cell culture centrifuge, 5810R	Eppendorf, Hamburg
Cooling table centrifuge, 5417R	Eppendorf, Hamburg
Table centrifuge, 5471C	Eppendorf, Hamburg
Chemiluminescence ECL films	GE Healthcare, Freiburg
CO ₂ incubators	Binder, Tuttlingen
Cryo tubes	Greiner Bio-One, Frickenhausen
Developer Optimax	Protec, Dorfwiesen
DNA/RNA UV Cleaner Box	Biosan, Riga, Latvia
Electroporation cuvettes, Gene Pulser	Bio-Rad, München
Electroporator, Gene Pulser Xcell System	Bio-Rad, München
EMSA gel chamber, X952.1	Roth, Karlsruhe
Film Cassettes	Roth, Karlsruhe
Flow Cytometers:	
Attune Acoustic Focusing Cytometer	Life Technologies, Carlsbad, USA
LSR II	BD, Heidelberg
Freezers	Liebherr, Ochsenhausen
Geldocumentation System	Intas, Göttingen

Gel dryer 583	Bio-Rad, München
Heatblock	Techne, Staffordshire, UK
Incubators	Sartorius, Göttingen; Heraeus, Hanau
Incubator Shaker I26	New Brunswick Scientific, Hamburg
Irradiation chamber HWM-D 2000 ¹³⁷ Cs	Wälischmiller Engineering, Markdorf
LightCycler480	Roche, Mannheim
LightCycler plates 96 well	4titude, Berlin
MACS columns	Miltenyi Biotec, Bergisch Gladbach
MACS rack	Miltenyi Biotec, Bergisch Gladbach
Magnetic rack	Qiagen, Hilden
Magnetic stirrer	IKA Labortechnik, Staufen
Microscopes	Leica, Wetzlar
Microtiter plate (U- or V-shape), 96-well	Greiner Bio-One, Frickenhausen
Microwave	SHARP, Hamburg
Nanodrop 2000	Thermo Fisher Scientific, Waltham, USA
Petri dishes	Greiner Bio-One, Frickenhausen
pH-Meter	Sartorius, Göttingen
Photometer	Eppendorf, Hamburg
Photometer µQuant	Bio-Tek, Bad Friedrichshall
Pipettes	Eppendorf, Hamburg
Plastic cuvettes	Brand, Wertheim
Plastic filter tips TipOne (RNase free)	StarLab, Hamburg
Plastic pipettes	Greiner Bio-One, Frickenhausen
Plastic tips	Eppendorf, Hamburg
Power supplies	Consort, Turnhout, Belgium
Precision scales	Kern, Balingen
PVDF membrane	Merck Millipore, Darmstadt
Rotator	NeoLab, Heidelberg
SDS-PAGE chamber	Roth, Karlsruhe
Semi-dry blotter	PHASE, Lübeck; Peqlab, Erlangen

Sorter:

FACS Aria Cell Sorter	BD, Heidelberg
FACS Star plus	BD, Heidelberg
Streptavidin-coated plates	Thermo Fisher Scientific, Waltham, USA
Thermocycler	Eppendorf, Hamburg
Thermomix comfort	Eppendorf, Hamburg
Tissue Culture Hoods Safeflow 1.2	Nunc, Wiesbaden
Tubes	Eppendorf, Hamburg
Typhoon Scanner	GE Healthcare, Freiburg
ViCell-XR cell viability analyzer	Beckman Coulter, Krefeld
Vortexer	Scientific Industries, Bohemia, USA
Whatman paper	Roth, Karlsruhe
Water Bath	Thermo HAAKE, Karlsruhe

5.2 Chemicals

5.2.1 General chemicals

Adenosine triphosphate (ATP)	Sigma-Aldrich, Taufkirchen
Acrylamide/Bisacrylamide	Roth, Karlsruhe
Agar	Roth, Karlsruhe
Agarose	Biozym, Hessisch Oldendorf
Ammonium persulfate (APS)	Bio-Rad, München
Ampicillin	Roth, Karlsruhe
Atufect transfection reagent	Silence Therapeutics, Berlin
Autoradiography developing solution	Sigma-Aldrich, Taufkirchen
Autoradiography fixing solution	Sigma-Aldrich, Taufkirchen
Boric acid	Roth, Karlsruhe
Bovine serum albumin (BSA)	GE Healthcare, Freiburg
Brefeldin-A	Sigma-Aldrich, Taufkirchen
Calcium chloride	Roth, Karlsruhe

Disodium hydrogen phosphate	Roth, Freiburg
Dimethyl sulfoxide (DMSO)	Sigma-Aldrich, Taufkirchen
DNA 1kb plus ladder	Invitrogen, Carlsbad, USA
dNTP-Mix	Thermo Fisher Scientific, Waltham, USA
Dithiothreitol (DTT)	Sigma-Aldrich, Taufkirchen
Ethylenediaminetetraacetic acid (EDTA)	Roth, Freiburg
Ethyleneglycol-bis(2-aminoethylether)- N,N,N',N'-tetraacetic acid (EGTA)	Sigma-Aldrich, Taufkirchen
Ethanol (p. a.)	Merck, Darmstadt
Ethidiumbromide	Roth, Freiburg
Ethidium monoazide bromide	Sigma-Aldrich, Taufkirchen
Ficoll 400	Roth, Freiburg
Glycerol	Roth, Freiburg
Glycine	Roth, Freiburg
Heparine	Sigma-Aldrich, Taufkirchen
HEPES	Roth, Freiburg
Isopropyl alcohol (p.a.)	Merck, Darmstadt
LB	Roth, Freiburg
Lumi-Glo ECL reagent	NEB, Frankfurt
Lymphoprep	Stemcell Technologies, Köln
Magnesium chloride	Roth, Freiburg
Methanol (p.a.)	Merck, Darmstadt
Nonidet P40 substitute (NP-40)	Sigma-Aldrich, Taufkirchen
PageRuler Prestained Protein Ladder	Thermo Fisher Scientific, Waltham, USA
Paraformaldehyde (PFA)	Sigma-Aldrich, Taufkirchen
Phenol:chloroform:isoamylalcohol (125:24:1)	Thermo Fisher Scientific, Waltham, USA
Polybrene	Sigma-Aldrich, Taufkirchen
Poly dI-dC	Roche, Mannheim
Potassium chloride	Roth, Freiburg
Potassium hydrogen phosphate	Roth, Freiburg
Protease inhibitor mix (Roche complete)	Roche, Mannheim

Protein-G-Sepharose	Invitrogen, Carlsbad, USA
Protein loading buffer (Rotiload)	Roth, Freiburg
Saccharose	Roth, Freiburg
Saponine	Roth, Freiburg
Sodium acetate	Roth, Freiburg
Sodium azide	Roth, Freiburg
Sodium chloride	Roth, Freiburg
Sodium dodecyl sulfate (SDS)	Roth, Freiburg
Sodium fluoride	Sigma-Aldrich, Taufkirchen
Sodium vanadate	Roth, Freiburg
Strep-Tactin Sepharose	IBA, Göttingen
Sulfate latex beads	Life Technologies, Carlsbad, USA
Sulfuric acid	Merck, Darmstadt
Tetramethylethylenediamine (TEMED)	Roth, Freiburg
Tris(hydroxymethyl)-aminomethan (Tris)	Roth, Freiburg
TritonX-100	Roth, Freiburg
Trypan blue	Invitrogen, Carlsbad, USA
Tween 20	Roth, Freiburg
X-tremeGENE HP Transfection Reagent	Roche, Mannheim
³² P- α -dATP	Perkin Elmer, Wiesbaden
β -Glycerophosphate	Sigma-Aldrich, Taufkirchen
β -Mercaptoethanol	Roth, Freiburg

5.2.2 Cell culture

DMEM, Gibco	Life Technologies, Carlsbad, USA
Fetal calf serum (FCS)	Life Technologies, Carlsbad, USA
L-glutamine	Life Technologies, Carlsbad, USA
IMDM	Life Technologies, Carlsbad, USA
Non-essential amino acids (NEAA)	Life Technologies, Carlsbad, USA
Optimem	Life Technologies, Carlsbad, USA

Penicillin/streptomycin (P/S)	Life Technologies, Carlsbad, USA
RPMI 1640	Life Technologies, Carlsbad, USA
RPMI 1640 (advanced)	Life Technologies, Carlsbad, USA
Sodium pyruvate	Life Technologies, Carlsbad, USA
Trypsin/EDTA	Life Technologies, Carlsbad, USA
β -Mercaptoethanol	Life Technologies, Carlsbad, USA

5.2.3 Stimulants, inhibitors and cytokines

Actinomycin D	Sigma-Aldrich, Taufkirchen
Ionomycin	Calbiochem, Schwalbach
Murine IL-12	BD, Heidelberg
Murine IL-6	R&D Systems, Minneapolis, USA
Murine TGF β	R&D Systems, Minneapolis, USA
Ovalbumin peptide (OVA, chicken, aa 323-339)	Biotrend, Köln
Phorbol 12-myristate 13-acetate (PMA)	Merck Millipore, Darmstadt

5.3 Enzymes and Kits

CD4 ⁺ T cell Isolation Kit (mouse)	Miltenyi Biotec, Bergisch Gladbach
CD4 ⁺ T cell Isolation Kit (human)	Miltenyi Biotec, Bergisch Gladbach
DreamTaq DNA polymerase	Thermo Scientific, Waltham, USA
Dynabeads human T-Activator CD3/CD28	Life Technologies, Carlsbad, USA
Gel Extraction Kit	Qiagen, Hilden
Herculase II DNA Polymerase	Agilent Technologies, Waldbronn
Indol-1	Life Technologies, Carlsbad, USA
Magna RIP TM Kit	Merck Millipore, Darmstadt
KAPA SYBR FAST qPCR Mastermix	Peqlab, Erlangen
Klenow Polymerase	NEB, Frankfurt
LightCycler 480 SYBR Green I Mastermix	Roche, Mannheim
Naive CD4 ⁺ T cell Isolation Kit, mouse	Miltenyi Biotec, Bergisch Gladbach

QIAshredder	Qiagen, Hilden
QIAQuick Nucleotide Removal Kit	Qiagen, Hilden
PCR Purification Kit	Qiagen, Hilden
Plasmid Maxi Kit	Qiagen, Hilden
Plasmid Mini Kit	Qiagen, Hilden
Proteinase K	NEB, Frankfurt
Rapid DNA ligation Kit	Roche, Mannheim
Restriction enzymes	NEB, Frankfurt
Restriction buffers	NEB, Frankfurt
RNaseH	Life Technologies, Darmstadt
RNeasy RNA isolation Kit	Qiagen, Hilden
RQ1 RNase-Free DNase	Promega, Mannheim
Superscript First Strand Synthesis Kit	Invitrogen, Carlsbad, USA
SuperScript II Reverse Transcriptase	Invitrogen, Carlsbad, USA
T4 DNA ligase	NEB, Frankfurt
3,3',5,5'-Tetramethylbenzidine (TMB)	eBioscience, Frankfurt am Main
Verso cDNA Synthesis Kit	Thermo Fisher Scientific, Waltham, USA

5.4 Mice strains

BALB/c	Charles River
C57BL/6	Charles River or Jackson Laboratory
<i>Malt1</i> ^{-/-} and <i>wt</i>	from J. Ruland and A. Gewies (Klinikum rechts der Isar, Technische Universität München)
R26/CAG-CARΔ1 ^{stop-fl} <i>Cd4</i> -Cre	a truncated, signaling-deficient version of the human CAR receptor is expressed in CD4 ⁺ T cells making them susceptible for adenoviral transduction (Heger et al., 2015); obtained from M. Schmidt-Supprian (Klinikum rechts der Isar, Technische Universität München)
<i>Malt1</i> ^{-/-} R26/CAG-CARΔ1 ^{stop-fl} <i>Cd4</i> -Cre	from J. Ruland and A. Gewies (Klinikum rechts der Isar, Technische Universität München)

OT-II (C57BL/6Tg(TcraTcrb)425Cbn/Crl) express α - and β -chain TCR that pairs with the CD4 co-receptor and is specific for chicken ovalbumin (OVA, 323-339); obtained from Charles River

5.5 Eukaryotic cell lines

A549 human lung adenocarcinoma epithelial cell line

HEK293A human embryonic kidney cell line; contains stably integrated copy of the E1 gene that is required to generate recombinant adenovirus

HEK293T human embryonic kidney cell line; transformed with SV40 large T antigen

Jurkat T cells human T cell line; derived from acute T cell leukemia

MALTI^{-/-} Jurkat T cells human T cell line; exon2 was deleted by CRISPR/Cas9 (generated by T. Gehring, AG Krappmann)

MEF mouse embryonic fibroblasts

5.6 Bacteria

TOP10 *Escherichia coli*, F-mcrA Δ (mrr-hsdRMS-mcrBC) ϕ 80lacZ Δ M15 Δ lacX74 nupG recA1 araD139 Δ (ara-leu)7697 galE15 galK16 rpsL(StrR) endA1 λ -

5.7 Vectors and oligonucleotides

5.7.1 Vectors

General vectors	Information
pcAT7-CDMS2	Minigene vector with constitutive exon3 and exon7 of the <i>CD45</i> gene (Motta-Mena et al., 2010). Obtained from Prof. Dr. Florian Heyd.
pHAGE-PGK-L1-h Δ CD2-T2A	Lentiviral vector. Obtained from Dr. Marc Schmidt-Supprian.
pHAGE-PGK-L1-h Δ CD2-T2A-Flag-Strep-Strep (pHAGE-StrepTagII; mock)	Flag-Strep-Strep-Tag was cloned into pHAGE-PGK-L1-h Δ CD2-T2A by <i>SalI/SalI</i>

Table 1: List of general vectors.

Additional vectors	Information
pHAGE-MALT1A-Strep	MALT1 cDNA was transferred into pHAGE-StrepTagII (<i>NotI/SalI</i>).
pHAGE-MALT1A T6BM1 EA-Strep	Point mutation (E316A) was introduced by PCR-based mutagenesis. MALT1 cDNA was transferred into pHAGE-StrepTagII (<i>NotI/SalI</i>).
pHAGE-MALT1A T6BM3 EA-Strep	Point mutation (E806A) was introduced by PCR-based mutagenesis. MALT1 cDNA was transferred into pHAGE-StrepTagII (<i>NotI/SalI</i>).
pHAGE-MALT1A T6BM1/3 EA-Strep	Point mutations (E316A/E806A) were introduced by PCR-based mutagenesis. MALT1 cDNA was transferred into pHAGE-StrepTagII (<i>NotI/SalI</i>).
pHAGE-MALT1B-Strep	MALT1 cDNA was transferred into pHAGE-StrepTagII (<i>NotI/SalI</i>).
pHAGE-MALT1B T6BM2 EA-Strep	Point mutation (E642A) was introduced by PCR-based mutagenesis. MALT1 cDNA was transferred into pHAGE-StrepTagII (<i>NotI/SalI</i>).
pHAGE-MALT1B T6BM3 EA-Strep	Point mutation (E795A) was introduced by PCR-based mutagenesis. MALT1 cDNA was transferred into pHAGE-StrepTagII (<i>NotI/SalI</i>).
pHAGE-MALT1B T6BM2/3 EA-Strep	Point mutations (E642A/E795A) were introduced by PCR-based mutagenesis. MALT1 cDNA was transferred into pHAGE-StrepTagII (<i>NotI/SalI</i>).
Minigene pcAT7 M1	Genomic <i>MALT1</i> region (intron6 56 bp-exon7-intron7 51 bp) was amplified by PCR from human genomic clone pBACe3.6 (Source BioScience) and cloned into pcAT7-CDMS2 (<i>BglII/BglII</i>).
Minigene pcAT7 M2	Genomic <i>MALT1</i> region (intron6 100 bp-exon7-intron7 94 bp) was amplified by PCR from human genomic clone pBACe3.6 (Source

	BioScience) and cloned into pcAT7-CDMS2 (<i>BgIII/BgIII</i>).
Minigene pcAT7 M3	Genomic <i>MALTI</i> region (intron6 56 bp-exon7-intron7 197 bp) was amplified by PCR from human genomic clone pBACe3.6 (Source BioScience) and cloned into pcAT7-CDMS2 (<i>BgIII/BgIII</i>).
Minigene pcAT7 M4	Genomic <i>MALTI</i> region (intron6 200 bp-exon7-intron7 51 bp) was amplified by PCR from human genomic clone pBACe3.6 (Source BioScience) and cloned into pcAT7-CDMS2 (<i>BgIII/BgIII</i>).
Minigene pcAT7 M5	Genomic <i>MALTI</i> region (intron6 200 bp-exon7-intron7 197 bp) was amplified by PCR from human genomic clone pBACe3.6 (Source BioScience) and cloned into pcAT7-CDMS2 (<i>BgIII/BgIII</i>).
Minigene pcAT7 M6	Genomic <i>MALTI</i> region (intron6 506 bp-exon7-intron7 539 bp) was amplified by PCR from human genomic clone pBACe3.6 (Source BioScience) and cloned into pcAT7-CDMS2 (<i>BgIII/BgIII</i>).
pMD2.G	Lentiviral envelope plasmid (Addgene ID 12259)
psPAX2	Lentiviral packaging plasmid (Addgene ID 12260)

Table 2: List of additional vectors.

5.7.2 shRNAs

Primary adenoviruses containing shRNAs against hnRNP U were obtained from Sirion Biotech, München.

shRNA	Sequence 5'-3'
sh-hnRNP U #1	CCATAACTGTGCAGTTGAATT
sh-hnRNP U #2	GGCTGGTCACTAACCACAAGT

Table 3: Sequences of shRNAs for adenoviral knockdown of hnRNP U.

5.7.3 siRNAs and morpholino

siRNA libraries:

siGENOME smart pool siRNA library (radioactive PCR) Dharmacon, Lafayette, USA

ON-TARGET*plus* smart pool siRNA library (qPCR) Dharmacon, Lafayette, USA

Smart pool siRNAs:

si-control (ON-TARGET*plus* Non-Targeting Pool) Dharmacon, Lafayette, USA

si-hnRNP U (ON-TARGET*plus* smart pool siRNA,
human hnRNP U) Dharmacon, Lafayette, USA

individual siRNAs: Eurogentec, Seraing, Belgium

siRNA	Sequence 5'-3'
si-control	si-GFP
si-hnRNP U #1	ACAGAAAGGCGGAGAUAAAUU
si-hnRNP U #2	GAAGAAAGAUUGUGAAGUUUU
si-hnRNP U #3	GAUGAAGACUAUAAGCAAAUU

Table 4: Sequences of individual siRNAs.

Morpholino (MO) sequences:

GeneTools, Philomath

Morpholino	Sequence 5'-3'
AMO	GAACCAAAGGATTGCACTACCTTCA
cMO	CCTCTTACCTCAGTTACAATTTATA

Table 5: Sequences of morpholinos.

5.7.4 EMSA oligonucleotides

Target	Sequence 5'-3'
NF- κ B (H2K) fw	GATCCAGGGCTGGGGATTCCCCATCTCCACAGG
NF- κ B (H2K) rev	GATCCCTGTGGAGATGGGGAATCCCCAGCCCTG
OCT1 fw	GATCTGTGGAATGCAAATCACTAGAA
OCT1 rev	GATCTTCTAGTGATTTGCATTCGACA

Table 6: EMSA oligonucleotide sequences.

5.7.5 Primer for qPCR and semi-qPCR

Target (mouse)	Sequence 5'-3'
<i>Malt1</i> ex6 fw	ACCGAGACAGTCAAGATAGC
<i>Malt1</i> ex9/10 rev	GACTTTGTCCTTTGCCAAAGG
<i>Malt1</i> ex5 fw	AAGTCCTATGCCTCACTACCAGTG
<i>Malt1</i> ex7/8 rev	GTTTAATTCATCTTCAGTGCCTCC
<i>Malt1</i> ex6/8 rev	GATGCCCAAATTGTTTAATTCATCTATG
<i>Hmbs</i> fw	GCGCTAACTGGTCTGTAGGG
<i>Hmbs</i> rev	TGAGGGAAAGGCAGATATGGAGG
<i>Il2</i> fw	GAGTGCCAATTCGATGATGAG
<i>Il2</i> rev	AGGGCTTGTTGAGATGATGC
<i>hnRNP U</i> fw	ATCTCGAGAGACCGTCTGAG
<i>hnRNP U</i> rev	CTTCACCAAGCAACATTCCAC
<i>hnRNP D</i> fw	TGCAACTTATCCCCAACAGG
<i>hnRNP D</i> rev	TCCATTCAGGAACTTGATAGAAAA
<i>hnRNP H2</i> fw	CATACCTGAAGTGGATTTTCTGTC
<i>hnRNP H2</i> rev	CTGACCTTCACCACGAACC
<i>hnRNP K</i> fw	TCTGAAGATCGGATCATTACCA
<i>hnRNP K</i> rev	TCTTGCATTAGAATCCTTCAACAT
<i>hnRNP L</i> fw	TGACTGAGGAGAACTTCTTTGAGA
<i>hnRNP L</i> rev	CTCTTCGAGTCCCCTCCAG
<i>hnRNP LL</i> fw	AGACATGATGGCTATGGATCGC
<i>hnRNP LL</i> rev	CACTAACCATTACAACGGAGCCA

<i>hnRNP R</i> fw	TCTGGAAGAGTTCAGTAAAGTCACA
<i>hnRNP R</i> rev	GTGCTGCTGACTTGTGATCC
<i>Srsf3</i> fw	TCGTCGTCCTCGAGATGATT
<i>Srsf3</i> rev	CCTATCTCTAGAAAGTGACCTGCTC
<i>Srsf9</i> fw	CGAGATCGAGCTCAAGAACC
<i>Srsf9</i> rev	GTAACCGTTTCTTCCATAGATCG

Table 7: Murine primer sequences.

Target (human)	Sequence 5'-3'
<i>MALT1</i> ex6 fw (radioactive PCR)	TAATGATCGAGACAGTCAAGATAGC
<i>MALT1</i> ex9/10 rev (radioactive PCR)	AACCTTGTCCTTCGCCAAAG
<i>MALT1A</i> fw	GAAGGTAGAAATCATCATAGGAAG
<i>MALT1A</i> rev	GCTTTGAGCTTGGGGTGCTCC
<i>MALT1B</i> fw	AAGCCCTATTCCTCACTACCAGTGG
<i>MALT1B</i> rev	GGATGACCAAGATTATTTAATTCATCTATG
<i>RP2</i> fw	GCACCACGTCCAATGACAT
<i>RP2</i> rev	GTGCGGCTGCTTCCATAA
<i>PPIB</i> fw	CCAGGGGAGATGGCACA
<i>PPIB</i> rev	CTTCGCACCACCTCCA
<i>GAPDH</i> fw	ACCACAGTCCATGCCATCAC
<i>GAPDH</i> rev	TCCACCACCCTGTTGCTGTA
<i>18S</i> rRNA fw	GCTTAATTTGACTCAACACGGGA
<i>18S</i> rRNA rev	AGCTATCAATCTGTCAATCCTGTC
<i>hnRNP U</i> fw	CGGTCCTCAAATGAAAGGA
<i>hnRNP U</i> rev	CTATGGCCACCACCTCTGTT
<i>MALT1</i> in1-ex2 fw	TGGAAGAAAGCTGTTGACTTGA
<i>MALT1</i> in1-ex2 rev	TCCTTCAGGCTCCAGTACCTT
<i>MALT1</i> in5-ex6 fw	TGTTATGTTTTGGAGCGTATTTTT
<i>MALT1</i> in5-ex6 rev	CAAATCCACATAAGGCACCTA
<i>MALT1</i> ex6-in6 fw	GACAGTCAAGATAGCAAGAAG
<i>MALT1</i> ex6-in6 rev	CTTTGCTTAATTAACGTTGCAG
<i>MALT1</i> in6/ex7-in7 fw	TTTTCTGAAACAAGGAAGAACAGA

<i>MALTI</i> in6/ex7-in7 rev	GTAGGCTAAAAGCACTCCAC
<i>MALTI</i> in7 fw	AGAACCTAACTGTATTGCAAATGTATG
<i>MALTI</i> in7 rev	CTTCAGTATTAGGCTCAACTCATT
<i>MALTI</i> in7/ex8-in8 fw	ACACTATAACATGATTCACTGGC
<i>MALTI</i> in7/ex8-in8 rev	TGTATTACTCACCAGGATGACC
<i>MALTI</i> in8 fw	AAAGAAGAATGTTGTATAGGGAAAGC
<i>MALTI</i> in8 rev	TGTCCACTACTGTCCGGGAGAT
<i>MALTI</i> ex9-in9 fw	AGCCTTTGGGTGAGTAGAAC
<i>MALTI</i> ex9-in9 rev	AGCCTCCTCTTCTAAACCTTC
<i>CD45</i> fw (minigene)	GGGAGCTTGGTACCACGCGTCGACC
<i>CD45</i> rev (minigene)	CAGCGCTTCCAGAAGGGCTCAGAGTGG

Table 8: Human primer sequences.

5.8 Antibodies

5.8.1 Antibodies for cell purification, stimulation and differentiation

anti-CD28 (37.51)	BD, Heidelberg
anti-CD28 (37N)	produced by V. Heissmeyer and E. Kremmer
anti-CD3 (145-2C11)	BD, Heidelberg
anti-CD3 (145-2C11)	produced by V. Heissmeyer and E. Kremmer
anti-IFN γ (Xmg1.2)	produced by V. Heissmeyer and E. Kremmer
anti-IL-12 (C17.8)	produced by V. Heissmeyer and E. Kremmer
anti-IL-2 (JES6-5H4)	Miltenyi Biotec, Bergisch Gladbach
anti-IL-4 (11B11)	produced by V. Heissmeyer and E. Kremmer
anti-TCR β -Biotin	eBioscience, Frankfurt am Main
rabbit anti-syrian hamster IgG	JacksonImmunoResearch, Newmarket, UK

5.8.2 FACS antibodies

anti-CD2-APC (RPA-2.10)	eBioscience, Frankfurt am Main
anti-CD25-PE (PC61.5)	eBioscience, Frankfurt am Main
anti-CD4-PE-Cy7 (GK1.5)	eBioscience, Frankfurt am Main

anti-CD4-PerCP (RM4-5)	eBioscience, Frankfurt am Main
anti-CD44-AlexaFluor 405 (IM7)	Caltag, Buckingham, UK
anti-CD45.2-APC-Cy7 (30-F11)	eBioscience, Frankfurt am Main
anti-CD62L-AlexaFluor 647 (MEL-14)	BioLegend, San Diego, USA
anti-CD69-APC (H1.2F3)	eBioscience, Frankfurt am Main
anti-CXCR5 (RF8B2, unconjugated)	BD, Heidelberg
anti-IFN γ -APC (XMG1.2)	eBioscience, Frankfurt am Main
anti-IL-2-APC (JES6-5H4)	eBioscience, Frankfurt am Main
anti-IL-2-FITC (JES6-5H4)	eBioscience, Frankfurt am Main
anti-IL-17A-PE (eBio17B7)	eBioscience, Frankfurt am Main
anti-PD-1-FITC (J43)	eBioscience, Frankfurt am Main
biotinylated goat anti-rat IgG	Abcam, Cambridge, UK
Streptavidin-PE	BD, Heidelberg

5.8.3 Primary antibodies for Western Blot

anti- β -ACTIN (I-19)	Santa Cruz, Heidelberg
anti-BCL10 (EP606Y)	Abcam, Cambridge, UK
anti-CARMA1 (1D12)	NEB, Frankfurt am Main
anti-CYLD (E10)	Santa Cruz, Heidelberg
anti-ERK (442704)	Merck Millipore, Darmstadt
anti-hnRNP U (3G6)	Abcam, Cambridge, UK
anti-I κ B α (L35A5)	NEB, Frankfurt am Main
anti-JNK1/2 (9252)	NEB, Frankfurt am Main
anti-MALT1 (mouse, 2494)	NEB, Frankfurt am Main
anti-MALT1 (human, B12)	Santa Cruz, Heidelberg
anti-MALT1 (mouse, H300)	Santa Cruz, Heidelberg
anti-MALT1A (GRTDEAVEC)	produced by E. Kremmer
anti-NEMO (Clone 54, WB)	BD, Heidelberg
anti-NEMO (FL-419, IP)	Santa Cruz, Heidelberg
anti-phospho-ERK (9101)	NEB, Frankfurt am Main

anti-phospho-I κ B α (9246)	NEB, Frankfurt am Main
anti-phospho-JNK (9255)	NEB, Frankfurt am Main
anti-phospho-p38 (9211)	NEB, Frankfurt am Main
anti-p38 (C-20)	Santa Cruz, Heidelberg
anti-TRAF6 (EP591Y)	Abcam, Cambridge, UK

5.8.4 Secondary antibodies for Western Blot

HRP-conjugated anti-rabbit	JacksonImmunoResearch, Newmarket, UK
HRP-conjugated anti-mouse	JacksonImmunoResearch, Newmarket, UK
HRP-conjugated anti-goat	JacksonImmunoResearch, Newmarket, UK

5.8.5 RNA-binding protein immunoprecipitation (RIP) antibodies

anti-hnRNP U (CS207320)	Merck Millipore, Darmstadt
normal mouse IgG (CS200621)	Merck Millipore, Darmstadt

5.9 Buffers and solutions

Agar plates:	LB (20 g/l), Agar (15 g/l)
Annealing buffer:	Tris-HCl pH 8.0 (50 mM), NaCl (70 mM)
B1 buffer:	PBS (1x), BSA (0.1 % (w/v)), EDTA (2 mM)
Blocking buffer:	BSA in PBS-T (3 % (w/v))
Blotting buffer:	Tris pH 8.3 (48 mM), Glycine (39 mM), Methanol (20 % (v/v)), SDS (0.03 % (w/v))
CB buffer:	PBS (1x), BSA (0.5 % (w/v)), EDTA (2 mM)
Co-IP buffer:	HEPES pH 7.5 (25 mM), NaCl (150 mM), Glycerol (1 mM), NP-40 (0.2 % (v/v)), DTT (1 mM), NaF (10 mM), β -Glycerophosphate (8 mM), NaVanadate (300 μ M), Protease inhibitor mix
DNA loading buffer:	Glycerol (30 %), Orange G (0.35 %)
FACS buffer:	PBS (1x), FCS (2 % (w/v)), NaN ₃ (0.01 % (v/v))

IC buffer:	PBS (1x), Saponine (0.5 % (w/v)), NaN ₃ (0.01 % (v/v))
High-salt buffer:	HEPES pH 7.9 (20 mM), NaCl (350 mM), Glycerol (20 % (v/v)), MgCl ₂ (1 mM), EDTA (0.5 mM), EGTA (0.1 mM), NP-40 (1 %), DTT (1 mM), NaF (10 mM), β-Glycerophosphate (8 mM), NaVanadate (300 μM), Protease inhibitor mix
LB medium:	LB (20 g/l)
PBS (1x):	NaCl (137 mM), Na ₂ HPO ₄ (10 mM), KCl (2.7 mM), KH ₂ PO ₄ (1.7 mM)
PBS-T (WB):	PBS, Tween-20 (0.1 % (v/v))
PBS-T (ELASA):	PBS, Tween-20 (0.05 % (v/v))
Poly dI-dC:	Poly dI-dC (2 mg/ml), Tris pH 8.0 (10 mM), NaCl (100 mM)
Polyacrylamide gel, native:	TBE buffer (1x), Acrylamide/Bisacrylamide (5 %), APS (0.75 % (v/v)), TEMED (0.075 % (v/v))
Proteinase K buffer (RIP):	RIP wash buffer (1x, Merck Millipore), SDS (1 % (v/v)), Proteinase K (12 % (v/v))
RIP lysis buffer:	RIP lysis stock (1x, Merck Millipore), Protease inhibitor cocktail (0.5 % (v/v)), RNase inhibitor (0.25 % (v/v))
RIP IP buffer:	RIP wash buffer (1x, Merck Millipore), EDTA (2 mM), RNase inhibitor (0.55 % (v/v))
SDS electrophoresis buffer (1x):	Tris pH 8.8 (25 mM), Glycine (192 mM), SDS (0.1 % (w/v))
Separation gel:	Tris/HCl pH=8.8 (375 mM), Acrylamide/Bisacrylamide (7.5-11 %), SDS (0.1 %), APS (0.075 %), TEMED (0.05 %)
Shift buffer (2x):	HEPES pH 7.9 (20 mM), KCl (120 mM), Ficoll (4 % (w/v))
Stacking gel:	Tris/HCl pH 6.8 (125 mM), Acrylamide/Bisacrylamide (5 %), SDS (0.1 %), APS (0.1 %), TEMED (0.1 %)
Stripping buffer:	Glycine (0.2 M), SDS (0.1 %), Tween-20 (1 % (v/v)), pH 2.2
TAC (Tris ammonium chloride) lysis buffer:	Tris pH 7.2 (20 mM), NH ₄ Cl (0.83 % (w/v))
TBE buffer:	Tris (50 mM), Boric acid (50 mM), EDTA (1 mM), pH 8.3
TE (Tris EDTA) buffer:	Tris/HCl pH 8.0 (10 mM), EDTA (1 mM)

6 Methods

6.1 Cell culture

6.1.1 Storage of cell lines

For the storage of suspension or adherent cells, 1×10^7 cells were pelleted and resuspended in 1 ml freezing medium (DMEM/RPMI, 20 % FCS, 15 % DMSO). After transfer into cryo tubes, samples were put into an isopropanol-containing freezing chamber over night at -80°C . For long-term storage, cells were stored in liquid nitrogen.

6.1.2 Cultivation of adherent cells

A549, HEK293T, HEK293A and MEF cells were cultured in DMEM medium supplemented with 10 % FCS and 100 U/ml P/S. Cells were splitted after they reached 80 % confluency. To detach cells from dishes, cells were washed with PBS and treated with 0.5–1.5 ml 0.05 % trypsin/EDTA solution for approximately 5 min. The reaction was stopped by adding fresh DMEM medium. Finally, cells were diluted in flasks or seeded in appropriate dishes for further experiments.

6.1.3 Cultivation of suspension cells

For cultivation of Jurkat T cells, RPMI medium supplemented with 10 % FCS and 100 U/ml P/S was used. Jurkat T cells were kept at a density between 0.5×10^6 and 1.5×10^6 cells/ml. Primary murine CD4^+ T cells were cultured in RPMI medium supplemented with 10 % heat-inactivated FCS, 1 % P/S, 1 % NEAA, 1 % HEPES, 1 % L-glutamine, 1 % sodium pyruvate and 0.1 % β -mercaptoethanol. For primary human CD4^+ T cells, advanced RPMI medium supplemented with 10 % heat-inactivated FCS and 2 mM L-glutamine was used.

6.1.4 Isolation and cultivation of primary murine CD4^+ T cells

For stimulation and knockdown experiments, primary murine CD4^+ T cells were isolated from spleen and lymph nodes (axial, inguinal and cervical) from BALB/c, OT-II or R26/CAG-CAR $\Delta 1^{\text{stop-fl}}$ *Cd4*-Cre mice by negative magnetic-activated cell sorting (MACS)

selection using the murine CD4⁺ T cell isolation kit (Miltenyi Biotec). First, spleen and lymph nodes were put into primary T cell medium (RPMI medium + 10 % heat-inactivated FCS, 1 % P/S, 1 % NEAA, 1 % HEPES, 1 % L-glutamine, 1 % sodium pyruvate and 0.1 % β -mercaptoethanol) and grinded through a cell strainer (100 μ M). To separate the cells from residual tissue particles, the homogenate was pelleted by centrifugation (1300 rpm, 8 min). Afterwards, the pellet was resuspended in TAC lysis buffer for 5 min on ice to destroy erythrocytes. Samples were washed, centrifuged and refiltered through a cell strainer to further eliminate residual tissue particles. The remaining cells were resuspended in ice-cold CB buffer (500 μ l/mouse) before adding a cocktail of biotin-conjugated antibodies (100 μ l/mouse, Miltenyi Biotec) to deplete non-CD4⁺ T cells. After incubation for 5 min at 4 °C, samples were filled up with 300 μ l of ice-cold CB buffer and incubated with magnetically labeled anti-biotin microbeads (200 μ l/mouse, Miltenyi Biotec) for 10 min at 4 °C. Finally, the cell suspension was applied to LS columns (Miltenyi Biotec) in a MACS separator, whereby the magnetically labeled cells were retained in the columns and the unlabeled CD4⁺ T cells were enriched in the flow-through. The separated CD4⁺ T cells were pelleted and resuspended in an appropriate volume of primary T cell medium. For differentiation experiments, naive CD4⁺ T cells from *wt*, *Malt1*^{-/-} or *Malt1*^{-/-}R26/CAG-CARΔ1^{stop-fl}*Cd4*-Cre mice were isolated using the naive, murine CD4⁺ T cell isolation kit (Miltenyi Biotec), which additionally contains anti-CD62L antibodies in the biotin-conjugated antibody cocktail.

6.1.5 Isolation and cultivation of primary human CD4⁺ T cells

For isolation of human CD4⁺ T cells, blood was taken from healthy donors and treated with heparine (1000 U/50 ml blood). Blood was centrifuged (300 x g, 10 min, RT, no break) to separate plasma (upper layer), buffy coat (intermediate layer) and erythrocytes (lowest layer). After removal of the plasma fraction, the intermediate buffy coat layer containing leukocytes and platelets was collected (approx. 10-18 ml/50 ml blood) and diluted with PBS up to a volume of 35 ml. To isolate mononuclear cells (MNCs), diluted buffy coat was carefully layered onto 15 ml Lymphoprep density gradient medium (Stemcell Technologies) and centrifuged (160 x g, 20 min, RT, no break). About 20 ml supernatant were removed without touching the next layer and the sample was again centrifuged (350 x g, 20 min, RT, no break). Finally, the intermediate layer containing the MNCs was collected and washed three times with PBMC buffer B1 (300 x g, 8 min, 4 °C). CD4⁺ T cells were isolated by negative MACS

selection using the human CD4⁺ T cell isolation kit (Miltenyi Biotec) according to the manufacturer's instructions (see 6.1.4). Purified cells were resuspended in human, primary T cell medium (Advanced RPMI 1640 + 10 % heat-inactivated FCS, 1 % P/S, 2 mM L-glutamine) at a density of 2×10^6 cells/ml. Written consent and approval by the ethics board of the Medical Faculty at the Technical University Munich was obtained for the use of peripheral blood from healthy donors.

6.1.6 Immunization and isolation of different murine T cell subsets

To obtain CD4⁺CD62L⁺CD44⁻ naive T cells, CD4⁺CD62L⁻CD44⁺ effector T cells and CD4⁺CXCR5⁺PD-1⁺ T_{FH} cells, BALB/c mice were immunized i.v. with approx. 2×10^8 sheep erythrocytes (Acila AG). After one week, spleens were collected, homogenized and single cell suspensions were prepared. To enrich for T cells, B cells were depleted by using anti-CD19 microbeads (Miltenyi, 10 μ l per 10^7 cells) according to the manufacturer's instructions. Samples are loaded onto MACS columns and CD19⁺ cells are retained within the columns. Purified cells were stained with the following antibodies and reagents for 20 min at 4 °C: anti-CXCR5, biotinylated goat anti-rat IgG, Streptavidin-PE, anti-CD4-PerCP, anti-PD-1-FITC, anti-CD62L-AlexaFluor 647 and anti-CD44-AlexaFluor 405. After washing, different T cell subsets (CD4⁺CD62L⁺CD44⁻ naive T cells, CD4⁺CD62L⁻CD44⁺ effector T cells and CD4⁺CXCR5⁺PD-1⁺ T_{FH} cells) were sorted on a FACS Aria cell sorter (BD) and subsequently lysed in Trizol for RNA extraction. Immunization, purification and sorting were performed by J. Kranich, Institute for Immunology, LMU München.

6.2 Cell transfection and transduction

6.2.1 Transfection of Jurkat T cells by electroporation

Transfection of Jurkat T cells with minigene constructs (M1–M6) was performed by electroporation. Thereby electric pulses are used to induce pores in the cell membrane, which enable the uptake of foreign DNA. 2.5×10^6 Jurkat T cells in 200 μ l Jurkat T cell medium were mixed with 1 μ g plasmid DNA and transferred into an electroporation cuvette (0.4 cm). Cells were electroporated at 180 V and 1000 μ F using a Gene Pulser (Bio-Rad) and transferred into pre-warmed RPMI medium. Cells were analyzed after 24 h of incubation.

6.2.2 Transfection of Jurkat T cells with siRNA and morpholino

Transfection of cells with siRNAs enables silencing of specific genes by promoting mRNA degradation, a process that is known as RNA interference (RNAi). A siRNA represents a short RNA stretch of about 21–23 nt and interacts with the RNA-induced silencing complex (RISC). The guide strand of the siRNA guides the RISC complex to complementary target mRNAs promoting mRNA destruction. For siRNA transfection, 0.5 μ l siRNA (100 μ M stock) was diluted in 100 μ l Optimem medium and mixed with 100 μ l of a mixture containing 1 μ l Atufect (1 μ g/ml) and 99 μ l Optimem. Atufect contains cationic lipids, which bind siRNAs and form liposomes that are taken up by the cell via fusion with the cell membrane. After 30 min incubation at 37 °C, the siRNA mixture was added dropwise to $0.5 \times 10^6/800 \mu$ l Jurkat T cells. Cells were feeded with 1 ml medium 6 h post transfection and further cultivated until 48 h post transfection.

Morpholinos (MO) are nonionic DNA analogs that bind to specific target sites in the RNA to prevent splice site selection. To efficiently enter the cells, vivo MOs were used which contain an additional delivery moiety. For knockdown of MALT1A, a vivo MO targeting the exon7-intron7 boundary of the *Malt1* pre-mRNA (AMO) was designed and a control vivo MO (cMO) was used for comparison. Murine CD4⁺ T cells (3×10^6 cells/ml) or MEFs (0.5×10^6 cells) were transfected with 5 nmol of AMO or cMO and cultured for 3 h (for RNA analyses) or 18 h (for protein analyses).

6.2.3 Lentiviral transduction of Jurkat T cells

To generate stable MALT1 expressing cell lines, we lentivirally transduced MALT1-deficient Jurkat T cells with different pHAGE-h Δ CD2-T2A-MALT1 constructs. The T2A sequence allows translation of both truncated human surface marker CD2 (h Δ CD2) and MALT1 from the same mRNA by a mechanism called ribosomal skipping. Thereby the formation of the glycyl-prolyl peptide bond at the 2A C-terminus is inhibited resulting in a translational stop and the release of the nascent polypeptide from the ribosome (Szymczak et al., 2004). Subsequently, translation of downstream sequences is resumed by the ribosome, which leads to the generation of two distinct proteins (Szymczak et al., 2004).

First, lentiviruses were produced by transfecting HEK293T cells with MALT1 expression plasmids and lentiviral packaging vectors. In more detail, 1×10^6 HEK293T cells were seeded

in a 10 cm² dish in 8 ml DMEM medium one day before transfection. The next day, HEK293T cells (~ 20 % confluency) were transfected with 1 µg of the lentiviral envelope plasmid pMD2.G, 1.5 µg of the packaging vector psPAX2 and 2 µg MALT1 transfer plasmid (pHAGE-hΔCD2-T2A-MALT1-SrepTagII) using X-tremeGENE HP DNA Transfection Reagent (Roche Diagnostics) according to the manufacturer's instructions. After 3 days, the supernatant containing the virus particles was removed and sterile filtered (0.45 µM). 500 µl virus together with 8 µg/ml polybrene was added to 2x 10⁵ MALT1-deficient Jurkat T cells (500 µl virus). 24 h later, cells were washed with PBS and resuspended in 1 ml fresh RPMI medium. After one week in culture, infection efficiency was determined by analyzing hΔCD2 expression using flow cytometry or by checking MALT1 expression levels via Western Blot.

6.2.4 Adenoviral transduction of primary, murine CD4⁺ T cells

For adenoviral transduction of murine CD4⁺ T cells with MALT1, full-length MALT1A, MALT1B or MALT1A C464A mutant were cloned in the pCAGAdDu-IRES-eGFP vector. 1x 10⁵ HEK293A cells were seeded in 6 well plates and transfected with 3 µg linearized plasmids using jetPEI reagent. When all cells show cytopathic effects (CPE), supernatant and cells were harvested and primary virus was collected by three freeze-thaw cycles (Warth and Heissmeyer, 2013). Cloning of adenoviral plasmids and primary virus production was performed by S. Warth, Research Unit Molecular Immune Regulation, Helmholtz Zentrum München.

The primary virus lysate was amplified in HEK293A cells. Thereby, 5x 10⁶ HEK293A cells were seeded in a 20 cm tissue culture dish one day before infection. At about 90 % confluency, cells were infected with primary virus lysate and incubated until cells show CPE, but before detachment. Cells and supernatant were harvested and disrupted by three freeze-thaw-cycles. After centrifugation (800 x g, 15 min, 4 °C), concentrated virus was aliquoted and stored at -80 °C. Adenovirus titer was determined by infecting A549 cells with several virus concentrations. In more detail, 1x 10⁵ A549 cells were seeded in a 12-well plate in 1 ml DMEM medium. Concentrated virus was diluted in medium (1:10, 1:100, 1:500, 1:1000, 1:2000) and 10 µl dilution was added to one well. After 36 h, cells were detached, washed with PBS and GFP expression was analyzed by flow cytometry (Attune). Virus titer was calculated the following: Titer (TU/ml) = (1x 10⁵ A549 cells x (% GFP cells/100))/ml.

Primary adenoviruses encoding control or sh-hnRNP U #1 and #2 were purchased from Sirion Biotec and amplified and titrated as indicated above.

Concentrated virus was used for the infection of primary, murine CD4⁺ T cells. For differentiation experiments, naive CD4⁺ T cells from *Malt1*^{-/-}R26/CAG-CARΔ1^{stop-fl}*Cd4*-Cre mice were isolated and transduced with GFP control, MALT1A, MALT1B or MALT1A C464A virus using an MOI (multiplicity of infection) of 50 in an infection volume of 165 μl per 10⁶ cells in a 15 ml tube. For knockdown experiments, CD4⁺ T cells from R26/CAG-CARΔ1^{stop-fl}*Cd4*-Cre mice were infected with control or sh-hnRNP U virus (MOI of 50). After 5 h incubation at 37 °C, cells were washed twice with PBS, resuspended in primary T cell medium and rested for 40 h before analysis. GFP⁺ cells of CD4⁺ T cells (infected with control or sh-hnRNP U adenoviruses) were sorted if RNA and intracellular IL-2 levels were analyzed.

6.3 Cell stimulation and differentiation

6.3.1 Stimulation of Jurkat T cells and primary human CD4⁺ T cells

Jurkat T cells were stimulated with P/I (Phorbol 12-myristate 13-acetate (PMA)/Ionomycin) using a concentration of 200 ng/ml PMA and 300 ng/ml Ionomycin. P/I stimulation acts downstream of TCR/CD28 as PMA directly stimulates PKCθ and Ionomycin triggers Ca²⁺ release from the endoplasmatic reticulum into the cytosol. Stimulation was performed in tubes at 37 °C.

Primary human CD4⁺ T cells were stimulated with human T-Activator CD3/CD28 Dynabeads (Life Technologies). Thereby, 2x 10⁶ cells (in 1 ml) were incubated with 50 μl pre-washed Dynabeads at 37 °C for 3h.

6.3.2 Stimulation of primary murine CD4⁺ T cells

Primary murine CD4⁺ T cells were stimulated with P/I, anti-CD3 and/or anti-CD28 antibodies or OVA-loaded APCs in primary T cell medium. For P/I stimulation, 30 ng/ml PMA and 300 ng/ml Ionomycin were used. Anti-CD3, anti-CD28 or anti-CD3/CD28 stimulation was performed either on pre-coated plates or with pre-coated sulfate latex beads (Life Technologies). For plate-bound stimulation, plates were coated with rabbit anti-hamster IgG

(20 μ l in 1 ml PBS per 6-well) over night at 4 °C. Afterwards, plates were washed two times with PBS before cells were stimulated with anti-CD3 (0.5 μ g/ml) or anti-CD28 (1 μ g/ml) or both antibodies and added to the pre-coated wells. Cells were stimulated at a density between 1×10^6 and 5×10^6 cells per ml. For lower cell numbers, stimulation conditions were adjusted. For the analysis of cell surface marker expression of control or sh-hnRNP U infected cells, 0.1 - 0.5×10^6 T cells were stimulated by using 96-well plates pre-coated with anti-CD3 (0.5 μ g/ml in PBS over night at 4 °C) and soluble anti-CD28 (1 μ g/ml).

If cells were stimulated with sulfate latex beads, anti-CD3 (13.3 μ g/ml) and/or anti-CD28 (26.6 μ g/ml) antibodies were added to a mixture of 250 μ l beads and 750 μ l sterile phosphate buffer (5 mM) and incubated over night at RT by rotation. Beads were washed three times with phosphate buffer (200 x g, 2 min, RT) and finally resuspended in phosphate buffer containing 2 mM BSA. Beads were counted and incubated with primary, murine CD4⁺ T cells in a cell to bead ratio of 3:1.

Stimulation of CD4⁺ T cells from OT-II mice was performed by using APCs loaded with OVA peptide (Figure 6.1).

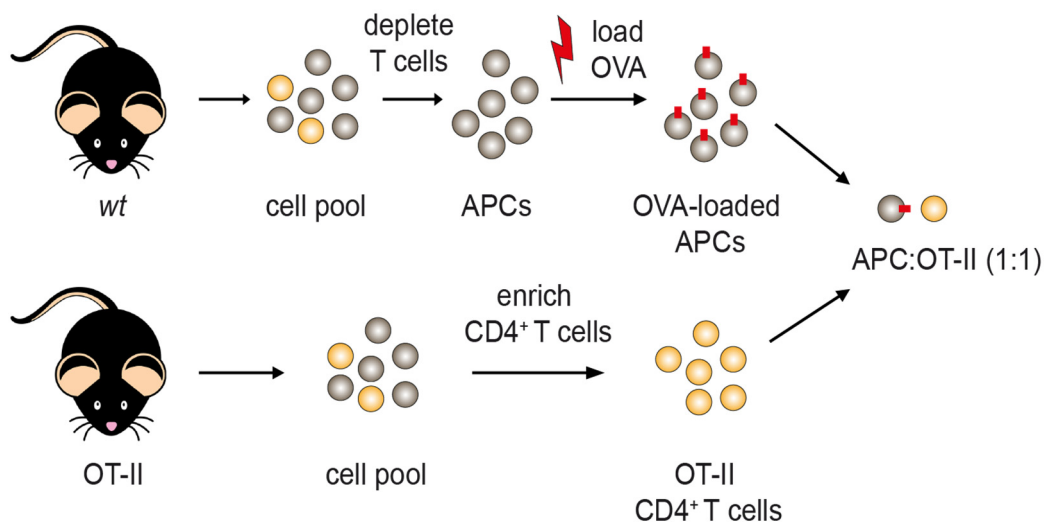


Figure 6.1: Schematic of stimulation of OT-II CD4⁺ T cells with T cell-depleted, OVA-loaded APCs.

To obtain APCs, spleen and lymph nodes from C57BL/6 *wt* mice were homogenized, lysed in TAC lysis buffer and resuspended in CB buffer as indicated above (see 6.1.4). The cell suspension was depleted for T cells by adding 30 μ l anti-TCR β (H57-597, eBioscience) and samples were incubated for 5 min at 4 °C. Afterwards, the suspension was treated with

magnetically labeled anti-biotin microbeads (200 μ l/mouse, Miltenyi Biotec) for 10 min at 4 °C before it was applied to LS columns (Miltenyi Biotec) in a MACS separator. The purified cells represent the APCs, which were subsequently irradiated (2000 rad), washed with CB buffer and pulsed with 1 μ g/ml OVA peptide (aa 323-339, Biotrend) for 1 h at 37 °C. 2×10^6 APCs were incubated with 2×10^6 OT-II CD4⁺ T cells (ratio 1:1) at 37°C before FACS analysis or RNA lysis.

6.3.3 *In vitro* differentiation of murine CD4⁺ T cells

Polarization into TH1 and TH17 cells was performed using naive CD4⁺ T cells from *wt* or *Malt1*^{-/-} mice or naive CD4⁺ T cells from *Malt1*^{-/-}R26/CAG-CAR Δ 1^{stop-fl}*Cd4*-Cre mice transduced with GFP control, MALT1A, MALT1B or MALT1 C464A viruses (see section 6.2.4). For TH1 conditions, medium was supplemented with IL-12 (10 ng/ml) and anti-IL-4 (10 μ g/ml); for TH17 conditions, TGF β (10 μ g/ml), IL-6 (60 ng/ml), anti-IL-12 (10 μ g/ml), anti-IL-4 (10 μ g/ml), anti-IFN γ (5 μ g/ml) and anti-IL-2 (2.5 μ g/ml) were added to the primary medium. Naive CD4⁺ T cells (0.2×10^6) were resuspended in differentiation medium (100 μ l) and transferred into a 96-well plate. T cells were stimulated with anti-CD3 (145-2C11, produced by V. Heissmeyer and E. Kremmer) and irradiated APCs (2×10^6) in a ratio 1:10 and were cultured at 37 °C. APCs were isolated from CD45.1 mice (see section 6.3.1) and irradiated with 2000 rad. After 72 h incubation time, T cells were re-stimulated with PMA (20 nM) and Ionomycin (1 μ M) for 4 h before they were analyzed for intracellular IFN γ and IL-17A expression using flow cytometry (see section 6.4.2). Experiments were performed in cooperation with D. Hu, Research Unit Molecular Immune Regulation, Helmholtz Zentrum München/Institute for Immunology, Biomedical Center, LMU München.

6.4 Flow cytometry and cell sorting

Cell populations were analyzed regarding their surface protein expression and intracellular cytokine levels either on an Attune Acoustic Focusing Cytometer (Life Technologies) or on a LSR II (BD) or on a LSR Fortessa (BD). For sorting, FACS Star plus (BD) or FACS Aria cell sorter (BD) were used.

6.4.1 Staining of surface molecules

To check h Δ CD2 surface expression of infected MALT1-deficient Jurkat T cells, ca. 0.2×10^6 cells were collected and resuspended in 500 μ l FACS buffer. Cells were stained with anti-CD2-APC antibody (human, dilution 1:500) for 10 min at RT. Afterwards samples were washed with FACS buffer, taken up in ca. 200 μ l FACS buffer and acquired on Attune Acoustic Focusing Cytometer.

For staining of CD69 and CD25 in primary murine CD4⁺ T cells, cells (0.2 - 1×10^6) were collected after stimulation and were resuspended in FACS buffer. To prevent unspecific antibody binding to Fc receptors, samples were treated with anti-CD16/32 (mouse, dilution 1:50) for 10 min at 4 °C. Afterwards, staining with anti-CD69-APC (mouse, 1:100) and anti-CD25-PE (mouse, 1:100) was performed for 10-15 min at 4 °C in the dark. Samples were washed, resuspended in FACS buffer and acquired on Attune Cytometer or LSR II.

6.4.2 Intracellular cytokine staining

For intracellular IL-2 staining, primary murine CD4⁺ T cells (0.5 - 1×10^6) were stimulated for 6 h with anti-CD3/CD28. 3 h before staining, cells were treated with Brefeldin-A (10 ng/ml, Sigma) to prevent exocytosis of signaling molecules. After stimulation, cells were collected, centrifuged (300 x g, 5 min, 4 °C), resuspended in FACS buffer and incubated with ethidium monoazide bromide (dilution 1:100) to distinguish between live and dead cells. Thereby, samples were incubated in the dark for 15 min at RT before they were exposed to light (10 min, 4 °C). Afterwards, samples were washed and fixed in 2 % PFA for 15 min at RT. Then, cells were washed and permeabilized in IC buffer (10 min, RT). Unspecific antibody binding was blocked with anti-CD16/32 (mouse, dilution 1:50 in Saponine buffer, 15 min, 4 °C) before samples were incubated with anti-IL-2-FITC or anti-IL-2-APC (both mouse, dilution 1:100 in IC buffer) for 30 min on ice. Afterwards, cells were washed (300 x g, 5 min, 4 °C) and filled up with FACS buffer to wash out unbound antibodies (> 15 min, RT). Samples were again washed (300 x g, 5 min, 4 °C), resuspended in FACS buffer and acquired on Attune Cytometer.

In differentiation experiments, cells were re-stimulated with PMA (20 nM) and Ionomycin (1 μ M) in the presence of Brefeldin-A for 2 h before staining. After cells were resuspended in FACS buffer, live-dead cell staining was conducted by treating the samples with a fixable

dead cell staining solution (indol-1, Life Technologies) for 30 min at 4 °C. Samples were washed and surface proteins CD45.2 and CD4 were stained by adding anti-CD45.2-APC-Cy7 and anti-CD4-PE-Cy7 (both mouse, dilution 1:200) for 15 min at 4 °C. Cells were fixed with 4 % PFA for 10 min at 20 °C and permeabilized for 20 min at 4 °C using PBS/0.5 % Saponine/1 % BSA. For intracellular staining of IL-17A and IFN γ , samples were treated with anti-IL-17A-PE and anti-IFN γ -APC (both mouse, dilution 1:200) for 50 min at 4°C. Samples were washed and acquired on LSR Fortessa. Staining was performed in cooperation with D. Hu, Research Unit Molecular Immune Regulation, Helmholtz Zentrum München/Institute for Immunology, Biomedical Center, LMU München.

6.4.3 Sorting of primary murine CD4⁺ T cells

Different T cell subsets (CD4⁺CD62L⁺CD44⁻ naive T cells, CD4⁺CD62L⁻CD44⁺ effector T cells and CD4⁺CXCR5⁺PD-1⁺ T_{FH} cells) were sorted on a FACS Aria cell sorter (BD) after samples have been stained with the respective antibodies. Sorting was performed by J. Kranich, Institute for Immunology, LMU München. CD4⁺ T cells, which were infected with control or sh-hnRNP U adenoviruses, were resuspended in FACS buffer, filtered and subsequently sorted for GFP⁺ cells using FACS Star plus.

6.5 Molecular biology methods

6.5.1 Polymerase chain reaction (PCR)

Amplification of DNA was performed using polymerase chain reaction (PCR).

Thereby, the following standard protocol was used:

Component	Amount
Template DNA	30 ng
5' primer (10 μ M)	1.25 μ l
3' primer (10 μ M)	1.25 μ l
dNTP (10 mM)	1,25 μ l
Herculase buffer (10x)	10 μ l
DNA polymerase (Herculase)	1 μ l
	Ad 50 μ l H ₂ O

Table 9: PCR standard protocol.

PCR program:

Step	Temperature	Time
Melting	94 °C	10 min
Melting	94 °C	1 min
Annealing	T _m primer -5 °C	1 min
Extension	72 °C	30 sec/1 kb
Extension	72 °C	10 min

} 30 cycles

Table 10: PCR standard program.

PCR products were checked for correct amplification on an agarose gel. Purification of PCR products was performed using PCR Purification Kit (Qiagen). For the generation of MALT1 TRAF6 binding mutants, megaprimer PCR was used to introduce glutamate (E) to alanine (A) point mutations. First, two primers were designed to generate the megaprimer: one primer bears the desired mutation, whereas the other primer flanks the coding sequence. After purification, the generated PCR product was used in a second PCR round. Thereby, the megaprimer was combined with a third primer to amplify the whole gene sequence. Finally, the PCR product can be cloned into the target vector.

6.5.2 DNA restriction digestion, agarose gel electrophoresis and DNA extraction

PCR products or plasmid DNA were digested using endonucleases from NEB and the appropriate buffers. After restriction digest, DNA was mixed with 6x DNA loading buffer and separated on an agarose gel. For gel preparation, agarose was dissolved in TBE buffer and supplemented with ethidium bromide. Agarose gels were run in TBE buffer at 8 V/cm. To determine DNA fragment size, 3 µl 1 kb plus DNA ladder was loaded. DNA bands were visualized with UV light and were cut out for extraction using the Gel Extraction Kit (Qiagen) according to the manufacturer's instruction.

6.5.3 DNA ligation and transformation of *Escherichia coli*

For ligation of digested plasmids and PCR products, Rapid DNA ligation Kit (Roche) containing the T4 DNA ligase was used according to the manufacturer's protocol. Depending on the size ratio between vector and PCR fragment, ligation was performed using a molar ratio of 1:3 to 1:5 vector to insert. The complete ligation mixture was added to competent *Escherichia coli* (*E. coli*) TOP10 cells and was incubated for 30 min on ice. After a heat-

shock at 42 °C for 45 sec, competent cells were cooled down on ice for 5 min and subsequently supplemented with 400 µl LB medium. Cells were raised in a shaker at 37 °C for 60 min and afterwards plated on LB agar plates containing the appropriate antibiotic. Plates were incubated over night at 37 °C.

6.5.4 Cultivation of *E. coli* and plasmid preparation

To isolate the generated plasmid DNA, LB medium was prepared and supplemented with the appropriate antibiotic (e.g. ampicillin 100 µg/ml). 3 ml of LB medium were inoculated with one colony from LB agar plates and cultivated in a shaker (180 rpm) over night at 37 °C. Plasmid DNA was isolated using the Plasmid Mini Kit (Qiagen) according to the manufacturer's protocol. To generate larger DNA amounts, 100-500 ng of the purified plasmid were re-transformed into competent *E. coli* cells (see 6.1.4). Afterwards, the cells were directly transferred into 150-200 ml LB medium and grown over night at 37 °C. For plasmid isolation, the Plasmid Maxi Kit (Qiagen) was used.

6.5.5 DNA sequencing

Purified DNA and the appropriate sequencing primers were send to Eurofins MWG Operon (Ebersberg) for sequencing.

6.5.6 RNA isolation

For extraction of RNA, $0.5-2 \times 10^6$ cells were lysed in 350 µl RLT lysis buffer (Qiagen). Afterwards, lysates were transferred onto shredder columns for homogenization (Qiagen). RNA was isolated according to the protocol of the Qiagen RNeasy RNA isolation Kit. In a next step, RNA concentration was measured using Nanodrop and RNA levels were adjusted up to 1 µg. Genomic DNA was removed by adding 1 µl DNase I (1 U) (Promega) and the corresponding buffers for 30 min at 37 °C. Afterwards, the samples were treated with 1 µl stop solution at 65 °C for 10 min to inactivate the DNase I reaction before they were stored at -80 °C.

6.5.7 Reverse transcription into cDNA

Digested RNA samples were reverse transcribed into cDNA using Superscript First Strand Synthesis Kit (Invitrogen) or Verso cDNA Synthesis Kit (Thermo Fisher Scientific) according to the manufacturer's instructions. Thereby, random hexamers were used as primers for the Reverse Transcriptase. If reverse transcription was performed with Superscript First Strand Kit, samples were treated with RNaseH (1.5 U) (Life Technologies) at 37 °C for 20 min to degrade the RNA template. Generated cDNA was stored at -80 °C.

6.5.8 Quantitative real-time PCR (qPCR) and semi-quantitative PCR (semi-qPCR)

Quantitative real-time PCR (qPCR) is a useful method to quantify RNA amounts, in which DNA amplification can be detected by using a fluorescent dye LightCycler 480 SYBR Green I Mastermix (Roche) or KAPA SYBR FAST qPCR Mastermix (Peqlab) that binds double stranded DNA. The fluorescence increases with each cycle of amplification and can be detected with a LightCycler 480 (LC-480, Roche). The following standard protocol was used:

Component	Amount
Template cDNA	2 µl
5' primer (20 µM)	1 µl
3' primer (20 µM)	1 µl
SYBR Green I Mastermix (2x)	10 µl
	Ad 20 µl H ₂ O

Table 11: qPCR standard protocol.

Step	Temperature	Time
Melting	95 °C	10 min
Melting	95 °C	10 sec
Annealing	60 °C	10 sec
Extension	72 °C	10 sec
Melting curve	65 °C – 95 °C	

} 40–45 cycles

Table 12: qPCR standard program.

To quantify target gene expression, murine hydroxymethylbilane synthase (*Hmbs*), human peptidylprolyl isomerase B (*PPIB*), human 18S ribosomal RNA (*18S* rRNA), human RNA polymerase II (*RP2*) or human glyceraldehyde-3-phosphate dehydrogenase (*GAPDH*) were used as internal controls. Relative expression levels were calculated using the $\Delta\Delta C_p$ method (Pfaffl, 2001).

For semi-qPCR, DreamTaq DNA polymerase and 10x DreamTaq green buffer (both Thermo Scientific) were used according to the following protocol:

Component	Amount
Template cDNA	2 μ l
5' primer (10 μ M)	1.25 μ l
3' primer (10 μ M)	1.25 μ l
dNTP (10 mM)	1 μ l
DreamTaq green buffer (10x)	10 μ l
DNA polymerase (DreamTaq)	0.3 μ l
	Ad 50 μ l H ₂ O

Table 13: Semi-qPCR standard protocol.

Step	Temperature	Time
Melting	94 °C	10 min
Melting	94 °C	10 sec
Annealing	T _m primer -5 °C	10 sec
Extension	72 °C	10 sec
Extension	72 °C	10 min

} 25–30 cycles

Table 14: Semi-qPCR standard program.

PCR samples were loaded on a 2-3 % agarose gel together with 3 μ l 1 kb plus DNA ladder. DNA bands were visualized with UV light using a Geldocumentation system (Intas). In minigene experiments, alternatively spliced products were quantified by densitometry using Adobe Photoshop. Percentage of exon7 inclusion was calculated relative to total PCR product.

6.6 Biochemical and immunological methods

6.6.1 Preparation of whole cell lysates

For analysis of protein expression levels and activation of downstream signaling pathways including NF- κ B DNA binding (see section 6.6.7), 1×10^6 – 5×10^6 cells were harvested (1800 rpm, 5 min, 4 °C), washed with PBS and subsequently lysed in 80–120 μ l high-salt buffer. Lysates were incubated on a shaker for 10–20 min at 4 °C before insoluble cellular debris were removed by centrifugation (14 000 rpm, 15 min, 4 °C). For Western Blot analysis, samples were mixed with 4x SDS loading buffer (Rotiload, Roth) and boiled for

5–10 min at 95 °C. Signaling potential of MALT1 TRAF6 binding mutants was analyzed in cooperation with T. Seeholzer, AG Krappmann.

6.6.2 Co-immunoprecipitation and Strep-Tactin pulldown

For protein interaction studies, 1×10^7 – 3×10^6 cells were lysed in 900 μ l Co-IP buffer supplemented with protease inhibitors. Lysates were incubated for 20 min at 4 °C in an overhead rotator before samples were cleared by centrifugation (14 000 rpm, 15 min, 4 °C). 30 μ l supernatant were collected as lysate controls and were mixed with 4x SDS loading buffer (Rotiload, Roth) and boiled for 5 min at 95 °C. The residual supernatant (ca. 830 μ l) was used for binding studies. Immunoprecipitations (IPs) were carried out by using antibodies against NEMO (9 μ l) or MALT1A (15 μ l) and samples were incubated in an overhead rotator overnight at 4 °C. After antibody incubation, 20 μ l Protein G Sepharose (1:1 suspension) was added and lysates were rotated for additional 1–2 h at 4 °C. For Strep-Tactin pulldowns (StrepT-PDs), Strep-tagged MALT1 proteins were precipitated by using 30 μ l Strep-Tactin Sepharose (1:1 suspension, IBA) at 4 °C overnight. After incubation with Protein G Sepharose or StrepTactin Sepharose, beads were washed four times with 500 μ l ice-cold Co-IP buffer without protease inhibitors (200 x g, 5 min, 4 °C). Supernatant was completely removed by aspiration and ca. 20 μ l 2x SDS loading buffer (Rotiload) was added to the beads. Samples were boiled at 95 °C for 8 min before they were separated by SDS-PAGE.

6.6.3 RNA-binding protein immunoprecipitation

RNA-binding protein immunoprecipitation (RIP) is a useful method to analyze whether specific nuclear or cytosolic proteins associate with specific RNA molecules. Analysis of hnRNP U binding to *MALT1* pre-mRNA in Jurkat T cells was performed using Magna RIP™ Kit (Merck Millipore). First, 2×10^7 Jurkat T cells were harvested, washed with PBS (1500 rpm, 5 min, 4 °C) and lysed in 100 μ l RIP lysis buffer (complete) for 5 min at 4 °C. Lysates were stored at -80 °C for 24 h. For immunoprecipitation, 100 μ l pre-washed protein A/G magnetic beads (in RIP wash buffer) were labeled with 5 μ g anti-hnRNP U or 5 μ g normal mouse IgG antibody (both Merck Millipore) for 30 min at RT in a rotator. Beads-antibody complexes were washed with RIP wash buffer and placed in a magnetic separator (Qiagen) to remove the supernatant. In the meantime, cell lysates were thawed and centrifuged (14 000 rpm, 10 min, 4 °C) to pellet insoluble cellular debris. Afterwards, 10 μ l of

the lysate supernatant were removed and stored at -80 °C as input fraction, while 100 µl of the lysate supernatant together with 900 µl RIP immunoprecipitation (RIP IP) buffer were added to the antibody-beads complexes and incubated overnight at 4 °C. Afterwards the supernatant was removed by magnetic separation and beads were washed six times with RIP wash buffer. The immunoprecipitates were incubated with 150 µl Proteinase K buffer for 30 min at 55 °C to digest RNA-bound proteins. After transferring the tubes into the magnetic rack, supernatant was collected and mixed with 250 µl RIP wash buffer. In the meantime, input samples were treated with 140 µl Proteinase K buffer for 30 min at 55 °C before adding 250 µl RIP wash buffer. To purify RNA, IP and input samples were mixed with 400 µl phenol:chloroform:isoamylalcohol (125:24:1, Thermo Fisher Scientific). After centrifugation (14 000 rpm, 10 min, RT), the aqueous phase was removed and treated with 400 µl chloroform. The mixture was again centrifuged (14 000 rpm, 10 min, RT) and 300 µl aqueous phase were transferred into a new reaction tube. For precipitation of RNA, 50 µl salt solution I, 15 µl salt solution II, 5 µl precipitation enhancer and 850 µl ethanol were added to each sample before storage at -80 °C overnight. After thawing and centrifugation (14 000 rpm, 30 min, 4 °C), the supernatant was removed, pellets were washed with 1 ml 80 % ethanol (14 000 rpm, 30 min, 4 °C), dried at RT and resuspended in 20 µl RNase free water. Finally, RNA was reverse transcribed into cDNA and *MALTI* pre-mRNA enrichment was analyzed by qPCR (see sections 6.5.7 and 6.5.8) normalizing IP samples relative to input fractions.

6.6.4 SDS polyacrylamide gel electrophoresis (SDS-PAGE)

Proteins of cellular lysates were separated by SDS-PAGE, which was performed under reducing conditions. Different concentrations of acrylamide (7–15 %) were used for the generation of separation gels with different pore sizes. APS (ammonium persulfate) and TEMED were added to the mixture to enable polymerization. After full polymerization of the separation gel, a 5 % polyacrylamide stacking gel containing pockets for the lysate samples was layered on top of the separation gel. When gels were fully polymerized, protein lysates were loaded. A prestained protein ladder (Thermo Fisher Scientific) was also loaded to estimate the molecular weight of the separated proteins. Electrophoresis was performed in SDS electrophoresis buffer at 90 V for 30 min before voltage was increased to 110 V for 60 min.

6.6.5 Western Blot (WB)

To enable detection of proteins separated by SDS-PAGE, proteins were transferred onto PVDF membranes using a semi-dry transfer system. Thereby, PVDF membranes were activated in methanol and Whatman filter papers were soaked in 1x blotting buffer. The SDS gel and the membrane were placed between soaked Whatman filter papers in the blotting apparatus. Proteins are transferred to the PVDF membrane by using an electric field (70 mA per gel for 110 min).

After blotting, membranes were blocked with 3 % BSA/PBS-T for 60 min to avoid unspecific antibody binding. Blocked membranes were incubated with primary antibody (dilution 1:1000 in 1.5 % BSA/PBS-T) overnight at 4 °C. Membranes were washed at least three times with PBS-T for 5 min at RT to remove unspecifically bound antibodies. Afterwards, HRP-coupled secondary antibody (dilution 1:10 000 in 1.5 % BSA/PBS-T) was added for 1 h at RT. Membranes were again washed with PBS-T to remove unbound antibodies. HRP activity was detected by using enhanced chemiluminescence (ECL) substrate (Cell Signaling) in a 1:20 dilution in water. HRP catalyzes oxidation of the substrate and is accompanied by the emission of light, which was detected by ECL films exposed to the membrane. For detection of further proteins on the same membrane, membranes were washed with PBS-T and treated with stripping buffer for 30 min at RT to remove all bound primary and secondary antibodies. Membranes were washed at least three times with PBS-T for 5 min, blocked with 3 % BSA solution and incubated with a specific primary and secondary antibody as described before.

6.6.6 MALT1 activity detection using MALT1 activity based probes

MALT1 activity based probes (ABPs) can be used to monitor cellular MALT1 activity (Eitelhuber et al., 2011). The MALT1 ABPs consist of a specific recognition element LRSR, an electrophile (AOMK) that forms a covalent bond with the active cysteine and a certain detection marker. An ABP coupled to the fluorophore BODIPY (boron-dipyrrromethene) was used for measuring MALT1 activity of different MALT1-Strep constructs. In this assay, Jurkat T cells ($2-5 \times 10^7$) were lysed in 900 μ l Co-IP buffer, centrifuged (14 000 rpm, 10 min, 4 °C) and overexpressed MALT1-Strep constructs were precipitated using Strep-Tactin Sepharose (see section 6.6.2). After three washing steps with Co-IP buffer, bead-bound MALT1-Strep was incubated with 3 μ M fluorescent MALT1-ABP (BODIPY) for 1 h at 30 °C, mixed with 4x SDS loading buffer (Rotiload, Roth) and boiled. Proteins were

separated by SDS-PAGE and fluorescence was detected by a Typhoon Scanner (FITC laser 488nm/filter 526 SP).

A biotin-coupled MALT1-ABP was used to detect active MALT1 in primary CD4⁺ T cells in a plate-bound assay called ELASA (enzyme-linked activity sorbent assay). Cells (1×10^7) were lysed in 200 μ l Co-IP buffer, centrifuged (14 000 rpm, 10 min, 4 °C) and extract was incubated with 0.1 μ M biotinylated MALT1 ABP (Biotin K). Extract was transferred to streptavidin-coated plates (Thermo Scientific) and incubated overnight at 4 °C. After washing in PBS-T (0.05 % Tween-20) and blocking with 2 % BSA/PBS-T, detection was performed by incubation with MALT1 primary antibody (2494; 1:800 in 1 % BSA/ PBS-T; 1 h, RT) and HRP-coupled secondary antibody (1:1500 in 1 % BSA/PBS-T; 1 h, RT). 3-5 washing steps with PBS-T were used after antibody incubation. Luminescence was determined after TMB substrate (eBioscience) incubation for 10-20 min and subsequent stop reaction with 1 M H₂SO₄ in a photometer (Bio-Tek) at 450 nm and 570 nm.

6.6.7 Electrophoretic mobility shift assay (EMSA)

Electrophoretic mobility shift assays (EMSAs) enable the visualization of transcription factor binding to DNA. Thereby, radioactive labeled oligonucleotides containing specific DNA response elements are incubated with protein lysates, and the mixture is separated on a native polyacrylamide gel, in which protein-DNA complexes migrate more slowly than free unbound DNA. Due to the radioactive labeling, DNA-transcription factor complexes can be detected with X-Ray films.

To produce radioactive labeled DNA probes, single oligonucleotides were annealed resulting in the formation of 5' overhanging dsDNA-oligonucleotides. Overhangs were filled in with radioactive nucleotides by Klenow polymerase according to the following protocol:

Component	Amount
DNA oligonucleotide	400 ng
Klenow buffer (10x)	2.5 μ l
dNTP-A (10 μ M)	1.8 μ l
[³² P]- α -dATP	30 μ Ci
Klenow Fragment	1 U
	ad 25 μ l H ₂ O

Table 15: Labling of DNA probes.

The reaction was incubated for 30 min at 37 °C. Afterwards, samples were purified using QIAQuick Nucleotide Removal Kit (Qiagen).

To determine DNA binding activity of NF- κ B and OCT1, EMSAs were performed using cells which were lysed in high-salt lysis buffer (see section 6.6.1) and 32 P- α -dATP-labeled NF- κ B (H2K) or OCT1 DNA binding site probes. Assays were conducted according to the following protocol:

Component	Amount
Protein extract	~ 5 μ g
2x Shift buffer	10 μ l
BSA	10 μ g
DTT (100 mM)	1 μ l
Poly dI-dC (2 μ g/ μ l)	1 μ l
[32]P- α -dATP-labeled probe	1 μ l (10 000–20 000 cpm)
	ad 20 μ l H ₂ O

Table 16: EMSA standard protocol.

Reaction mixture was incubated for 30 min at RT and separated on a native polyacrylamide gel (5 %) in 1x TBE buffer at 26 mA/gel. Gels were dried on a Whatman filter paper at 80 °C for 1 h and exposed to autoradiography films. To determine NF- κ B fold induction, intensities of NF- κ B bands were quantified relative to OCT1 signal using ImageJ software.

6.7 Statistical analysis

All experiments were performed at least three times unless otherwise indicated. Values represent the mean \pm standard deviation (SD). Experiments were analyzed by using unpaired Student's *t*-test. Statistical significance values are * p < 0.05; ** p < 0.01; *** p < 0.001.

7 Abbreviations

° C	° Celsius
18S rRNA	18S ribosomal RNA
A/Ala	alanine
aa	amino acid
ABP	activity based probe
Ac	acidic amino acid
API2	cellular inhibitor of apoptosis 2
AMO	MALT1A morpholino
AOMK	acyloxymethyl ketone
AP-1	activator protein-1
APC	antigen presenting cell
APC	allophycoyanin
APS	ammonium persulfate
Ar	aromatic amino acid
ARS	activation responsive motif
ATF2	activating transcription factor 2
ATP	adenosine triphosphate
BCL-6	B cell chronic lymphocytic leukemia/lymphoma 6
BCL10	B cell chronic lymphocytic leukemia/lymphoma 10
BCR	B cell receptor
BODIPY	boron-dipyrromethene
BPS	branch point sequences
BSA	bovine serum albumin
C/Cys	cysteine
Ca ²⁺	calcium
CAG	chicken actin promoter and cytomegalovirus enhancer
CaMKII	calmodulin-dependent protein kinase II
CAR	coxsackievirus and adenovirus receptor
CARD	caspase-recruitment domain

CARMA1	CARD-containing MAGUK 1
Cas9	CRISPR-associated protein-9
CBM	CARMA1-BCL10-MALT1
CC	coiled-coil
CCR	CC chemokine receptor
CD	cluster of differentiation
CD62L	CD62 ligand
cDNA	complementary DNA
Ci	Curie
cIAP	cellular inhibitor of apoptosis
CLIP	crosslinking and immunoprecipitation
cMO	control morpholino
Co-IP	Co-immunoprecipitation
CPE	cytopathic effects
cpm	counts per minute
CRISPR	Clustered Regularly Interspaced Short Palindromic Repeats
C-terminus	Carboxyl-terminus
CTLA-4	cytotoxic T lymphocyte antigen-4
CXCR	CXC chemokine receptor
CYLD	cylindromatosis
D/Asp	aspartate
DAG	diacylglycerol
dATP	desoxyadenosine triphosphate
DD	death domain
DMEM	Dulbecco's Modified Eagle Medium
DMSO	dimethyl sulfoxide
DNA	deoxyribonucleic acid
dNTP	deoxyribonucleotide triphosphate
ds	double-stranded
DTT	dithiothreitol

E/Glu	glutamate
EAE	experimentally induced autoimmune encephalomyelitis
ECL	enhanced chemiluminescence
EDTA	ethylenediaminetetraacetic acid
eGFP	enhanced green fluorescent protein
EGTA	Ethyleneglycol-bis(2-aminoethylether)-N,N,N',N'-tetraacetic acid
ELASA	enzyme-linked activity sorbent assay
EMSA	electrophoretic mobility shift assay
ERK	extracellular signal-regulated kinase
ESE	exonic splicing enhancers
ESS	exonic splicing silencers
FACS	fluorescence-activated cell sorting
FCS	fetal calf serum
FITC	fluorescein isothiocyanate
FOXP3	forkhead box p3
G/Gly	glycine
g	gravity
GADS	GRB2-related adapter downstream of Shc
GAPDH	glyceraldehyde-3-phosphate dehydrogenase
GATA3	GATA binding protein 3
GDP	guanosine diphosphate
GEF	guanine nucleotide exchange factor
GFP	green fluorescent protein
GRB2	growth factor receptor-bound protein 2
GSK3	glycogen synthase kinase
GTP	guanosine triphosphate
GUK	guanylate kinase
H/His	histidine
h	human
h	hour

H ₂ SO ₄	sulfuric acid
HEK	human embryonic kidney
HEPES	2-[4-(2-Hydroxyethyl)-1-piperazino]-ethansulfonic acid
HEV	high-endothelial venules
HMBS	hydroxymethylbilane synthase
hnRNP	heterogeneous nuclear ribonucleoproteins
HOIL1	heme-oxidized IRP2 ubiquitin ligase 1
HOIP	HOIL1-interacting protein
HPK1	hematopoietic progenitor kinase 1
HRP	horseradish peroxidase
I	Ionomycin
IC	intracellular
ICOS	inducible T cell co-stimulator
IFN γ	interferon gamma
Ig	immunoglobulin
IKK	I κ B kinase
IL	interleukin
IMDM	Iscove's Modified Dulbecco's Medium
IP	immunoprecipitation
IP ₃	inositol 1,4,5-trisphosphate
IRAK	interleukin 1 receptor associated kinase 1
IRP2	iron regulatory protein 2
IS	immunological synapse
ISE	intronic splicing enhancers
ISS	intronic splicing silencers
ITAM	immunoreceptor tyrosine-based activation motif
iTreg	inducible Treg
I κ B	inhibitor of NF- κ B
JAK	janus kinase
JNK	c-Jun N-terminal kinase

K/Lys	lysine
kb	kilo base
KCL	potassium chloride
kDa	kilo Dalton
KH ₂ PO ₄	potassium hydrogen phosphate
LAT	linker for activation of T cells
LB	Luria-Bertani (medium)
LCK	lymphocyte-specific protein tyrosine kinase
LEF	lymphoid enhancer binding factor 1
LUBAC	linear ubiquitin chain assembly complex
MACS	magnetic-activated cell sorting
MAGUK	membrane associated guanylate kinase
MALT1	mucosa associated lymphoid tissue lymphoma translocation protein 1
MAPK	mitogen activated protein kinase
MAP3K	MAPK kinase kinase
MAP2K	MAPK kinase
MEF	mouse embryonic fibroblast
MFI	mean fluorescence intensity
mg	milligram
MgCl ₂	magnesium chloride
MHC	major histocompatibility complex
MIB2	mindbomb E3 ubiquitin protein ligase 2
min	minute
MKK	MAPK kinase
ml	milliliter
MNC	mononuclear cells
MO	morpholino
MOI	multiplicity of infection
mRNA	messenger RNA
MyD88	myloid differentiation factor 88

Na ₂ HPO ₄	disodium hydrogen phosphate
NaCl	sodium chloride
NaF	sodium fluoride
NaN ₃	sodium azide
NEAA	non-essential amino acids
NEMO	NF-κB essential modulator
NES	nuclear export sequence
NFAT	nuclear factor of activated T cells
NF-κB	nuclear factor kappa B
ng	nanogram
NH ₄ Cl	ammonium chloride
NLS	nuclear localization sequence
nm	nanometer
NP-40	nonidet P40 substitute
NSCLC	non-small cell lung cancer
nt	nucleotide
N-terminus	amino-terminus
nTreg	natural Tregs
OD	optical density
OVA	ovalbumin
P	proline
P/S	penicillin/streptomycin
PBMC	peripheral blood mononuclear cells
PBS	phosphate buffered saline
PBS-T	PBS-Tween 20
PCR	polymerase chain reaction
PD-1	programmed cell death protein-1
PDK1	phosphoinositide-dependent kinase 1
PDZ	PSD-95/DLG/ZO1 homology
PE	phycoerythrin

PFA	paraformaldehyde
PH	pleckstrin homology
PI3K	phosphoinositide 3 kinase
PIP ₂	phosphatidyl inositol 4,5-bisphosphate
PIP ₃	phosphatidyl inositol 3,4,5-trisphosphate
PKB	protein kinase B
PKC	protein kinase C
PLC γ 1	phospholipase C gamma 1
PLK1	polo-like kinase 1
PM	paracaspase mutant
PMA	phorbol 12-myristate 13-acetate
PP2A	protein phosphatase 2A
PPIB	peptidylprolyl isomerase B
PPT	polypyrimidine tract
pre-mRNA	precursor messenger RNA
PSF	PTB-associated splicing factor
PTB	polypyrimidine tract binding protein
Q/Gln	glutamine
qPCR	quantitative polymerase chain reaction
R	arginine
Ras	rat sarcoma
RasGRP	Ras guanyl nucleotide-releasing protein
RBM12B	RNA-binding motif protein 12B
RBMS1	RNA-binding motif single-stranded-interacting protein 1
RHD	Rel homology domain
RING	really interesting new gene
RISC	RNA-induced silencing complex
RNA	ribonucleic acid
RNAi	RNA interference
RNase	ribonuclease

ROR γ t	RAR-related orphan receptor gamma t
RP2	RNA polymerase II
rpm	rounds per minute
RRM	RNA recognition motif
RT	room temperature
RT-PCR	real-time PCR
S	serine
SAF-A	scaffold attachment factor A
Sam68	Src-associated in mitosis 68 kDa
SCF	Skp1-Cullin-Roc1/Rbx/Hrt1-F-box
SD	standard deviation
SDS	Sodium dodecyl sulfate
SDS-PAGE	SDS polyacrylamide gel electrophoresis
semi-qPCR	semi-quantitative PCR
SH2	Src homology 2
SH3	Src homology 3
SHARPIN	SHANK-associated RH domain interacting protein
shRNA	small hairpin RNA
siRNA	small interfering RNA
SLP76	SH2-domain containing leukocyte protein of 76 kDa
SMAC	supramolecular activation cluster
snRNP	small nuclear ribonucleoprotein particles
SOS	son of sevenless
SPRM1	sperm-associated POU domain protein 1
SR	serine/arginine-rich
Src	sarcoma
SRSF	serine/arginine-rich splicing factor
SS	splice site
StrepT-PD	Strep-Tactin pulldown
SV40	simian virus 40

T/Thr	threonine
T6BM	TRAF6 binding motif
TAB	TAK1 binding protein
TAC	tris ammonium chloride
TAD	transactivation domain
TAK	transforming growth factor beta activated kinase
TBE	Tris borate EDTA
TCF7	transcription factor 7
TCR	T cell receptor
TE	Tris EDTA
TEMED	Tetramethylethylenediamine
T _{FH}	follicular T helper
TGF β	transforming growth factor beta
T _H	T helper
TLR	toll like receptor
T _m	melting temperature
TMB	3,3',5,5'-Tetramethylbenzidine
TNF	tumour necrosis factor
TNFAIP3	tumour necrosis factor alpha induced protein 3
TRAF	tumor-necrosis factor associated receptor-associated factor
TRAP150	thyroid-hormone receptor-associated protein 150
Treg	regulatory T cell
Tris	Tris(hydroxymethyl)-aminomethan
U	Unit
U2AF	U2 auxiliary factor
Ubc13	E2 ubiquitin-conjugating enzyme 13
Uev1A	ubiquitin E2 variant 1AA
USA	United States of America
UTR	untranslated region
UV	ultraviolet radiation

V	valine
V	volt
WT	wildtype
ZAP70	zeta-chain-associated protein 70 kDa
β -TrCP	beta-transducin repeat containing protein
γ c	common gamma chain
μ g	microgram
μ l	microliter

8 References

- Abbas, A.K., Lichtman, A.H.H., and Pillai, S. 2014. Cellular and Molecular Immunology. Elsevier Health Sciences.
- Alarcon, B., Mestre, D., and Martinez-Martin, N. (2011). The immunological synapse: a cause or consequence of T-cell receptor triggering? *Immunology*. 133, 420-425.
- Baaten, B.J., Li, C.R., and Bradley, L.M. (2010). Multifaceted regulation of T cells by CD44. *Commun Integr Biol*. 3, 508-512.
- Bachmann, M.F., and Oxenius, A. (2007). Interleukin 2: from immunostimulation to immunoregulation and back again. *EMBO Rep*. 8, 1142-1148.
- Baens, M., Bonsignore, L., Somers, R., Vanderheydt, C., Weeks, S.D., Gunnarsson, J., Nilsson, E., Roth, R.G., Thome, M., and Marynen, P. (2014). MALT1 auto-proteolysis is essential for NF-kappaB-dependent gene transcription in activated lymphocytes. *PLoS One*. 9, e103774.
- Baumjohann, D., Preite, S., Reboldi, A., Ronchi, F., Ansel, K.M., Lanzavecchia, A., and Sallusto, F. (2013). Persistent antigen and germinal center B cells sustain T follicular helper cell responses and phenotype. *Immunity*. 38, 596-605.
- Berard, M., and Tough, D.F. (2002). Qualitative differences between naive and memory T cells. *Immunology*. 106, 127-138.
- Bertin, J., Wang, L., Guo, Y., Jacobson, M.D., Poyet, J.L., Srinivasula, S.M., Merriam, S., DiStefano, P.S., and Alnemri, E.S. (2001). CARD11 and CARD14 are novel caspase recruitment domain (CARD)/membrane-associated guanylate kinase (MAGUK) family members that interact with BCL10 and activate NF-kappa B. *J Biol Chem*. 276, 11877-11882.
- Bidere, N., Ngo, V.N., Lee, J., Collins, C., Zheng, L., Wan, F., Davis, R.E., Lenz, G., Anderson, D.E., Arnoult, D., Vazquez, A., Sakai, K., Zhang, J., Meng, Z., Veenstra, T.D., Staudt, L.M., and Lenardo, M.J. (2009). Casein kinase 1alpha governs antigen-receptor-induced NF-kappaB activation and human lymphoma cell survival. *Nature*. 458, 92-96.
- Birzele, F., Fauti, T., Stahl, H., Lenter, M.C., Simon, E., Knebel, D., Weith, A., Hildebrandt, T., and Mennerich, D. (2011). Next-generation insights into regulatory T cells: expression profiling and FoxP3 occupancy in Human. *Nucleic Acids Res*. 39, 7946-7960.
- Black, D.L. (2003). Mechanisms of alternative pre-messenger RNA splicing. *Annu Rev Biochem*. 72, 291-336.
- Blonska, M., and Lin, X. (2009). CARMA1-mediated NF-kappaB and JNK activation in lymphocytes. *Immunol Rev*. 228, 199-211.
- Blonska, M., and Lin, X. (2011). NF-kappaB signaling pathways regulated by CARMA family of scaffold proteins. *Cell Res*. 21, 55-70.
- Blonska, M., Pappu, B.P., Matsumoto, R., Li, H., Su, B., Wang, D., and Lin, X. (2007). The CARMA1-Bcl10 signaling complex selectively regulates JNK2 kinase in the T cell receptor-signaling pathway. *Immunity*. 26, 55-66.

- Boehm, T. (2012). Evolution of vertebrate immunity. *Curr Biol.* *22*, R722-732.
- Bornancin, F., Renner, F., Touil, R., Sic, H., Kolb, Y., Touil-Allaoui, I., Rush, J.S., Smith, P.A., Bigaud, M., Junker-Walker, U., Burkhart, C., Dawson, J., Niwa, S., Katopodis, A., Nuesslein-Hildesheim, B., Weckbecker, G., Zenke, G., Kinzel, B., Traggiai, E., Brenner, D., Brustle, A., St Paul, M., Zamurovic, N., McCoy, K.D., Rolink, A., Regnier, C.H., Mak, T.W., Ohashi, P.S., Patel, D.D., and Calzascia, T. (2015). Deficiency of MALT1 paracaspase activity results in unbalanced regulatory and effector T and B cell responses leading to multiorgan inflammation. *J Immunol.* *194*, 3723-3734.
- Brenner, D., Brechmann, M., Rohling, S., Tapernoux, M., Mock, T., Winter, D., Lehmann, W.D., Kiefer, F., Thome, M., Krammer, P.H., and Arnold, R. (2009). Phosphorylation of CARMA1 by HPK1 is critical for NF-kappaB activation in T cells. *Proc Natl Acad Sci U S A.* *106*, 14508-14513.
- Brownlie, R.J., and Zamoyska, R. (2013). T cell receptor signalling networks: branched, diversified and bounded. *Nat Rev Immunol.* *13*, 257-269.
- Brustle, A., Brenner, D., Knobbe-Thomsen, C.B., Cox, M., Lang, P.A., Lang, K.S., and Mak, T.W. (2015). MALT1 is an intrinsic regulator of regulatory T cells. *Cell Death Differ.*
- Brustle, A., Brenner, D., Knobbe, C.B., Lang, P.A., Virtanen, C., Hershenfield, B.M., Reardon, C., Lacher, S.M., Ruland, J., Ohashi, P.S., and Mak, T.W. (2012). The NF-kappaB regulator MALT1 determines the encephalitogenic potential of Th17 cells. *J Clin Invest.* *122*, 4698-4709.
- Busch, A., and Hertel, K.J. (2012). Evolution of SR protein and hnRNP splicing regulatory factors. *Wiley Interdiscip Rev RNA.* *3*, 1-12.
- Chang, J.T., Wherry, E.J., and Goldrath, A.W. (2014). Molecular regulation of effector and memory T cell differentiation. *Nat Immunol.* *15*, 1104-1115.
- Chaplin, D.D. (2010). Overview of the immune response. *J Allergy Clin Immunol.* *125*, S3-23.
- Chen, L., and Flies, D.B. (2013). Molecular mechanisms of T cell co-stimulation and co-inhibition. *Nat Rev Immunol.* *13*, 227-242.
- Chen, M., and Manley, J.L. (2009). Mechanisms of alternative splicing regulation: insights from molecular and genomics approaches. *Nat Rev Mol Cell Biol.* *10*, 741-754.
- Chen, W., Jin, W., Hardegen, N., Lei, K.J., Li, L., Marinos, N., McGrady, G., and Wahl, S.M. (2003). Conversion of peripheral CD4+CD25- naive T cells to CD4+CD25+ regulatory T cells by TGF-beta induction of transcription factor Foxp3. *J Exp Med.* *198*, 1875-1886.
- Cheng, J., Hamilton, K.S., and Kane, L.P. (2014). Phosphorylation of Carma1, but not Bcl10, by Akt regulates TCR/CD28-mediated NF-kappaB induction and cytokine production. *Mol Immunol.* *59*, 110-116.
- Cho, S., Hoang, A., Sinha, R., Zhong, X.-Y., Fu, X.-D., Krainer, A.R., and Ghosh, G. (2011). Interaction between the RNA binding domains of Ser-Arg splicing factor 1 and U1-70K

- snRNP protein determines early spliceosome assembly. *Proceedings of the National Academy of Sciences of the United States of America*. *108*, 8233-8238.
- Chuang, S.M., Wang, I.C., and Yang, J.L. (2000). Roles of JNK, p38 and ERK mitogen-activated protein kinases in the growth inhibition and apoptosis induced by cadmium. *Carcinogenesis*. *21*, 1423-1432.
- Coornaert, B., Baens, M., Heyninck, K., Bekaert, T., Haegman, M., Staal, J., Sun, L., Chen, Z.J., Marynen, P., and Beyaert, R. (2008). T cell antigen receptor stimulation induces MALT1 paracaspase-mediated cleavage of the NF-kappaB inhibitor A20. *Nat Immunol*. *9*, 263-271.
- Das, J., Chen, C.H., Yang, L., Cohn, L., Ray, P., and Ray, A. (2001). A critical role for NF-kappa B in GATA3 expression and TH2 differentiation in allergic airway inflammation. *Nature immunology*. *2*, 45-50.
- Davidson, D., Chow, L.M., Fournel, M., and Veillette, A. (1992). Differential regulation of T cell antigen responsiveness by isoforms of the src-related tyrosine protein kinase p59fyn. *J Exp Med*. *175*, 1483-1492.
- Davidson, T.S., DiPaolo, R.J., Andersson, J., and Shevach, E.M. (2007). Cutting Edge: IL-2 is essential for TGF-beta-mediated induction of Foxp3+ T regulatory cells. *Journal of immunology (Baltimore, Md : 1950)*. *178*, 4022-4026.
- De Conti, L., Baralle, M., and Buratti, E. (2013). Exon and intron definition in pre-mRNA splicing. *Wiley Interdiscip Rev RNA*. *4*, 49-60.
- Deng, L., Wang, C., Spencer, E., Yang, L., Braun, A., You, J., Slaughter, C., Pickart, C., and Chen, Z.J. (2000). Activation of the I kappa B kinase complex by TRAF6 requires a dimeric ubiquitin-conjugating enzyme complex and a unique polyubiquitin chain. *Cell*. *103*, 351-361.
- Deo, S.S., Mistry, K.J., Kakade, A.M., and Niphadkar, P.V. (2010). Role played by Th2 type cytokines in IgE mediated allergy and asthma. *Lung India*. *27*, 66-71.
- Dong, C., Yang, D.D., Tournier, C., Whitmarsh, A.J., Xu, J., Davis, R.J., and Flavell, R.A. (2000). JNK is required for effector T-cell function but not for T-cell activation. *Nature*. *405*, 91-94.
- Douanne, T., Gavard, J., and Bidere, N. (2016). The paracaspase MALT1 cleaves the LUBAC subunit HOIL1 during antigen receptor signaling. *J Cell Sci*. *129*, 1775-1780.
- Douglas, A.G.L., and Wood, M.J.A. (2011). RNA splicing: disease and therapy. *Briefings in functional genomics*. *10*, 151-164.
- Douglas, P., Ye, R., Morrice, N., Britton, S., Trinkle-Mulcahy, L., and Lees-Miller, S.P. (2015). Phosphorylation of SAF-A/hnRNP-U Serine 59 by Polo-Like Kinase 1 Is Required for Mitosis. *Molecular and cellular biology*. *35*, 2699-2713.
- Dreyfuss, G., Matunis, M.J., Pinol-Roma, S., and Burd, C.G. (1993). hnRNP proteins and the biogenesis of mRNA. *Annu Rev Biochem*. *62*, 289-321.
- Dubois, S.M., Alexia, C., Wu, Y., Leclair, H.M., Leveau, C., Schol, E., Fest, T., Tarte, K., Chen, Z.J., Gavard, J., and Bidere, N. (2014). A catalytic-independent role for the LUBAC in

- NF-kappaB activation upon antigen receptor engagement and in lymphoma cells. *Blood*. *123*, 2199-2203.
- Duwel, M., Welteke, V., Oeckinghaus, A., Baens, M., Kloo, B., Ferch, U., Darnay, B.G., Ruland, J., Marynen, P., and Krappmann, D. (2009). A20 negatively regulates T cell receptor signaling to NF-kappaB by cleaving Malt1 ubiquitin chains. *J Immunol*. *182*, 7718-7728.
- Eitelhuber, A.C., Vosyka, O., Nagel, D., Bognar, M., Lenze, D., Lammens, K., Schlauderer, F., Hlahla, D., Hopfner, K.P., Lenz, G., Hummel, M., Verhelst, S.H., and Krappmann, D. (2015). Activity-based probes for detection of active MALT1 paracaspase in immune cells and lymphomas. *Chem Biol*. *22*, 129-138.
- Eitelhuber, A.C., Warth, S., Schimmack, G., Duwel, M., Hadian, K., Demski, K., Beisker, W., Shinohara, H., Kurosaki, T., Heissmeyer, V., and Krappmann, D. (2011). Dephosphorylation of Carma1 by PP2A negatively regulates T-cell activation. *Embo j*. *30*, 594-605.
- Elton, L., Carpentier, I., Staal, J., Driege, Y., Haegman, M., and Beyaert, R. (2015). MALT1 cleaves the E3 ubiquitin ligase HOIL-1 in activated T cells, generating a dominant negative inhibitor of LUBAC-induced NF-kappaB signaling. *Febs j*.
- Fredericks, A.M., Cygan, K.J., Brown, B.A., and Fairbrother, W.G. (2015). RNA-Binding Proteins: Splicing Factors and Disease. *Biomolecules*. *5*, 893-909.
- Funke, L., Dakoji, S., and Bredt, D.S. (2005). Membrane-associated guanylate kinases regulate adhesion and plasticity at cell junctions. *Annual Review of Biochemistry*. *74*, 219-245.
- Gaide, O., Favier, B., Legler, D.F., Bonnet, D., Brissoni, B., Valitutti, S., Bron, C., Tschopp, J., and Thome, M. (2002). CARMA1 is a critical lipid raft-associated regulator of TCR-induced NF-kappa B activation. *Nat Immunol*. *3*, 836-843.
- Gaide, O., Martinon, F., Micheau, O., Bonnet, D., Thome, M., and Tschopp, J. (2001). Carma1, a CARD-containing binding partner of Bcl10, induces Bcl10 phosphorylation and NF-kappaB activation. *FEBS Lett*. *496*, 121-127.
- Gascoigne, N.R. (2008). Do T cells need endogenous peptides for activation? *Nat Rev Immunol*. *8*, 895-900.
- Germain, R.N. (2002). T-cell development and the CD4-CD8 lineage decision. *Nat Rev Immunol*. *2*, 309-322.
- Gerondakis, S., Fulford, T.S., Messina, N.L., and Grumont, R.J. (2014). NF-kappaB control of T cell development. *Nat Immunol*. *15*, 15-25.
- Gewies, A., Gorka, O., Bergmann, H., Pechloff, K., Petermann, F., Jeltsch, K.M., Rudelius, M., Kriegsmann, M., Weichert, W., Horsch, M., Beckers, J., Wurst, W., Heikenwalder, M., Korn, T., Heissmeyer, V., and Ruland, J. (2014). Uncoupling Malt1 threshold function from paracaspase activity results in destructive autoimmune inflammation. *Cell Rep*. *9*, 1292-1305.
- Gilmore, T.D. (2006). Introduction to NF-kappaB: players, pathways, perspectives. *Oncogene*. *25*, 6680-6684.

- Goehle, R.W., Shultz, J.C., Murudkar, C., Usanovic, S., Lamour, N.F., Massey, D.H., Zhang, L., Camidge, D.R., Shay, J.W., Minna, J.D., and Chalfant, C.E. (2010). hnRNP L regulates the tumorigenic capacity of lung cancer xenografts in mice via caspase-9 pre-mRNA processing. *J Clin Invest.* *120*, 3923-3939.
- Gonzalez, S., Gonzalez-Rodriguez, A.P., Suarez-Alvarez, B., Lopez-Soto, A., Huergo-Zapico, L., and Lopez-Larrea, C. (2011). Conceptual aspects of self and nonself discrimination. *Self Nonsel.* *2*, 19-25.
- Griesbach, R.A. (2012). MALT1 und NEMO determinieren T-Zell-Aktivierung und -Differenzierung (Unpublished doctoral dissertation). Ludwig-Maximilians-Universität München, Germany.
- Guilet, C., and Vito, P. (2000). Caspase recruitment domain (CARD)-dependent cytoplasmic filaments mediate bcl10-induced NF-kappaB activation. *J Cell Biol.* *148*, 1131-1140.
- Guil, S., Long, J.C., and Caceres, J.F. (2006). hnRNP A1 relocalization to the stress granules reflects a role in the stress response. *Molecular and cellular biology.* *26*, 5744-5758.
- Guy, C.S., and Vignali, D.A. (2009). Organization of proximal signal initiation at the TCR:CD3 complex. *Immunol Rev.* *232*, 7-21.
- Hachmann, J., Edgington-Mitchell, L.E., Poreba, M., Sanman, L.E., Drag, M., Bogoyo, M., and Salvesen, G.S. (2015). Probes to monitor activity of the paracaspase MALT1. *Chem Biol.* *22*, 139-147.
- Hachmann, J., Snipas, S.J., van Raam, B.J., Cancino, E.M., Houlihan, E.J., Poreba, M., Kasperkiewicz, P., Drag, M., and Salvesen, G.S. (2012). Mechanism and specificity of the human paracaspase MALT1. *Biochem J.* *443*, 287-295.
- Hailfinger, S., Nogai, H., Pelzer, C., Jaworski, M., Cabalzar, K., Charton, J.E., Guzzardi, M., Decaillet, C., Grau, M., Dorken, B., Lenz, P., Lenz, G., and Thome, M. (2011). Malt1-dependent RelB cleavage promotes canonical NF-kappaB activation in lymphocytes and lymphoma cell lines. *Proc Natl Acad Sci U S A.* *108*, 14596-14601.
- Hara, H., Bakal, C., Wada, T., Bouchard, D., Rottapel, R., Saito, T., and Penninger, J.M. (2004). The molecular adapter Carma1 controls entry of IkappaB kinase into the central immune synapse. *J Exp Med.* *200*, 1167-1177.
- Hara, H., and Saito, T. (2009). CARD9 versus CARMA1 in innate and adaptive immunity. *Trends Immunol.* *30*, 234-242.
- Hara, H., Wada, T., Bakal, C., Kozieradzki, I., Suzuki, S., Suzuki, N., Nghiem, M., Griffiths, E.K., Krawczyk, C., Bauer, B., D'Acquisto, F., Ghosh, S., Yeh, W.C., Baier, G., Rottapel, R., and Penninger, J.M. (2003). The MAGUK family protein CARD11 is essential for lymphocyte activation. *Immunity.* *18*, 763-775.
- Hara, H., Yokosuka, T., Hirakawa, H., Ishihara, C., Yasukawa, S., Yamazaki, M., Koseki, H., Yoshida, H., and Saito, T. (2015). Clustering of CARMA1 through SH3-GUK domain interactions is required for its activation of NF-kappaB signalling. *Nat Commun.* *6*, 5555.

- Hasegawa, Y., Brockdorff, N., Kawano, S., Tsutui, K., Tsutui, K., and Nakagawa, S. (2010). The matrix protein hnRNP U is required for chromosomal localization of Xist RNA. *Developmental cell*. *19*, 469-476.
- Hayden, M.S., and Ghosh, S. (2012). NF-kappaB, the first quarter-century: remarkable progress and outstanding questions. *Genes Dev*. *26*, 203-234.
- Heger, K., Kober, M., Riess, D., Drees, C., de Vries, I., Bertossi, A., Roers, A., Sixt, M., and Schmidt-Supprian, M. (2015). A novel Cre recombinase reporter mouse strain facilitates selective and efficient infection of primary immune cells with adenoviral vectors. *Eur J Immunol*. *45*, 1614-1620.
- Heissmeyer, V., Macian, F., Im, S.H., Varma, R., Feske, S., Venuprasad, K., Gu, H., Liu, Y.C., Dustin, M.L., and Rao, A. (2004). Calcineurin imposes T cell unresponsiveness through targeted proteolysis of signaling proteins. *Nat Immunol*. *5*, 255-265.
- Hermiston, M.L., Xu, Z., and Weiss, A. (2003). CD45: a critical regulator of signaling thresholds in immune cells. *Annu Rev Immunol*. *21*, 107-137.
- Heyd, F., and Lynch, K.W. (2010). Phosphorylation-dependent regulation of PSF by GSK3 controls CD45 alternative splicing. *Mol Cell*. *40*, 126-137.
- Heyd, F., and Lynch, K.W. (2011). Degrade, move, regroup: signaling control of splicing proteins. *Trends Biochem Sci*. *36*, 397-404.
- Hinz, M., and Scheidereit, C. (2014). The IκB kinase complex in NF-κB regulation and beyond. *EMBO reports*. *15*, 46-61.
- Hong, C., Luckey, M.A., Ligons, D.L., Waickman, A.T., Park, J.-Y., Kim, G.Y., Keller, H.R., Etzensperger, R., Tai, X., Lazarevic, V., Feigenbaum, L., Catalfamo, M., Walsh, S.T.R., and Park, J.-H. (2014). Activated T cells secrete an alternatively spliced form of common gamma-chain that inhibits cytokine signaling and exacerbates inflammation. *Immunity*. *40*, 910-923.
- Huang, W., and August, A. (2015). The signaling symphony: T cell receptor tunes cytokine-mediated T cell differentiation. *J Leukoc Biol*. *97*, 477-485.
- Huelga, S.C., Vu, A.Q., Arnold, J.D., Liang, T.Y., Liu, P.P., Yan, B.Y., Donohue, J.P., Shiue, L., Hoon, S., Brenner, S., Ares, M., Jr., and Yeo, G.W. (2012). Integrative genome-wide analysis reveals cooperative regulation of alternative splicing by hnRNP proteins. *Cell reports*. *1*, 167-178.
- Hulpiau, P., Driège, Y., Staal, J., and Beyaert, R. (2015). MALT1 is not alone after all: identification of novel paracaspases. *Cell Mol Life Sci*.
- Hutchison, S., LeBel, C., Blanchette, M., and Chabot, B. (2002). Distinct sets of adjacent heterogeneous nuclear ribonucleoprotein (hnRNP) A1/A2 binding sites control 5' splice site selection in the hnRNP A1 mRNA precursor. *The Journal of biological chemistry*. *277*, 29745-29752.
- Ip, J.Y., Tong, A., Pan, Q., Topp, J.D., Blencowe, B.J., and Lynch, K.W. (2007). Global analysis of alternative splicing during T-cell activation. *RNA*. *13*, 563-572.

- Ishiguro, K., Ando, T., Goto, H., and Xavier, R. (2007). Bcl10 is phosphorylated on Ser138 by Ca²⁺/calmodulin-dependent protein kinase II. *Mol Immunol.* *44*, 2095-2100.
- Ishiguro, K., Green, T., Rapley, J., Wachtel, H., Giallourakis, C., Landry, A., Cao, Z., Lu, N., Takafumi, A., Goto, H., Daly, M.J., and Xavier, R.J. (2006). Ca²⁺/calmodulin-dependent protein kinase II is a modulator of CARMA1-mediated NF-kappaB activation. *Mol Cell Biol.* *26*, 5497-5508.
- Israel, A. (2010). The IKK complex, a central regulator of NF-kappaB activation. *Cold Spring Harb Perspect Biol.* *2*, a000158.
- Ivanov, II, McKenzie, B.S., Zhou, L., Tadokoro, C.E., Lepelley, A., Lafaille, J.J., Cua, D.J., and Littman, D.R. (2006). The orphan nuclear receptor RORgamma directs the differentiation program of proinflammatory IL-17+ T helper cells. *Cell.* *126*, 1121-1133.
- Izquierdo, J.M., Majos, N., Bonnal, S., Martinez, C., Castelo, R., Guigo, R., Bilbao, D., and Valcarcel, J. (2005). Regulation of Fas alternative splicing by antagonistic effects of TIA-1 and PTB on exon definition. *Molecular cell.* *19*, 475-484.
- Jabara, H.H., Ohsumi, T., Chou, J., Massaad, M.J., Benson, H., Megarbane, A., Chouery, E., Mikhael, R., Gorka, O., Gewies, A., Portales, P., Nakayama, T., Hosokawa, H., Revy, P., Herrod, H., Le Deist, F., Lefranc, G., Ruland, J., and Geha, R.S. (2013). A homozygous mucosa-associated lymphoid tissue 1 (MALT1) mutation in a family with combined immunodeficiency. *J Allergy Clin Immunol.* *132*, 151-158.
- Janssens, S., Burns, K., Tschopp, J., and Beyaert, R. (2002). Regulation of interleukin-1- and lipopolysaccharide-induced NF-kappaB activation by alternative splicing of MyD88. *Curr Biol.* *12*, 467-471.
- Jattani, R.P., Tritapoe, J.M., and Pomerantz, J.L. (2016). Intramolecular Interactions and Regulation of Cofactor Binding by the Four Repressive Elements in the Caspase Recruitment Domain-containing Protein 11 (CARD11) Inhibitory Domain. *J Biol Chem.* *291*, 8338-8348.
- Jaworski, M., Marsland, B.J., Gehrig, J., Held, W., Favre, S., Luther, S.A., Perroud, M., Golshayan, D., Gaide, O., and Thome, M. (2014). Malt1 protease inactivation efficiently dampens immune responses but causes spontaneous autoimmunity. *Embo j.* *33*, 2765-2781.
- Jaworski, M., and Thome, M. (2015). The paracaspase MALT1: biological function and potential for therapeutic inhibition. *Cell Mol Life Sci.*
- Jeltsch, K.M., Hu, D., Brenner, S., Zoller, J., Heinz, G.A., Nagel, D., Vogel, K.U., Rehage, N., Warth, S.C., Edelmann, S.L., Gloury, R., Martin, N., Lohs, C., Lech, M., Stehklein, J.E., Geerlof, A., Kremmer, E., Weber, A., Anders, H.J., Schmitz, I., Schmidt-Supprian, M., Fu, M., Holtmann, H., Krappmann, D., Ruland, J., Kallies, A., Heikenwalder, M., and Heissmeyer, V. (2014). Cleavage of roquin and regnase-1 by the paracaspase MALT1 releases their cooperatively repressed targets to promote T(H)17 differentiation. *Nat Immunol.* *15*, 1079-1089.
- Jin, Y., Yang, Y., and Zhang, P. (2011). New insights into RNA secondary structure in the alternative splicing of pre-mRNAs. *RNA biology.* *8*, 450-457.

- Johnson, G.L., and Lapadat, R. (2002). Mitogen-activated protein kinase pathways mediated by ERK, JNK, and p38 protein kinases. *Science*. *298*, 1911-1912.
- Jun, J.E., Wilson, L.E., Vinuesa, C.G., Lesage, S., Blery, M., Miosge, L.A., Cook, M.C., Kucharska, E.M., Hara, H., Penninger, J.M., Domashenz, H., Hong, N.A., Glynne, R.J., Nelms, K.A., and Goodnow, C.C. (2003). Identifying the MAGUK protein Carma-1 as a central regulator of humoral immune responses and atopy by genome-wide mouse mutagenesis. *Immunity*. *18*, 751-762.
- Kamma, H., Portman, D.S., and Dreyfuss, G. (1995). Cell type-specific expression of hnRNP proteins. *Experimental cell research*. *221*, 187-196.
- Kao, W.P., Yang, C.Y., Su, T.W., Wang, Y.T., Lo, Y.C., and Lin, S.C. (2015). The versatile roles of CARDS in regulating apoptosis, inflammation, and NF-kappaB signaling. *Apoptosis*. *20*, 174-195.
- Karin, M. (1999). How NF-kappaB is activated: the role of the IkappaB kinase (IKK) complex. *Oncogene*. *18*, 6867-6874.
- Keren, H., Lev-Maor, G., and Ast, G. (2010). Alternative splicing and evolution: diversification, exon definition and function. *Nature reviews Genetics*. *11*, 345-355.
- Kiledjian, M., and Dreyfuss, G. (1992). Primary structure and binding activity of the hnRNP U protein: binding RNA through RGG box. *The EMBO journal*. *11*, 2655-2664.
- Kim, M.K., and Nikodem, V.M. (1999). hnRNP U inhibits carboxy-terminal domain phosphorylation by TFIIF and represses RNA polymerase II elongation. *Mol Cell Biol*. *19*, 6833-6844.
- King, C.G., Kobayashi, T., Cejas, P.J., Kim, T., Yoon, K., Kim, G.K., Chiffoleau, E., Hickman, S.P., Walsh, P.T., Turka, L.A., and Choi, Y. (2006). TRAF6 is a T cell-intrinsic negative regulator required for the maintenance of immune homeostasis. *Nat Med*. *12*, 1088-1092.
- Klein, T., Fung, S.Y., Renner, F., Blank, M.A., Dufour, A., Kang, S., Bolger-Munro, M., Scurll, J.M., Priatel, J.J., Schweigler, P., Melkko, S., Gold, M.R., Viner, R.I., Regnier, C.H., Turvey, S.E., and Overall, C.M. (2015). The paracaspase MALT1 cleaves HOIL1 reducing linear ubiquitination by LUBAC to dampen lymphocyte NF-kappaB signalling. *Nat Commun*. *6*, 8777.
- Korn, T., Bettelli, E., Oukka, M., and Kuchroo, V.K. (2009). IL-17 and Th17 Cells. *Annu Rev Immunol*. *27*, 485-517.
- Kornblihtt, A.R., Schor, I.E., Allo, M., Dujardin, G., Petrillo, E., and Munoz, M.J. (2013). Alternative splicing: a pivotal step between eukaryotic transcription and translation. *Nature reviews Molecular cell biology*. *14*, 153-165.
- Kortum, R.L., Rouquette-Jazdanian, A.K., and Samelson, L.E. (2013). Ras and extracellular signal-regulated kinase signaling in thymocytes and T cells. *Trends Immunol*. *34*, 259-268.

- Kukalev, A., Nord, Y., Palmberg, C., Bergman, T., and Percipalle, P. (2005). Actin and hnRNP U cooperate for productive transcription by RNA polymerase II. *Nat Struct Mol Biol.* *12*, 238-244.
- Kumari, S., Curado, S., Mayya, V., and Dustin, M.L. (2014). T cell antigen receptor activation and actin cytoskeleton remodeling. *Biochim Biophys Acta.* *1838*, 546-556.
- Lamason, R.L., McCully, R.R., Lew, S.M., and Pomerantz, J.L. (2010). Oncogenic CARD11 mutations induce hyperactive signaling by disrupting autoinhibition by the PKC-responsive inhibitory domain. *Biochemistry.* *49*, 8240-8250.
- Langel, F.D., Jain, N.A., Rossman, J.S., Kingeter, L.M., Kashyap, A.K., and Schaefer, B.C. (2008). Multiple protein domains mediate interaction between Bcl10 and MALT1. *J Biol Chem.* *283*, 32419-32431.
- Leeman, J.R., and Gilmore, T.D. (2008). Alternative splicing in the NF-kappaB signaling pathway. *Gene.* *423*, 97-107.
- Lenz, G., Davis, R.E., Ngo, V.N., Lam, L., George, T.C., Wright, G.W., Dave, S.S., Zhao, H., Xu, W., Rosenwald, A., Ott, G., Muller-Hermelink, H.K., Gascoyne, R.D., Connors, J.M., Rimsza, L.M., Campo, E., Jaffe, E.S., Delabie, J., Smeland, E.B., Fisher, R.I., Chan, W.C., and Staudt, L.M. (2008). Oncogenic CARD11 mutations in human diffuse large B cell lymphoma. *Science.* *319*, 1676-1679.
- Leppek, K., Schott, J., Reitter, S., Poetz, F., Hammond, M.C., and Stoecklin, G. (2013). Roquin promotes constitutive mRNA decay via a conserved class of stem-loop recognition motifs. *Cell.* *153*, 869-881.
- Ley, K. (2014). The second touch hypothesis: T cell activation, homing and polarization. *F1000Res.* *3*, 37.
- Li, S., Yang, X., Shao, J., and Shen, Y. (2012). Structural insights into the assembly of CARMA1 and BCL10. *PLoS One.* *7*, e42775.
- Lim, L.P., and Burge, C.B. (2001). A computational analysis of sequence features involved in recognition of short introns. *Proceedings of the National Academy of Sciences of the United States of America.* *98*, 11193-11198.
- Liu, J., and Lin, A. (2005). Role of JNK activation in apoptosis: a double-edged sword. *Cell Res.* *15*, 36-42.
- Lobry, C., Lopez, T., Israel, A., and Weil, R. (2007). Negative feedback loop in T cell activation through IkappaB kinase-induced phosphorylation and degradation of Bcl10. *Proc Natl Acad Sci U S A.* *104*, 908-913.
- Love, P.E., and Hayes, S.M. (2010). ITAM-mediated signaling by the T-cell antigen receptor. *Cold Spring Harb Perspect Biol.* *2*, a002485.
- Lucas, P.C., Yonezumi, M., Inohara, N., McAllister-Lucas, L.M., Abazeed, M.E., Chen, F.F., Yamaoka, S., Seto, M., and Nunez, G. (2001). Bcl10 and MALT1, independent targets of chromosomal translocation in malt lymphoma, cooperate in a novel NF-kappa B signaling pathway. *J Biol Chem.* *276*, 19012-19019.

- Luckheeram, R.V., Zhou, R., Verma, A.D., and Xia, B. (2012). CD4(+)T cells: differentiation and functions. *Clin Dev Immunol.* 2012, 925135.
- Luco, R.F., Allo, M., Schor, I.E., Kornblihtt, A.R., and Misteli, T. (2011). Epigenetics in alternative pre-mRNA splicing. *Cell.* 144, 16-26.
- Lynch, K.W. (2004). Consequences of regulated pre-mRNA splicing in the immune system. *Nature reviews Immunology.* 4, 931-940.
- Lynch, K.W. (2007). Regulation of alternative splicing by signal transduction pathways. *Advances in experimental medicine and biology.* 623, 161-174.
- Lynch, K.W., and Weiss, A. (2000). A model system for activation-induced alternative splicing of CD45 pre-mRNA in T cells implicates protein kinase C and Ras. *Mol Cell Biol.* 20, 70-80.
- Ma, C.S., Deenick, E.K., Batten, M., and Tangye, S.G. (2012). The origins, function, and regulation of T follicular helper cells. *J Exp Med.* 209, 1241-1253.
- Macian, F. (2005). NFAT proteins: key regulators of T-cell development and function. *Nat Rev Immunol.* 5, 472-484.
- Magistrelli, G., Jeannin, P., Herbault, N., Benoit De Coignac, A., Gauchat, J.F., Bonnefoy, J.Y., and Delneste, Y. (1999). A soluble form of CTLA-4 generated by alternative splicing is expressed by nonstimulated human T cells. *Eur J Immunol.* 29, 3596-3602.
- Malek, T.R. (2008). The biology of interleukin-2. *Annu Rev Immunol.* 26, 453-479.
- Malissen, B. (2008). CD3 ITAMs count! *Nat Immunol.* 9, 583-584.
- Marsland, B.J., Soos, T.J., Spath, G., Littman, D.R., and Kopf, M. (2004). Protein kinase C theta is critical for the development of in vivo T helper (Th)2 cell but not Th1 cell responses. *The Journal of experimental medicine.* 200, 181-189.
- Martinez, N.M., Agosto, L., Qiu, J., Mallory, M.J., Gazzara, M.R., Barash, Y., Fu, X.-D., and Lynch, K.W. (2015). Widespread JNK-dependent alternative splicing induces a positive feedback loop through CELF2-mediated regulation of MKK7 during T-cell activation. *Genes & development.* 29, 2054-2066.
- Martinez, N.M., and Lynch, K.W. (2013). Control of alternative splicing in immune responses: many regulators, many predictions, much still to learn. *Immunol Rev.* 253, 216-236.
- Martinez, N.M., Pan, Q., Cole, B.S., Yarosh, C.A., Babcock, G.A., Heyd, F., Zhu, W., Ajith, S., Blencowe, B.J., and Lynch, K.W. (2012). Alternative splicing networks regulated by signaling in human T cells. *RNA.* 18, 1029-1040.
- Matlin, A.J., Clark, F., and Smith, C.W. (2005). Understanding alternative splicing: towards a cellular code. *Nat Rev Mol Cell Biol.* 6, 386-398.
- Matsumoto, R., Wang, D., Blonska, M., Li, H., Kobayashi, M., Pappu, B., Chen, Y., Wang, D., and Lin, X. (2005). Phosphorylation of CARMA1 plays a critical role in T Cell receptor-mediated NF-kappaB activation. *Immunity.* 23, 575-585.

- Matsushita, K., Takeuchi, O., Standley, D.M., Kumagai, Y., Kawagoe, T., Miyake, T., Satoh, T., Kato, H., Tsujimura, T., Nakamura, H., and Akira, S. (2009). Zc3h12a is an RNase essential for controlling immune responses by regulating mRNA decay. *Nature*. *458*, 1185-1190.
- Matter, N., Herrlich, P., and Konig, H. (2002). Signal-dependent regulation of splicing via phosphorylation of Sam68. *Nature*. *420*, 691-695.
- Mc Guire, C., Elton, L., Wieghofer, P., Staal, J., Voet, S., Demeyer, A., Nagel, D., Krappmann, D., Prinz, M., Beyaert, R., and van Loo, G. (2014). Pharmacological inhibition of MALT1 protease activity protects mice in a mouse model of multiple sclerosis. *J Neuroinflammation*. *11*, 124.
- McAllister-Lucas, L.M., Inohara, N., Lucas, P.C., Ruland, J., Benito, A., Li, Q., Chen, S., Chen, F.F., Yamaoka, S., Verma, I.M., Mak, T.W., and Nunez, G. (2001). Bim1, a MAGUK family member linking protein kinase C activation to Bcl10-mediated NF-kappaB induction. *J Biol Chem*. *276*, 30589-30597.
- McCully, R.R., and Pomerantz, J.L. (2008). The protein kinase C-responsive inhibitory domain of CARD11 functions in NF-kappaB activation to regulate the association of multiple signaling cofactors that differentially depend on Bcl10 and MALT1 for association. *Mol Cell Biol*. *28*, 5668-5686.
- McKinnon, M.L., Rozmus, J., Fung, S.Y., Hirschfeld, A.F., Del Bel, K.L., Thomas, L., Marr, N., Martin, S.D., Marwaha, A.K., Priatel, J.J., Tan, R., Senger, C., Tsang, A., Prendiville, J., Junker, A.K., Seear, M., Schultz, K.R., Sly, L.M., Holt, R.A., Patel, M.S., Friedman, J.M., and Turvey, S.E. (2014). Combined immunodeficiency associated with homozygous MALT1 mutations. *J Allergy Clin Immunol*. *133*, 1458-1462, 1462.e1451-1457.
- McNeela, E.A., and Mills, K.H. (2001). Manipulating the immune system: humoral versus cell-mediated immunity. *Adv Drug Deliv Rev*. *51*, 43-54.
- Medoff, B.D., Seed, B., Jakobek, R., Zora, J., Yang, Y., Luster, A.D., and Xavier, R. (2006). CARMA1 is critical for the development of allergic airway inflammation in a murine model of asthma. *Journal of immunology (Baltimore, Md : 1950)*. *176*, 7272-7277.
- Michel, M., Wilhelmi, I., Schultz, A.S., Preussner, M., and Heyd, F. (2014). Activation-induced tumor necrosis factor receptor-associated factor 3 (Traf3) alternative splicing controls the noncanonical nuclear factor kappaB pathway and chemokine expression in human T cells. *J Biol Chem*. *289*, 13651-13660.
- Moreno-Garcia, M.E., Sommer, K., Haftmann, C., Sontheimer, C., Andrews, S.F., and Rawlings, D.J. (2009). Serine 649 phosphorylation within the protein kinase C-regulated domain down-regulates CARMA1 activity in lymphocytes. *J Immunol*. *183*, 7362-7370.
- Motta-Mena, L.B., Heyd, F., and Lynch, K.W. (2010). Context-dependent regulatory mechanism of the splicing factor hnRNP L. *Molecular cell*. *37*, 223-234.
- Murphy, K.P., Travers, P., Walport, M., and Janeway, C. 2008. *Janeway's Immunobiology*. Garland Science.

- Nagel, D., Spranger, S., Vincendeau, M., Grau, M., Raffegerst, S., Kloo, B., Hlahla, D., Neuenschwander, M., Peter von Kries, J., Hadian, K., Dorken, B., Lenz, P., Lenz, G., Schendel, D.J., and Krappmann, D. (2012). Pharmacologic inhibition of MALT1 protease by phenothiazines as a therapeutic approach for the treatment of aggressive ABC-DLBCL. *Cancer Cell*. 22, 825-837.
- Naro, C., and Sette, C. (2013). Phosphorylation-mediated regulation of alternative splicing in cancer. *Int J Cell Biol*. 2013, 151839.
- Nasim, F.-U.H., Hutchison, S., Cordeau, M., and Chabot, B. (2002). High-affinity hnRNP A1 binding sites and duplex-forming inverted repeats have similar effects on 5' splice site selection in support of a common looping out and repression mechanism. *RNA (New York, N Y)*. 8, 1078-1089.
- Noels, H., van Loo, G., Hagens, S., Broeckx, V., Beyaert, R., Marynen, P., and Baens, M. (2007). A Novel TRAF6 binding site in MALT1 defines distinct mechanisms of NF-kappaB activation by API2middle dotMALT1 fusions. *J Biol Chem*. 282, 10180-10189.
- Oberdoerffer, S., Moita, L.F., Neems, D., Freitas, R.P., Hacohen, N., and Rao, A. (2008). Regulation of CD45 alternative splicing by heterogeneous ribonucleoprotein, hnRNPLL. *Science*. 321, 686-691.
- Obrdlik, A., Kukalev, A., Louvet, E., Farrants, A.K., Caputo, L., and Percipalle, P. (2008). The histone acetyltransferase PCAF associates with actin and hnRNP U for RNA polymerase II transcription. *Mol Cell Biol*. 28, 6342-6357.
- Oeckinghaus, A., and Ghosh, S. (2009). The NF-kappaB family of transcription factors and its regulation. *Cold Spring Harb Perspect Biol*. 1, a000034.
- Oeckinghaus, A., Wegener, E., Welteke, V., Ferch, U., Arslan, S.C., Ruland, J., Scheidereit, C., and Krappmann, D. (2007). Malt1 ubiquitination triggers NF-kappaB signaling upon T-cell activation. *Embo j*. 26, 4634-4645.
- Padhan, K., and Varma, R. (2010). Immunological synapse: a multi-protein signalling cellular apparatus for controlling gene expression. *Immunology*. 129, 322-328.
- Pan, Q., Shai, O., Lee, L.J., Frey, B.J., and Blencowe, B.J. (2008). Deep surveying of alternative splicing complexity in the human transcriptome by high-throughput sequencing. *Nat Genet*. 40, 1413-1415.
- Park, S.G., Schulze-Luehrman, J., Hayden, M.S., Hashimoto, N., Ogawa, W., Kasuga, M., and Ghosh, S. (2009). The kinase PDK1 integrates T cell antigen receptor and CD28 coreceptor signaling to induce NF-kappaB and activate T cells. *Nat Immunol*. 10, 158-166.
- Parkin, J., and Cohen, B. (2001). An overview of the immune system. *Lancet*. 357, 1777-1789.
- Paul, S., and Schaefer, B.C. (2013). A new look at T cell receptor signaling to nuclear factor-kappaB. *Trends Immunol*. 34, 269-281.

- Pelzer, C., Cabalzar, K., Wolf, A., Gonzalez, M., Lenz, G., and Thome, M. (2013). The protease activity of the paracaspase MALT1 is controlled by monoubiquitination. *Nat Immunol.* *14*, 337-345.
- Pfaffl, M.W. (2001). A new mathematical model for relative quantification in real-time RT-PCR. *Nucleic Acids Res.* *29*, e45.
- Pinol-Roma, S. (1997). HnRNP proteins and the nuclear export of mRNA. *Seminars in cell & developmental biology.* *8*, 57-63.
- Pinol-Roma, S., and Dreyfuss, G. (1992). Shuttling of pre-mRNA binding proteins between nucleus and cytoplasm. *Nature.* *355*, 730-732.
- Pitcher, L.A., and van Oers, N.S. (2003). T-cell receptor signal transmission: who gives an ITAM? *Trends Immunol.* *24*, 554-560.
- Pohl, M., Bortfeldt, R.H., Grutzmann, K., and Schuster, S. (2013). Alternative splicing of mutually exclusive exons--a review. *Bio Systems.* *114*, 31-38.
- Punwani, D., Wang, H., Chan, A.Y., Cowan, M.J., Mallott, J., Sunderam, U., Mollenauer, M., Srinivasan, R., Brenner, S.E., Mulder, A., Claas, F.H.J., Weiss, A., and Puck, J.M. (2015). Combined immunodeficiency due to MALT1 mutations, treated by hematopoietic cell transplantation. *Journal of clinical immunology.* *35*, 135-146.
- Purvis, H.A., Stoop, J.N., Mann, J., Woods, S., Kozijn, A.E., Hambleton, S., Robinson, J.H., Isaacs, J.D., Anderson, A.E., and Hilkens, C.M. (2010). Low-strength T-cell activation promotes Th17 responses. *Blood.* *116*, 4829-4837.
- Qiao, Q., Yang, C., Zheng, C., Fontan, L., David, L., Yu, X., Bracken, C., Rosen, M., Melnick, A., Egelman, E.H., and Wu, H. (2013). Structural architecture of the CARMA1/Bcl10/MALT1 signalosome: nucleation-induced filamentous assembly. *Mol Cell.* *51*, 766-779.
- Rao, N., Nguyen, S., Ngo, K., and Fung-Leung, W.P. (2005). A novel splice variant of interleukin-1 receptor (IL-1R)-associated kinase 1 plays a negative regulatory role in Toll/IL-1R-induced inflammatory signaling. *Mol Cell Biol.* *25*, 6521-6532.
- Rebeaud, F., Hailfinger, S., Posevitz-Fejfar, A., Tapernoux, M., Moser, R., Rueda, D., Gaide, O., Guzzardi, M., Iancu, E.M., Rufer, N., Fasel, N., and Thome, M. (2008). The proteolytic activity of the paracaspase MALT1 is key in T cell activation. *Nat Immunol.* *9*, 272-281.
- Risso, A., Smilovich, D., Capra, M.C., Baldissarro, I., Yan, G., Bargellesi, A., and Cosulich, M.E. (1991). CD69 in resting and activated T lymphocytes. Its association with a GTP binding protein and biochemical requirements for its expression. *Journal of immunology (Baltimore, Md : 1950).* *146*, 4105-4114.
- Roca, X., Sachidanandam, R., and Krainer, A.R. (2005). Determinants of the inherent strength of human 5' splice sites. *RNA (New York, N Y).* *11*, 683-698.
- Rohrbach, S., Muller-Werdan, U., Werdan, K., Koch, S., Gellerich, N.F., and Holtz, J. (2005). Apoptosis-modulating interaction of the neuregulin/erbB pathway with anthracyclines in regulating Bcl-xS and Bcl-xL in cardiomyocytes. *J Mol Cell Cardiol.* *38*, 485-493.

- Rosebeck, S., Lim, M.S., Elenitoba-Johnson, K.S., McAllister-Lucas, L.M., and Lucas, P.C. (2016). API2-MALT1 oncoprotein promotes lymphomagenesis via unique program of substrate ubiquitination and proteolysis. *World J Biol Chem.* 7, 128-137.
- Rothrock, C., Cannon, B., Hahm, B., and Lynch, K.W. (2003). A conserved signal-responsive sequence mediates activation-induced alternative splicing of CD45. *Mol Cell.* 12, 1317-1324.
- Rothrock, C.R., House, A.E., and Lynch, K.W. (2005). HnRNP L represses exon splicing via a regulated exonic splicing silencer. *EMBO J.* 24, 2792-2802.
- Ruefli-Brasse, A.A., French, D.M., and Dixit, V.M. (2003). Regulation of NF-kappaB-dependent lymphocyte activation and development by paracaspase. *Science.* 302, 1581-1584.
- Ruland, J., Duncan, G.S., Wakeham, A., and Mak, T.W. (2003). Differential requirement for Malt1 in T and B cell antigen receptor signaling. *Immunity.* 19, 749-758.
- Sakaguchi, S., Wing, K., Onishi, Y., Prieto-Martin, P., and Yamaguchi, T. (2009). Regulatory T cells: how do they suppress immune responses? *Int Immunol.* 21, 1105-1111.
- Sandberg, R., Neilson, J.R., Sarma, A., Sharp, P.A., and Burge, C.B. (2008). Proliferating cells express mRNAs with shortened 3' untranslated regions and fewer microRNA target sites. *Science.* 320, 1643-1647.
- Satpathy, S., Wagner, S.A., Beli, P., Gupta, R., Kristiansen, T.A., Malinova, D., Francavilla, C., Tolar, P., Bishop, G.A., Hostager, B.S., and Choudhary, C. (2015). Systems-wide analysis of BCR signalosomes and downstream phosphorylation and ubiquitylation. *Mol Syst Biol.* 11, 810.
- Scharschmidt, E., Wegener, E., Heissmeyer, V., Rao, A., and Krappmann, D. (2004). Degradation of Bcl10 induced by T-cell activation negatively regulates NF-kappa B signaling. *Mol Cell Biol.* 24, 3860-3873.
- Schmitz, M.L., and Krappmann, D. (2006). Controlling NF-kappaB activation in T cells by costimulatory receptors. *Cell Death Differ.* 13, 834-842.
- Schulze-Luehrmann, J., and Ghosh, S. (2006). Antigen-receptor signaling to nuclear factor kappa B. *Immunity.* 25, 701-715.
- Seol, D.W., and Billiar, T.R. (1999). A caspase-9 variant missing the catalytic site is an endogenous inhibitor of apoptosis. *The Journal of biological chemistry.* 274, 2072-2076.
- Serre, K., Mohr, E., Benezech, C., Bird, R., Khan, M., Caamano, J.H., Cunningham, A.F., and MacLennan, I.C.M. (2011). Selective effects of NF-kappaB1 deficiency in CD4⁺ T cells on Th2 and TFh induction by alum-precipitated protein vaccines. *European journal of immunology.* 41, 1573-1582.
- Shambharkar, P.B., Blonska, M., Pappu, B.P., Li, H., You, Y., Sakurai, H., Darnay, B.G., Hara, H., Penninger, J., and Lin, X. (2007). Phosphorylation and ubiquitination of the IkappaB kinase complex by two distinct signaling pathways. *EMBO J.* 26, 1794-1805.
- Sharma, S., Falick, A.M., and Black, D.L. (2005). Polypyrimidine tract binding protein blocks the 5' splice site-dependent assembly of U2AF and the prespliceosomal E complex. *Mol Cell.* 19, 485-496.

- Sharpe, A.H., and Abbas, A.K. (2006). T-cell costimulation--biology, therapeutic potential, and challenges. *N Engl J Med.* 355, 973-975.
- Shaulian, E., and Karin, M. (2002). AP-1 as a regulator of cell life and death. *Nat Cell Biol.* 4, E131-136.
- Shih, V.F., Tsui, R., Caldwell, A., and Hoffmann, A. (2011). A single NFkappaB system for both canonical and non-canonical signaling. *Cell Res.* 21, 86-102.
- Shin, C., and Manley, J.L. (2004). Cell signalling and the control of pre-mRNA splicing. *Nature reviews Molecular cell biology.* 5, 727-738.
- Shiow, L.R., Rosen, D.B., Brdickova, N., Xu, Y., An, J., Lanier, L.L., Cyster, J.G., and Matloubian, M. (2006). CD69 acts downstream of interferon-alpha/beta to inhibit S1P1 and lymphocyte egress from lymphoid organs. *Nature.* 440, 540-544.
- Shukla, S., and Oberdoerffer, S. (2012). Co-transcriptional regulation of alternative pre-mRNA splicing. *Biochim Biophys Acta.* 1819, 673-683.
- Smith-Garvin, J.E., Koretzky, G.A., and Jordan, M.S. (2009). T cell activation. *Annu Rev Immunol.* 27, 591-619.
- Sommer, K., Guo, B., Pomerantz, J.L., Bandaranayake, A.D., Moreno-Garcia, M.E., Ovechkina, Y.L., and Rawlings, D.J. (2005). Phosphorylation of the CARMA1 linker controls NF-kappaB activation. *Immunity.* 23, 561-574.
- Srinivasula, S.M., Ahmad, M., Guo, Y., Zhan, Y., Lazebnik, Y., Fernandes-Alnemri, T., and Alnemri, E.S. (1999). Identification of an endogenous dominant-negative short isoform of caspase-9 that can regulate apoptosis. *Cancer research.* 59, 999-1002.
- Staal, J., and Beyaert, R. (2012). A two-step activation mechanism of MALT1 paracaspase. *J Mol Biol.* 419, 1-3.
- Staal, J., Driège, Y., Bekaert, T., Demeyer, A., Muyllaert, D., Van Damme, P., Gevaert, K., and Beyaert, R. (2011). T-cell receptor-induced JNK activation requires proteolytic inactivation of CYLD by MALT1. *Embo j.* 30, 1742-1752.
- Stamm, S. (2008). Regulation of alternative splicing by reversible protein phosphorylation. *The Journal of biological chemistry.* 283, 1223-1227.
- Stempin, C.C., Chi, L., Giraldo-Vela, J.P., High, A.A., Hacker, H., and Redecke, V. (2011). The E3 ubiquitin ligase mind bomb-2 (MIB2) protein controls B-cell CLL/lymphoma 10 (BCL10)-dependent NF-kappaB activation. *J Biol Chem.* 286, 37147-37157.
- Stone, J.C. (2011). Regulation and Function of the RasGRP Family of Ras Activators in Blood Cells. *Genes Cancer.* 2, 320-334.
- Sun, L., Deng, L., Ea, C.K., Xia, Z.P., and Chen, Z.J. (2004). The TRAF6 ubiquitin ligase and TAK1 kinase mediate IKK activation by BCL10 and MALT1 in T lymphocytes. *Mol Cell.* 14, 289-301.
- Sun, S.C. (2010). CYLD: a tumor suppressor deubiquitinase regulating NF-kappaB activation and diverse biological processes. *Cell Death Differ.* 17, 25-34.

- Swain, S.L., Weinberg, A.D., English, M., and Huston, G. (1990). IL-4 directs the development of Th2-like helper effectors. *J Immunol.* *145*, 3796-3806.
- Szabo, S.J., Kim, S.T., Costa, G.L., Zhang, X., Fathman, C.G., and Glimcher, L.H. (2000). A novel transcription factor, T-bet, directs Th1 lineage commitment. *Cell.* *100*, 655-669.
- Szymczak, A.L., Workman, C.J., Wang, Y., Vignali, K.M., Dilioglou, S., Vanin, E.F., and Vignali, D.A.A. (2004). Correction of multi-gene deficiency in vivo using a single 'self-cleaving' 2A peptide-based retroviral vector. *Nature biotechnology.* *22*, 589-594.
- Tanner, M.J., Hanel, W., Gaffen, S.L., and Lin, X. (2007). CARMA1 coiled-coil domain is involved in the oligomerization and subcellular localization of CARMA1 and is required for T cell receptor-induced NF-kappaB activation. *J Biol Chem.* *282*, 17141-17147.
- Tazi, J., Bakkour, N., and Stamm, S. (2009). Alternative splicing and disease. *Biochim Biophys Acta.* *1792*, 14-26.
- Thaker, Y.R., Schneider, H., and Rudd, C.E. (2015). TCR and CD28 activate the transcription factor NF-kappaB in T-cells via distinct adaptor signaling complexes. *Immunol Lett.* *163*, 113-119.
- Thome, M., Charton, J.E., Pelzer, C., and Hailfinger, S. (2010). Antigen receptor signaling to NF-kappaB via CARMA1, BCL10, and MALT1. *Cold Spring Harb Perspect Biol.* *2*, a003004.
- Tokunaga, F., and Iwai, K. (2012). LUBAC, a novel ubiquitin ligase for linear ubiquitination, is crucial for inflammation and immune responses. *Microbes Infect.* *14*, 563-572.
- Tong, A., Nguyen, J., and Lynch, K.W. (2005). Differential expression of CD45 isoforms is controlled by the combined activity of basal and inducible splicing-regulatory elements in each of the variable exons. *The Journal of biological chemistry.* *280*, 38297-38304.
- Topp, J.D., Jackson, J., Melton, A.A., and Lynch, K.W. (2008). A cell-based screen for splicing regulators identifies hnRNP LL as a distinct signal-induced repressor of CD45 variable exon 4. *RNA (New York, N Y).* *14*, 2038-2049.
- Tube, N.J., Pagan, A.J., Taylor, J.J., Nelson, R.W., Linehan, J.L., Ertelt, J.M., Huseby, E.S., Way, S.S., and Jenkins, M.K. (2013). Single naive CD4+ T cells from a diverse repertoire produce different effector cell types during infection. *Cell.* *153*, 785-796.
- Uehata, T., Iwasaki, H., Vandenbon, A., Matsushita, K., Hernandez-Cuellar, E., Kuniyoshi, K., Satoh, T., Mino, T., Suzuki, Y., Standley, D.M., Tsujimura, T., Rakugi, H., Isaka, Y., Takeuchi, O., and Akira, S. (2013). Malt1-induced cleavage of regnase-1 in CD4(+) helper T cells regulates immune activation. *Cell.* *153*, 1036-1049.
- Uren, A.G., O'Rourke, K., Aravind, L.A., Pisabarro, M.T., Seshagiri, S., Koonin, E.V., and Dixit, V.M. (2000). Identification of paracaspases and metacaspases: two ancient families of caspase-like proteins, one of which plays a key role in MALT lymphoma. *Mol Cell.* *6*, 961-967.
- van der Houven van Oordt, W., Diaz-Meco, M.T., Lozano, J., Krainer, A.R., Moscat, J., and Caceres, J.F. (2000). The MKK(3/6)-p38-signaling cascade alters the subcellular distribution

- of hnRNP A1 and modulates alternative splicing regulation. *The Journal of cell biology*. *149*, 307-316.
- van Panhuys, N. (2016). TCR Signal Strength Alters T-DC Activation and Interaction Times and Directs the Outcome of Differentiation. *Front Immunol*. *7*, 6.
- van Panhuys, N., Klauschen, F., and Germain, R.N. (2014). T-cell-receptor-dependent signal intensity dominantly controls CD4(+) T cell polarization In Vivo. *Immunity*. *41*, 63-74.
- Vercammen, D., Declercq, W., Vandenabeele, P., and Van Breusegem, F. (2007). Are metacaspases caspases? *J Cell Biol*. *179*, 375-380.
- Vu, N.T., Park, M.A., Shultz, J.C., Goehle, R.W., Hoeflerlin, L.A., Shultz, M.D., Smith, S.A., Lynch, K.W., and Chalfant, C.E. (2013). hnRNP U enhances caspase-9 splicing and is modulated by AKT-dependent phosphorylation of hnRNP L. *The Journal of biological chemistry*. *288*, 8575-8584.
- Vyas, J.M., Van der Veen, A.G., and Ploegh, H.L. (2008). The known unknowns of antigen processing and presentation. *Nat Rev Immunol*. *8*, 607-618.
- Wahl, M.C., Will, C.L., and Luhrmann, R. (2009). The spliceosome: design principles of a dynamic RNP machine. *Cell*. *136*, 701-718.
- Waite, J.C., and Skokos, D. (2012). Th17 response and inflammatory autoimmune diseases. *Int J Inflam*. *2012*, 819467.
- Wang, D., Matsumoto, R., You, Y., Che, T., Lin, X.Y., Gaffen, S.L., and Lin, X. (2004). CD3/CD28 costimulation-induced NF-kappaB activation is mediated by recruitment of protein kinase C-theta, Bcl10, and IkappaB kinase beta to the immunological synapse through CARMA1. *Mol Cell Biol*. *24*, 164-171.
- Wang, E.T., Sandberg, R., Luo, S., Khrebtkova, I., Zhang, L., Mayr, C., Kingsmore, S.F., Schroth, G.P., and Burge, C.B. (2008). Alternative isoform regulation in human tissue transcriptomes. *Nature*. *456*, 470-476.
- Warrington, R., Watson, W., Kim, H.L., and Antonetti, F.R. (2011). An introduction to immunology and immunopathology. *Allergy Asthma Clin Immunol*. *7 Suppl 1*, S1.
- Warth, S.C., and Heissmeyer, V. (2013). Adenoviral transduction of naive CD4 T cells to study Treg differentiation. *J Vis Exp*.
- Wegener, E., and Krappmann, D. (2007). CARD-Bcl10-Malt1 signalosomes: missing link to NF-kappaB. *Sci STKE*. *2007*, pe21.
- Wegener, E., Oeckinghaus, A., Papadopoulou, N., Lavitas, L., Schmidt-Supprian, M., Ferch, U., Mak, T.W., Ruland, J., Heissmeyer, V., and Krappmann, D. (2006). Essential role for IkappaB kinase beta in remodeling Carma1-Bcl10-Malt1 complexes upon T cell activation. *Mol Cell*. *23*, 13-23.
- Wiesmann, C., Leder, L., Blank, J., Bernardi, A., Melkko, S., Decock, A., D'Arcy, A., Villard, F., Erbel, P., Hughes, N., Freuler, F., Nikolay, R., Alves, J., Bornancin, F., and Renatus, M. (2012). Structural determinants of MALT1 protease activity. *J Mol Biol*. *419*, 4-21.

- Willinger, T., Freeman, T., Herbert, M., Hasegawa, H., McMichael, A.J., and Callan, M.F. (2006). Human naive CD8 T cells down-regulate expression of the WNT pathway transcription factors lymphoid enhancer binding factor 1 and transcription factor 7 (T cell factor-1) following antigen encounter in vitro and in vivo. *J Immunol.* *176*, 1439-1446.
- Willis, T.G., Jadayel, D.M., Du, M.Q., Peng, H., Perry, A.R., Abdul-Rauf, M., Price, H., Karran, L., Majekodunmi, O., Wlodarska, I., Pan, L., Crook, T., Hamoudi, R., Isaacson, P.G., and Dyer, M.J. (1999). Bcl10 is involved in t(1;14)(p22;q32) of MALT B cell lymphoma and mutated in multiple tumor types. *Cell.* *96*, 35-45.
- Wu, C.J., and Ashwell, J.D. (2008). NEMO recognition of ubiquitinated Bcl10 is required for T cell receptor-mediated NF-kappaB activation. *Proc Natl Acad Sci U S A.* *105*, 3023-3028.
- Wu, Z., Jia, X., de la Cruz, L., Su, X.-C., Marzolf, B., Troisch, P., Zak, D., Hamilton, A., Whittle, B., Yu, D., Sheahan, D., Bertram, E., Aderem, A., Otting, G., Goodnow, C.C., and Hoyne, G.F. (2008). Memory T cell RNA rearrangement programmed by heterogeneous nuclear ribonucleoprotein hnRNPLL. *Immunity.* *29*, 863-875.
- Xiao, R., Tang, P., Yang, B., Huang, J., Zhou, Y., Shao, C., Li, H., Sun, H., Zhang, Y., and Fu, X.-D. (2012). Nuclear matrix factor hnRNP U/SAF-A exerts a global control of alternative splicing by regulating U2 snRNP maturation. *Molecular cell.* *45*, 656-668.
- Yamamoto, M., Okamoto, T., Takeda, K., Sato, S., Sanjo, H., Uematsu, S., Saitoh, T., Yamamoto, N., Sakurai, H., Ishii, K.J., Yamaoka, S., Kawai, T., Matsuura, Y., Takeuchi, O., and Akira, S. (2006). Key function for the Ubc13 E2 ubiquitin-conjugating enzyme in immune receptor signaling. *Nat Immunol.* *7*, 962-970.
- Yang, Y., Kelly, P., Shaffer, A.L., 3rd, Schmitz, R., Yoo, H.M., Liu, X., Huang da, W., Webster, D., Young, R.M., Nakagawa, M., Ceribelli, M., Wright, G.W., Yang, Y., Zhao, H., Yu, X., Xu, W., Chan, W.C., Jaffe, E.S., Gascoyne, R.D., Campo, E., Rosenwald, A., Ott, G., Delabie, J., Rimsza, L., and Staudt, L.M. (2016). Targeting Non-proteolytic Protein Ubiquitination for the Treatment of Diffuse Large B Cell Lymphoma. *Cancer Cell.* *29*, 494-507.
- Ye, H., Arron, J.R., Lamothe, B., Cirilli, M., Kobayashi, T., Shevde, N.K., Segal, D., Dzivenu, O.K., Vologodskaya, M., Yim, M., Du, K., Singh, S., Pike, J.W., Darnay, B.G., Choi, Y., and Wu, H. (2002). Distinct molecular mechanism for initiating TRAF6 signalling. *Nature.* *418*, 443-447.
- Ye, J., Beetz, N., O'Keeffe, S., Tapia, J.C., Macpherson, L., Chen, W.V., Bassel-Duby, R., Olson, E.N., and Maniatis, T. (2015). hnRNP U protein is required for normal pre-mRNA splicing and postnatal heart development and function. *Proceedings of the National Academy of Sciences of the United States of America.* *112*, E3020-3029.
- Yu, J.W., Hoffman, S., Beal, A.M., Dykon, A., Ringenberg, M.A., Hughes, A.C., Dare, L., Anderson, A.D., Finger, J., Kasparcova, V., Rickard, D., Berger, S.B., Ramanjulu, J., Emery, J.G., Gough, P.J., Bertin, J., and Foley, K.P. (2015). MALT1 Protease Activity Is Required for Innate and Adaptive Immune Responses. *PLoS One.* *10*, e0127083.

- Yu, J.W., Jeffrey, P.D., Ha, J.Y., Yang, X., and Shi, Y. (2011). Crystal structure of the mucosa-associated lymphoid tissue lymphoma translocation 1 (MALT1) paracaspase region. *Proc Natl Acad Sci U S A*. *108*, 21004-21009.
- Yu, Y., Smoligovets, A.A., and Groves, J.T. (2013). Modulation of T cell signaling by the actin cytoskeleton. *J Cell Sci*. *126*, 1049-1058.
- Yugami, M., Kabe, Y., Yamaguchi, Y., Wada, T., and Handa, H. (2007). hnRNP-U enhances the expression of specific genes by stabilizing mRNA. *FEBS letters*. *581*, 1-7.
- Zarubin, T., and Han, J. (2005). Activation and signaling of the p38 MAP kinase pathway. *Cell Res*. *15*, 11-18.
- Zeng, H., Di, L., Fu, G., Chen, Y., Gao, X., Xu, L., Lin, X., and Wen, R. (2007). Phosphorylation of Bcl10 negatively regulates T-cell receptor-mediated NF-kappaB activation. *Mol Cell Biol*. *27*, 5235-5245.
- Zhang, W., and Liu, H.T. (2002). MAPK signal pathways in the regulation of cell proliferation in mammalian cells. *Cell Res*. *12*, 9-18.
- Zhao, W., Wang, L., Zhang, M., Wang, P., Qi, J., Zhang, L., and Gao, C. (2012). Nuclear to cytoplasmic translocation of heterogeneous nuclear ribonucleoprotein U enhances TLR-induced proinflammatory cytokine production by stabilizing mRNAs in macrophages. *Journal of immunology (Baltimore, Md : 1950)*. *188*, 3179-3187.
- Zhu, J., Mayeda, A., and Krainer, A.R. (2001). Exon identity established through differential antagonism between exonic splicing silencer-bound hnRNP A1 and enhancer-bound SR proteins. *Molecular cell*. *8*, 1351-1361.
- Zhu, J., Yamane, H., and Paul, W.E. (2010). Differentiation of effector CD4 T cell populations (*). *Annu Rev Immunol*. *28*, 445-489.
- Zikherman, J., and Weiss, A. (2008). Alternative splicing of CD45: the tip of the iceberg. *Immunity*. *29*, 839-841.

9 Appendix

9.1 Publications

Articles:

Meininger, I., Griesbach, R.A., Hu, D., Gehring, T., Seeholzer, T., Bertossi, A., Kranich, J., Oeckinghaus, A., Eitelhuber, A.C., Greczmiel, U., Gewies, A., Schmidt-Supprian, M., Ruland, J., Brocker, T., Heissmeyer, V., Heyd, F., and Krappmann, D. (2016). Alternative splicing of MALT1 controls signalling and activation of CD4(+) T cells. *Nat Commun.* 7, 11292.

Wilson, D.L., Meininger, I., Strater, Z., Steiner, S., Tomlin, F., Wu, J., Jamali, H., Krappmann, D., and Gotz, M.G. (2016). Synthesis and Evaluation of Macrocyclic Peptide Aldehydes as Potent and Selective Inhibitors of the 20S Proteasome. *ACS Med Chem Lett.* 7, 250-255.

Review:

Meininger, I., and Krappmann, D. (2016). Lymphocyte signaling and activation by the CARMA1-BCL10-MALT1 signalosome. *Biol Chem.* Advance online publication. doi:10.1515/hsz-2016-0216

9.2 Acknowledgments

There are many people I would like to thank for helping and supporting me within the last four years.

First, I would like to express my gratitude to my supervisor Daniel Krappmann for his guidance, support and the excellent working conditions that he provided.

I also want to thank the members of my thesis committee for reviewing my thesis: Prof. Dr. Michael Boshart, Prof. Dr. Angelika Böttger, Prof. Dr. Dirk Eick, Prof. Dr. Barbara Conradt and Prof. Dr. Marc Bramkamp.

Many thanks go to the members of my HELENA thesis committee, Dr. Jan Kranich and Prof. Dr. Michael Sattler, for critical discussions and advices.

I am very thankful to all collaboration partners, who contributed to this study. Special thanks go to Prof. Dr. Florian Heyd for sharing his knowledge and expertise.

I also would like to thank all present and former colleagues for their help and the very pleasant working atmosphere: Wolfgang Beisker, Arianna Bertossi, Miriam Bognar, Jara Brenke, Stefanie Brandner, Katrin Demski, Scalett Dornauer, Andrea Eitelhuber, Torben Gehring, Laura Glockner, Richard Griesbach, Kamyar Hadian, Daniela Hlahla, Kerstin Kutzner, Zhoulei Li, Daniel Nagel, Larissa Ringelstetter, Gisela Schimmack, Kenji Schorpp, Thomas Seeholzer, Andrea Takacs, Michelle Vincendeau, Aurelia Weber and Simone Woods.

Many thanks go to my family and friends, especially to Patrick, who always supported and encouraged me during the last four years.

Eidesstattliche Erklärung

Ich, Isabel Meininger, versichere hiermit an Eides statt, dass die vorgelegte Dissertation mit dem Titel „Alternative splicing of MALT1 controls signaling and activation of CD4⁺ T cells“ von mir selbständig und ohne unerlaubte Hilfe angefertigt ist.

München, den
(Unterschrift)

Erklärung

Hiermit erkläre ich, *

- dass die Dissertation nicht ganz oder in wesentlichen Teilen einer anderen Prüfungskommission vorgelegt worden ist.
- dass ich mich anderweitig einer Doktorprüfung ohne Erfolg **nicht** unterzogen habe.
- ~~dass ich mich mit Erfolg der Doktorprüfung im Hauptfach
und in den Nebenfächern
bei der Fakultät für der
(Hochschule/Universität)
unterzogen habe.~~
- ~~dass ich ohne Erfolg versucht habe, eine Dissertation einzureichen oder mich der Doktorprüfung zu unterziehen.~~

München, den.....
(Unterschrift)

*) Nichtzutreffendes streichen